





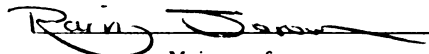
3 1293 00895 7189

This is to certify that the
thesis entitled
DURABILITY CHARACTERISTICS OF POLYMER-MODIFIED
GLASS FIBER REINFORCED
CONCRETE

presented by
Makoto Yohena

has been accepted towards fulfillment
of the requirements for

M.S. degree in Civil Engineering


Major professor

Date 3/10/90

LIBRARY

Michigan State University

PLACE IN RETURN BOX to remove this checkout from your record.
 TO AVOID FINES return on or before date due.

DATE DUE	DATE DUE	DATE DUE
_____	_____	_____
_____	_____	_____
_____	_____	_____
_____	_____	_____
_____	_____	_____
_____	_____	_____
_____	_____	_____

**DURABILITY CHARACTERISTICS OF POLYMER-MODIFIED
GLASS FIBER REINFORCED
CONCRETE**

By

Makoto Yohena

A THESIS

**Submitted to
Michigan State University
in partial fulfillment of requirements
for the degree of**

MASTER OF SCIENCE

Department of Civil and Environmental Engineering

1990

ABSTRACT

DURABILITY CHARACTERISTICS OF POLYMER-MODIFIED GLASS FIBER REINFORCED CONCRETE

by

Makoto Yohena

The main thrust of this research was to assess the effectiveness of polymer emulsions in enhancing the durability characteristics of GFRC materials. Polymer modification led to significant improvements in the flexural strength and toughness characteristics of GFRC materials. Aging in air in interior conditions had no significant effects on the flexural performance of GFRC materials with or without polymer emulsion. Accelerated aging in hot water led to major drops in flexural strength and particularly toughness of GFRC. Although polymer-modified GFRC materials had higher flexural strength and toughness at all periods of hot water immersion, polymer modification could not prevent the loss in flexural performance of GFRC with accelerated aging. Scanning Electron Microscope (SEM) observations suggested that the loss in flexural performance with accelerated aging was caused by the penetration of cement hydration products in between the glass filaments.

ACKNOWLEDGEMENTS

Financial support for this investigation was provided by the Research Excellence Fund of the State of Michigan, Okinawa Prefectural Government Human Resources Development Foundation, and Institute of International Education. The author is especially thankful to his adviser, Dr. Parviz Soroushian for his continuous support and encouragement. Mr. Ben L. Tilsen of Concast, Inc. and Mr. Mike Rich of the Composite Materials and Structures Center at Michigan State University played important roles in the initiation and successful completion of the investigation.

1888

1889

1890

1891

1892

1893

1894

1895

1896

1897

1898

1899

1900

1901

1902

1903

1904

1905

1906

1907

1908

1909

1910

1911

1912

1913

1914

TABLE OF CONTENTS

LIST OF TABLES	vi
LIST OF FIGURES	viii
1. INTRODUCTION, OBJECTIVES & SCOPE	1
2. GLASS FIBER REINFORCED CONCRETE: STATE-OF-THE-ART	5
2.1 Glass Fibers	5
2.2 Manufacturing and Mix Proportioning of GFRC	11
2.3 Quality Control	60
2.4 Fresh Mix Properties	69
2.5 Hardened Material Mechanical Properties	75
2.6 Physical Properties	97
2.7 Durability Properties	103
2.8 Bond and Interface Zone	162
2.9 Failure Mechanisms and Theoretical Studies	168
2.10 Design	183
2.11 Applications	200
3. EXPERIMENTAL PROGRAM	210
3.1 Objectives	210
3.2 Experimental Design	210
3.3 Materials, Mix Proportions and Construction	212
3.4 Test Procedures	214

4.	EXPERIMENTAL RESULTS & DISCUSSION	219
4.1	Flexural Load-Deflection Behavior	219
4.2	Flexural Strength and Toughness Test Results	221
4.3	Polymer Effects on Aging in Air	235
4.4	Polymer Effects on Aging in Hot Water	248
5.	SUMMARY AND CONCLUSIONS	262
	LIST OF REFERENCES	265

1.	EXPERIMENTAL METHOD AND DISCUSSION	219
1.1	General Methods and Apparatus	219
1.2	General Methods and Apparatus	221
1.3	General Methods and Apparatus	223
1.4	General Methods and Apparatus	225
1.5	General Methods and Apparatus	227
2.	RESULTS AND DISCUSSION	229
2.1	General Methods and Apparatus	229
2.2	General Methods and Apparatus	231
2.3	General Methods and Apparatus	233
2.4	General Methods and Apparatus	235
2.5	General Methods and Apparatus	237
2.6	General Methods and Apparatus	239
2.7	General Methods and Apparatus	241
2.8	General Methods and Apparatus	243
2.9	General Methods and Apparatus	245
2.10	General Methods and Apparatus	247
2.11	General Methods and Apparatus	249
2.12	General Methods and Apparatus	251
2.13	General Methods and Apparatus	253
2.14	General Methods and Apparatus	255
2.15	General Methods and Apparatus	257
2.16	General Methods and Apparatus	259
2.17	General Methods and Apparatus	261
2.18	General Methods and Apparatus	263
2.19	General Methods and Apparatus	265
2.20	General Methods and Apparatus	267
2.21	General Methods and Apparatus	269
2.22	General Methods and Apparatus	271
2.23	General Methods and Apparatus	273
2.24	General Methods and Apparatus	275
2.25	General Methods and Apparatus	277
2.26	General Methods and Apparatus	279
2.27	General Methods and Apparatus	281
2.28	General Methods and Apparatus	283
2.29	General Methods and Apparatus	285
2.30	General Methods and Apparatus	287
2.31	General Methods and Apparatus	289
2.32	General Methods and Apparatus	291
2.33	General Methods and Apparatus	293
2.34	General Methods and Apparatus	295
2.35	General Methods and Apparatus	297
2.36	General Methods and Apparatus	299
2.37	General Methods and Apparatus	301
2.38	General Methods and Apparatus	303
2.39	General Methods and Apparatus	305
2.40	General Methods and Apparatus	307
2.41	General Methods and Apparatus	309
2.42	General Methods and Apparatus	311
2.43	General Methods and Apparatus	313
2.44	General Methods and Apparatus	315
2.45	General Methods and Apparatus	317
2.46	General Methods and Apparatus	319
2.47	General Methods and Apparatus	321
2.48	General Methods and Apparatus	323
2.49	General Methods and Apparatus	325
2.50	General Methods and Apparatus	327
2.51	General Methods and Apparatus	329
2.52	General Methods and Apparatus	331
2.53	General Methods and Apparatus	333
2.54	General Methods and Apparatus	335
2.55	General Methods and Apparatus	337
2.56	General Methods and Apparatus	339
2.57	General Methods and Apparatus	341
2.58	General Methods and Apparatus	343
2.59	General Methods and Apparatus	345
2.60	General Methods and Apparatus	347
2.61	General Methods and Apparatus	349
2.62	General Methods and Apparatus	351
2.63	General Methods and Apparatus	353
2.64	General Methods and Apparatus	355
2.65	General Methods and Apparatus	357
2.66	General Methods and Apparatus	359
2.67	General Methods and Apparatus	361
2.68	General Methods and Apparatus	363
2.69	General Methods and Apparatus	365
2.70	General Methods and Apparatus	367
2.71	General Methods and Apparatus	369
2.72	General Methods and Apparatus	371
2.73	General Methods and Apparatus	373
2.74	General Methods and Apparatus	375
2.75	General Methods and Apparatus	377
2.76	General Methods and Apparatus	379
2.77	General Methods and Apparatus	381
2.78	General Methods and Apparatus	383
2.79	General Methods and Apparatus	385
2.80	General Methods and Apparatus	387
2.81	General Methods and Apparatus	389
2.82	General Methods and Apparatus	391
2.83	General Methods and Apparatus	393
2.84	General Methods and Apparatus	395
2.85	General Methods and Apparatus	397
2.86	General Methods and Apparatus	399
2.87	General Methods and Apparatus	401
2.88	General Methods and Apparatus	403
2.89	General Methods and Apparatus	405
2.90	General Methods and Apparatus	407
2.91	General Methods and Apparatus	409
2.92	General Methods and Apparatus	411
2.93	General Methods and Apparatus	413
2.94	General Methods and Apparatus	415
2.95	General Methods and Apparatus	417
2.96	General Methods and Apparatus	419
2.97	General Methods and Apparatus	421
2.98	General Methods and Apparatus	423
2.99	General Methods and Apparatus	425
2.100	General Methods and Apparatus	427

LIST OF TABLES

Table 2.1.1	Simplified Compositions of Glass Fibers	6
Table 2.1.2	Properties of Single Filaments of Glass	7
Table 2.2.1	Specification for Silican Sand	38
Table 2.3.1	PCI Specification for Alkali Resistant Glass Fiber - Test Requirement	62
Table 2.4.1	Mix Proportion and Fluidity	73
Table 2.4.2	Comparative Mixing Test Results	74
Table 2.5.1	Typical Mean Properties of GFRC Tested at an Early Age	93
Table 2.7.1	Bending, Tensile, and Impact Strength of GFRC at 10 Years for Various Glass Contents and Glass Length	113
Table 2.7.2	GFRC Strength at 10 Years as Percentage of the 28-day Values	113
Table 2.10.1	Typical Design Stresses for GFRC	194
Table 2.10.2	Values for K1 and K2	195
Table 2.10.3	Values for Z and I	196
Table 3.1	Properties of AR-Glass Fiber	213
Table 3.2	Silica Sand Sieve Analysis	213
Table 4.1	Flexural Test Results - Unaged GFRC	222
Table 4.2	Flexural Test Results - 12 Hour Aging	223
Table 4.3	Flexural Test Results - 1 Day Aging	223
Table 4.4	Flexural Test Results - 5 Day Aging	224
Table 4.5	Flexural Test Results - 10 Day Aging	224
Table 4.6	Flexural Test Results - 15 Day Aging	225
Table 4.7	Flexural Test Results - 20 Day Aging	225
Table 4.8	Flexural Test Results - 30 Day Aging	226

2218

2219

2220

2221

2222

2223

2224

2225

2226

2227

2228

2229

2230

Table 4.9	Flexural Test Results - 50 Day Aging	226
Table 4.10	Statistical Characteristics for LOP-Aging in Air	237
Table 4.11	Statistical Characteristics for MOR-Aging in Air	239
Table 4.12	Statistical Characteristics for Flexural Toughness - Aging in Air	239
Table 4.13	Polymer Effects in LOP-Aging in Air	240
Table 4.14	Polymer Effects in MOR-Aging in Air	240
Table 4.15	Polymer Effects in Flexural Toughness-Aging in Air	240
Table 4.16	Statistical Characteristics for LOP-50 Days in Hot Water	252
Table 4.17	Statistical Characteristics for MOR-50 Days in Hot Water	252
Table 4.18	Statistical Characteristics for Flexural Toughness - 50 Days in Hot Water	252
Table 4.19	Polymer Effects in LOP - 50 Days in Hot Water	253
Table 4.20	Polymer Effects in MOR - 50 Days in Hot Water	253
Table 4.21	Polymer Effects in Flexural Toughness - 50 Days in Hot Water	253

Page 1

Page 2

Page 3

Page 4

Page 5

Page 6

Page 7

Page 8

Page 9

Page 10

Page 11

Page 12

Page 13

Page 14

Page 15

Page 16

Page 17

Page 18

Page 19

LIST OF FIGURES

Figure 2.1.1	Weight Loss of Glass at Various Zirconia Content	7
Figure 2.1.2	Glass Fiber Roving	10
Figure 2.1.3	Chopped Strands	10
Figure 2.1.4	Manufacturing Process	10
Figure 2.2.1	Main Stages in the Automated Production of GFRP Sheets Using the Spray-Suction Process	14
Figure 2.2.2	GFRP Fabrication by Winding	14
Figure 2.2.3	Arrangement of Basic Spray Head	18
Figure 2.2.4	Spray Type Available	18
Figure 2.2.5	Production of Roving Boom	21
Figure 2.2.6	Relationship of Mould Width to Depth Where Access for Spraying Could be Difficult	27
Figure 2.2.7	Moulding Technique for Flat Products	28
Figure 2.2.8	Moulding Technique for Ribbed Edge	29
Figure 2.2.9	Moulding Technique for Rising Shutter Edge	30
Figure 2.2.10	Moulding Technique for Internal Corners	31
Figure 2.2.11	Moulding Technique for External Corners	32
Figure 2.2.12	Moulding Technique for Sandwich Panel With Organic Core	33
Figure 2.2.13	Moulding Technique for Sandwich Panel With Styrofoam Core	34
Figure 2.2.14	The Effect of Sand Content on the Drying Shrinkage of GFRP, Measured at 50°C and 20% RH	37
Figure 2.2.15	Strength Development Profiles for GFRP Cured at 20°C and 100% RH	55

Page

Page

Page

Page

Page

Page

Page

Page

Page

Page

Page

Page

Page

Page

Page

Figure 2.2.16	Strength Development Profiles of Heat-Treated GFRC Compared with the Material Cured at 20°C and 100% RH	55
Figure 2.3.1	Typical Flexural Test and Tensile Test Graphs	69
Figure 2.4.1	Test Container for Determining Fluidity	71
Figure 2.4.2	Fluidity and Flow of Typical GFRC Premix Vs. Fiber Content	71
Figure 2.5.1	Representative Tensile Load-Extension Curve for Unaged GFRC	76
Figure 2.5.2	Tensile Stress-Strain Curve of a 28-Day Old GFRC Sample Containing 4 Vol% Fibers of Length 30 mm (1.18 in.)	78
Figure 2.5.3	Schematic Stress-Strain Curves for GFRC	79
Figure 2.5.4	Stress-Strain Curve in Tension and Bending (a) After 28 days in water (b) After 2 years in water	80
Figure 2.5.5	Load-Deflection Curve From a 4-point Bending Test on a 28 Day Old GFRC Sample Containing 4 Vol% Fibers, 30 mm (1.18 in.) Long, Crosshead Speed 2mm/min (0.08 in/min)	81
Figure 2.5.6	Typical Izod Impact Strength for GFRC Stored in Water	83
Figure 2.5.7	Compressive and Shear Strengths	85
Figure 2.5.8	Typical Variation of MOR with Fiber Volume Fraction - Sprayed with 37 mm or 1.46 in. Long Fibers	87
Figure 2.5.9	Typical Variation of MOR with Fiber Length for GFRC Containing 5% by Weight of AR-Glass Fiber	89
Figure 2.5.10	Creep of Spray Dewatered GFRC with Cement Past Matrix in Dry Conditions	95
Figure 2.5.11	Effect of Matrix Type on Creep of GFRC Loaded in Flexure at 1 Month: Creep Under Water	96

Page 1

Page 2

Page 3

Page 4

Page 5

Page 6

Page 7

Page 8

Page 9

Page 10

Page 11

Page 12

Figure 2.5.12	Fatigue Performance of Hand Spray GFRP Containing 5% by Weight of AR-Glass Fiber: (a) Flexural Fatigue (b) Tensile Fatigue	97
Figure 2.6.1	The Effect of Silica Sand on Shrinkage	99
Figure 2.6.2	Relationship Between Linear Coefficient of Thermal Expansion of Cement Paste and Ambient Relative Humidity	101
Figure 2.6.3	Relationship of Sound Reduction and Frequency	103
Figure 2.7.1	Effect of Aging (50°C, 122°F Water for 1 Month) on the Change in the Load-Deflection Curve of GFRP with AR-Glass Fibers	104
Figure 2.7.2	MOR Against Log Time for Composite Made with E-Glass - Air and Water Storage	105
Figure 2.7.3	Flexural Yield Strength Versus Freeze-Thaw Cycles	109
Figure 2.7.4	Flexural Ultimate Strength Versus Freeze-Thaw Cycles	110
Figure 2.7.5	Bending Strength of GFRP Composite Stored in Air at 20°C, 40% RH, Fiber Length 30 mm (1.18 in.)	114
Figure 2.7.6	Bending Strength of GFRP Composites Stored Under Water at 20°C, Fiber Length 30 mm (1.18 in.)	115
Figure 2.7.7	Bending Strength of GFRP Composites Stored on the Natural Weathering Site of Garston, Fiber Length 30 mm (1.18 in.)	116
Figure 2.7.8	MOR and LOP (Proportional Elastic Limit-PEL) Versus Age for AR-Glass Fiber Composites Stored in Various Environments: (a) Stored in Natural U.K. Weathering Condition (b) Stored in Water at 64 to 68°F (18 to 20°C) (c) Stored in Air at 68°F (20°C) and 40% Relative Humidity	117

Figure 2

Figure 3

Figure 4

Figure 5

Figure 6

Figure 7

Figure 8

Figure 9

Figure 10

Figure 11

Figure 12

Figure 13

Figure 14

Figure 15

Figure 16

Figure 17

Figure 2.7.9	Variations in the LOP Stress and Strain in Tension with Fiber-Volume Fractions	118
Figure 2.7.10	Reduction in Strength of AR-Glass Filaments Removed from Aged GFRC	120
Figure 2.7.11	Strand-In-Cement (SIC) Specimen	124
Figure 2.7.12	SIC Strength Retention in Water at Various Temperatures	126
Figure 2.7.13	"Arrhenius" Plots	127
Figure 2.7.14	"Normalized Arrhenius" Plot	128
Figure 2.7.15	Strength Retention of GFRC Composites in Water at Various Temperatures	130
Figure 2.7.16	Strength Retention of GFRC Composites in Water and Weathering	134
Figure 2.7.17	"Normalized Arrhenius" Plot Including Weathering Data	134
Figure 2.7.18	How to Improve Durability of GFRC	135
Figure 2.7.19	Strength of Glass Fiber Strand With Various Coatings in Wet OPC Paste at 80°C (176°F)	137
Figure 2.7.20	MOR of GFRC Using Specially Coated AR-Glass Fibers After Accelerated Aging in 80°C (176°F) Water	137
Figure 2.7.21	MOR (Open Symbols) and LOP (Solid Symbols) of GFRC Composites Containing (a) OPC, (b) 60% OPC, 40% Fly Ash, (c) Pozament, and (d) 60% OPC, 40% Fly Ash Modified by Styrene Butadiene, Stored in Natural Weather in U.K.	139
Figure 2.7.22	Ultimate Tensile Strength of GFRC Composites (a) OPC, (b) 60% OPC, 40% Fly Ash, (c) Pozament, and (d) 60% OPC, 40% Fly Ash Modified by Styrene Butadiene, Stored in Natural Weather in U.K.	140

Figure 2.7.23	Impact Strength of GFRC Composite Containing (a) OPC, (b) 60% OPC, 40% Fly Ash, (c) Pozament, and (d) 60% OPC, 40% Fly Ash Modified by Styrene Butadiene, Stored in Natural Weather in U.K.	140
Figure 2.7.24	Effect of Aging in Water at 20°C on the (a) MOR, and (b) Toughness (W.F.) of GFRC Composites Prepared from Matrices of OPC and Cements with 5% Fly Ash	141
Figure 2.7.25	Effect of Fly Ash Content on the MOR and Toughness (W.F.) Values of GFRC Composites Aged in Water at 20°C for (a) 150 Days and (b) 1 Year	141
Figure 2.7.26	Effect of Accelerated Aging in 50°C Water and MOR and Toughness (WOF) of Composite with AR-Glass Fibers with Various Treatments of Silica Fume	144
Figure 2.7.27	Typical Tensile Stress-Strain Curve for AR-Glass and Forton P-GFRC After (a) 28 Days Curing at 20°C (68°F) and (b) the Next 26 Weeks Under Water at 50°C (122°F)	147
Figure 2.7.28	Bending and Tensile Strength Development as a Function of Time, Curing Under water at 20°C (68°F)	147
Figure 2.7.29	Bending and Tensile Strength Development, Curing at 20°C (68°F)	148
Figure 2.7.30	Impact Strength Development	148
Figure 2.7.31	Tensile Strength Development Under Accelerated Aging at 50°C (122°F) Under Water	149
Figure 2.7.32	Development Strain at Ultimate Tensile Stress Under Accelerated Aging at 50°C (122°F) Under Water	149
Figure 2.7.33	Development of Limit Proportionality in Tension Under Accelerated Aging at 50°C (122°F) Under Water	150

Fig.

Fig.

Fig.

Fig.

Fig.

Fig.

Fig.

Fig.

Fig.

Fig.

Fig.

Fig.

Figure 2.7.34	Tensile Young's Modulus Development Under Accelerated Aging at 50°C (122°F) Under Water	150
Figure 2.7.35	Bending Strength Development Under Accelerated Aging at 50°C (122°F) Under Water	151
Figure 2.7.36	Impact Strength Development Under Accelerated Aging at 50°C (122°F) Under Water	151
Figure 2.7.37	MOR of GFRC Made from HAC and AR Glass Fibers	154
Figure 2.7.38	UTS of GFRC Made from HAC and AR-Glass Fibers	154
Figure 2.7.39	Impact Strength of AR-GFRC With HAC	155
Figure 2.7.40	MOR and Impact Strength of GFRC with E-Glass	155
Figure 2.7.41	Stress-Strain Diagram of AR-GFRC/HAC, Water Stored	155
Figure 2.7.42	MOR and LOP in Bending for GFRC Made With: (a) Frodingham Supersulphated Cement, (b) Quick-Setting Supersulphated Cement, and (c) OPC; Stored Under Water at 20°C	158
Figure 2.7.43	Impact Strength for GFRC Made With: (a) Frodingham Supersulphated Cement, (b) Quick-Setting Supersulphated Cement and (c) OPC; Stored Under Water at 20°C	158
Figure 2.7.44	Tensile Stress-Strain Curves for GFRC Made with Frodingham Supersulphated Cement Stored: (a) in Air at 65% RH; (b) on Natural Weathering Site at U.K.; and (c) Under Water at 20°C for 5 Years	159
Figure 2.7.45	Ultimate Failure Strain in Tension of GFRC Made with Frodingham and Quick-Setting Supersulphated Cement Stored in (a) Air at 65% RH, (b) Water at 20°C and (c) Natural Weathering	159

Page 1
Page 2
Page 3
Page 4
Page 5
Page 6
Page 7
Page 8
Page 9
Page 10
Page 11
Page 12
Page 13
Page 14
Page 15
Page 16
Page 17
Page 18
Page 19
Page 20
Page 21
Page 22
Page 23
Page 24
Page 25
Page 26
Page 27
Page 28
Page 29
Page 30
Page 31
Page 32
Page 33
Page 34
Page 35
Page 36
Page 37
Page 38
Page 39
Page 40
Page 41
Page 42
Page 43
Page 44
Page 45
Page 46
Page 47
Page 48
Page 49
Page 50
Page 51
Page 52
Page 53
Page 54
Page 55
Page 56
Page 57
Page 58
Page 59
Page 60
Page 61
Page 62
Page 63
Page 64
Page 65
Page 66
Page 67
Page 68
Page 69
Page 70
Page 71
Page 72
Page 73
Page 74
Page 75
Page 76
Page 77
Page 78
Page 79
Page 80
Page 81
Page 82
Page 83
Page 84
Page 85
Page 86
Page 87
Page 88
Page 89
Page 90
Page 91
Page 92
Page 93
Page 94
Page 95
Page 96
Page 97
Page 98
Page 99
Page 100

Figure 2.7.46	Changes in (a) the Bending, and (b) Impact Strength of GFRC by the Accelerative Test	161
Figure 2.7.47	Changes in (a) the Bending and (b) Impact Strength of GFRC Under Natural Exposure	162
Figure 2.8.1	Schematic View of Specimen	163
Figure 2.8.2	Relationship Between Tensile Load and Anchor Length	164
Figure 2.8.3	Relationship Between Tensile Load and Anchor Angle	165
Figure 2.8.4	Relationship Between Tensile Load and W/C	166
Figure 2.9.1	Stress-Strain Curves of Strong Fibers and Brittle Matrices	169
Figure 2.9.2	Ranges of Composite Stress-Strain Curves Made with Brittle Matrices and Strong Fibers	170
Figure 2.9.3	Typical Stress-Strain Curves for GFRC Materials Calculated from Equations 4, 6, 7 and 8	173
Figure 2.9.4	Schematic Representation of Bending of Fibers Bridging a Traverse Crack During Fracture	181
Figure 2.10.1	Reduction of MOR	191
Figure 2.10.2	Bending Behavior of GFRC	192
Figure 2.11.1	GFRC Cladding Panels	203
Figure 2.11.2	Replacement of Conventional Cladding Panels	203
Figure 2.11.3	Timber Replacement	204
Figure 2.11.4	GFRC "Timber" Cladding Detail	204
Figure 2.11.5	FRP Panel Replacement Application	205
Figure 2.11.6	Permanent Formwork	205
Figure 2.11.7	Sewer Linings	206

Eq

Eq

Eq

Eq

Eq

Eq

Eq

Eq

Eq

Eq

Eq

Eq

Eq

Eq

Eq

Figure 2.11.8	GFRC Permanent Coffe Unit	206
Figure 2.11.9	Asbestos Cement Replacement (a) Roof Tiles (b) Roof Tiles Detail	207
Figure 2.11.10	The Marine Industry. Floating Pontoons	208
Figure 2.11.11	The Agricultural Industry. Field Drinking Trough	208
Figure 2.11.12	The Agricultural Industry. Sheep Dip Troughs	209
Figure 2.11.13	The Leisure Industry. Kiosk	209
Figure 3.1	GFRC Panel and Specimens	216
Figure 3.2	Water Bath for Accelerated Aging	217
Figure 3.3	Third-Point Loading with a Load Cell and Two Transducers	217
Figure 3.4	Computer-Based Data Acquisition System	218
Figure 3.5	JEOL T-330 SEM	218
Figure 4.1	Typical Load-Deflection Curves - Unaged GFRC	220
Figure 4.2	Multiple Cracking (a) Polymer 0% (b) Polymer 15%	220
Figure 4.3	Typical Load-Deflection Curves - Aged GFRC (50 Days in 50°C, 122°F Water)	221
Figure 4.4	LOP, MOR vs. Time - Polymer 0% (a) Aging in Dry Air (b) Aging in Hot Water	227
Figure 4.5	LOP, MOR vs. Time - Polymer 5% (a) Aging in Dry Air (b) Aging in Hot Water	228
Figure 4.6	LOP, MOR vs. Time - Polymer 10% (a) Aging in Dry Air (b) Aging in Hot Water	229

Fig.

Fig.

Fig.

Fig.

Fig.

Fig.

Fig.

Fig.

Fig.

Fig.

Fig.

Fig.

Fig.

Fig.

Fig.

Fig.

Fig.

Fig.

Fig.

Figure 4.7	LOP, MOR vs. Time - Polymer 15% (a) Aging in Dry Air (b) Aging in Hot Water	230
Figure 4.8	Toughness vs. Time - Polymer 0% (a) Aging in Dry Air (b) Aging in Hot Water	231
Figure 4.9	Toughness vs. Time - Polymer 5% (a) Aging in Dry Air (b) Aging in Hot Water	232
Figure 4.10	Toughness vs. Time - Polymer 10% (a) Aging in Dry Air (b) Aging in Hot Water	233
Figure 4.11	Toughness vs. Time - Polymer 15% (a) Aging in Dry Air (b) Aging in Hot Water	234
Figure 4.12	LOP and MOR of Unaged and Aged in Air	236
Figure 4.13	Toughness of Unaged and Aged in Air	236
Figure 4.14	LOP and MOR with Time - GFRG Aged in Air	237
Figure 4.15	Toughness with Time - GFRG Aged in Air	237
Figure 4.16	Inclined Crack - Unaged GFRG	241
Figure 4.17	Fractured Surface - Unaged GFRG	241
Figure 4.18	Fiber Pull-Out With No Fracture of Filaments	243
Figure 4.19	Smooth Surface of Filaments - Aging in Air	243
Figure 4.20	Free Space In-Between Filaments - Unaged GFRG	244
Figure 4.21	Free Space In-Between Filaments - Aging in Air	244
Figure 4.22	Crack Developed Along Fiber - Aging in Air	245
Figure 4.23	Debonding Between Matrix and Filaments	245
Figure 4.24	Hydration Products Attracted to Filaments - Polymer 0%	246
Figure 4.25	Polymer Particles Attracted to Filaments - Polymer 15%	246

Figure 4.26	Polymer Particles - Polymer 15%	247
Figure 4.27	LOP and MOR of Unaged and Aged in Hot Water	249
Figure 4.28	Toughness of Unaged Aged in Hot Water	249
Figure 4.29	Linear Regression Curves of MOR with Time - Aging in Hot Water	250
Figure 4.30	Linear Regression Curves of Toughness With Time - Aging in Hot Water	250
Figure 4.31	Perpendicular Crack - Aging in Hot Water	254
Figure 4.32	Fractured Surface - Aging in Hot Water	254
Figure 4.33	Penetration of Hydration Products - Polymer 0%	
	(a) Magnification 350	
	(b) Magnification 2000	257
Figure 4.34	Penetration of Hydration Products - Polymer 15%	
	(a) Magnification 200	
	(b) Magnification 1000	258
Figure 4.35	Smooth Surface of Filaments	
	(a) Polymer 0% (50 Days in Hot Water)	
	(b) Polymer 15% (50 Days in Hot Water)	259
Figure 4.36	Fractured Filament and Grooves Caused by Pull-Out	260
Figure 4.37	Fractured Filaments with Little Pull-Out	260
Figure 4.38	Natural Weathering Exposure at Michigan State University	261

(

1 copy

reinf

of ve

glass

direc

resis

the t

glass

2222

rein

dry

mic

elas

lowe

prop

be u

star

tube

rete

1322

2122

CHAPTER 1

INTRODUCTION, OBJECTIVES & SCOPE

Glass fiber reinforced concrete (GFRC) may be viewed as a composite material, based on a matrix of cement or mortar reinforced with an addition of glass fibers at about 5 to 8% of weight. Cementitious matrices reinforced with short glass fibers are superior to plain cement as far as the direct tensile strength, flexural strength, impact resistance and fire resistance are concerned. For example, the tensile and flexural strengths of unaged GFRC with 5% glass fiber addition are about twice and four times that of matrix itself, respectively.

The idea of using dispersed glass fibers as reinforcement for cement was initially developed by Biryukovich, et al. (1964), Reference 1, in the Soviet Union, where they reported improvements in tensile strength, elasticity and other properties of cement products. However, because of uncertainties regarding long-term properties, glass fiber reinforced concrete (GFRC) could not be used practically.

The practical use of GFRC as a construction material started with the development of an alkali-resistant glass fiber in the early 1970's. Majumdar and Nurse (1974), Reference 2, at the U.K. Building Research Establishment (BRE) used an alkali-resistant glass fiber which had a high zirconia content and demonstrated desirable resistance to

the

the

the

the

the

the

the

the

the

the

the

the

the

the

the

the

the

the

the

the

the

the

the

the

the

the

the

the highly alkaline environment of ordinary Portland cement. The research at BRE led to major developments and commercial production of GFRC in U.K. As a result of these efforts, the use of GFRC as a construction material, mainly as an attractive replacement for asbestos cement, spread worldwide. It was estimated in 1980 that the world production of alkali-resistant glass fibers was about 5000 tons per annum. Typical applications of GFRC include cladding panels, permanent concrete formwork, and pipe linings (Reference 3).

Although the overall performance of GFRC is improved through the use of alkali-resistant glass fibers, GFRC still shows a reduction in strength and ductility with time when it is exposed to wet environments (References 4 to 8). Therefore, applications of GFRC are limited to non-structural uses, and designers of GFRC must consider this reduction in strength with time. For this reason, GFRC researchers have mostly concentrated their efforts on achieving improvements in the long-term durability of the composite (References 5, 6, 7).

Although the ultimate causes of the wet aging response are still debated, two factors have been suggested to cause the loss in strength and ductility of GFRC in wet environments. One is chemical, the other is physical. The former is that the alkali-resistant glass fibers are subjected to some alkali attack in moist cement environment and lose some of their tensile strength. The physical cause

66

67

68

69

70

71

72

73

74

75

76

77

78

79

80

81

82

83

84

85

86

87

of GFRC aging results from the tendency of the cement hydration products, especially calcium hydroxides, to fill up spaces between and around the filaments of glass fibers and bind the filaments as GFRC ages in moist conditions. This causes local concentration of stress under load at the surface of fibers, resulting in embrittlement of GFRC (Reference 7).

Bijen (1983), Reference 21, showed some improvements in the durability of GFRC by adding polymer emulsions into the matrix. The polymer-modified glass fiber reinforced cement (Forton P-GFRC) composites contained non-alkali-resistant glass fibers (E-glass fibers) instead of alkali-resistant glass fibers and a polymer in the form of water-dispersed particles. It is suggested that when the fiber bundles are mixed with polymer-modified mortar, the glass fiber filaments are surrounded by the polymer particles and thus are screened off and protected against the migration of cement hydration products, as well as possible chemical attack.

The use of polymer-modified GFRC has grown in the recent years partly due to shortening of moist curing period resulting from polymer modification.

The objectives of this investigation were (1) to establish and compare the durability characteristics of polymer-modified GFRC with different polymer additions using

accelerated aging tests, and (2) to identify the failure and deterioration mechanisms in polymer-modified GFRC using scanning electron microscope (SEM).

The polymer type used at 0%, 5%, 10% and 15% weight of cement was acrylic emulsion, and the glass fibers were alkali-resistant. The specimens were manufactured through spraying, and all had a constant glass fiber weight fraction of 6%. Accelerated aging was achieved through immersion in water at 50°C (122°F); comparisons were made between aging under water and in air. The aging process was studied through the measurement of flexural strength and toughness, and also by scanning electron microscope photography.

This thesis is organized in five chapters. A comprehensive review of the literature, covering all the key aspects of GFRC production, properties and applications, is presented in Chapter 2. The experimental program conducted in this investigation is introduced in Chapter 3. The experimental results, together with statistical analysis and discussions of results, are presented in Chapter 4. Chapter 5 summarizes this investigation, and presents the conclusions derived from the analysis of the results produced in this study.

2.1

be in

divid

2.1.2

avail

ATC

need

the r

made

alkal

resis

Port.

ATC

glass

or tl

resis

Prod.

2.1.3

Major

impr

CHAPTER 2

GLASS FIBER REINFORCED CONCRETE: STATE-OF-THE-ART

2.1 GLASS FIBERS

There are clearly various of glass fibers which could be incorporated into cement-based matrices; they can be divided into two main categories:

- * Non-alkali resistant
- * Alkali resistant

2.1.1 Non-Alkali Resistant Glass Fibers

Before alkali resistant glass fibers were readily available 'E' glass and 'A' glass were commonly used in GFRC. The E glass or borosilicate glass was more widely used than A glass, and it is now the standard fiber used for the reinforcement of plastics. The A glass is a cheap fiber made from scrap sheet or bottle glass. Since these non-alkali resistant glass fibers do not have adequate resistance to the high alkalinity (PH=12-13) of ordinary Portland cement, they nowadays have little practical in GFRC. However, if special coatings are provided to these glass fibers, or the fibers are used with low-alkali cement or the less alkaline high-alumina cement, Non-alkali resistant glass fibers will have some potentials for GFRC production because of their low cost (Reference 10).

2.1.2 Alkali-Resistant (AR) Glass Fibers

In the late 1960's, investigations carried out by Majumdar and Nurse (1974), Reference 2, led to great improvements in resistance to of glass fibers to alkali

attack

other g

been de

chemical

glass

of eac

proper

and ty

reinfo

differ

high a

and A

resis

terms

an al

more

resis

Table

(Refe

attack by including zirconia sand in the glass formulation. Other glass formulations based on high zirconia content have been developed elsewhere. Table 2.1.1 shows approximate chemical composition of AR-glass fiber, E glass fiber and A glass fiber (References 9, 10). Although the compositions of each glass fiber differs largely, their physical properties, as shown in Table 2.1.2, are not so different and typically satisfy the requirements for use as reinforcement in cement paste or mortar. The major difference among them is their ability of resistance against high alkalinity, and AR-glass fiber is much superior to E and A glass fibers. Figure 2.1.1 also shows the alkali resistance of glass fibers at different ZrO_2 contents in terms of the weight loss of glass fibers after immersion in an alkaline solution, and it suggests that glass fiber with more than 15% Zirconia content have satisfactory alkali resistance (Reference 7).

Table 2.1.1 Simplified Compositions of Glass Fibers (Reference 9).

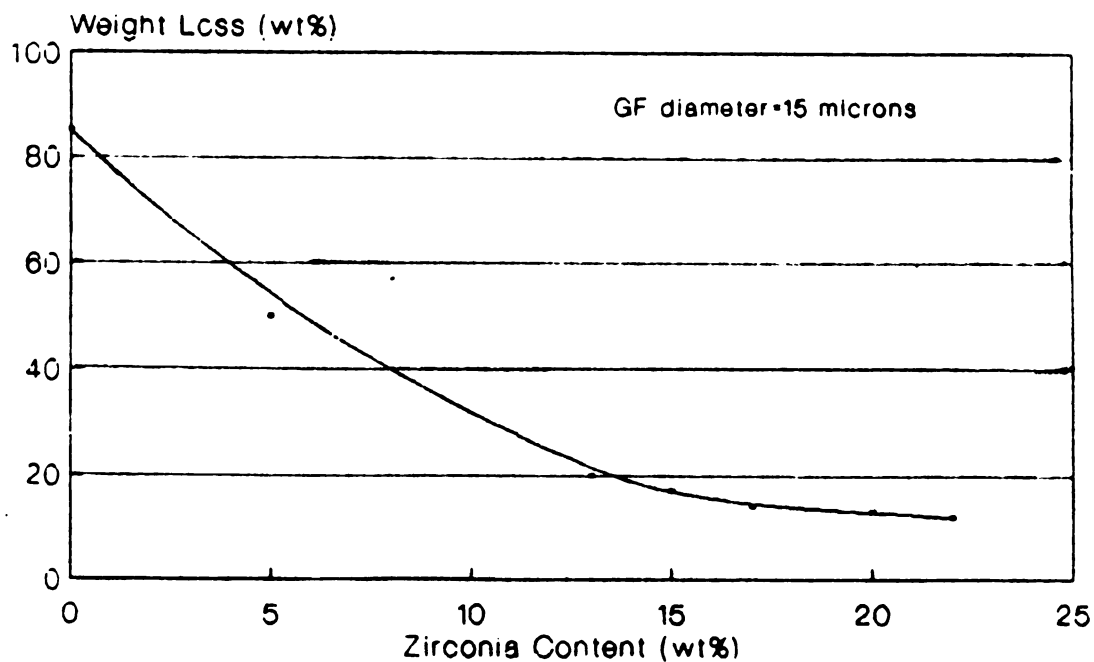
Component	AR-glass	E-glass	A-glass
SiO ₂	6.5 %	55 %	72 %
Al ₂ O ₃	1 %	15 %	2 %
B ₂ O ₃	—	10 %	—
CaO	4 %	21 %	10 %
MgO	—	—	3 %
Na ₂ O	15 %	1 %	13 %
K ₂ O	1 %	—	—
ZrO ₂	17 %	—	—

(wt%)



Table 2.1.2 Properties of Single Filaments of Glass (Reference 2).

	AR-glass	E-glass	A-glass
Density (tm^{-3})	2.68	2.53	2.46
Tensile strength (Nmm^{-2})	3600	3700	3100
Young's modulus (Nmm^{-2})	70000	77000	74000
Extention at break (%)	3.6	4.8	4.7



Weight Loss of GF after Immersing in 10% NaOH
Solution at 80 C (176F) for 100 Hrs (wt%).

Figure 2.1.1 Weight Loss of Glass at Various Zirconia Content (Reference 7).

2.1.3 Forms of Glass Fibers

The single filaments of glass are of the order of 10 to 20 microns in diameter. The only form of glass available as single filaments is called glass wool. This glass wool is extremely difficult to mix with cement; formation of fiber balls during mixing makes the uniform dispersion of glass wool rather difficult. Therefore, the usual forms of glass fiber are rovings and chopped strands.

Rovings are continuous strands of glass fiber grouped together in a parallel bundle and wound to form a square-ended package referred to as a cheese. The individual strands consist of 100 to 200 filaments bonded together by an organic water-based emulsion, and about 30 strands are grouped to form roving. Figure 2.1.2 shows a roving of glass fiber. The spray-up method, the most commonly used manufacturing technique for GFRP, uses this form of glass fiber.

Chopped strands consist of rovings chopped into uniform lengths between 6 mm (.24 in.) and 50 mm (2 in.). They are purchased by specifying the cut length. Since chopped strand fibers are used in the pre-mix process, greater strand integrity is required. This is obtained by modifying the coating applied to bind the filaments such that stiffer fiber is produced with greater integrity and resistance to abrasion during the mixing process. Chopped strands are shown in Figure 2.1.3.

strand

essent

apple

for AR

lincon

the fi

gas be

to a s

which

temper

filare

speed

its b

in Pi

2.1.4 Manufacturing of Glass Fibers

The manufacturing methods used for rovings and chopped strands of glass fibers for GFRC applications are essentially the same as those used for E glass fibers applied to FRP, but high melting temperatures are necessary for AR-glass fibers because of their high content of Zirconia. In modern glass fiber manufacturing facilities the fiber is produced on a continuous basis in electrical or gas heated furnaces. Molten glass passes from the furnace to a series of electrically heated outlets, called bushings, which are made from a platinum-based alloy to withstand high temperatures. Molten glass exudes and is drawn into filaments of diameter of 10-20 microns, depending on drawing speed through a bushing with hundreds of small nozzles in its base. The fiber making process is shown schematically in Figure 2.1.4.

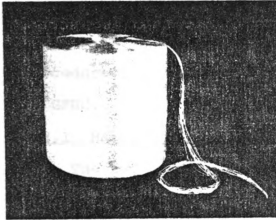
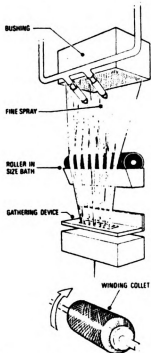


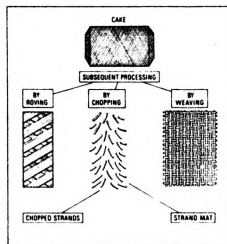
Figure 2.1.2 Glass Fiber Roving (Reference 10).



Figure 2.1.3 Chopped Strands (Reference 10).



(a) From Bushing to Cake



(b) From Cake to Finished Product

Figure 2.1.4 Manufacturing Process (References 9, 11)

1.2 MAY

The

(GRC) v

material

reviews

procedur

to GRC

1.2.1

Th

premi

subdivi

(a

(

1.2.1

Direct

gun f

acomi

chopp

length

2.2 MANUFACTURING AND MIX PROPORTIONING OF GFRC

The properties of glass fiber reinforced concrete (GFRC) vary with adopted manufacturing method, constituent materials, mix design, and curing conditions. This chapter reviews the manufacturing methods and equipment, mix design procedures, curing and finishing techniques commonly applied to GFRC.

2.2.1 Manufacturing Methods

The two basic techniques in use are spraying and premixing, and each method may be further divided into subdivisions as follows:

(a) Spraying

Direct Spraying

Spray Suction

Winding

Spinning

(b) Premixing

Contact Moulding

Pressing

Extrusion

2.2.1.1 Spraying Techniques

Direct Spraying:

A slurry mortar is fed at a metered rate to the spray gun from a specially developed pump unit, where it is atomized by compressed air. Glass fiber roving is fed to a chopper/feeder unit which cuts the fiber into predetermined lengths, and compressed air is again used to inject them

into

more

more

spray

flat

both

Spray

spray

proc

down

water

post

water

use

fac

proc

fib

of

aut

(Re

W

Proc

Proc

ope

cop

into the slurry stream. Relatively high fiber contents (more than 8% of weight) can be incorporated into cement matrices using the direct spraying technique. This direct spray process can be easily mechanized to produce basically flat or shallow profiled items by mechanizing movements of both the mould and the spray head (References 9, 12).

Spray Suction:

In principle, this process is similar to the direct spray process except for the use of a vacuum-dewatering process. By this dewatering process the GFRC can be laid down using the spraying method but with a much higher water/cement ratio than could be tolerated if conventional post-manufacturing processes were being used. The high water content enables a highly atomized slurry spray to be used giving greater control of thickness uniformity, and facilitates mass production of primarily flat sheet. GFRC produced by this method makes the most effective use of fiber properties and has the highest strength and stiffness of the sprayed materials. The process can be readily automated for standard sheets as shown in Figure 2.2.1 (References 9, 12).

Winding:

Figure 2.2.2 shows the main elements in the winding process for the production of pipes, noting that similar procedures can be adopted for the manufacture of sheets or open sections by cutting and re-forming the freshly made composites. The continuous glass fiber rovings are

1971

1972

1973

1974

1975

1976

1977

1978

1979

1980

1981

1982

1983

1984

1985

1986

1987

1988

1989

1990

1991

1992

impregnated with cement slurry by passing them through a cement bath; they are then wound onto a suitable mandrel at a predetermined angle and pitch. Additional slurry and chopped fiber can be sprayed onto the mandrel during the winding process and roller pressure combined with suction can be used to remove excess cement paste and water. Fiber volumes in excess of 15% have been achieved and hence very high strengths are possible (References 9, 12).

Spinning:

This method has been employed for the production of pipe products and considerable development work has been required to design and manufacture equipment suitable to achieve the desired product characteristics. The mould is located on a spinning bed and rotated at the required speed for placement of the outer fiber reinforcement. The fiber and slurry systems are mounted on a boom which is powered through the mould and facilitates the dispensation of a continuous slurry and fiber mixture along the length of the mould. Once the placing processes are complete the rotational speed of the mould is increased in order to produce the required dewatering characteristics and draw off the excess water (References 9, 12).

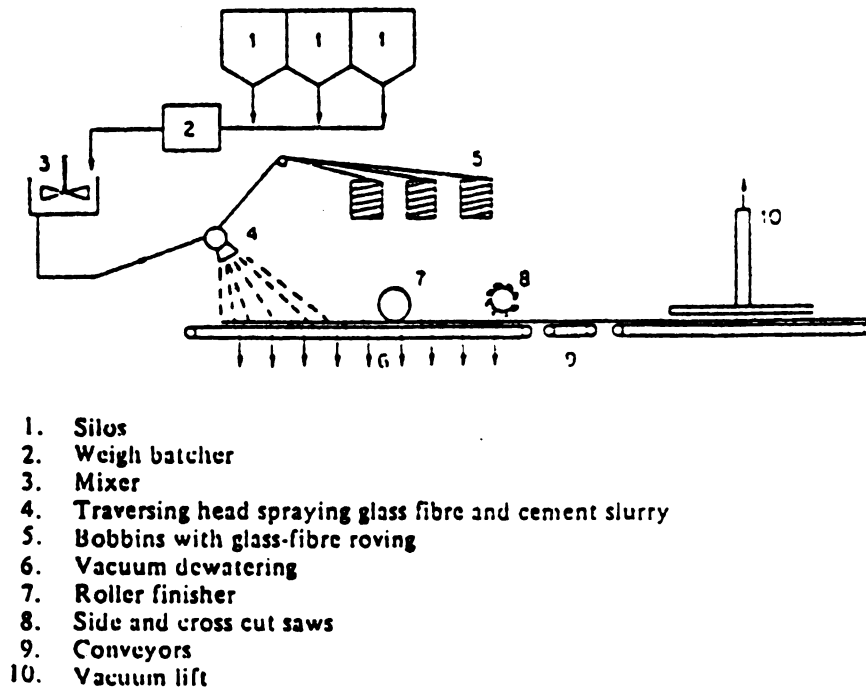


Figure 2.2.1 Main Stages in the Automated Production of GFR Sheets Using the Spray-Suction Process (Reference 9).

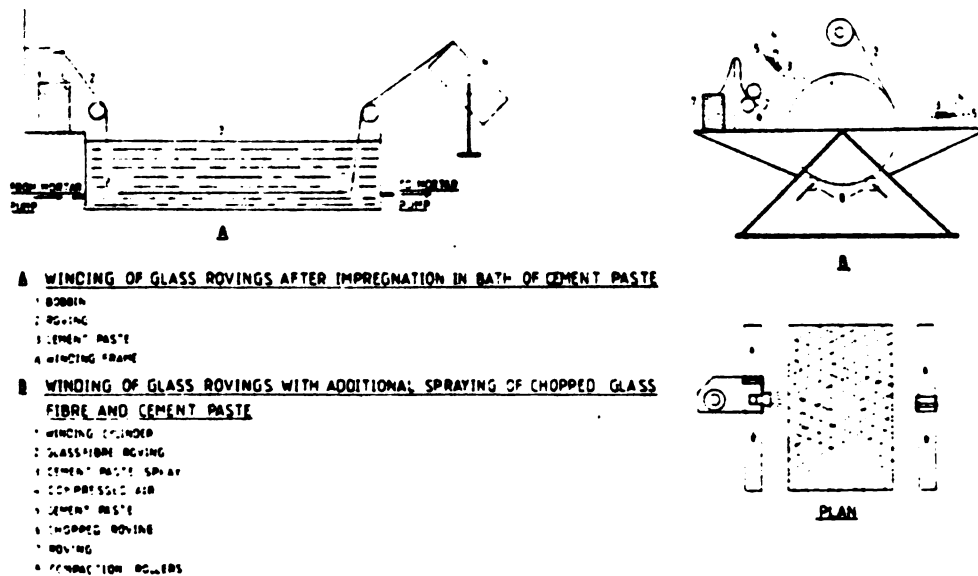


Figure 2.2.2 GFR Fabrication by Winding (Reference 12).

2.2.1.2 Equipment for Spraying Methods

Since direct spray work and dewatering spray work are at present the major GFRC production processes employed, the equipment used in these procedures, namely the pump unit, spray heads, roving feed systems, vacuum equipment, automated spray-up equipment and the automated traverse unit are described in this section.

Pump Unit:

The pump unit is the piece of equipment that processes the matrix or mortar component of the GFRC composite. Freshly mixed mortar (or in some cases the raw materials) is transported by the pump unit at set rates to the spray head or gun. The unit can therefore be regulated to produce a precisely maintained mortar output at the gun nozzle. It is essential that the speed of the pump is carefully selected to ensure that the delivery rate conforms with the relative velocity at which mortar can pass through the pipeline. Very stiff mixes are directly influenced in their rate of output by the pipeline friction, with only marginal relationship to static heads. Consequently, when low water/cement ratio mixes are processed, admixture may be required to assist the pumpability of the mix.

Spray Heads:

The spray head for GFRC is the unit that processes the mortar and glass fiber, transforming these two components from separate materials into one homogeneous well dispersed

composite. This process is a continuous flow, so that separate inputs are blended via the spray heads respective output rates and inclusion angle to produce, at lay-out, a two dimensional uniform dispersion of glass fibers. The components of a spray head are seen in Figure 2.2.3. As seen in this figure, the basic components are the chopper gun unit and the mortar spray head. The chopper gun unit takes the roving, chops it into uniform lengths of fiber and sprays it into the mortar spray system. The mortar spray head receives the mortar from the pump and sprays it out in the form of a rain of mortar with the required fineness, velocity and spray cone angle.

Basically the four types of spray head systems are available, and those are shown in Figure 2.2.4. Single head gun is an early production model of spray head, and it is still widely used in GFRP industry. Twin mortar head spray head employs two standard spray heads located on either side of chopper gun, and it has been used successfully but suffers from being a heavy spray head for manual work. The system in which twin chopper guns are located on each side of a mortar spray has been used in some works, but it is not in practical use. The concentric spray head is a newly developed type of spray head. It combines the mortar spray head with the chopper gun by locating the mortar spray head around the nozzle of the chopper gun, and the chopped fiber

is sprayed out in the center of a concentric ring of mortar. This spray head produces a good spray pattern that contains the fiber and considerably reduces waste. Its disadvantage is a tendency to block easily if particles of sand or cement greater than 1 mm are present in the mortar. However, concentric spray head is providing to be a viable step forward in spray head design (Reference 13).

Roving Feed System:

In order that the wound package forming the roving cheese can be efficiently fed to the chopper head, a suitable 'path' has to be established. This has evolved resembling the fishing rod method of supporting the fishing line, namely a series of spaced eyes through which the line or roving is made to pass. A production roving boom and stand are shown in Figure 2.2.5. This unit is provided with castors to enable the drop from the last support eye to be positioned close to the spray head. Experience has shown that the vertical height between the roving bundle and the first support eye should be around 1 m (3.3 ft). This enables the heavily coiled roving to open out easily on take-up and prevents snagging at the eye. The horizontal displacement of the guide eyes should be such that excessive over-run can be avoided when the chopper drive is turned off. This over-run is also a function of the length of the

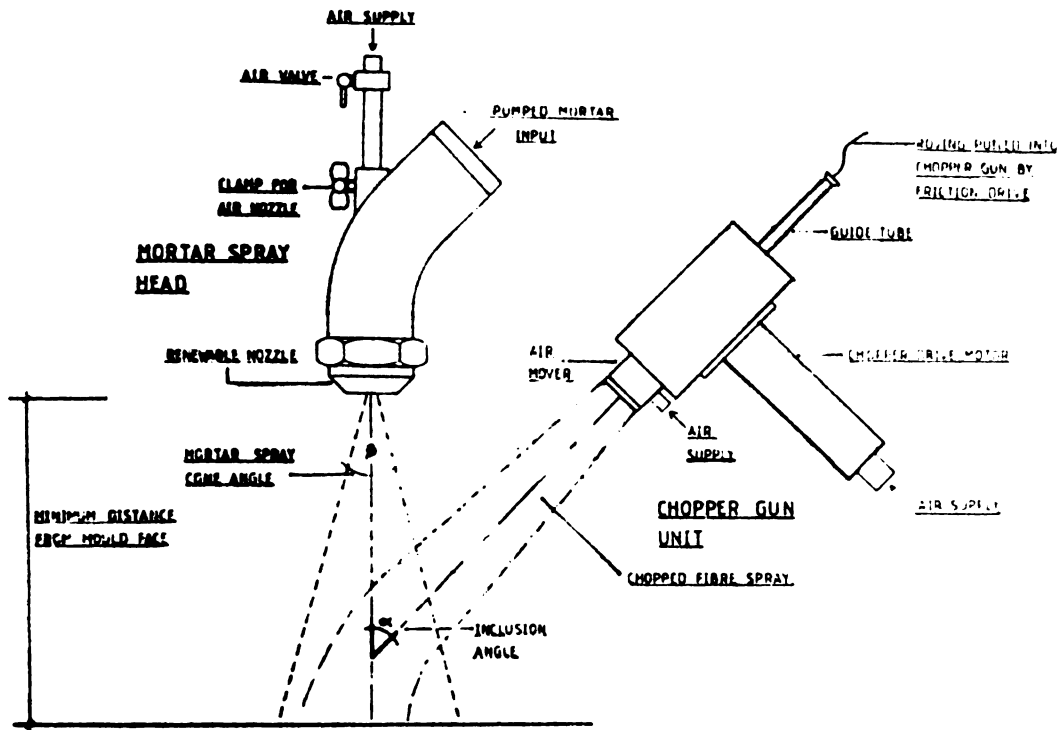


Figure 2.2.3 Arrangement of Basic Spray Head (Reference 12).

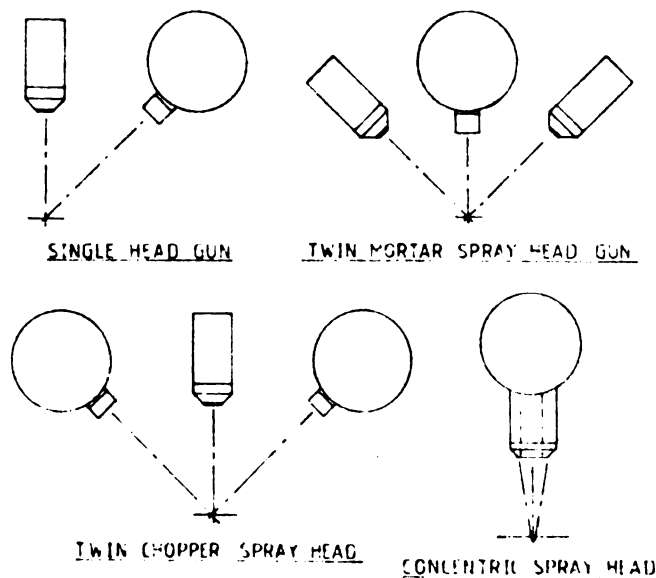


Figure 2.2.4 Spray Type Available (Reference 12).

drop fr

distanc

cheese

Vacuum

Va

method

is red

the lo

proces

upward

extra

conti

shall

tight

grid

cente

onto

requi

fini

sepa

time

wate

Pina

inve

epra

flit

drop from the last guide eye to the chopper head, and the distance of the horizontal run of eyes above the roving cheese (Reference 13).

Vacuum Equipment:

Vacuum extraction of surplus water in spray-suction method has certain advantages. Shrinkage of the composite is reduced and the strength properties are improved due to the lower water/cement ratio and increased density. Two processes now in practice are downward vacuum extraction and upward vacuum extraction. Equipment for downward vacuum extraction can take the form of either a stage or a continuous process, but both operate in the same manner. A shallow box of suitable dimensions is produced with airtight sides and base but a stiffened top that contains a grid of holes at approximately 10 mm (0.4 in) center-to-center, with a 4 mm (0.16 in.) diameter. GFRC is sprayed onto the top covered with a filter paper or fabric until the required thickness is reached and troweling gives a uniform finish. The box is connected to a vacuum pump and is separated by a filter system. Vacuuming commences and the time and degree of vacuum is fixed by experiment. Surplus water is tapped out of the system and the vacuum removed. Finally, the board is taken off by either suction lift or inversion of the box (Reference 13).

In the upward vacuum extraction process, GFRC is sprayed onto the mould or shallow profiled plate, and then a filter cloth or paper is placed onto the top of the wet

copy

the

the

ing

the

san-

Sen-

Equ-

(Re

composite. Following this the vacuum box is positioned over the top of the composite with the perforated plate against the filter material. Air is extracted and, provided an airtight seal is obtained around the perimeter of the mould and the vacuum box, the mould is sucked against the box. This sandwiches the GFRC which takes on the profile of the mould. Hence water is extracted by pressing and vacuum suction. Equipment for this type can produce detailed finishes (Reference 13).

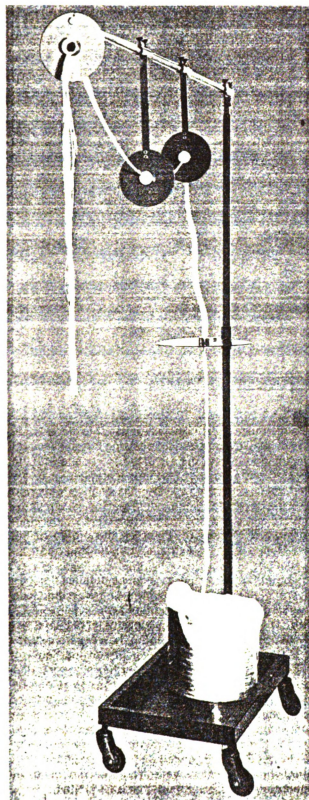


Figure 2.2.5 Production Roving Boom (Reference 12).

Automated Spray-Up Equipment:

This unit holds the spray head assembly and passes across the mould. There are two systems using this technique, continuous plant process and station plant process (Reference 13).

In the continuous plant process, the mortar pump and spray head is arranged, and the process initiated by the traverse unit, which conveys the spray head across the mould. GFRC is sprayed onto a primary conveyor, which is an open weave synthetic material capable of permitting water to pass through during the vacuum process. The primary conveyor receives the spray of GFRC and a continuous lay-up of uniform thickness is achieved by adjustment of its forward motion together with the cross traverse motion of the spray head. Setting these two rates of traverse is critical to ensure a uniform board thickness. The primary conveyor passes over the vacuum box where excess water is sucked downwards and out of the wet composite. This is performed by a liquid ring vacuum pump. After vacuum treatment, the wet board is cut and side trimmed. The cross cut is achieved by a flying shear type cross cutter which travels automatically with the board so as to produce a square cut. Two adjustable side trims cut the board to the required width. An automatic length selector initiates the moving carriage cross cutter to cut the board to the finished length. A secondary conveyor is driven by the

primary

ready

S

table

The sl

head

would

board

Final

and t

devel

palle

for c

2.2.

Cont

Shor

inti

prod

meth

proc

fi

toge

pre

Gene

tha

less

primary conveyor and serves to remove the finished board ready to be stacked for curing (Reference 13).

Station flat sheet plant involves four stages with a table transferring the composite from one stage to the next. The sheet is sprayed-up by continuous sweeps of the spray head mounted on a traverse unit which progresses along the mould table. As the table moves from station 1 to 2 the board is formed. Dewatering takes place at station 3. Finally, at station 4, the sheet is removed from the table and transported by vacuum lift or transfer machines developed for this purpose. The boards are then stacked on pallets which are built up 12 high and transferred as a unit for overnight curing (Reference 13).

2.2.1.3 Premixing Techniques

Contact Moulding:

This process follows normal precasting techniques. Short strands of glass fiber and cement paste or mortar are intimately mixed and then further processed to produce a product by casting in open moulds. A problem with this method is the damage done to glass fibers during the mixing process, causing the fracture and filamentization of glass fibers. Moreover, glass fibers tend to tangle and matt together if care is not taken in the mixing process; it is preferable to use adequate admixtures for good dispersion. Generally, fiber length in this process should be shorter than those used spray methods and fiber content is also less. The orientation of fibers tends to be three-

dimensi

limited

are de

repeats

method

boxes,

furnitu

suffic

and ma

than m

Press:

I

excess

proper

suppor

demon.

(0.8

press

exper

turnt

dawat

from

admix

fibre

proce

small

(Ref

dimensional random in the mixer but may be altered to a limited extent by the production process. The moulds used are dependent on the product to be made and the number of repeats required. Typical items manufactured using this method include litterbin, planters, buried cable junction boxes, gas and water services boxes, bar spacers and garden furniture. The normal external mould vibration systems are sufficient to produce flow and obtain the required density and material properties, although the mix is less mobile than most concretes (References 9, 11).

Pressing:

In premixed GFRC, the application of pressure to remove excess water will result in much improved mechanical properties and results in the material being self-supporting, allowing the components to be immediately demoulded. Flat sheets between 10 mm (0.4 in.) and 20 mm (0.8 in.) thick have been produced by this process at pressures between 0.15 MN/m^2 and 10 MN/m^2 , and have been used experimentally to produce items as complex as stereo turntable base plates and speaker housings. Vacuum-assisted dewatering process using paper-felt filters may be conducted from either one or both mould faces but a water thickening admixture is required to prevent water expulsion before the fibrous mix has had time to uniformly fill the mould. The process is ideal for the production of large numbers of small components since immediate demoulding is possible (References 9, 11).

From

produ

nix

of the

used

sand

room

chop

The

mean

and

nix

thr

lif

pro

fol

use

loc

be

al

9,

2.

(n

re

Extrusion:

Extruded sections with complex shapes have been produced commercially but careful attention is required in mix design to prevent bleeding through the mix or blocking of the die, and carefully controlled vibration should be used to obtain a GFRC formulation that can be extruded. The sand/cement slurry is premixed to a water/cement ratio normally below 0.30, the fiber is added directly from a chopper unit and blending is carried out in the mixer unit. The mixed material is then deposited in a hopper and by means of internal vibration, at a predetermined frequency and amplitude, fluidizing effects are created causing the mix to flow into the receiving mould which is propelled through the machine. The moulds are then handled by vacuum lifting and taken for curing. This method of production produces GFRC with approximately 60% fiber orientation that follows the material flow, a feature which is particularly useful when considering long thin products requiring longitudinal strength. Examples of the type of product being considered include replacement of timber, steel or aluminum sections, window frames and guttering (References 9, 11).

2.2.1.4 Moulding Techniques (Reference 14)

Materials suitable for the mould are steel, wood (natural timber and manufactured board), glass fiber reinforced plastics, concrete and GFRC, and all materials

need consideration as suitable for the adopted manufacturing conditions. The design of GFRC moulds should take the following points into consideration:

1. All moulds must be robust enough to take the day-to-day wear common in production. Naturally, the number of castings made from the mould would, to some extent, dictate the material choice for the mould. Deflection in the mould due to the cast-in GFRC and to the mould weight itself must be considered.
2. Ideally, all corners should be to a radius of 10 mm (0.4 in.) or have fillets of 45° . Draw angles of 5° are the optimum.
3. Cast-jacking points help demoulding and increase the mould life. In-built air connections are also significant in this respect.
4. The spray gun must be able to gain access to all parts of the mould. Hand placing into inaccessible mould features is a poor design feature and will produce a weak, porous composite, instead of the required durable, well-compacted, high quality GFRC needed for service conditions. Figure 2.2.6 indicates the relationship of width to depth in a mould high lighting the access potential. If intersection falls on a hatched area then spray access is possible. The dark zone indicates marginal accessibility.
5. Spray production gives only one mould face unless bonded panels are produced. Non-moulded faces will

have a textured or trowelled finish that is only as good as the operator's skill. Overworking exposes fibers at the surface.

6. Surface ribs and channels should be wide enough to allow roller access for adequate compaction. Fine details will require extra compaction with a stiff brush prior to roller compaction. In this case the arris will be void of fibers and highly likely to be spoilt on demoulding and handling due to spalling.
7. Small details in the mould will take the worst battering. If made from timber they may need frequent replacement. Stainless steel or plastics are more suitable.

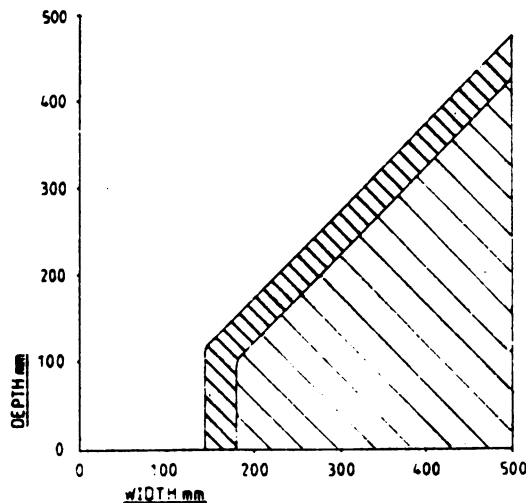


Figure 2.2.6 Relationship of Mould Width to Depth Where Access for Spraying Could be Difficult (Reference 14).

wide.

A. E.

Flat

1.

2.

3.

4.

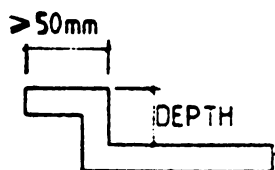
Fi
E

The following moulding techniques for each section are widely used in GFRP industry:

A. EDGES

Flat Products (Figure 2.2.7):

1. Return edge is attached to the mould with depth equal to the design thickness and of width at least 50 mm (1.97 in.).
2. The GFRP is sprayed into the mould, tucking the material into the corner with special purpose tool. Final layer not sprayed yet (Figure 2.2.7 b).
3. Overspray folded over, back onto panel surface (Figure 2.2.7 c).
4. Final layer is sprayed, rolled and trowelled to achieve design thickness (Figure 2.2.7 d).



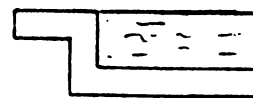
(a)



(b)



(c)



(d)

Figure 2.2.7 Moulding Technique for Flat Products (Reference 14).

Rbb

1.

2.

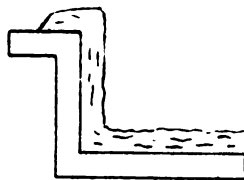
3.

4.

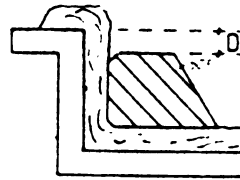
1
2

Ribbed Edge (Figure 2.2.8)

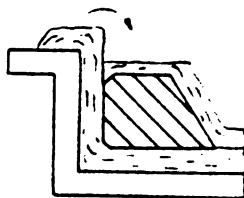
1. Spray in layers, roller compact and check to ensure correct thickness on side-wall and base (Figure 2.2.8 a).
2. Place the precut foam former in the mould and check with gauge to ensure that the former is D mm below mould top (Figure 2.2.8 b).
3. Spray over the former to meet last spray. Turn over overspray from mould edge and roller compact (Figure 2.2.8 c).
4. Spray to correct thickness. Pay attention to thickness at a and b and ensure that the overlap at b is sufficient (Figure 2.2.8 d).



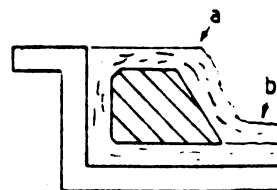
(a)



(b)



(c)



(d)

Figure 2.2.8 Moulding Technique for Ribbed Edge (Reference 14).

Rising Shutter Edge (Figure 2.2.9)

- 1 .** Spray base of shutter as normal. Then lay foam core as described for ribbed edge method above (Figure 2.2.9 a).
- 2 .** Locate rising shutter and spray up vertical face and over mould edge (Figure 2.2.9 b).
- 3 .** Fold back overspray; place rib foam core in place. Spray over core and spray up to the design thickness. Roller compact and trowel to complete panel in normal way (Figure 2.2.9 c).

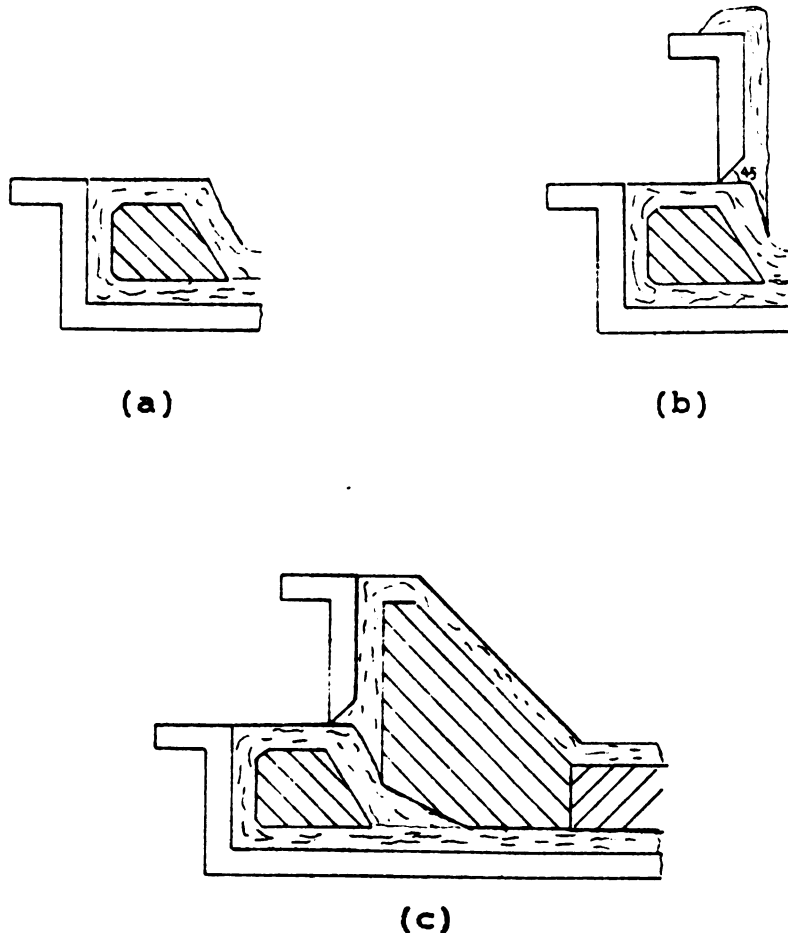


Figure 2.2.9 Moulding Technique for Rising Shutter Edge (Reference 14).

5.

1.

1.

2.

3.

B. CORNERS

Internal Corners (Figure 2.2.10)

1. When using a compaction roller care must be taken not to disturb the side wall material as shown in Figure 2.2.10 (a). If a disturbance occurs, it is not good practice to replace with a trowel. It is better to respray the disturbed area.
2. This method of using a float or trowel to finish internal edge (Figure 2.2.10 b) is not a good practice. The tendency is cut into the composite and give a thin section right in the corner. Special rollers can be produced to compact the corners.
3. Alternatively, a special angle tool (Figure 2.2.10 c) can be manufactured to compact the corner material.

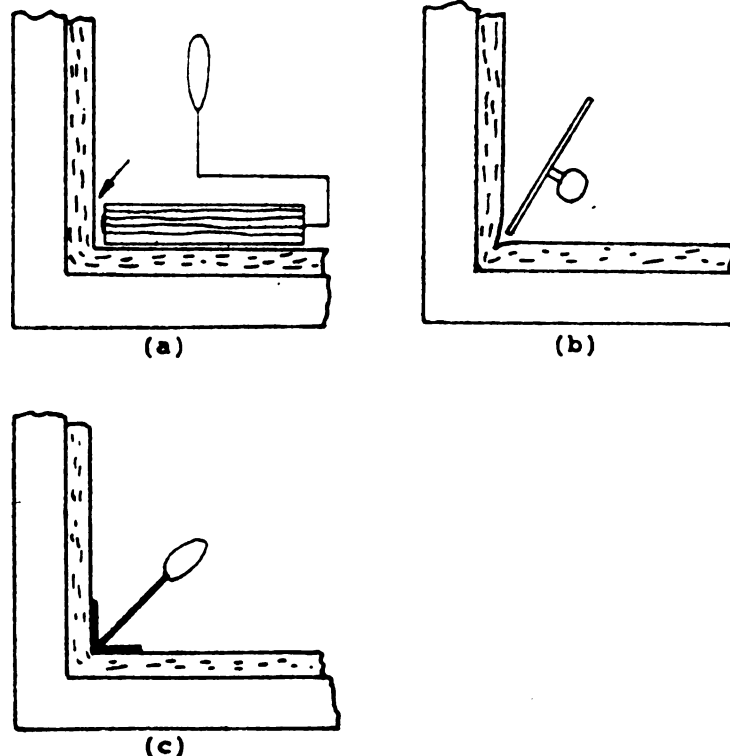


Figure 2.2.10 Moulding Technique for Internal Corners (Reference 14).

Extern

1.

2.

Fig
(16)

External Corners (Figure 2.2.11)

1. If support is not given to the edge of the GFRC, the material will spread and squeeze away from the mould (Figure 2.2.11 a), leaving a pocket or void down the edge. Thinning will also occur.
2. The above situation can be avoided by supporting the side of the sprayed material with a trowel, while roller compacting or trowelling the top edge (Figure 2.2.11 b).

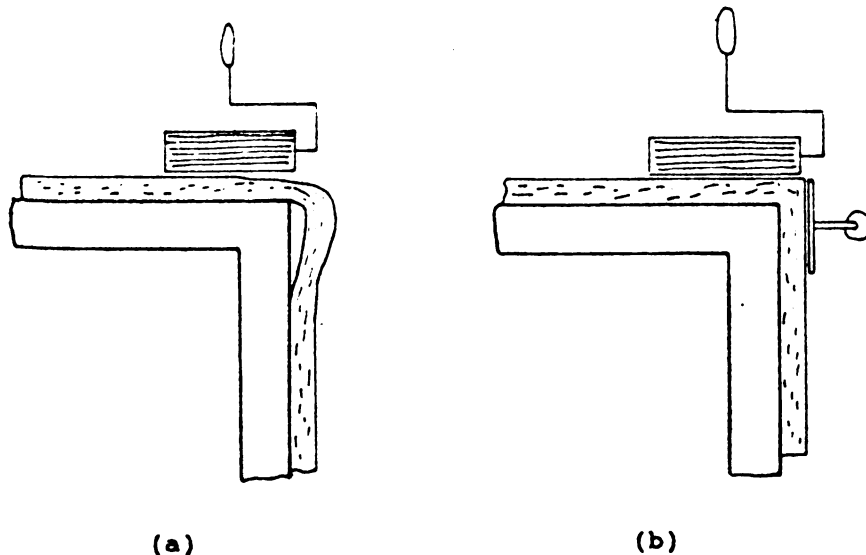


Figure 2.2.11 Moulding Technique for External Corners (Reference 14).

C. S.

Organ:

1.

2.

3.

4.

Fl
Or

C. SANDWICH PANELS

Organic Foam Core (Figure 2.2.12)

1. Spray and compact mould face and sides as normal, checking thickness (Figure 2.2.12 a).
2. Precut foam blocks fitting loosely together are coated with mortar and binding agent, and are placed in the mould with chamfered blocks at the edges (Figure 2.2.12 b); care is required not to disturb the vertical GFRC edges.
3. Check top surface of the foam core to be at correct height (Figure 2.2.12 c); spray 3 mm (0.1 in) layer of GFRC, then fold over the overspray from edge, and roller compact.
4. Complete spraying the top surface of foam and roller compact. Finish with trowel and straight edge to check level (Figure 2.2.12 d).

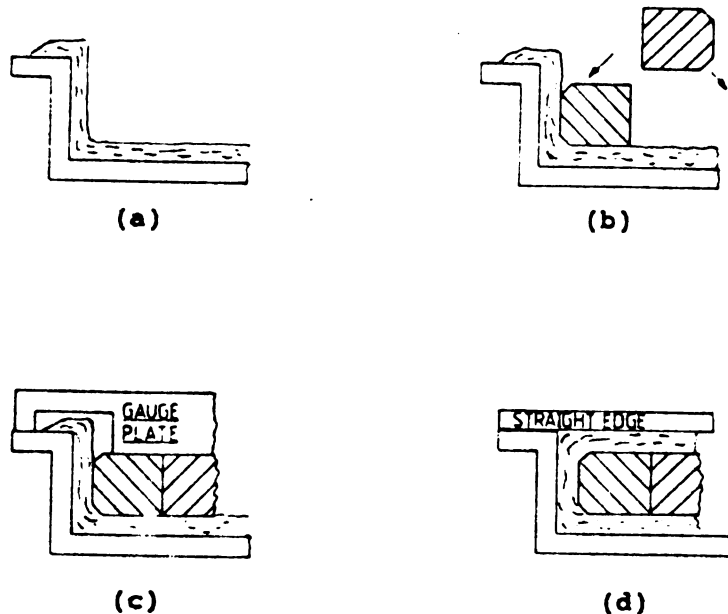


Figure 2.2.12 Moulding Technique for Sandwich Panel with Organic Foam Core (Reference 14).

Styrofoam Concrete Core (Figure 2.2.13)

1. Spray and compact mould face and sides as normal, checking thicknesses (Figure 2.2.13 a).
2. Fill moulds with styrofoam concrete mix. Tamp to remove air pockets. Use gauge plate to check depth (Figure 2.2.13 b). Spray 3 mm (0.1 in.) layer of GFRC and fold over overspray from the mould edge and roller compact.
3. Spray over with GFRC in layers, and roller compact to achieve the required thickness (Figure 2.2.13 c).
4. Ensure that a grid of 6 mm (0.24 in.) air holes is present in the back face (Figure 2.2.13 d) since the entrained air in the styropor concrete will expand and bow the back if pressure is allowed to build up.

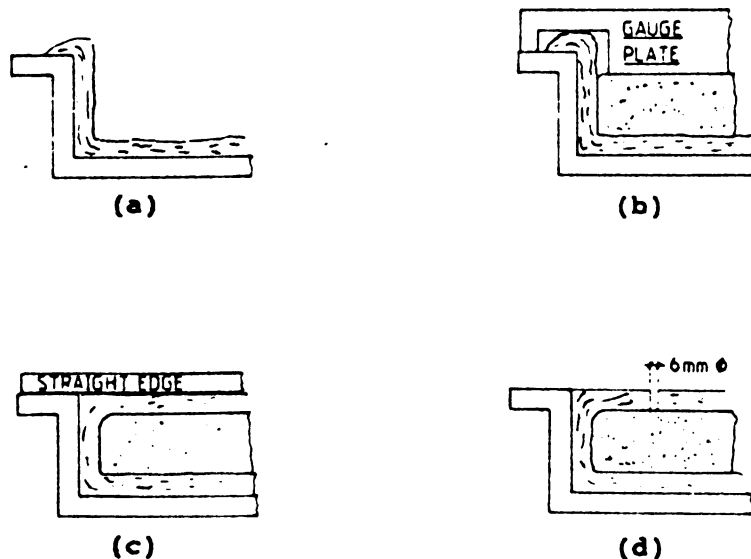


Figure 2.2.13 Moulding Technique for Sandwich Panel with Styrofoam Concrete Core (Reference 14).

2.2.2 Mix Design Procedures

Mix design of GFRG depends upon strength requirements, the amount of details, the form surface, density, fire rating, and other physical properties. There are many different ingredients which could theoretically be incorporated into the mix in order to alter the material properties, enabling it to perform satisfactorily in a given environment. This section describes the constituents of GFRG mixes, and then reviews the mix proportions required for specific uses (References 11, 15).

2.2.2.1 Constituents of GFRG Matrices

Cement:

The Portland cement for GFRG must meet the requirements of ASTM C-150: "Specification for Portland Cement." Type I Portland cement is recommended and commonly used. Type III may be suitable when variations in the sprayability of the cement slurry and those properties of the composite affected by cement fineness are accommodated. However, as with all concrete, some applications may require special types of cement (References 11, 15).

Alternative cements to ordinary Portland cement, sulfate resisting cement, high alumina cement, high early strength cement, and white Portland cement, could also be utilized. Situations that would require sulfate resisting cement may not warrant this choice with GFRG mix proportioning, but it may be prudent to include fly-ash in the matrix instead of sand. If circumstances necessitate

h

g

r

p

c

C

w

R

R

w

t

a

R

S

f

v

s

c

high alumina cement in the mix, then consideration should be given to the possibility of using 'E' glass as reinforcement. When rapid demoulding is required in production, regulated set cement may be considered. This cement can produce a set 5 minutes after mixing. Consequently, purpose-built mixing and dispensing equipment would be required. This rapid setting gives a strength that may allow demoulding in just 15 minutes after mixing the matrix. If white composites are required, then naturally white Portland cement has to be used, but it may be possible to apply white cement only for the mist coat (with a polymer admixture), and back this up with rapid hardening cement mortar for the bulk of the composite (References 11, 15).

Sand:

The use of sand in the GFRC mix reduces drying shrinkage and the possibility of subsequent cracking. Sand when incorporated into the GFRC mix will reduce drying shrinkages to the levels shown in Figure 2.2.14, where sand content is given in terms of sand/cement ratio by weight. At sand/cement ratios in excess of about 1.5:1, the porosity in the cement binder phase may become excessive, due to an air-entrainment effect, leading to reductions in the strength of the cured GFRC. Therefore, with higher sand content mixes (say with a sand/cement ratio of 1:1 and over), care must be taken in manufacturing technique and in the choice of stresses to be used in component design. Washed and dried silica sand, or sands free of contaminants

and

144

reco

can

qual

glas

mod.

Fi

Sh

11

and lumps meeting the compositional requirements of ASTM C-144 "Specification for Aggregate for Masonry Mortar," are recommended. Dry sand is preferred since an accurate check can be kept on water incorporated into the mix. Good-quality silica sands, of the types used in foundry work and glass-making, with stiff particles having a high Young's modulus, and in suitable grain sizes and shapes are readily

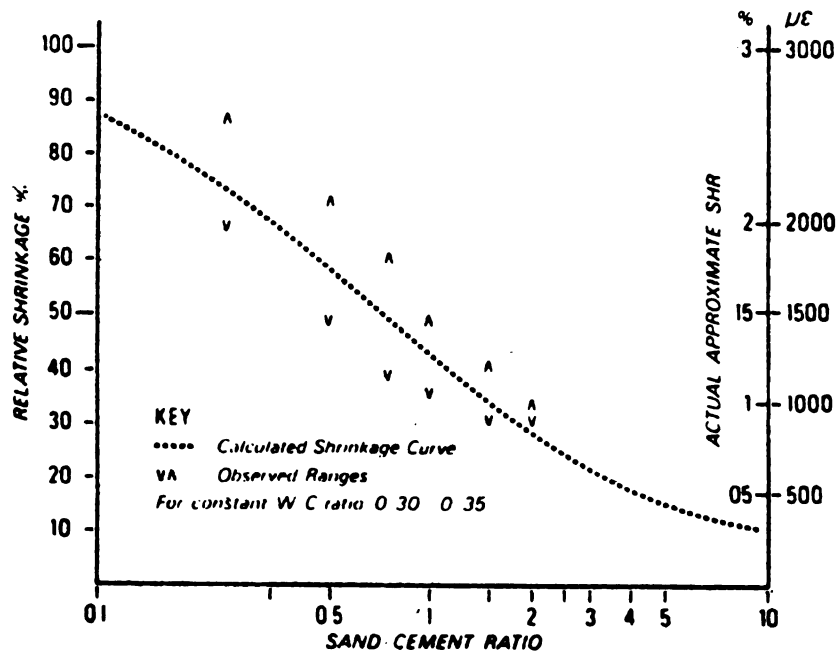


Figure 2.2.14 The Effect of Sand Content on the Drying Shrinkage of GFRc, Measured at 50 C and 20% RH (Reference 11).

27

61

wo

ge

de

62

02

72

—

—

—

—

—

—

—

—

—

—

—

—

—

—

—

—

—

—

—

available. Table 2.2.1 details a viable specification of silica sand. The sand must be free of large particles which would block the spray nozzle. Also, clay lumps and silt in general are undesirable as they can increase the water demand. For these reasons, washed, graded and dried silica sand which is free from soluble salts, clay particles and organic matter is strongly recommended (References 11, 15).

Table 2.2.1 Specification for Silica Sand (Reference 11).

Chemical Composition	Silica	96-98%
	Moisture	2% _{max}
	Soluble Salts (Sulfates, Chlorides and Alkalies)	1% _{max}
	Loss on Ignition	0.5% _{max}
Physical Composition	Maximum particle size	100% passing a No. 16 (1.18 mm) sieve
	Fine fraction	< 2% passing a No. 100 (150 μ m) sieve
	Grain shape	rounded/subrounded

We:

se:

con

the

the

dis

of

ma

th

wa

co

an

in

Pe

wh

ad

es

Ma

Pe

hy

hy

w.

l.

z.

Water:

Impurities in water can adversely interfere with the setting of the cement, may reduce the strength of the cured composite and may also lead to poor long-term performance of the hardened cement binder phase. To sum up the situation the mixing water should be fit for drinking and contain dissolved solids less than 2000 ppm. However, while the use of drinking water is always safe for concrete and GFRC manufacture, non-potable water may often be satisfactory for the purpose. The rules to apply in this case are that the water should not taste salty or brackish and the best way to confirm that it is satisfactory is to carry out setting-time and strength tests on GFRC specimens made with it to the intended formulation (References 11, 15).

Pozzolanic Admixture:

A pozzolan is a finely divided form of reactive silica which reacts with calcium hydroxide in cement paste to form additional calcium silicate hydrate which has desirable effects on the density and microstructure of concrete materials, especially at interfaces between cementitious paste and mix inclusions where the concentration of calcium hydroxide is generally high. Moreover, reduction of calcium hydroxide results in reduced alkalinity of concrete pore water, controlling the damage of glass fibers (Reference 16).

Pozzolanic admixtures commonly used in cementitious materials include fly ash, silica fume, blast furnace slag,

and

con.

or

in

ble.

ncs

poz

poz

rec

and

A.

th

Va

18

ma

re

fl

an

de

co

w.

re

co

t.

d.

s

and natural pozzolans. Fly ash and natural pozzolans should conform to ASTM C-618: "Specification for Fly Ash and Raw or Calcined Natural Pozzolan for Use as a Mineral Admixture in Portland Cement Concrete." Portland cements can also be blended with pozzolans as specified in ASTM C-595, and the most important blends are designated Type IP (15% to 40% pozzolan) and Type I-PM (0 to 15% pozzolans). Two pozzolanic materials which have been established in the recent years as commonly used mineral admixtures are fly ash and silica fume (Reference 15, 17).

A. FLY ASH

Fly ash is the finely divided residue resulting from the combustion of ground or powdered coal (Reference 16). Various authors, including Singh, et. al. (1984), Reference 18, have suggested that the chemical nature of the cement matrix in GFRC can be improved (i.e., its alkalinity can be reduced) by adding fly ash. The round shape and fineness of fly ash particles also improve the flowability of the mix and fiber dispersibility when the pre-mix manufacturing method. Lee (1983), Reference 11, suggests that in combination with an air-entraining agent, the GFRC modified with fly ash provides a material with improved fire resistance. The fly ash and air entraining agent combination helps to produce connected porosity channels through which the rapidly evolving steam can escape without disruption the material by explosive spalling of its surfaces, and it also reduces the water of hydration to be

dr
in
a.
in
a.
E
re
fr
S
h
f
i
a
e
t
t
p
f
f
G
t
M
c
C
P
C

driven off in a fire. All other advantages of using fly ash in plain concrete (e.g., reduced permeability, reduced alkali-aggregate reactivity, improved sulfate resistance, increased long-term strength, and economic advantages) would also apply to GFRC (Reference 16, 17).

B. SILICA FUME

Silica fume is a by-product resulting from the reduction of high-purity quartz with coal in electric arc furnaces in the production of silicon and silicon alloys. Silica fume is distinguished from fly ash by its fineness, high pozzolanic reactivity and high silica content. The fineness and high pozzolanic reactivity of silica fume make it highly effective in enhancing the structural density and adhesion capacity in the bulk of the cement paste and especially within the interface zones between the paste and the mix inclusions (e.g., fibers), Reference 16. According to Bentur (1989), Reference 19, silica fume has great potentials in the improving of the durability of GFRC. The filling of spaces between and around the filaments of glass fibers by CH is one of the main reasons for embrittlement of GFRC. The 0.1 μm silica fume particles can penetrate into the space between filaments which are usually less than 3 μm wide, thereby preventing the growth of massive CH crystals between the filaments of glass fiber strands. Other advantages associated with the use of silica fume in plain concrete (reduced permeability, potentials for developing very high strength, improved chemical resistance,

etc.) would also apply to GFRC. It should be noted that silica fume tends to make the mix rather sticky and damages the workability of fresh mix; this phenomenon should be accounted for in the pre-mix method of manufacturing GFRC, and even in spray-up method where silica fume makes the fresh slurry less fluid and affects the output of the slurry (References 16, 17).

Chemical Admixture:

Standard commercially available chemical admixtures such as air-entraining agents, water reducers, high range water reducers, accelerators, and retardes may be used to impart specific properties to GFRC. These admixtures should conform to the requirements of ASTM C-494: "Specification for Chemical Admixtures for Concrete," or ASTM C-260: "Specification for Air-Entraining Admixtures for Concrete."

A. AIR-ENTRAINING AGENTS

The air-entraining agents formulated for use in concrete and mortars can be either natural substances such as wood resins, animal fatty acids and lignosulphonates, or synthetic compounds like alkylaryl sulphonates, alkyl sulphates and alkyl naphthalene sulphonates. The purpose of including an air-entraining agent into a GFRC formulation is to produce discrete uniform bubbles of 0.05-1.5 mm (0.002-0.059 in.) diameter at about 0.1 mm (0.004 in.) spacing, and to stabilize this system. The bubbles are introduced by the mixing action and become entrained by the admixture's

surfactant, anionic action (References 10, 11, 17).

The normal consequence of air entrainment include improved freeze-thaw resistance, improved workability and cohesiveness of fresh mix, and a reduction in strength. However, air-entrainment may not affect the strength of lean concrete or mortar mixes (cement contents below 300 kg/m³ or 500 lb/yd³), since the lower strengths at air contents needed for good frost protection may be entirely offset by the corresponding decrease in water/cement ratio (noting that air entrainment tends to reduce water requirements for workability), References 11, 19.

B. WATER-REDUCING AGENTS

A water-reducing agent lowers the water required to attain a given fluidity. The fluidity and sprayability of GFRM mixes tend to decrease as the sand content is increased or as the water/cement ratio is lowered. Achieving the desired fluidity with less water at a constant cement content leads to general improvements in strength, impermeability, and durability of GFRM. Water-reducing agents can be divided into two categories based on the general composition of their active ingredients. The first category includes the salts and derivatives of lignosulfonates; the other category consists of salts and derivatives of hydroxycarboxylic acids. The common feature of both categories is that these compounds are absorbed primarily at the solid-water interface, and the action experienced is one of a deflocculating effect, breaking the

matrix components into the basic particles which are uniformly dispersed. This deflocculating action is believed to be the basis of water reduction (Reference 17).

Although water-reducing agent improves the workability of the fresh mix, they may not necessarily improve its cohesiveness, and may act as a retarder which prolongs the setting time of the fresh mix. Some water reducers also tend to accelerate the loss of fluidity (slump loss) with time, limiting the time available for the handling of fresh mix (References 11, 17).

C. HIGH-RANGE WATER-REDUCING AGENTS

High-Range Water-Reducers can drastically improve the workability of mortar or concrete mixes. High-range water-reducing agent is an ASTM terminology, and perhaps the name "superplasticizer" is more familiar to concrete engineers (Reference 15). A high-range water-reducing agent can achieve water reductions of the order of 15 to 30%. The composition of this admixture consists of linear polymers containing sulfonic acid groups attached to the polymer backbone at regular intervals. Two major polymer types are naphthalene sulphonate formaldehyde condensates and sulphonated melamine formaldehyde condensate. The action of both is similar, and better performance is achieved by adding the admixture after preliminary mixing. The sulphonic acid groups are responsible for neutralizing the surface charges on the cement particles and causing dispersion (References 10, 11, 17).

If added at amounts comparable to conventional water-reducing agents, water reductions are similar (5 to 10%); however, the effectiveness of these materials is that the undesirable side effects (air entrainment and set retardation) are absent or at least very much reduced. Thus, they can be used at high rates of addition, typically in amounts exceeding 1% of active ingredient by weight of cement, whereas conventional water-reducing agents can not be used in such large quantities. High-range water-reducing agents enjoy the advantages of low water requirement, but (depending on the specific type of admixture) the improved workability may only last for some 30 to 40 minutes (References 10, 17).

D. SET ACCELERATING AGENTS

Set accelerators can enable certain products to be demoulded quickly, thus increasing the efficiency in precast manufacturing process. Set accelerators can be divided into three groups: soluble inorganic salts, soluble organic compounds, and miscellaneous solid materials (Reference 10). The most predictable accelerator (as far as both the setting time and hardening rate are concerned) is calcium chloride, and it has been used successfully in GFRP, where (unlike reinforced concrete) there is no possibility of it promoting corrosive attack on the reinforcing medium, glass fiber (Reference 11).

Conventional accelerators can be expected to increase

1-day strength, the increase being dependent on the type and dosage of the admixture. An optimum dose of calcium chloride (2% by weight of cement) will approximately double the 1-day compressive strength of mortar or concrete. These increases diminish with time and later strengths (at 28 days or more) may actually be lower than the strength of mortars or concretes without an accelerating agent. Trials are always necessary before production runs can be confidently undertaken (References 10, 17).

E. SET RETARDING AGENTS

When a complicated product is being produced that may require the inclusion of a light weight filling material for insulation and so forth, together with fixing and other accessories, it may be beneficial to add a set retarding agent to the formulation. This ensures that the first layers of GFRG placed into the mould have not passed the initial setting phase prior to being turned over at the edge and trowelled into the final packing coat. In hot climates such as Middle East where ambient temperatures may be so high that they significantly shorten the available working time of the slurry, the use of a set retarding agent is more common than adding water to the mix for prolonging the working time. Any excess water will lead to reduced strength in the cured GFRG (References 10, 11).

Set retarders can be divided into several categories, based on their chemical composition: (1) lignosulfonic acids and their salts, (2) hydroxycarboxylic acids and their

salts, (3) sugars and their derivatives, and (4) inorganic salts. Categories 1 and 2 also possess water reducing properties, and they can be classified under both groups.

Lignosulfonate-based admixtures are prepared from pulp and paper industrial wastes, and studies have indicated that most of the retarding properties of these agents may be due to compounds that belong to categories 2 and 3. Some inorganic salts (e.g., borates, phosphates, and zinc and lead salts) can act as retarders, but are not used commercially (Reference 17).

Polymeric Admixtures:

Polymers, either as emulsions or impregnants are beginning to find wider use in concretes where they impart some interesting effects. It is possible to increase the flexural strength of concrete by the inclusion of polymethymethacrylate; although it tends to embrittle the concrete to some extent, this polymer admixture improves the resistance to chloride and sulphate attack and freeze-thaw damage (Reference 20).

According to Lee (1983), Reference 11, acrylic copolymers in mortar can significantly improve the tensile strengths, but in GFRC the effects may not be so marked at economical addition rates, say 10% of the total mix. However, using cement composites contains E-glass fibers instead of alkali-resistant glass fibers and a thermoplastic polymer in the form of water-dispersed particles (latex),

Bi

fi

th

ce

at

th

2.

(a

ni

Gl

Ce

F:

We

Ac

(h

re

2:

G:

Ce

P:

Bijen (1983), Reference 21, concluded that the glass fiber filaments are surrounded by the polymer particles and are thus screened off and protected against the migration of cement hydration products, as well as possible chemical attack, and thus long-term durability has been improved by the addition of this type of polymer.

2.2.2.2 Mix Proportioning Examples:

The following are basic mixes for general use in GFRC:

(a) For spraying without dewatering the most commonly used mix consists are (Reference 11):

Glass Fiber	5% AR glass fibers, 34-38 mm (1.34-1.50 in.) long;
Cement	Type I or Type III Portland cement;
Fine Aggregate	Fine silica sand with sand/cement ratio in the range 0.3:1.0 to 0.5:1.0;
Water	Water/cement ratio in the range 0.28:1.0 to 0.33:1.0;
Admixtures	Generally not necessary, unless required by a particular application.

(b) For GFRC panels with spraying method (PCI recommendation), the mix would lie in the range (Reference 22):

Glass Fiber	5% by weight of total mix, using 38 mm (1.5 in.) to 51 mm (2 in.) fiber lengths;
Cement	Type I or Type III Portland cement
Fine Aggregate	Sand/cement ratios of 1:3 to 1:1;

Water	Water/cement ratio about 0.3:1.0;
Admixtures	5% by volume of the total mix of an acrylic thermoplastic copolymer dispersion to provide a blend of acceptable composition properties and processibility.

(c) For spray-suction method the most commonly used mix is (Reference 11):

Glass Fiber	5% AR glass fibers, 34-38 mm (1.34-1.50 in.) long;
Cement	Type I or Type III Portland cement;
Fine Aggregate	Sand/cement ratio in the range 0.3:1.0 to 0.5:1.0;
Water	The water/cement ratio would be generally about 0.5-0.55 initially, being reduced to 0.25-0.30 after dewatering;
Admixtures	May be used for specified properties.

(d) For premixing method, there is a wider range of mixes as this process is used for a wide range of products, generally with a lower strength requirement. A suitable mix would be:

Glass Fiber	3.5-5% AR glass fibers, 12-25 mm (0.5-1.0 in.) long;
Cement	Usually Type I or Type III Portland cement, although special cements are used for particular processes;

P

W

A

(

u

G

C

W

A

(

t

G

C

W

A

Fine Aggregate Fine silica sand with sand/cement ratio in range 0.3:1.0 to 0.5:1.0;

Water Water/cement ratio in range 0.28-0.33;

Admixtures Water-reducing agents or high-range water-reducing agents are commonly used to keep water/cement ratio to minimum.

(e) For the pressing process of premix method the commonly used mix consists of (Reference 23):

Glass Fiber 2.5-5% AR glass fibers;

Cement Ordinary Portland cement;

Water Water/dry solids ratio >0.3;

Admixtures Fly ash may be blended to cement with fly ash/cement ratio 1:1, and water-reducers or high-range water-reducers are also used;

(f) For the extrusion process of premix (Ram extrusion through a die, Reference 23):

Glass Fiber 2.5% AR glass fibers, with 22 mm (7/8 in.);

Cement Ordinary Portland cement;

Water To give water/dry solids ratio 0.4:1.0;

Admixtures Blended fly ash with fly ash/cement ratio 1:1, and water-reducers or high-range water-reducers are used.

(9

11

GI

Ce

Wa

Ad

2.

cc

(1

1

2

(

1

(g) For fire-resistant mix with spraying method (Reference 11):

Glass Fiber	5% AR glass fibers, 34-38 mm (1.34-1.50 in.) long;
Cement	Type I or Type III Portland cement;
Water	To give water/cement ratio 0.47:1.0;
Admixtures	Blended fly ash with fly ash/cement ratio 0.67:1.0, and an air-entraining agent must be used.

2.2.2.3 Mixing Procedures:

General procedures of loading and mixing of constituents in GFRC production are discussed below.

(a) General mixing procedure for spraying method (Reference 23):

1. Charge the mixer (a high-shear mixer) with the gauging water and any liquid admixture specified.
2. Progressively add the sand and cement. Alternatively add the sand first and then the cement, while mixing (any powder admixture that is specified should be blended with a portion of the sand inclusion).

(b) General mixing procedure for premixing method (Reference 23):

1. Mix the matrix component first in a high shear mixer as described above. This will produce a well-dispersed mortar that assists fiber dispersion.

2.

2.

th

ho

th

us

ac

a.

cu

re

l.

f

T

2. Transfer the blended matrix material to a rotating pan mixer and gradually add the glass fibers. Just sufficient mixing time is used to disperse the fibers and to prevent fiber balling or built up around the paddle blades.

2.2.3 Curing:

In normal curing processes using standard GFRC mixes the component will usually remain in the mould for 12-24 hours. It is essential that moisture is retained during this period by covering the product with polythene sheet or using similar protection to avoid drying and to achieve adequate strength for demoulding. The temperature should also be maintained around 18-25°C (64-77°F), and accelerated curing systems with temperatures over 50°C (122°F) are not recommended and may be detrimental to strength (References 11, 23).

After initial overnight curing, the product is removed from the form and placed in a controlled curing environment. This environment may be provided by:

- (a) A humidity chamber room or fog room;
- (b) Thorough wetting then sealing in polythene;
- (c) Total immersion in water; or
- (d) The use of curing membranes to prevent surface evaporation.

SC

Ca

af

el

o.

h.

s

d

P

(

w

t

m

P

d

c

c

i

i

P

(

Controlled curing is important because the cure schedule not only affects strength gain, but improper curing can cause warpage due to variations in moisture content, and affect surface appearance (porosity, staining, efflorescence).

A typical GFRC mix is cement-rich and it must receive or retain sufficient moisture to accomplish cement hydration. GFRC products are usually thin and are susceptible to rapid drying. Incomplete strength development (low physical properties) will occur when products are cured in normal atmospheric conditions (References 11, 22).

At normal ambient temperatures ($18-25^{\circ}\text{C}$, $64-77^{\circ}\text{F}$), and when using ordinary Portland cement, a period of 10 days of total immersion or 28 days at high humidity is required for maximum strength levels to be reached. With Type III Portland cement these times may be reduced to 8 days and 14 days respectively. Lower temperatures will require considerably longer moist-curing periods. When GFRC is cured at $20^{\circ}\text{C}/100\%$ RH, which can be achieved through curing in a fog-room or by covering with polythene sheeting immediately after spraying, the strength development profiles shown in Figure 2.2.15 would be expected (References 11, 24).

high

item

of r

Howe

can

GPAC

24).

It is possible to reduce the curing period by using higher temperatures and this may be useful for mass produced items or where production rates are critical. The validity of reduced curing time can be seen in Figure 2.2.16. However, it should be noted that curing at high temperatures can have an undesirable effect on the ultimate strength of GFRC and this must be taken into account (References 11, 24).

SE
STRENGTH AS % OF 28 DAY FCM ROOM VALUE
100
90
80
70
60
50
40
30
20
10
0

Fig
at

STRENGTH AS % OF 28 DAY FCM ROOM VALUE
100
90
80
70
60
50
40
30
20
10
0

21
22
23
24

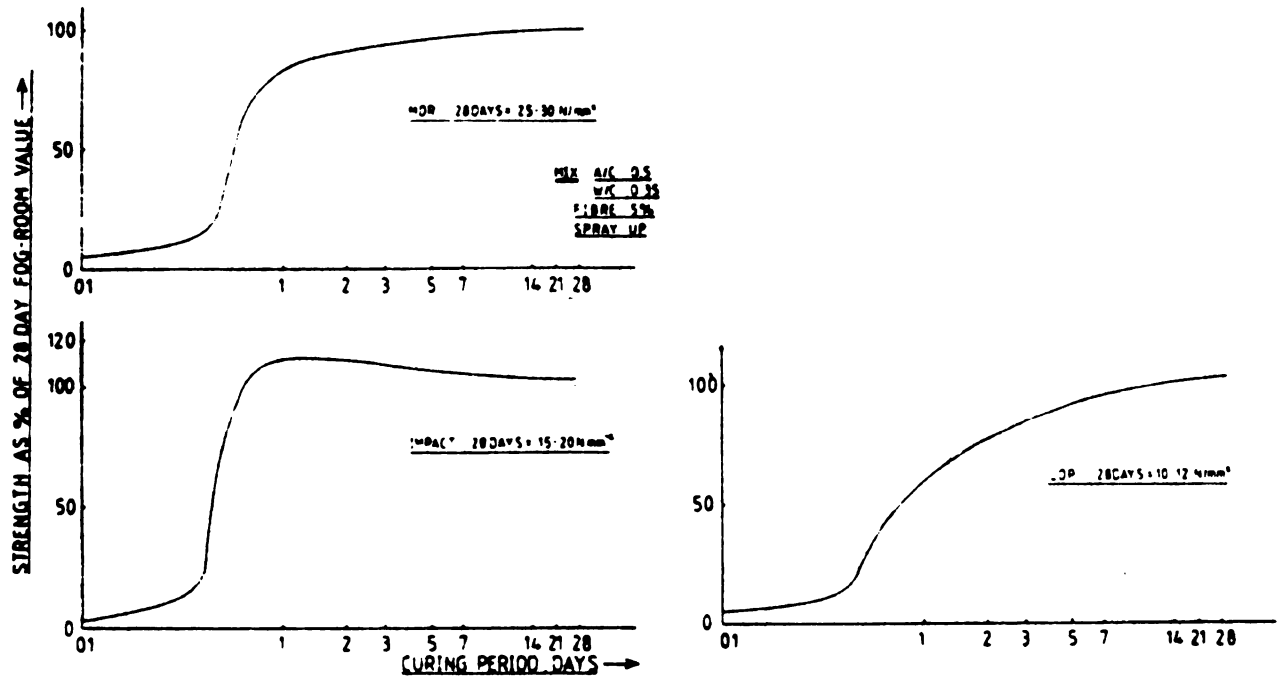


Figure 2.2.15 Strength Development Profiles for GFRC Cured at 20°C/100% RH (Reference 24).

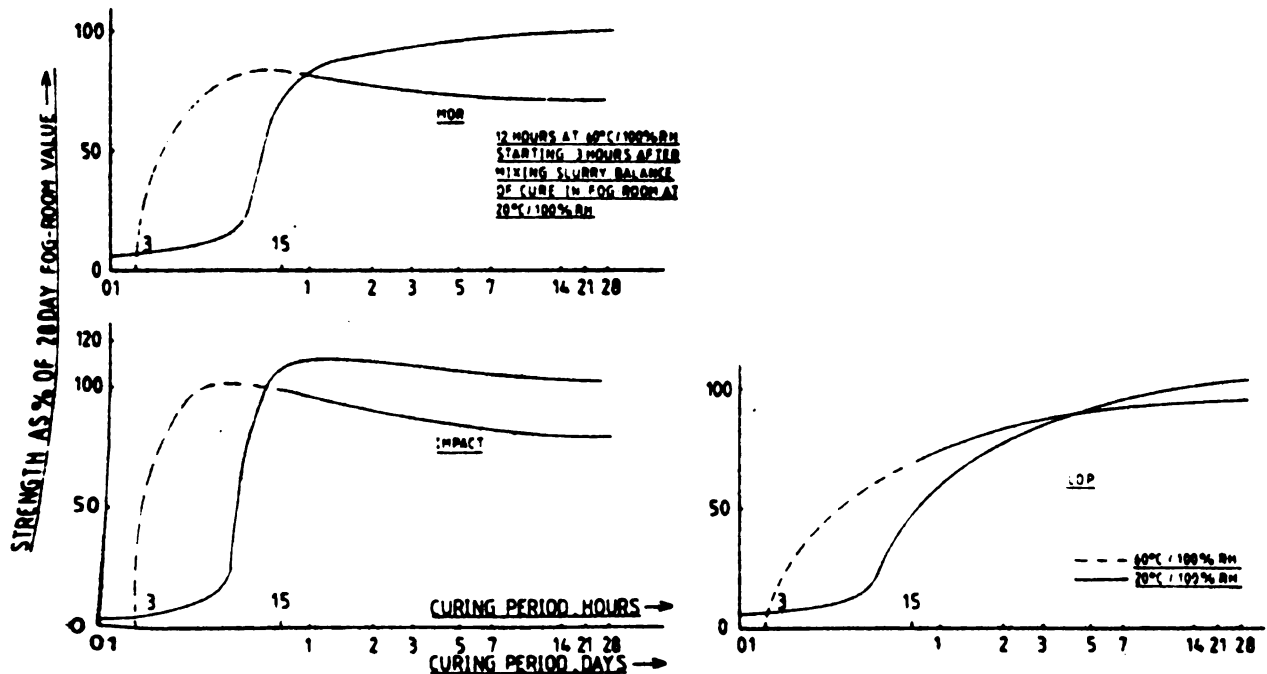


Figure 2.2.16 Strength Development Profiles of Heat-Treated GFRC Compared with the Material Cured at 20°C/100% RH (Reference 24).

2.2.

aes

sho

sho

nec

2.2.

can

app

acc

use

no

ca

pr

1.

2.

3.

4.

pe

2.2.4 Finishing Techniques:

A combination of the practical considerations and aesthetic factors influence the decision on how a product should be finished. Since many finishes have led both short- and long-term problems, considerable thought is necessary (Reference 25).

2.2.4.1 Textured Mould Finishes:

The finest satin grains to deep irregular indentations can be achieved with textured finishes from the mould. The application of a fine 'mist' coat without fibers is acceptable for internal finishes; in the case of external use, however, this practice may lead to surface crazing if not carefully controlled. For example, smooth GRP moulds can cause these crazing problems. Therefore, certain precautions are advisable when using smooth-faced moulds:

1. Minimum thickness of mist coats should be employed possibly including a polymer latex such as an acrylic in the formulation. This provides a 'flexible' surface which is tolerant to a degree of shrinkage stress.
2. The mould should, if possible, be roughened.
3. The demoulding surface should be sealed with a proprietary sealer.
4. It may be necessary to reduce the length of the chopped fiber immediately behind the mist coat.

With these precautions in mind, many textures are possible, as would be customary with precast concrete. If

the

rel

26)

2.2

emp

a n

sto

th

sa

fr

ho

co

et

ar

to

u,

r

d

(

2

E

c

t

c

the lightness of GFRG is to be exploited, however, the relief to the finish should be restricted (References 25, 26).

2.2.4.2 Light Etch Retarded Finishes:

A pleasant stone textured finish can be obtained by employing face-down retarders. These are used together with a mould release agent and are suitable for timber, wood, steel and plastic moulds. The result is a transformation of the glossy, craze-prone finish obtained from GRP moulds to a sandy texture finish that removes the cement rich surface from the GFRG and exposes the sand in the matrix. It may, however, be necessary to increase the thickness of the mist coat in order to prevent exposure of the glass fibers on the etched surface (Reference 25).

The mould release agent is first painted on the mould and left to dry. Then the retarder is applied and allowed to dry out. Filling of the mould can be allowed at any time up to 5 days after the application of the etch retarder. A range of etch retarders is available giving a variety of depths, but the lightest is probably the most satisfactory (Reference 25).

2.2.4.3 Colored Cements:

One of the most popular finishes is to use white cement plus a clear silicone coating. The advantage of white cement is that the color is in the material and, provided that care is taken during manufacture and curing, consistency of color from unit to unit can be maintained.

Although other pigmented cements are available, uniformity of color from panel to panel is difficult to achieve (Reference 26).

However, pigmentation is an area where further development is taking place. The best results are likely to be achieved with white Portland cement and inorganic pigments in a color range from light yellows to dark reds. To achieve the necessary uniform consistency, very accurate weigh batching is necessary in conjunction with the use of a high-speed mixer. This produces a high shear effect on the particles in suspension, ensuring an even distribution of the iron oxide throughout the matrix slurry, which is then sprayed in the usual way. After careful curing and drying, a coat of silicone should be applied to partially seal the surface. This ensures that further drying is controlled at a constant rate for all panels (Reference 26).

2.2.4.4 Stain Finishes:

A successful method of producing a pigmented surface on GFRC is to use a stain after demoulding. The proprietary stain available has an acid included in the formulation to clean off the top layers of cement and mould oil from the surface of the product. The solution is simply brushed on and left. Two applications are usually applied followed by a coating of silicone wax or liquid sealer to prevent lime bloom. This finish, if sealed carefully after application, has proved quite successful and practical to use. The buff stain is probably ferrous sulphate solution and the green is

cop

(Re

2.2

va

se

si

Th

se

a

2.

ha

1

2

3

4

V

S

H

R

C

V

copper sulphate, both assisted by an acid in the solution (Reference 25).

2.2.4.5 Sealers:

A range of proprietary sealers is available with varying influences on the surface of GFRC. The purpose of a sealer should be to penetrate the surface and reduce significantly the take-up of atmospheric dirt and pollution. This may mean that the surface appearance is changed by the sealer but a range of effects can occur from a deep gloss to a barely noticeable sheen (Reference 25).

2.2.4.6 Epoxy Gel-Coat Finishes:

The bonding of an epoxy resin finish by gel-moulding has many distinct advantages.

1. The finish is governed by the quality and surface of the mould.
2. The texture and shine of the finish obtained is constant.
3. Relatively complicated profiles can be produced.
4. Semi-transparent motifs and writing can be bonded into the surface.

The process involves coating the mould with a poly vinyl alcohol release agent as used in GRP moulding work. A special two-part epoxy resin is then applied by spraying or painting to form a thick uniform coating. Once 'tacky' a second thin coating is added again by either means and this acts as a bonding layer. The GFRC is then sprayed immediately onto the two-coat system and the process

completed as standard. When the GFRC is sufficiently hard to resist demoulding the unit is removed.

2.3 QUALITY CONTROL

To ensure effective design and to maintain material within the expected specification it is vitally necessary to monitor GFRC during production. In order to fulfill these requirements the quality control program must include control tests of materials, equipment checking, testing of the uncured composite, and physical and mechanical property testing of the cured composite. These tests are required to assure a consistent and uniform manufacturing process (Reference 12).

Specified properties of all material used in the manufacture of GFRC should be verified by appropriate ASTM tests, by either the material supplier or the GFRC manufacturer (Reference 27).

In order to establish evidence of proper manufacture and conformance with plant standards and project specification, a system of records should be kept to provide full information on material tests, mix designs, composite tests, and any other information specified for each project (Reference 27).

2.3.1 Material Checking:

2.3.1.1 Cement:

Obtain cement manufacture's test certificates and file data on cement fineness and strength test. If production

problems indicate that a particular batch of cement is causing a false set, the stockpile should be sampled and a check made on the setting time using the standard Vicat test apparatus. Troublesome stocks of cement should be put to one side. Lumpy cement should also be investigated with reference to the post-mixing state. If high-shear mixers are employed it may be possible to process lumpy cement, but with forced pan mixers blockages in the mortar spray head can occur. All cement should meet the requirements of the specified type in ASTM C-150. Mill certificates of cement should be kept on file in the plant for at least 2 years after cement use (References 27, 28).

2.3.1.2 Glass Fiber:

Table 2.3.1 shows the PCI specification for alkali-resistant glass fiber. Plant testing of glass fiber is not required if the glass fiber strand is certified as being manufactured with an alkali-resistant glass produced using zirconia and conforms to the specification requirements shown in Table 2.3.1 (Reference 27).

Table 2.3.1 PCI Specification for Alkali-Resistant Glass Fiber-Test Requirements (Reference 27).

Property	Specified Value	Method of Test	Frequency of Testing
Zirconia content, ZrO_2	16% min.	X-ray Spark Analysis	Monthly
Density	2.7 g/cm ³	ASTM D 3800	Yearly
Tensile Strength	185-355 x 10 ³ psi	ASTM D 2343 strand	Yearly
Young's modulus	11,400 x 10 ³ psi	Wax tensile	Monthly
Elongation at break	2 + 0.5%	ASTM D3379 ASTM D2343	Yearly
Filament diameter	13.5 ± 2µm	—	Twice daily
Roving tex	200 yds/lb ± 10%	ASTM D 861	Each 1,100 lb
End count	26 ± 6	Physical count	Daily
Loss on ignition (Size pick-up)	±20% from the nominal value stated by the supplier, or ±0.2%, whichever is the greater.	ASTM D 2587	Each 44,000 lb daily
Strength retention by Strand-in-Cement test.	Minimum value 48 x 10 ³ psi after 96 ± 1 hour in water at 80°C (±1°C)	"Method of Test for Strength Retention of Glassfibre in Cements and Mortars," GRCA S0104/0184, Jan. 1984 ⁽⁴⁷⁾ (See Note 1)	Each 110,000 lb

Note 1 The routine assessment procedure of testing after one aging period, as described on page 8 of GRCA S0104/0184 is to be used together with the standard cement mortar slurry specified in Note 2 on page 15 of that document

2.3.1.3 Sand:

The grading of sand should be checked regularly and compared with the limits of GFRG production and also with the specification offered by the supplier. It is advisable to retain a small quantity of sand of acceptable standard as a visual cross-check of what is indeed a satisfactory material (References 27, 28).

Usually dry sand is employed but when it is intended to use wet sand the free water content should be known. The decision is then made either to mix to a workability level by adding water or to add the amount of water necessary to maintain the water/cement ratio. Workability must always be within the stipulated range of the manufacturing process.

Ideally, batching by using whole bags of sand is often quicker and easier than weighing out additions or gauging by volume (Reference 28).

The above also applies in deciding whether to use wet or dry sand. If scales are used, then a simple calibration check should be performed with every shift (Reference 28).

2.3.1.4 Admixtures:

All relevant admixture information with respect to performance, quantities, and application methods should be on file at the plant. These admixtures must be clearly labeled and not transferred into unlabeled storage jars. Additions must be made to comply with the manufacturer's recommended dosage, or to an acceptable pre-production test level. The method of addition should be as sophisticated as possible, for example by using the proper admixture dispersing equipment which is obtainable from the admixture supplier. It should be noted that over- and under-dosage can be equally disastrous (References 27, 28).

2.3.1.5 Water:

It is recommended that water be added via gauging equipment which removes human error resulting from guess work. All dispensing equipment should be checked by an appointed person on a regular basis and a tabulated record kept of these checks together with the results obtained (Reference 28).

2.3.

spr

fro

fib

fib

rat

cor

has

spr

ens

is

2.

ou

ca

th

as

th

2

sy

ac

ni

up

(P

2.3.2 Equipment Checking:

There are three main checks carried out when setting up spray equipment: (1) the delivery rate of the cement slurry from the spray head; (2) the delivery rate of the chopped fiber; and (3) spray pattern setting (Reference 12).

The delivery rates of the cement slurry and the chopped fiber are checked over a given time period and the delivery rate is calculated in kg/min. or lb/min. to ensure the correct ratio of fiber to slurry. Once the spray equipment has been set to produce the required fiber content, the spray pattern from the spray head has to be checked to ensure that even distribution of fibers in the mortar cone is achieved (Reference 12, 28).

2.3.3 Production Checking in Wet State ('Green' State)

Assessment of the composite in the wet state is carried out on boards prepared at the same time as the unit is being cast. These boards are also used for long-term tests, and they are manufactured and cured by exactly the same regime as the product. Samples are cut from the board according to the specified cutting pattern (References 12, 27, 28).

2.3.3.1 Thickness:

The performance of GFRC products manufactured by spraying method depends on the correct thickness being achieved. Thickness should be checked frequently at a large number of places on the product surface during each spray up. This is best done using a simple penetration gauge (Reference 27).

spr

con

des

spr

con

de

al

in

am

co

gl

ce

2

w

l

i

f

(

(

t

n

s

2.3.3.2 Slurry Consistency Slump Test:

This test indicates whether a slurry is suitable for spraying. It also provides means of comparing the consistency of slurries made with varying materials, mix designs, etc. Stiff mixes may be difficult to pump and spray. The frequency of testing depends upon the quality control program established by the manufacturer.

With the use of high-range water-reducers in a mix design, the slump test may not be appropriate. As an alternate, each mixer may be equipped with an ammeter that indicates the relative resistance of the mixer motor. The ammeter reading should be maintained constant after a slurry consistency is determined to provide a good "wet-out" of the glass fibers with no segregation of the aggregate from the cement paste (References 27, 28).

2.3.3.3 Fiber Content (Washout Tests):

The average glass fiber content determined by the washout test should be recorded and be within the control limits of -0.5 to +1.0% by weight. The washout test is used in two ways: (1) as a routine estimate of the mean glass fiber content of the composite during GFRC production; and (2) to establish the competence of spray operators (Reference 27).

The uniformity of glass distribution through the thickness (top to bottom) is important and can be checked by means of the washout test with split samples. A convenient sample size is six coupons, 100 mm square (3.95 in. square).

The six coupons taken enable a measure of the variability of the fiber content within the test board to be established, usually expressed as the standard deviation and coefficient of variation. Sequential application of fiber and slurry may give non-uniformity that results in layers of varying glass contents, and may cause poor product performance. A variation of less than 10% is considered acceptable. It is recommended that the test be performed on a weekly basis (References 27, 28).

2.3.3.4 Unit Weight:

Most GFRG strength properties vary directly with the density of the slurry - the higher the density, the better the performance. The unit weight test (ASTM C-138) should be performed once per day before starting the production. The unit weight should not vary more than 48 kg/m (3 lb/ft) from the established unit weight for the particular mix design in use (Reference 27).

2.3.4 Production Checking in Post-Curing:

After the required curing period, sample coupons are cut from the board to check bulk density and absorption, flexural strength, and, if necessary, tensile strength (References 12, 27).

2.3.4.1 Bulk Density and Absorption (Reference 27):

These measurements assist in establishing the level of compaction of GFRG. The wet bulk density should not be less than 2003 kg/m (125 pcf) and the dry bulk density should not

be l

not

from

des

wei

cur

cop

tes

est

2.3

as

of

loc

re

th

de

as

da

p

de

be less than 1762 kg/m (110 pcf). The bulk density should not vary more than -80 kg/m (5 pcf) to +160 kg/m (10 pcf) from the established bulk density for the particular mix design in use. The absorption should not exceed 16% by weight when no copolymer dispersion is used in the mix as a curing aid, and should not exceed 13% by weight when 5% copolymer dispersion is used in the mix. The absorption test values should not vary more than +1% by weight from established absorption for the particular mix design in use.

2.3.4.2 Flexural Strength (References 12, 28):

The flexural strength of GFRC test coupons is expressed as the LOP, limit of proportionality, and the MOR, modulus of rupture. The LOP is determined from the point on the load/deformation plot where the initial pseudoelastic response deviates from the linear path. This coincides with the first crack developing in the matrix. The MOR is determined from the peak value in the load/deformation plot as shown in Figure 2.3.1.

In general four to six coupons are tested at 7 and 28 days, and the average result is used as an indication of the properties of the element manufactured. LOP is strongly dependent on the matrix properties and is influenced by:

- (i) The type of matrix being used (e.g. cement/sand);
- (ii) The degree of cure;
- (iii) The presence of surface cracks (e.g. mechanical damage, shrinkage cracking);

- (iv) Quality of matrix (e.g. degree of porosity, compaction).

MOR of the composite is determined by the presence of fibers and is dependent on:

- (i) The glass content of GFRC;
- (ii) The orientation of glass fibers;
- (iii) The degree of cure;
- (iv) The type of matrix;
- (v) The quality of the matrix (e.g. degree of porosity, compaction).

2.3.4.3 Tensile Strength (Reference 28):

Although this property can be measured rather easily using a variety of conventional testing equipment, the results obtained greatly depend on the preparation of the samples and the mode of operation of clamps.

The typical trace produced from a tensile test (see Figure 2.3.1) yields a two-stage failure. The first region shows pseudoelastic behavior of a relatively high modulus limited by the cracking of the matrix. The second region exhibits progressive multiple cracking at a lower modulus ending in the enlargement of one crack and the final break up of the sample. The point of modulus change and the stage when the matrix cracks is defined as the BOP, bend-over point, and the final load indicates the UTS, ultimate tensile strength.

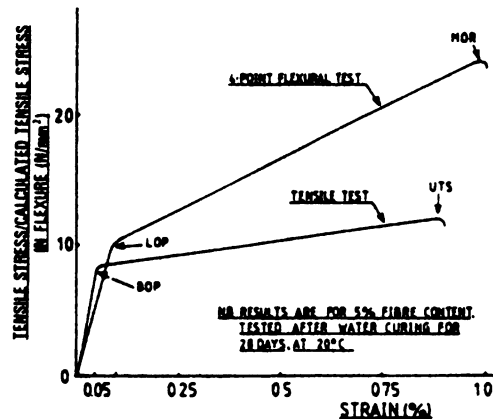


Figure 2.3.1 Typical Flexural Test and Tensile Test Graphs (Reference 28).

2.4 FRESH MIX PROPERTIES

GFRC manufacturing using premix method has certain advantages since spraying method is difficult to cast into complex shapes and thick placements, and relatively high installation costs of spraying method also encourage the manufacturer to use the premix technique. However, GFRC premix obviously has some problems related to fresh mix workability which spraying does not have. This chapter reviews the workability characteristics of GFRC premix (Reference 12).

2.4.1 Fluidity Test for GFRC Premix:

The conventional flow value is not a sufficient factor for representing the workability of GFRC because even GFRC mixes with relatively small flow values may still be workable and compaction could be achieved by external vibration. For this reason, it is necessary to develop a specific method for measuring the fluidity of GFRC mix.

Reference 29 suggests the testing method described below:

GFRC Mix is charged into a special container as shown in Figure 2.4.1. Under a vibration of 9000 r.p.m. generated by a table vibrator, the content is flown out of the container through a slit opening at the skirt. While GFRC mix is being discharged, the time for lowering level of GFRC mix in the container by 9 cm (3.54 in.) is measured in seconds. The relations between fiber content and this lowering time as well as the flow value are shown in Figure 2.4.2. The fiber content used in Figure 2.4.2 was decided through making measurements on five different 50 g (0.11 lb) samples taken from different points of the fresh mix.

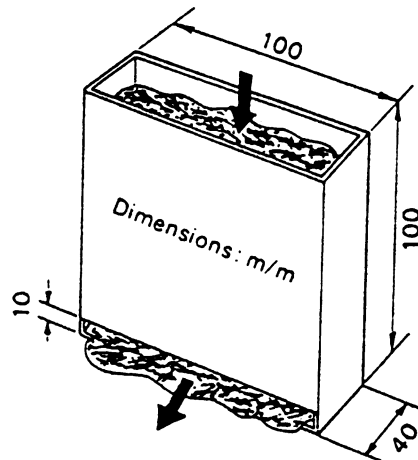


Figure 2.4.1 Test Container for Determining Fluidity (Reference 29).

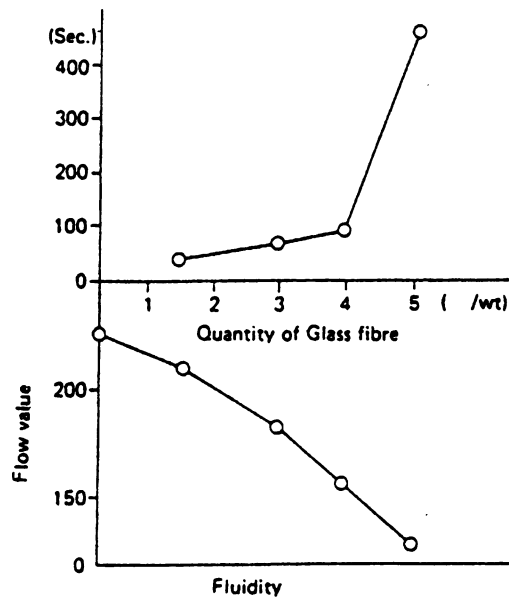


Figure 2.4.2 Fluidity and Flow of Typical GFRC Premix Vs. Fiber Content (Reference 29).

2.4.

Dis

nirt

imp

ceme

fi

Fig

Exc

seg

(Re

flu

wat

pro

pre

wat

be

suc

hav

fre

2.4.2 Effects of Mix Proportioning on Fluidity and Fiber Dispersability:

Table 2.4.1 shows the fluidity of different GFRC mixtures. In general, the fluidity of GFRC mix will be improved as the sand content is reduced. When the cement/sand ratio becomes smaller than 2, segregation of fibers from mortar occurs under vibration.

The increase in water/cement ratio is also observed in Figure 2.4.1 to increase the fluidity of mortar. Excessively fluid GFRC mixtures may, however, encourage segregation of fibers from the mortar under vibration (Reference 29). GFRC premix compositions with reasonable fluidity which contain relatively low sand contents with low water/cement ratio and seem to give desirable fresh mix properties. In order to reduce the water/cement ratio and prevent segregation tendencies, some admixtures such as water-reducing agents and adhesive (dispersing) agents may be used in GFRC premix (see Table 2.4.1 for the effects of such admixtures on fresh mix properties). These admixtures have been found to improve the dispersability of fibers in fresh mix (References 11, 29).

Table 2.4.1 Mix Proportion and Fluidity (Reference 29).

Cement/Sand (Wt proportion)	Water/ Cement (%)	Fibre quantity (% wt)	Fluidity	
			Flow value	Time (sec.)
1 : 3	50	1.5	—	Fibre segregated
1 : 2	50	1.5	—	Fibre segregated
1 : 1	35	0	216	—
1 : 1	35	1.5	148	a little segregated
2 : 1	35	1.5	158	135
3 : 1	35	0	230	—
3 : 1	35	1.5	206	35
Admixture agent				
Kind		Additive quantity.(%)	Fluidity (sec.)	Remarks
Adhesive agent (A)		2 ~ 7	60 ~ 270	
Adhesive agent (B)		0.01 ~ 0.1	60 ~ 108	
Water reducing agent (C)		0.1 ~ 0.5	100 ~ 30	

2.4.3 Effects of the Mixing Method:

The effects of different mixing processes on fresh GFRC premix properties are shown in Table 2.4.2. Manual mixing produced the best fluidity when compared with different mechanical mixing technique. When the revolution of the mixing agitators was in excess of 100 r.p.m., GFRC lost its fluidity to a considerable degree, and was susceptible to a hard discharge from the mixing drum. This may be attributable to raveling effect of agitators on fibers. On the contrary, exceedingly less revolution of the agitators will result in a bad mixing efficiency, and in that case fibers may not be well-dispersed in the mixture (Reference 29).

It is suggested that mixing efficiency also depends on the shapes of the agitators in the mixture. The results presented in Table 2.4.2 indicate that the mixer with no agitator or stirrer inside the mixing drum (Omni-Mixer) cause no damage and no agglomeration to fibers in the GFRC mix, and brought about better fluidity of the material. The mixer also showed a sufficient efficiency by producing GFRC mixtures in shorter time periods when compared with mixers with agitators. The fluidity of GFRC mixtures with high fiber contents (about 5% by mass) is expected to be lost drastically through mixing by any agitator mixers. When mixers without agitators were used, better fluidity was obtained in GFRC mixtures even at fiber contents as high as 7% by weight (Reference 29).

Table 2.4.2 Comparative Mixing Test Results (Reference 29).

Rev. of Agitators	Fluidity		State of mixture	State of fibre	Evaluation
	Flow value	Time (sec.)			
A. 360 rpm	bad	bad	good	ravellid	bad
B. 340	-	125	bad	ravellid	bad
C. 92	-	280	good	ravellid	good
D. 80	-	40	good	not ravellid	good
E. 74	-	40	good	not ravellid	good
F. 72	109	90	bad	not ravellid	good
G. 61	149	65	good	not ravellid	better
H. 59	-	135	bad	not ravellid	good
I. 0	150	-	good	not ravellid	better
J. Manual mixing	175	-	good	not ravellid	better

Note:

A, B, C, D, E-Drill Mixer;

F, G-Eirich Mixer;

H-Tilting Type Mixer;

I-Agitatorless Mixer

com

ori

giv

mat

per

mos

cor

be

wh

ap

si

to

2.

e:

st

i

b

c

c

t

c

h

2.5 HARDENED MATERIAL MECHANICAL PROPERTIES

An important role of fibers in the fibrous cement composites is to control the propagation of cracks originating from voids and other defects in the matrix, thus giving a reliable tensile strength to an otherwise brittle material with unreliable tensile behavior. AR-glass fibers perform this role in cement mortar matrices, and thus in most applications of GFRC it is the tensile strength of the composite which is the most important property, either in bending or in direct tension, and it is the tensile behavior which has been thoroughly investigated. In some applications, of course, other properties may be of significance, and therefore all mechanical properties need to be examined (References 30, 32).

2.5.1 Tensile Behavior:

When unaged GFRC is tested in tension, the load-extension curve produced takes a form which is shown schematically in Figure 2.5.1. In this diagram, the initial linear portion of the curve, Region 1, is determined by the fibers and matrix acting together as an elastic composite, the stiffness and stress being given by the law of mixtures (Reference 30). This behavior is followed up to, or close to, the failure strain of the matrix. In certain conditions with high fiber content it may extend beyond the matrix failure strain. In this region,

microcracking may be initiated but this is suppressed and restrained by the fibers, although this may be evidenced by slight deviations from linearity (References 30, 32).

Region 1 terminates at the proportional limit which for direct tension, has been the 'bend over point' (BOP) where there is a marked deviation from linearity to a region which may be almost horizontal (References 30, 31, 32).

Provided there are sufficient fibers to support the load after the matrix has cracked, a zone of multiple cracking of the matrix ensues - Region 2. As the first cracks propagate, the load at the cracked section is carried by the fibers and there is some extension over the debonded region. Away from the crack the load is transferred back from fiber to matrix by shear forces at the fiber-cement interface, until further cracks are formed, accompanied by further extension. This continues until the matrix is crossed by a series of closely spaced fine cracks, and the load is entirely carried by the fibers (References 30, 32).

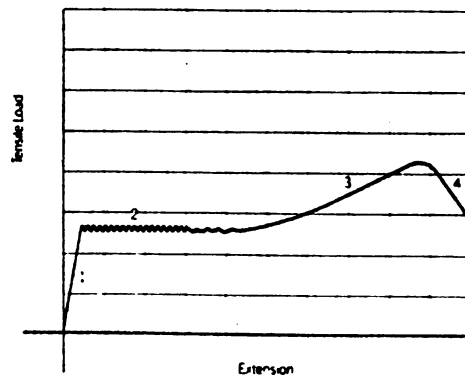


Figure 2.5.1 Representative Tensile Load-Extension Curve for Unaged GFRP (Reference 30).

The third region is where the load is being carried by the fibers alone and the slope is governed by stress-strain behavior of the fibers. The ultimate tensile strength (UTS) arises when the bridging fibers across one particular crack are either broken or pulled out of the matrix, although the failure is gradual rather than abrupt - Region 4 (References 30, 31, 32).

There are several important factors which must be considered in making effective use of glass fiber as reinforcement in GFRC:

- (a) The fibers should be significantly stiffer than the matrix;
- (b) The fiber content by volume must be greater than a critical volume fraction;
- (c) There must be good fiber/matrix bond;
- (d) Fiber length must be sufficient to develop the bond;
- (e) The fiber should have a high aspect ratio (the ratio of surface area to cross sectional area) achieved by using long thin fibers.

Although there must be sufficient fiber/matrix bond, it has been demonstrated that the bond should not be too good, otherwise the strain to failure will be small and failure will take place early in the region of multiple cracking - Region 2 (Reference 32). Figure 2.5.2 shows tensile stress-strain curve of GFRC containing 4 vol% fibers of length 30 mm (1.18 in.).

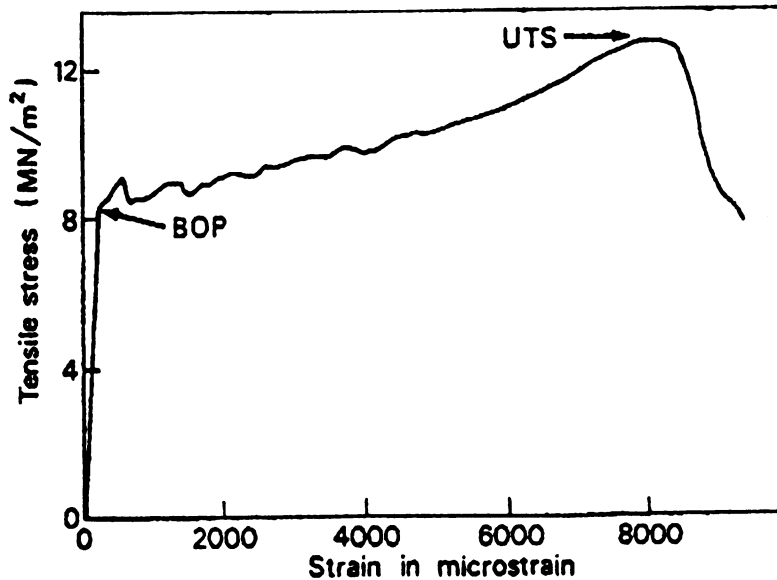


Figure 2.5.2 Tensile Stress-Strain Curve of a 28 Day Old GFRC Sample Containing 4 Vol% Fibers of Length 30 mm (1.18 in.), Reference 33.

2.5.2 Flexural Behavior:

An understanding of the flexural behavior of GFRC can be gained by examining and combining the tensile and compressive stress-strain curves. Whereas the tensile curve follows the behavior described above, the compressive stress-strain curve remains almost linear to failure with a slope similar to the initial part of the tensile curve. If the apparent stress and strain are calculated from simple bending theory, the resulting bending stress-strain curve lies between the compressive and tensile curves (Figure 2.5.3). It contains two points of interest, the limit of proportionality (LOP) and the highest calculated stress, termed the modulus of rupture (MOR), References 30, 32.

If the tensile and compressive stress-strain curves for any particular specimen of GFRC are known, the bending curve can be estimated. Such an estimate of the bending curve suggests that the LOP is similar to the BOP, but practical tests show that LOP is about 1.7 times the BOP. However, brittle materials often show higher strength in bending than in tension, so this is not surprising (Reference 30).

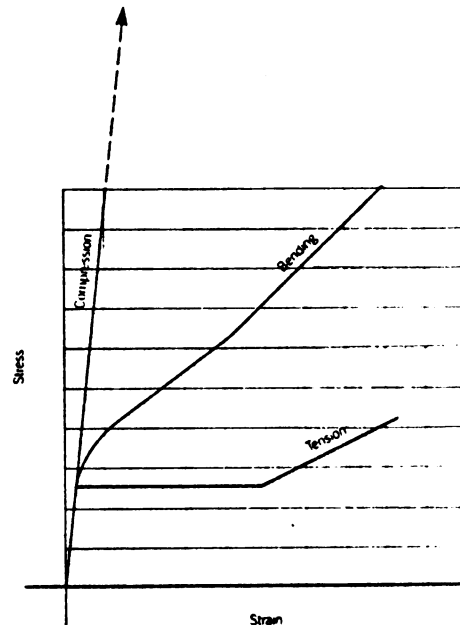


Figure 2.5.3 Schematic Stress-Strain Curves for GFRC (Reference 30).

The MOR is found to be commonly 2.5 to 3.0 times the UTS for rectangular sections. The greater the tensile strain to failure, the closer this ratio will become to 3.0. Conversely, as the strain to failure reduces (i.e., if Region 2 is limited) then the MOR/UTS ratio will decrease. It was demonstrated that there could be a reduction in MOR

du

th

GR

te

dc

fl

as

cu

to

st

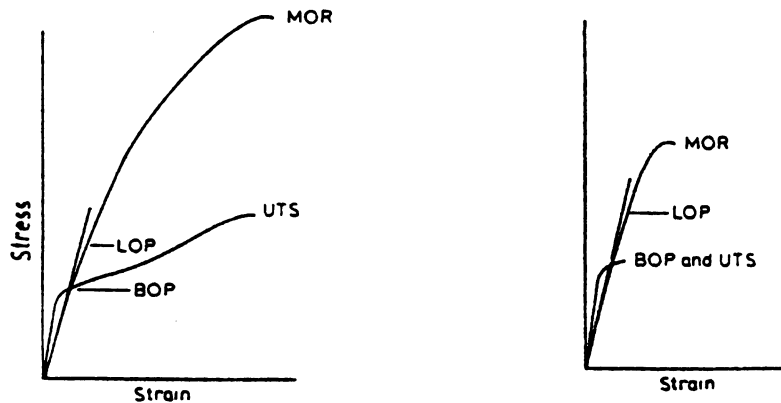
2

h

(

due to a reduction in the tensile strain capacity even if the tensile strength is maintained (References 30, 32).

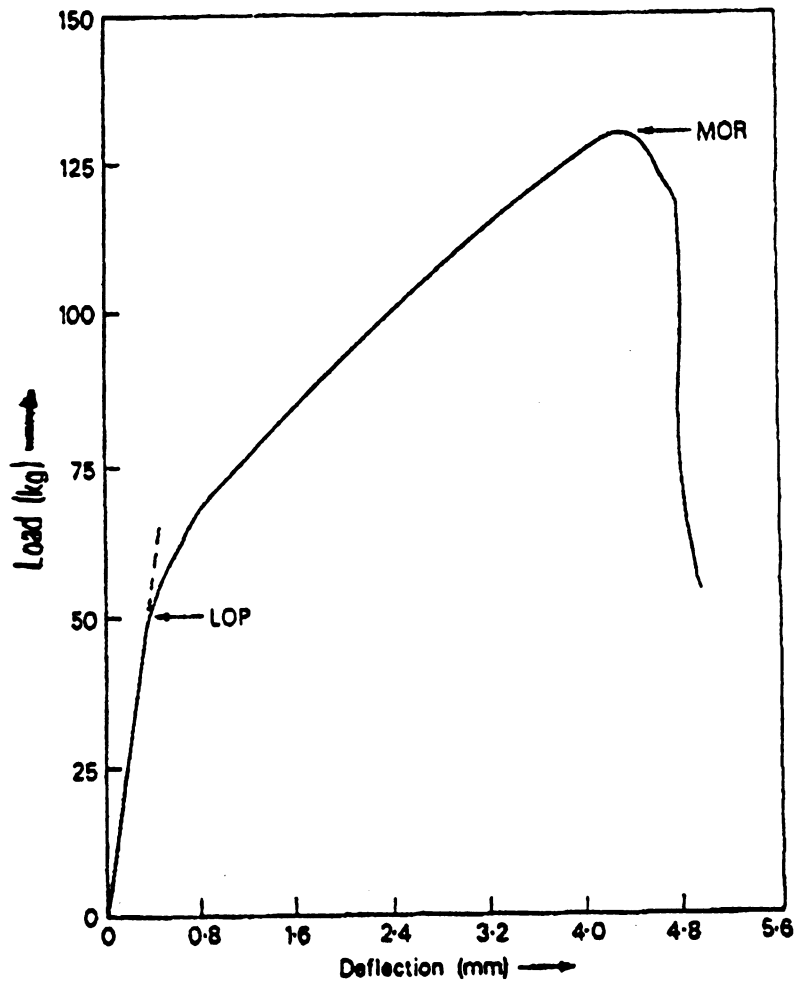
The other major feature of the flexural behavior of GFRC is that whereas there is a sharp discontinuity in the tensile stress-strain curve when cracking first occurs, this does not occur in flexure. Cracking develops gradually in flexure, starting at one face and spreading slowly inwards as the bending moment increases. Thus the load-deflection curve in bending is much smoother and the LOP is much harder to detect (Reference 32). Figure 2.5.4 shows the typical stress-strain curves in bending and tension, and Figure 2.5.5 shows the actual bending curve of unaged GFRC.



(a) After 28 days in water.

(b) After 2 Years in Water

Figure 2.5.4 Stress-Strain Curves in Tension and Bending (Reference 32).



$$\sigma = \frac{Wl}{bd^2}$$

Note:

where σ is the tensile stress in the outer element of the specimen, W is the applied load, l the span and b and d the specimen breadth and depth respectively.

Figure 2.5.5 Load Deflection Curve from a 4-Point Bending Test on a 28 Day Old GFRG Sample, Containing 4 Vol % Fibers, 30 mm (1.18 in.) Long, Crosshead Speed 2 mm/min. (0.08 in./min.), Reference 33.

2.5.3 Impact Resistance:

The impact resistance of GFRC is influenced strongly by the reinforcing fibers. Increasing fiber length from, for example, 25 to 50 mm (1 to 2 in.) or using alkali-resistant glass fibers increases the impact strength. Cured GFRC at 28 days has higher impact strengths than either unreinforced cement paste or asbestos cement (References 31, 32).

In addition to its higher impact resistance, GFRC's failure characteristics are different from those of asbestos cement or plain concrete. GFRC exhibits pseudo-ductile behavior for several years, and damage due to impact is usually confined to the area of impact without evidence of cracks propagating beyond this area (Reference 31).

Impact properties relate to the area under the tensile or flexural stress-strain curve; as these curves alter with time, the impact properties are reduced. Figure 2.5.6 shows a typical impact strength curve using the Izod swinging pendulum apparatus and plotted against time for water stored in GFRC. Upon prolonged aging, GFRC can be expected to become less ductile, and thus its impact resistance tends to diminish (References 31, 32).

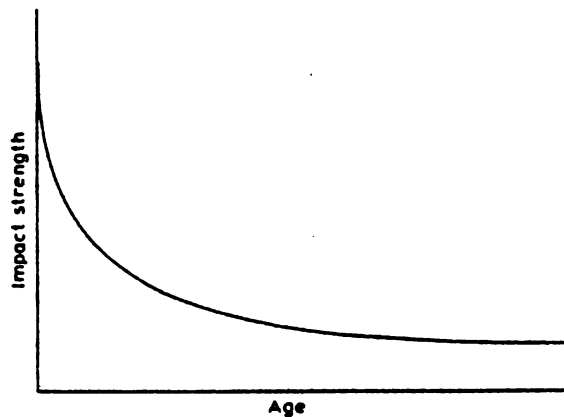


Figure 2.5.6 Typical Izod Impact Strength for GFRC Stored in Water (Reference 32).

2.5.4 Compressive and Shear Strengths:

The mode of failure and ultimate strength of GFRC under compression depends on the orientation of loading relative to the fibers. The in-plane compressive strength is about 70% of the across-plane strength (see Figure 2.5.7). Both strengths are strongly dependent on the type of matrix, and the compressive strength of GFRC is in fact close to that of the unreinforced matrix material (Reference 34).

Values were obtained from 25 mm (1 in.) cubes cut from extra thick sprayed sheets. Because GFRC is so frequently used as a much thinner sheet material, it was desirable to test coupons of representative thickness cut from normal sheets. Compressive strength values for a spray-dewatered materials containing 5% AR-glass fiber in a matrix with sand:cement ratio 1:3 lay in the range 64-83 MN/m² (9.3-12

ksi). Stress-strain curves were linear to about 45-55 MN/m² (6.5-8 ksi) with Young's Moduli in the range 27 to 31 MN/m² (3.9 to 4.5 ksi) and Poisson's ratio of 0.12 to 0.22. Test samples stored in natural weather for 5 years indicate a tendency for compressive strength to increase upon aging, and for the in-plane strength to approach the cross-plane strengths values (References 31, 34).

There are also two types of shear strength because panels made by spraying method have fibers randomly distributed in the plane of the section (Figure 2.5.7). Therefore, shear values vary with the type of load application as follows (Reference 31, 34):

- (a) Interlaminar shear with failure plane and shear direction parallel to the fiber plane. The value of shear strength is that of the matrix. This type of shear stress is encountered in the bending of single skins and vertical load-carrying bonding pads. The strength values are about 3 to 5 MN/m² (430 to 730 psi) and tend to increase slightly on wet aging.
- (b) In-plane shear with failure plane perpendicular to fibers and shear direction in the fiber plane. In-plane shear strength and ultimate tensile strength for a range of formulations of hand-sprayed GFRC after a variety of aging treatments are identical. Therefore, in the absence of direct in-plane shear measurements, tensile strength values may be used with confidence. In-plane shear stress can be generated by bolted

connections near the edge of a sheet. Values fall on wet aging from about 15 MN/m^2 (2175 psi) to about 5 MN/m^2 (725 psi).

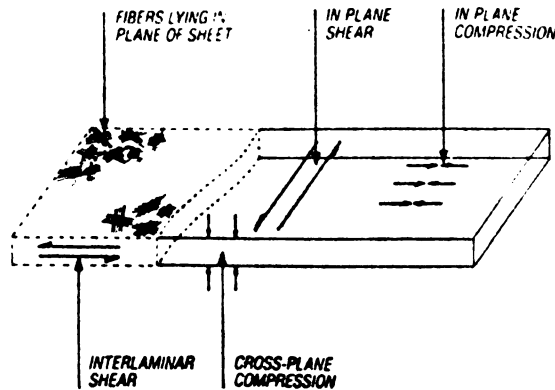


Figure 2.5.7 Compressive and Shear Strengths (Reference 31).

2.5.5 Factors Affecting the Mechanical Properties of GFR:

The principal factors affecting properties of GFR are:

Glass Fibers: The volume fraction, orientation, length, degree of filamentisation, strength and resistance to alkali attack of the fiber;

Matrix: The type, density and degree of cure which all have effect on the matrix as well as the fiber/matrix bond strength;

Manufacture: The method of incorporating the fiber into the matrix;

Environment: The conditions of use and age, particularly with regard to moisture and temperature.

These factors are generally not separable but are all inter-related to some degree. The effects of the above factors on GFRC mechanical performance are reviewed below (References 31, 32).

2.5.5.1 Glass Fibers:

Increasing the volume fraction of glass fibers in sprayed GFRC increases impact strength, MOR and UTS to levels roughly proportional to the increase in fiber content; below about 2% volume fraction, however, there is insufficient fiber to provide an effective reinforcing action. If the fiber content is reduced, there is a greater likelihood of obtaining areas of the GFRC composite which have little or no fiber in them. Greater attention must be paid to fiber distribution during manufacture to avoid this possibility. Those properties which are mainly dependent upon the matrix show little variation with fiber content, although LOP and BOP may be increased detectably at levels of fiber content more than 5% by volume. Above about 6% by volume there is difficulty with processing leading to poor compaction and generally reduced properties. Typical variation of MOR with fiber volume fraction for hand sprayed GFRC containing 37 mm (1.46 in.) long AR-glass fibers is shown in Figure 2.5.8 (References 35, 36).

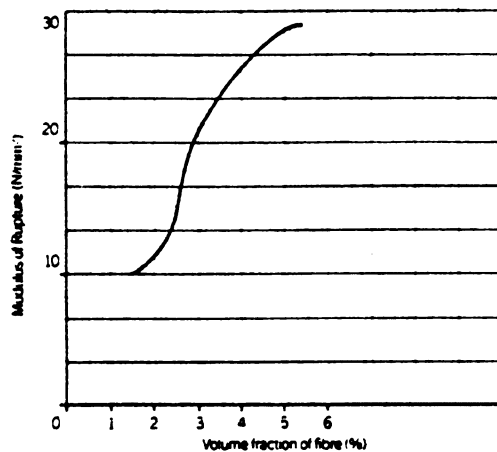


Figure 2.5.8 Typical Variation of MOR with Fiber Volume Fraction - Sprayed with 37 mm or 1.46 in. Long Fibers (Reference 36).

In premixed GFRC the random orientation of fibers and the use of shorter fibers reduce the reinforcement efficiency of fibers considerably when compared with sprayed GFRC having the same fiber content. Since the incorporation of more than 3.5% by volume of fiber leads to severe processing difficulties, the range of fiber content is usually limited to between 2% and 3.5% by volume. At lower glass content the properties of the GFRC are not generally attractive except for some applications, e.g. renders and screeds. Within this range of glass contents, the only property that varies significantly is impact strength, which increases with increasing glass content (Reference 36).

Although it is common practice to give glass content in terms of percentage by weight, it is volume fraction, V_f which determines the reinforcing effect. In low-density GFRC, 5% by weight may be as low as 2% by volume, whereas in GFRC with a density about 2 t/m^3 (62 lb/ft^3), 5% by weight is about 4% by volume (Reference 36).

As far as the effects of fiber length are concerned the use of longer strands of glass fiber increases their effectiveness as reinforcing agents. The effect is not linear. Typical variation of MOR with fiber length for hand sprayed GFRC containing 5% by weight of Glass fiber is shown in Figure 2.5.9.

For hand sprayed GFRC 4.1% volume fraction of fibers (5% by weight), the effect of changing the strand length between 25 mm (0.98 in.) and 50 mm (1.97 in.) is marginal for any property level except for impact strength, which shows an increase with increasing fiber length. Below 25 mm (0.98 in.) fiber length, the reinforcing efficiency drops markedly and with 12 mm (0.47 in.) or shorter fibers the property levels achieved are not dissimilar to the values for premixed GFRC. Above 50 mm (1.97 in.) fiber length, the incorporation of the fibers becomes difficult and compaction problems are encountered in manufacture (References 35, 36).

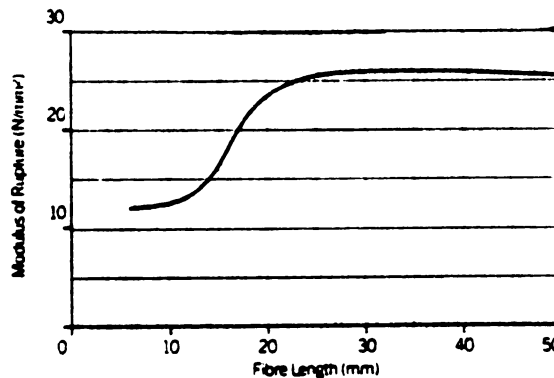


Figure 2.5.9 Typical Variation of MOR with Fiber Length for GFRC Containing 5% by Weight of AR-Glass Fiber (Reference 36) .

2.5.5.2 Matrix:

The matrix has the most important effects on the LOP, BOP and initial Young's modulus of GFRC. Thus to ensure consistent, reliable behavior and good LOP and BOP values, a well-compacted, well-cured matrix is required, with the minimum water/cement ratio compatible with the manufacturing process (Reference 32).

The earliest studies and first trials with GFRC used a neat cement matrix and longest running tests are based on this material. It was quickly recognized that shrinkage would be excessive and sand was introduced to the matrix in order to reduce shrinkage to an acceptable level. Increasing the sand content has the effect of reducing the initial strength of GFRC (MOR and UTS).

This reduction is particularly marked at sand contents greater than a sand/cement ratio of 0.5:1.0. Up to this point, the LOP and BOP values are maintained, before falling at higher sand contents. Increasing the sand content leads to increased porosity of the matrix caused by the increased water/cement ratio necessary to keep a workable mix. There must also be a reduction in the effective area of fiber bond due to the presence of sand. Thus there will be a decrease in the fiber/matrix bond leading to a reduction in the early-age strength. Where lower initial strengths are acceptable, increased sand contents up to a sand/cement ratio of 1.5:1.0 have been used (References 32, 36).

Up to a sand/cement ratio of 1:1, although the initial properties are somewhat reduced, the long-term ultimate strength will be close to that of the neat cement values provided the volume fraction of the glass fiber and the curing conditions are the same. The conditions necessary to achieve this are that the matrix must be well compacted using low water/cement ratios to ensure a minimum porosity, thus maintaining the fiber volume fraction at the optimum level. Also curing must be adequate such that continuing hydration of cement will allow the fiber/matrix bond to develop fully. Curing of GFRP is important to ensure adequate hydration of cement and therefore a good matrix/fiber bond. Inadequate curing leads to a weak matrix and poor material properties (Reference 32, 36).

2.5.5.3 Manufacturing Method:

Different methods of manufacture impose different characteristics on the material, particularly relating to fiber orientation and distribution. Also, each process has different requirements for mix proportions, water/cement ratios and use of admixtures which will have an effect on the matrix and the matrix controlled properties (Reference 32).

2.5.5.4 Environment:

The conditions of use of GFRG products and applications can have a considerable effect on the long-term properties. There is embrittlement and reduction in ultimate strength in wet conditions, the rate being dependent on the degree of exposure to moisture and the temperature. Extreme environmental situations, such as hot and wet conditions, create a very rapid drop in strength (Reference 32). This issue will be thoroughly covered later in discussions on the durability characteristics of GFRG.

2.5.6 Typical Mechanical Properties of GFRG:

The range of various mechanical properties are given in Table 2.5.1 for three GFRG formulations subjected to a satisfactory curing condition and tested at 28 days (References 32, 36).

The main difference between decatered and hand sprayed (non-dewatered) GFRG is the difference in density which has two effects. Firstly, although the fiber content by weight is the same, the higher density of the dewatered board gives

a higher fiber volume fraction leading to higher strengths. Secondly, the dewatered board has better compaction and reduced porosity, thus giving better fiber/matrix bond strength (Reference 32).

The values shown in Table 2.5.1 are for tests on coupons of GFRC, generally 200 mm (7.9 in.) x 50 mm (1.97 in.) x 8-10 mm (0.31-0.39 in.) thick, assuming random two-dimensional fiber distribution. In addition to the degree of anisotropy which may occur with machine spray, it should be noted that there can also be a 'top and bottom' effect. This is caused by the compacting and finishing treatment on the top surface, rolling or trowelling, which can cause differences in fiber concentration and distribution at the top face. The bottom or mould face will also tend to be better compacted. To take account of sample variations, generally six coupons from each test board are tested, taken in different directions, and equal numbers of coupons are tested with the top face and bottom face in tension (References 32, 36).

Table 2.5.1 Typical Mean Properties of GFRC Tested at an Early Age (Reference 36).

Process		Spray dewatered ¹	Hand Spray ²	Vibration Cast Premix ³
Dry bulk density	(t/m ³)	2.0-2.05	1.9-2.1	1.9-2.0
Compressive strength	N/mm ²	60-100	50-80	40-60
Modulus	kN/mm ²	13-25	10-20	13-18
Impact strength	Nmm/mm ²	11-25	10-25	8-14
Poisson's Ratio		0.24	0.24	0.24
Bending:				
LCP	N/mm ²	9-13	7-11	5-8
MOR	N/mm ²	28-42	21-31	10-14
Direct Tension:				
BOP	N/mm ²	7-9	5-7	4-6
UTS	N/mm ²	10-17	8-11	4-7
Strain to failure %		0.7-1.3	0.6-1.2	0.1-0.2
Shear:				
In-plane	N/mm ²	10-17	8-11	4-7
Interlaminar	N/mm ²	3-5	3-5	N.A.

Notes:

- 1 Sand: cement ratios of 0.1 to 0.5:1 and water: cement ratio 0.28
- 2 Sand: cement ratios of 0.33:1 to 1:1 and water: cement ratio 0.33
- 3 Sand: cement ratio of 0.5:1 and water: cement ratio of 0.33

The strain to failure and Young's modulus in Table 2.5.1 are as measured from the tensile test for short-term loading and are essentially typical for the matrix. Typical values of the impact strength as measured by Izod test are also shown in Table 2.5.1 (References 32, 36).

2.5.7 Creep Performance

So far GFRC has not been used to any great extent in situations in which it would be subjected to significant permanently applied or continuous stresses. The fact that

creep strains are generally less than moisture movements creates certain difficulties in measurement. Even in a controlled humidity laboratory, direct tensile creep measurements can be obscured by small changes in the moisture level of the environment. By measuring deflections in bending tests on simple strip specimens the moisture movement effects are suppressed and creep may be observed in normal laboratory conditions (References 36, 38).

The general form of creep strain variation with time for GFRc materials is shown in Figure 2.5.10, which gives results for neat cement paste-based samples tested in bending (Reference 34).

In common with other cement and concrete materials, the initial (elastic) deformation is followed by a further slow creep deformation when the load is maintained. The creep behavior of GFRc is very similar in general form to that of cement paste and sand/cement mortars. At bending stresses below the LOP, the creep behavior of spray-dewatered GFRc is identical to that of the matrix material. Creep strain is proportional to the initial strain and under long term loading will increase the initial strain by a factor between 2 and 4. This means, for example, that a panel installed horizontally which exhibits some deflection under self weight would be expected with time to show a deflection of approximately three times the initial amount. Both water content and aggregate content have major effects on creep rates - as they do for mortars (References 34, 36).

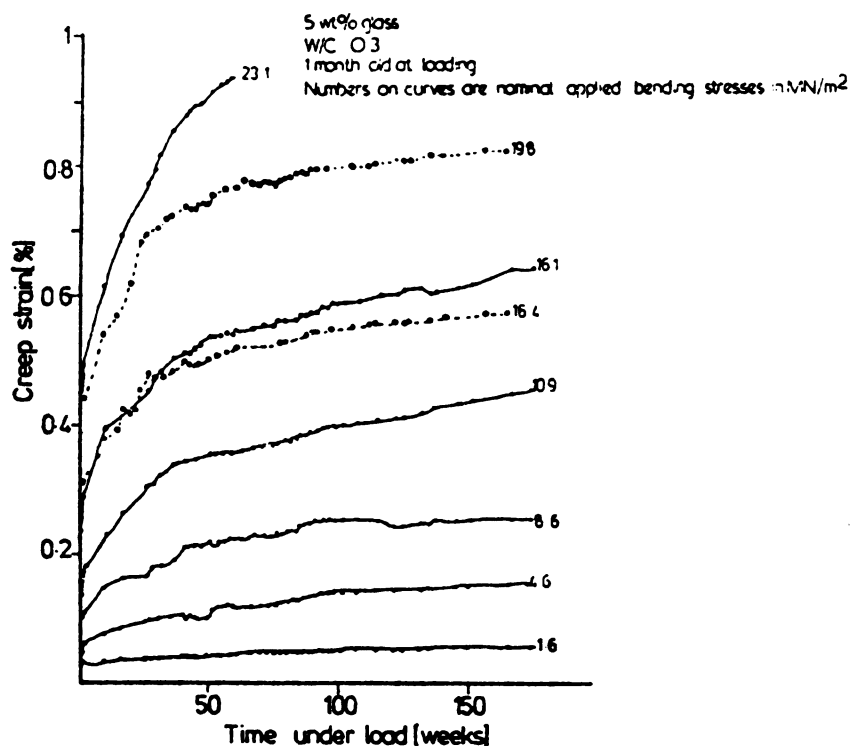


Figure 2.5.10 Creep of Spray Dewatered GFRC with Cement Paste Matrix in Dry Conditions (Reference 34).

The creep coefficients for a neat cement paste GFRC and a sand containing GFRC in wet conditions are shown in Figure 2.5.11. In dry conditions creep is initially somewhat greater but approaches the "wet creep" at the longer times. No stress rupture failures have been observed at stresses up to twice the normal recommended working stress level in experiments in which samples were kept under a constant bending load in dry air or under water at $18/20^{\circ}\text{C}$ (References 34, 36).

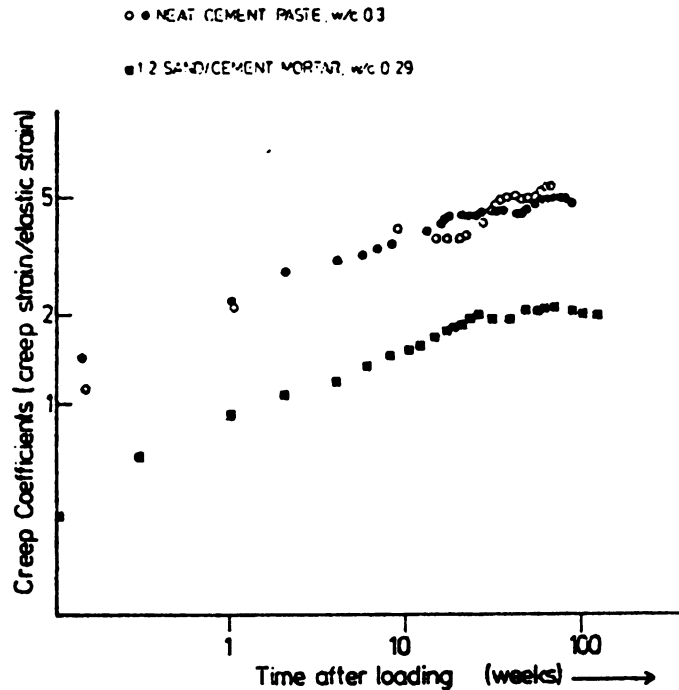


Figure 2.5.11 Effect of Matrix Type on Creep of GFRC Loaded in Flexure at 1 Month: Creep Under Water (Reference 34).

2.5.8 Fatigue Behavior:

Figure 2.5.12 gives the results of repeated load fatigue tests carried out in bending and direct tension on samples of hand-sprayed GFRC. A common form of S-N curve (stress versus cycles to failure) is obtained. Bending tests gave fatigue lives greater than 10^5 cycles at the LOP stress level and greater than 10^7 cycles at the normal flexural working stress levels (Reference 36).

Direct tension test results indicate lives in the excess of 10^4 cycles at the BOP and over 10^7 cycles at the normal tensile working stress levels (Reference 36).

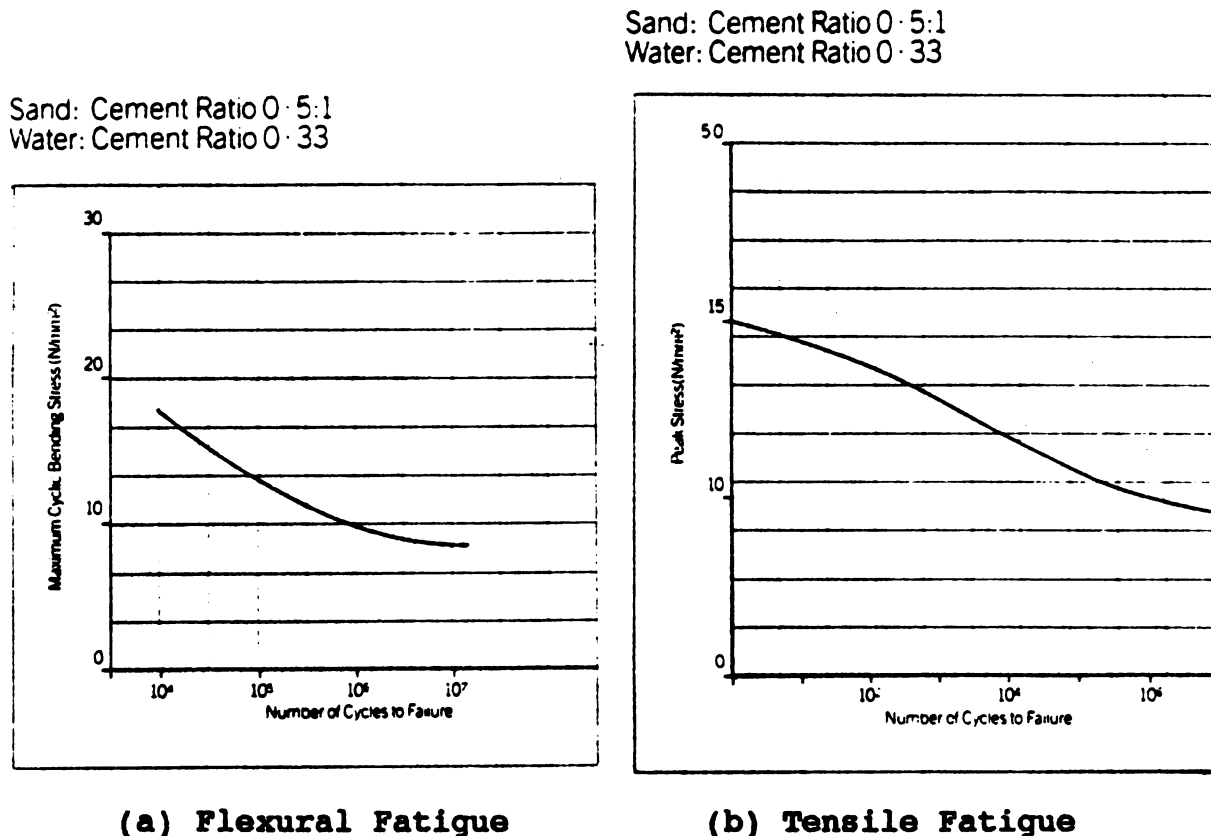


Figure 2.5.12 Fatigue Performance of Hand Spray GFRc Containing 5% by Weight of AR-Glass Fiber (Reference 36).

2.6 PHYSICAL PROPERTIES

The following physical properties of GFRc are reviewed in this section: Shrinkage, thermal expansion, thermal conductivity, permeability, density, and sound transmission.

2.6.1 Shrinkage:

As with all cement based materials, GFRc undergoes

dimensional changes as it is wetted and dried, but because GFRC typically has a cement-rich matrix these changes will be significantly larger than those experienced with conventional concrete (References 30, 31).

The complete drying shrinkage strain of GFRC made with a neat cement matrix is about 0.3% (with water/cement ratio of about 0.28 to 0.30), which is very high and the underlying cause of several problems with some of the early applications of GFRC. Sand was introduced into the matrix essentially to reduce shrinkage to an acceptable level, and silica sand has been found to have the best shrinkage reducing properties. The effect of silica sand content on the ultimate drying shrinkage of spray dewatered GFRC, with 5% by weight of glass fibers, is shown in Figure 2.6.1 (Reference 32).

The shrinkage rate, which is essentially the drying rate, is very important, as the slower the shrinkage movements, the greater will be the relaxation effect under restrained conditions. For the normal range of sand content (i.e., sand/cement ratio of 0.3 to 0.5), when dried at 50°C (122°F) after seven days of water curing, the total shrinkage is reached after about 8 days; at 4 days the shrinkage is about 80% and at 2 days it is about 60% of the total. For air drying at room temperature these ages have been estimated to be equivalent to 2 months, 28 days and 7-14 days respectively (Reference 30).

Since GFRC is a relatively impermeable material, changes in external humidity take a considerable period of time to affect the moisture content of GFRC. It takes about 20 days for 10 mm (0.39 in.) thick sprayed GFRC to approach equilibrium with changes in external humidity; it takes even longer for thicker sections (Reference 31).

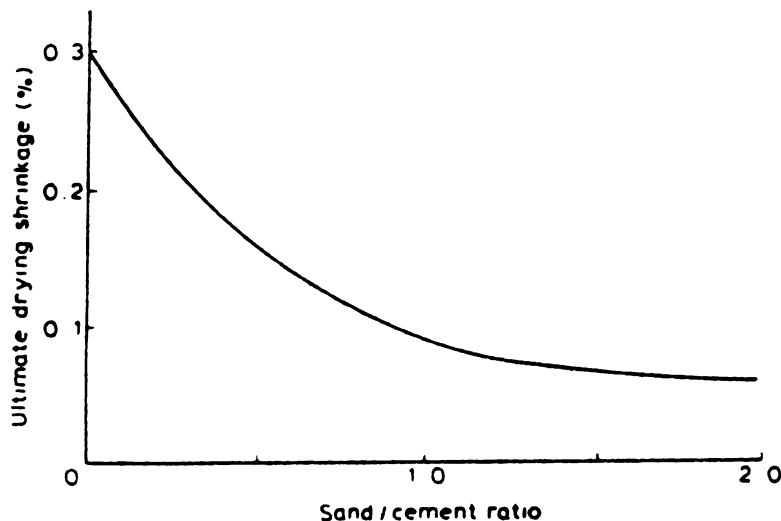


Figure 2.6.1 The Effect of Silica Sand on Shrinkage (Reference 32).

2.6.2 Thermal Strains:

Thermal expansion and contraction are governed by matrix properties, primarily the density and amount of sand addition or sand-cement ratio. The coefficient of thermal expansion is in the range of 11 to 16×10^{-6} mm/mm/°C (6 to

9×10^{-6} in./in. $^{\circ}$ F), which is within the range of values for other cementitious materials. GFRC in common with cement paste, and, to a less noticeable extent, mortar and concrete, exhibits an anomalous behavior in that the thermal expansion coefficient varies with the moisture content of the material. The coefficient has a value at the lower end of the range when the material is fully dry or fully saturated. At intermediate levels of moisture content (50% to 80% RH), the upper values apply. The reason for this behavior is that thermal strains are made up of two movements: the normal kinetic thermal movement and the swelling pressure, a complex effect caused by moisture transfer within the system. The behavior for neat cement paste is shown in Figure 2.6.2 (References 30, 31).

2.6.3 Thermal Conductivity:

Thermal conductivity of GFRC depends more or less linearly on density of the composite and its moisture content. The typical range of thermal conductivity is 0.5 to 1.0 W/m/ $^{\circ}$ C (3.5 to 7.0 BTU/in./hr./ft 2 / $^{\circ}$ F).

2.6.4 Permeability:

The porosity of the GFRC matrix tends to distribute water throughout the system uniformly and rapidly but does not seem to increase the transport of water from one side of the sheet to the other. Laboratory tests have shown that no signs of moisture would appear on the inside of a 10 mm (3/8 in.) sheet of GFRC with rain blown onto it by a 117 km/h (73 mph) wind. Water permeability of GFRC will range

from 7.3 to 16 10^{-9} gm/Pa*s*m (5 to 11 perm-in.) at 0.25 and 0.35 water-cement ratios, respectively. Highly compacted GFRC tends to have a lower water vapor permeability than less well compacted GFRC (Reference 30).

Most formulations of the material have a vapor permeance of less than 3 perms ($1.7 * 10^{-7}$ gm/Pa*s*m), making the need for an additional vapor barrier subject to vapor flow calculations.

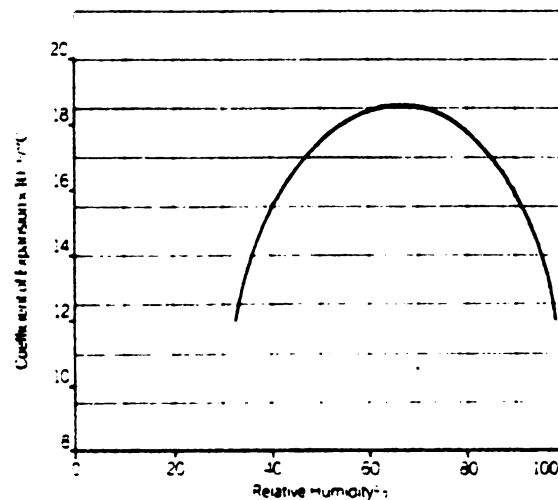


Figure 2.6.2 Relationship Between Linear Coefficient of Thermal Expansion of Cement Paste and Ambient Relative Humidity (Reference 31).

Air permeability of GFRC ranges from 4.6 perm-in. ($6.7 * 10^{-9}$ gm/Pa*s*m) for GFRC exposed to 40% RH to 0.2 perm-in. ($0.3 * 10^{-9}$ gm/Pa*s*m) for GFRC exposed to 90% RH (References 30, 31).

The air and water vapor permeances of GFRC decrease as a function of time a storage under natural weather conditions. These properties are similar to those of the cement matrix and compare favorably with those of other building materials (Reference 30).

2.6.5 Density:

The dry density of spray-up GFRC depends primarily on fiber content, water/cement ratio, polymer content, sand addition, compaction, and spray techniques. These factors also influence porosity. The typical range of density is 1700 to 2000 kg/m³ (105 to 125 pcf) for the hand sprayed material and 2000 to 2200 kg/m³ (125 to 138 pcf) for the spray-dewatered material. A knowledge of the density gives information on the general quality control procedures (References 30, 31, 32).

2.6.6 Sound Transmission

GFRC follows the mass law for sound reduction. For skins of similar design, but different weights, the STC increases approximately 6 units for each doubling of weight. GFRC's relatively high density offers good attenuation characteristics. A 10 mm (3/8 in.) sheet of GFRC at 0.2 kPa (4 psf) provides a sound transmission class (STC) of 34 (see Figure 2.6.3). However, a complete panel assembly will provide greater sound reduction conforming to most code requirement (Reference 30).

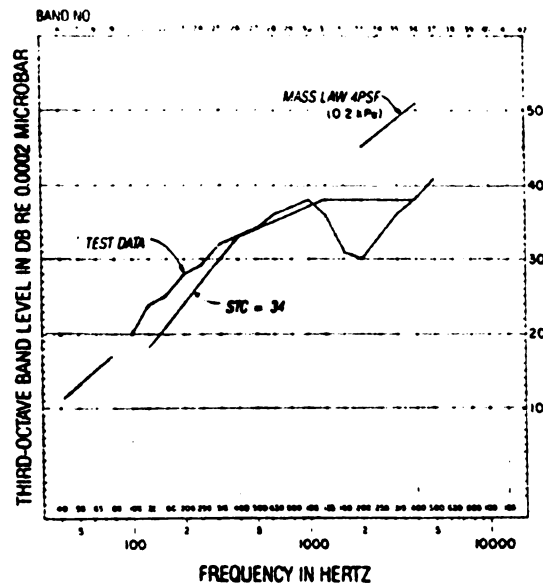


Figure 2.6.3 Relationship of Sound Reduction and Frequency (Reference 30).

2.7 DURABILITY PROPERTIES

2.7.1 General:

As a result of the reinforcement provided by randomly distributed glass fibers, the 28-day tensile strength of GFRC products is typically about 12.4 MPa (1800 psi). The value of the tensile strain at the peak tensile stress is typically 1%, which is about 100 times that of unreinforced matrix. This remarkably enhanced ductility makes it an attractive material for the production of various types of

thin building components, and facilitates the handle, transport, and erect thin GFRP panels (Reference 40).

However, on prolonged exposure to wet environments, GFRP tends to lose part of its tensile strength and most of its toughness (Figure 2.7.1), and eventually it becomes brittle. Early work with GFRP, using E-glass fibers, indicated that this decline in properties with aging is mainly the result of a chemical attack. The development of high zirconia glass fibers which are more resistant to alkali attack (known as AR-glass fibers), resulted in considerable improvements in the durability characteristics of GFRP (Figure 2.7.2 shows comparisons between AR-glass and E-glass on the basis of aging effects on MOR values); AR-glass, however, did not solve the problem completely. GFRP with AR-glass fibers also tends to lose part of its tensile strength and most of their toughness, although at a much slower rate than the GFRP composites with E-glass fibers (References 2, 41).

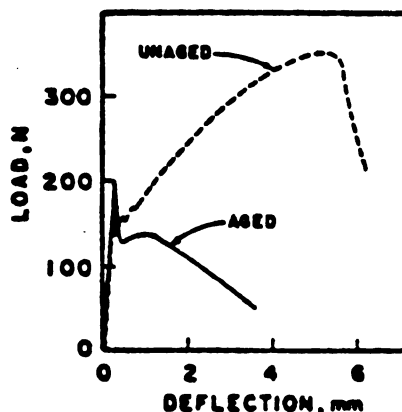


Figure 2.7.1 Effect of Aging (50°C , 122°F Water for 1 Month) on the Change in the Load-Deflection Curve of GFRP with AR-Glass Fibers (Reference 41).

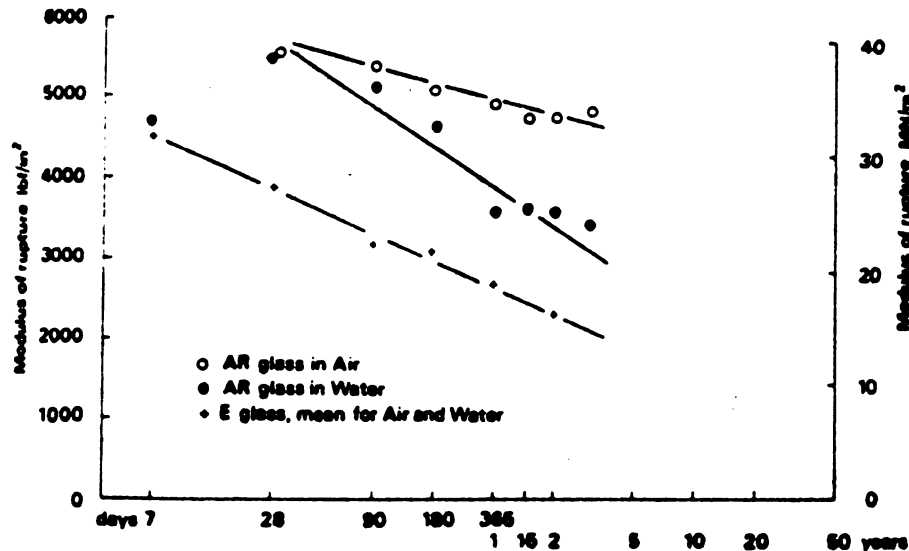


Figure 2.7.2 MOR Against Log Time for Composite Made with E-glass and AR-glass-Air and Water Storage (Reference 2).

As a result of the durability problems, the application of GFRP is limited to non-structural and semi-structural purposes. The justification for the use of GFRP in these applications is that even after prolonged exposure, the MOR of GFRP will not reduce below a lower limiting value, which is still relatively high, 10 to 20 MPa (1.45 to 2.9 ksi). This is basis for the design of GFRP panels. However, even in non-structural and semi-structural applications, there are sometimes objections to the use of GFRP because of the loss of toughness and possible embrittlement with time (Reference 41).

As a result of the durability characteristics of GFRP, the full potentials embodied in its mechanical properties

before aging has not been used effectively. Therefore, there is considerable interest in developing methods and means for improving the durability of GFRC (Reference 41).

2.7.2 Chemical Attack:

The rate of chemical attack on cementitious materials depends largely upon the extent to which reactive elements in the cement are exposed to aggressive agents and this is a function of permeability. The permeability of GFRC is lower than that of normal concretes, and consequently GFRC shows good resistance to chemical attack (References 31, 37).

It is generally true that dewatered GFRC offers slightly better chemical resistance than non-dewatered GFRC, due to its lower water/cement ratio and reduced porosity. GFRC also benefits from having a high cement content, which is another factor determining the chemical resistance of cement-based materials. Improved performance against chemical attack may be expected from the use of special cements e.g. high alumina cement or supersulfate cement (Reference 31).

2.7.2.1 Sulfate Resistance:

In the presence of moisture and sulphates a reaction takes place causing degradation of the cement; GFRC, however, is less sensitive to sulfate attack than most concretes (Reference 37).

Resistance to sulphate attack is increased by the use of sulphate resisting cement, and it is a usual practice to use this type of cement for the manufacture of GFRC which

may be in contact with sulphate solutions. Typical of such applications are silage tanks, drainage components, sewer linings and junction boxes which may be used in contact with sulphate bearing soils.

2.7.2.2 Acid and Alkali Attacks:

Portland cement releases calcium hydroxide during hydration and provides a highly alkaline environment (pH 12.5). Consequently, alkaline solutions present no particular hazard to GFRc.

Alkali-resistant glass is relatively unaffected by acidic environments although ordinary Portland cement may be degraded after long-term exposure to acids. Deleterious acid attack may occur due to the action of sour silage under certain conditions in sewers where bacterial action has produced sulphuric acid, and in certain types of soil, but can be countered by the use of sulphate resisting cement or high alumina cement (Reference 37).

2.7.2.3 Marine Environments (Reference 37):

Seawater and seaspray exposures of GFRc give mechanical property changes similar to those in fresh water exposure and natural weathering at equivalent temperatures. Some surface carbonation can occur which may detract from the appearance of GFRc, but which is not detrimental to mechanical properties (unlike in reinforced concrete where both exposure to salts and carbonation result in increased attack on the reinforcement).

2.7.3 Frost Attack:

Experience with GFRC in natural freeze-thaw environments has been good. In order to study the freeze-thaw durability of the material a series of laboratory studies have been performed (Reference 31).

ASTM C-666, "Standard Test Method for Resistance of Concrete to Rapid Freezing and Thawing," Procedure A, represents a severe standard freeze-thaw test. In this test, specimens are subjected to alternative cycles of freezing in water at 0°F (-18°C) for approximately 2 hours and thawing in water at 40°F (4°C) for approximately 1 1/2 hours. GFRC specimens were subjected to freeze-thaw cycles after 0, 8, and 26 weeks of accelerated aging. Unreinforced mortar specimens were subjected to freeze-thaw cycles after 0 and 26 weeks of accelerated aging. For each of these accelerated aging periods, six specimens were tested in flexure after 0, 100, 200 and 300 cycles of freezing and thawing (Reference 31, 37).

Flexural yield strength versus freeze-thaw cycles are plotted by solid lines in Figure 2.7.3 for GFRC specimens and by dashed lines for the companion unreinforced mortar specimens. All curves in Figure 2.7.3 represent matrix cracking strength. Numbers next to each curve indicate the number of weeks in accelerated aging conditions prior to exposure to freezing and thawing (References 31, 37).

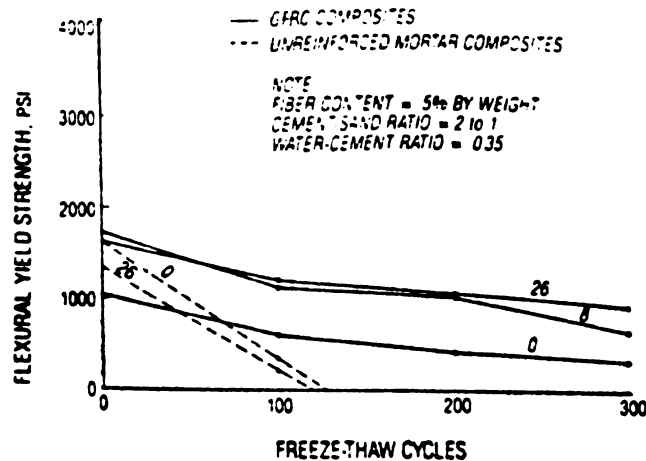


Figure 2.7.3 Flexural Yield Strength Versus Freeze-Thaw Cycles (Reference 37).

As shown in the figure, presence of the glass fibers effectively preserved the cement matrix against significant freeze-thaw deterioration. Without fibers, mortar specimens were observed to completely deteriorate before reaching 200 freeze-thaw cycles. In addition, the effect of accelerated aging prior to freeze-thaw exposure had very little effect on the resulting freeze-thaw resistance of the GFRP specimens (References 31, 37).

The ultimate strength versus freeze-thaw cycles relationships are plotted in Figure 2.7.4 for the GFRP specimens. Numbers next to each curve indicate the number of weeks in accelerated aging prior to freeze-thaw exposure. As shown in the figure, regardless of the aging conditions prior to the freeze-thaw tests, the ultimate flexural

strength decreases to approximately 10.3 MPa (1500 psi) after 100 cycles and approximately 6.9 MPa (1000 psi) after 300 cycles (Reference 37).

After 300 cycles the GFRc showed slight flaking and fiber prominence on the form side. There was severe flaking of the 'trowel' face and delamination cracks along the edges. The flakes, about 4 to 5 mm (5/32 to 13/64 in.) across and 1 mm (3/64 in.) thick, generally remained attached to the main body of the specimen by the glass fibers (Reference 37).

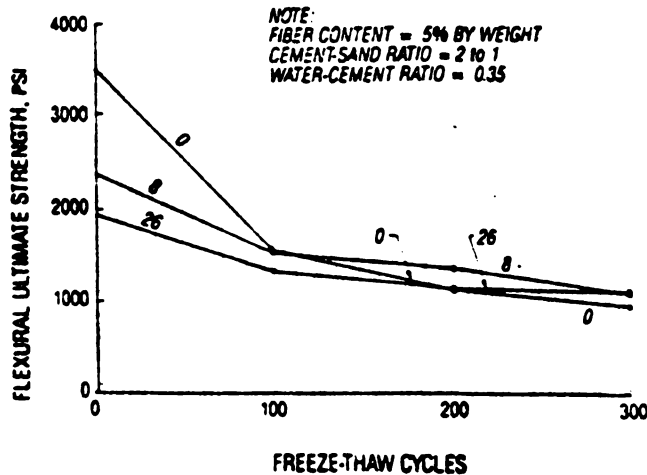


Figure 2.7.4 Flexural Ultimate Strength Versus Freeze-Thaw Cycles (Reference 37).

ASTM C-666, procedure A provides a relatively severe freeze-thaw condition at which most materials show some degradation. GFRc is no exception but it still compares favorably with other established construction materials, and

the conclusion is that freeze-thaw conditions do not pose a significant problem for the use of GFRG (Reference 37).

Freeze-thaw tests have been made on test samples cut from sprayed boards containing 5% AR-glass fiber by weight and 20% sand by total weight. The tests were conducted following the British Standard Test for Asbestos Cement Building Products, BS 4624; 1970 (50 freeze-thaw cycles). These tests involved samples that were artificially aged by soaking in 50°C (122°F) water for 90 days then subjected to 50 cycles of 16 hours at -20°C (-4°F) in air and 8 hours at 20°C (68°F) in air, followed by soaking water for 48 hours (Reference 37).

There was no visible change in the appearance of the samples after the tests, and the mechanical properties (ultimate flexural strength, modulus of elasticity, and impact resistance) were not affected (Reference 37).

2.7.4 Durability Under Natural Exposure Conditions:

Majumdar and Singh (1985), Reference 42, studied the properties of GFRG composites containing 2 to 8 vol% of AR-glass fibers of lengths 10 to 40 mm (0.39 in. to 1.57 in.) for periods of up to 10 years in various environments. These composites were made in the form of boards 8 to 10 mm (0.31 to 0.39 in.) manufactured by the spray-dewatering technique using a Portland cement matrix. The 150 mm x 50 mm (5.90 in. x 1.97 in.) specimens cut from the boards were first wet-cured for 7 days in the laboratory and then randomly distributed in three different environments: (a)

in air at 20°C, 40% RH; (b) under water at 20°C; and (c) natural weathering at Garston, UK.

An enormous amount of data has been produced in this test program because of the use of four fiber lengths 10, 20, 30 and 40 mm (0.39, 0.79, 1.18, 1.57 in.), and four levels of fiber contents, approximately 2, 4, 6 and 8 vol% in the GFRc boards (References 35, 42).

The bending, tensile and impact strength test results presented in Table 2.7.1 indicate that even after ten years of storage in various environments these properties of GFRc are still dependent on the fiber volume fraction in the composite. In this context, fiber length is found to be important only if the composites are kept in a relatively dry environment, where their strength at ten years sometimes shows an increase with increasing fiber length. When the composites are exposed to continuously wet or natural weathering conditions, no significant improvement in the long-term strength properties of GFRc can be expected by using longer fibers (Reference 42).

Assuming that the retention of initial strength properties at later ages is a suitable measure of the durability of a material, some ideas regarding the watering effects on the long-term behavior of GFRc containing various fiber proportions at different lengths can be obtained from the data given in Table 2.7.2 (Reference 42). The MOR results obtained at various times over the 10-year period

Table 2.7.1 Bending, Tensile, and Impact Strength of GFRC at 10 Years for Various Glass Contents and Glass Length (Reference 42).

Glass		Properties								
Content (vol %)	Length (mm)	MOR (MPa)*			UTS (MPa)*			IS (kJ m ⁻²)*		
		Air	Water	Weather	Air	Water	Weather	Air	Water	Weather
2.1	10	15.2	13.3	10.6	5.3	3.6	3.6	5.8	2.8	5.0
	20	15.7	14.5	11.0	4.9	4.5	3.0	7.5	2.9	4.3
	30	18.5	18.6	10.6	5.6	3.9	3.1	8.8	5.5	3.1
	40	19.4	14.7	15.0	6.5	5.6	4.6	8.9	2.0	3.2
4.4	10	23.8	18.3	17.2	7.8	5.2	5.3	13.3	2.9	6.2
	20	30.6	20.3	20.4	11.3	7.4	7.1	17.4	4.1	6.5
	30	36.0	19.4	22.4	12.8	7.9	7.7	20.7	3.9	5.2
	40	36.6	21.2	21.7	12.9	7.4	8.0	19.0	3.0	5.7
6.3	10	35.2	24.5	23.0	12.9	10.3	8.4	19.3	5.0	7.0
	20	41.5	24.7	27.4	15.1	10.9	9.9	25.6	3.9	11.5
	30	39.5	24.6	25.0	14.0	11.8	8.7	24.0	4.6	8.6
	40	47.9	25.8	29.6	18.6	10.5	10.1	24.5	3.3	8.9
8.2	10	40.7	28.3	28.1	15.3	10.2	9.3	23.2	7.5	11.3
	20	39.7	27.0	29.1	12.9	10.0	9.1	30.9	6.0	12.9
	30	49.1	32.3	27.1	18.1	12.3	9.6	24.7	6.6	8.9
	40	46.7	27.8	28.9	16.7	11.5	7.6	27.6	6.7	10.3

*MOR = Modulus of rupture; UTS = Ultimate tensile strength; IS = Impact strength.

Table 2.7.2 GFRC Strength at 10 Years as Percentage of the 28-day Values (Reference 42).

Glass		Modulus of rupture			Tensile strength			Impact strength			Ultimate failure strain*		
Content (vol %)	Length (mm)	Air	Water	Weather	Air	Water	Weather	Air	Water	Weather	Air	Water	Weather
2.1	10	83	79	63	98	61	61	77	38	68	—	—	—
	20	74	77	58	62	61	40	85	42	62	53	10	17
	30	78	83	47	76	51	41	90	89	50	121	7	9
	40	71	55	56	72	66	54	77	29	46	51	—	—
4.4	10	85	76	71	78	59	60	95	28	60	113	5	14
	20	81	63	63	82	62	60	102	26	41	136	6	6
	30	87	51	59	90	56	54	94	22	30	114	4	10
	40	88	56	57	81	53	58	86	19	37	91	4	11
6.3	10	86	67	63	81	69	56	78	24	35	124	9	15
	20	87	61	67	80	65	59	86	19	57	102	5	19
	30	87	60	61	80	75	55	86	15	38	81	5	13
	40	91	68	78	89	55	53	78	14	37	103	6	12
8.2	10	95	77	76	103	71	64	76	28	42	195	9	16
	20	84	80	86	76	71	65	65	23	50	85	9	25
	30	86	73	61	85	72	56	65	25	33	90	8	10
	40	88	67	69	75	63	42	77	24	37	73	6	7

*In tension.

have been plotted in Figures 2.7.5 to 2.7.7 to illustrate the effects of fiber content on the age-strength relationships in GFRC composites. These results show that the MOR values increase with fiber proportions and that this relative gain is maintained in the three storage conditions used for at least 10 years. In relatively dry air the MOR of GFRC composites remains essentially unchanged with time, but in water and on natural weathering significant reductions in strength take place. It should be noted that only a small proportion of the initial high failure strain of GFRC composites is retained at 10 years in wet environments. A low failure strain produces brittleness in the material and a very careful consideration of this property is necessary in design with GFRC (Reference 42).

Daniel and Schultz (1985), Reference 43, also suggested that the MOR decreased to nearly the strength level of the Limit of Proportionality (LOP) after 10 years of natural weathering in UK or in wet condition as shown in Figure 2.7.8.

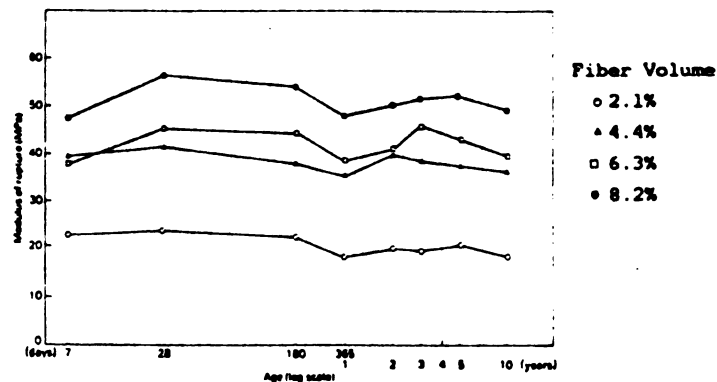


Figure 2.7.5 Bending Strength of GFRC Composites Stored in Air at 20°C, 40% RH, Fiber Length 30 mm (1.18 in.), Reference 35.

The effect of fiber content and the influence of the environment on the matrix cracking strength (or the stress at the LOP in tension) of 10-year-old GFRC are illustrated in Figure 2.7.9 (a). Matrix cracking strength of GFRC at 10 years showed an increase in fiber content, the extent of the increase depending on the different environments used. The latter is to be expected as the LOP is a matrix-controlled property, and its value depends on the curing conditions of the cement which controls its degree of hydration. The matrix cracking strain in tension for the 10-year-old GFRC (Figure 2.7.9 (b)) shows a similar trend, that is to say, these values increase with fiber content and are lower in air than in water (Reference 35).

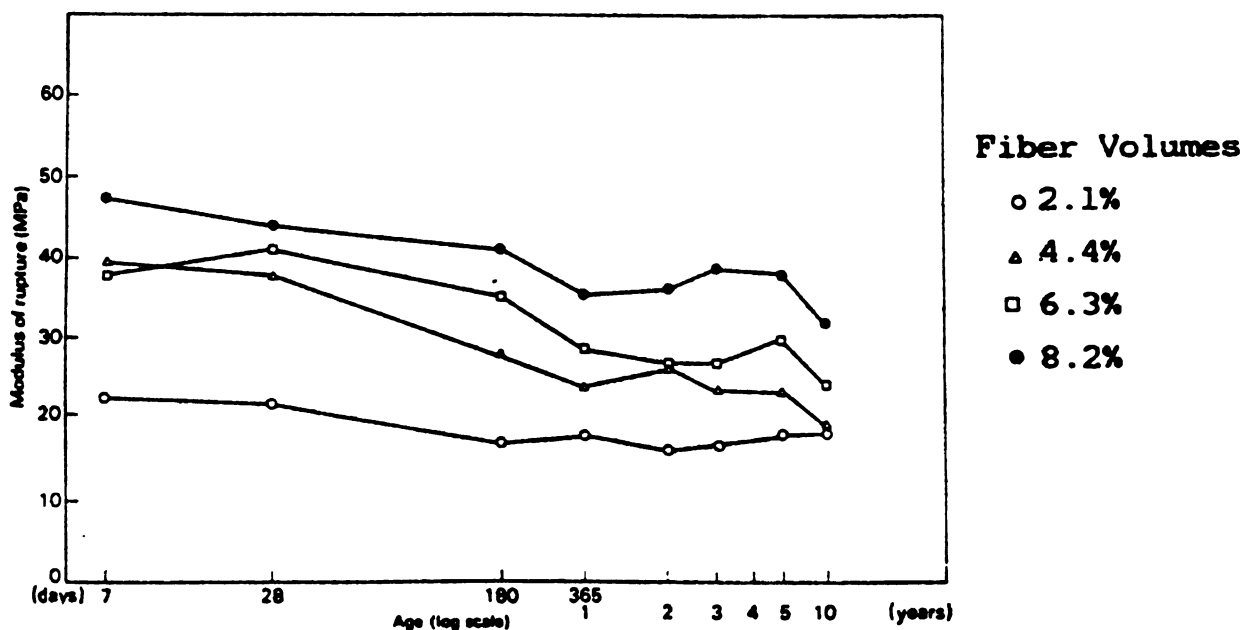


Figure 2.7.6 Bending Strength of GFRC Composites Stored Under Water at 20°C Fiber Length, 30 mm (1./18 in.), Reference 35.

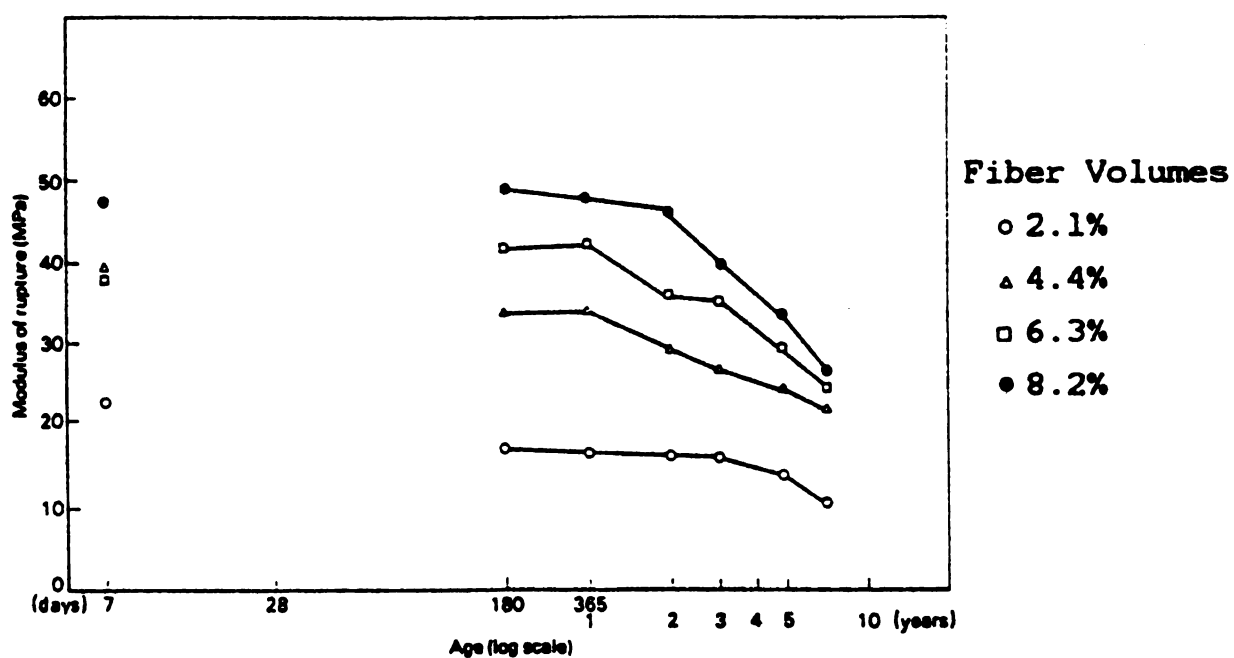
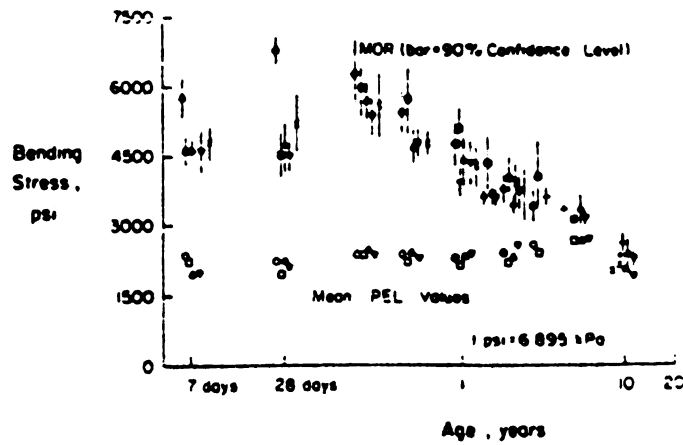
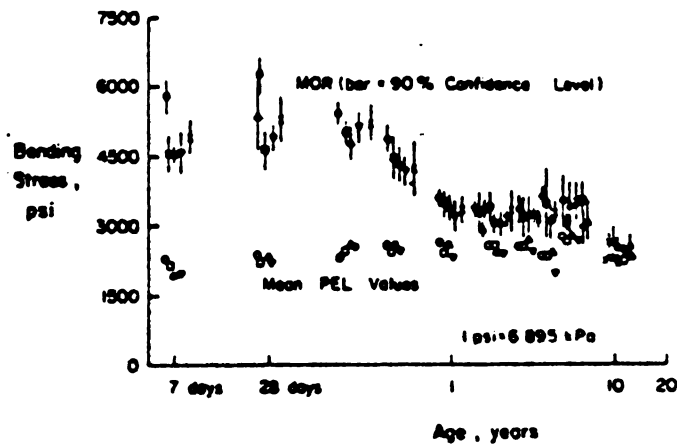


Figure 2.7.7 Bending Strength of GFRP Composites Stored on the Natural Weathering Site of Garston, Fiber Length 30 mm (1.18 in.), Reference 35.



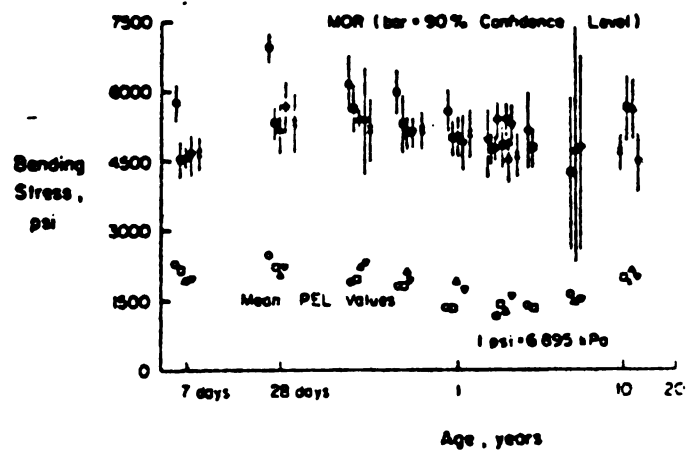
Note Different Symbols Indicate results
From Five Similar Boards

(a) Stored in Natural U.K. Weathering Conditions



Note Different Symbols Indicate Results
From Five Similar Boards

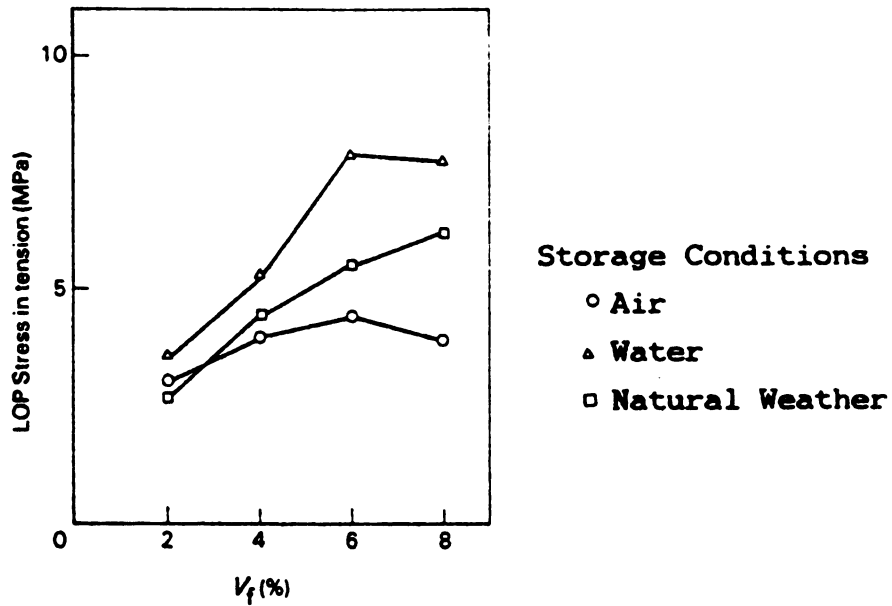
(b) Stored in Water at 64 to 68°F (18 to 20°C)



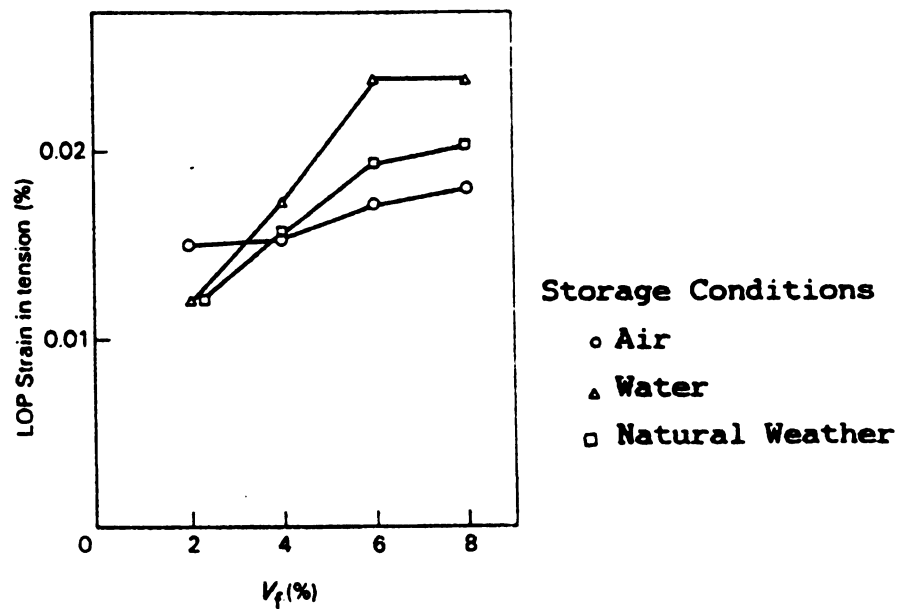
Note Different Symbols Indicate Results
From Five Similar Boards

(c) Stored in Air at 68°F (20°C) and 40% Relative Humidity

Figure 2.7.8 MOR and LOP (Proportional Elastic Limit-PEL) Versus Age for AR-Glass Fiber Composites Stored in Various Environments (Reference 43).



(a) LOP Stress



(b) LOP Strain

Figure 2.7.9 Variations in the LOP Stress and Strain in Tension with Fiber-Volume Fractions (at 10 Years) - Reference 35.

2.7.5 Aging Processes of GFRG:

Two processes have been suggested as causing the loss in strength and toughness of GFRG in wet environments:

- (a) Chemical attack on the glass fibers by the alkaline environment of cement.
- (b) Growth of hydration products between the glass filaments in GFRG.

These aging processes are described below (Reference 41).

2.7.5.1 Chemical Attack on Glass Fibers:

In a highly alkaline medium, like the one present in Portland cement matrix ($\text{pH} > 13$), the concentration of hydroxide ions is high enough to attack and break the glass network, which usually consists of -Si-O-Si- bonds. The chemical attack leads to the formation of defects on the surface of the glass, which in turn cause reduction in strength. The relations between the nature of these defects and the loss of strength can be readily established on the basis of the Griffith theory. The most direct way of estimating the extent of chemical attack is based on determining the change in the strength of glass filaments stored in cementitious environments, solutions of similar composition, or strands embedded in cement, like in the "Strand in Cement" (SIC) test, or of glass filaments removed from aged composites (Reference 41).

Tests of this kind clearly reveal the rapid strength loss due to chemical degradation in the case of E-glass.

Even with commercial AR-glass fibers, reduction in strength of glass filaments removed from GFRP materials aged in wet environment could be observed (Figure 2.7.10). The trends in Figure 2.7.10 indicate that the commercially available AR-glass fibers are not immune to chemical attack. However, it should be noted that the reduction in strength takes place mainly during the first two or three years, and then the strength becomes stable, for at least up to 10 years. Also, the strength stabilizes at values greater than about 1000 MPa, which is high enough in practice for providing useful reinforcing effects (Reference 41).

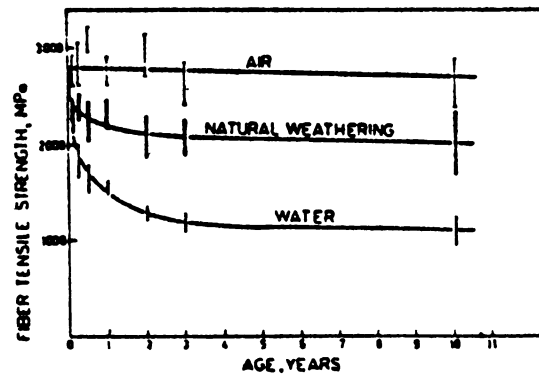


Figure 2.7.10 Reduction in Strength of AR-Glass Filaments Removed from Aged GFRP (Reference 41).

2.7.5.2 Growth of Hydration Products Between the Filaments:

It is well established that aging in wet environments results in considerable change in the microstructure of the cementitious matrix in the vicinity of the filaments. In young composite there are hardly any hydration products around the filaments, while after prolonged aging in wet conditions the spaces between the filaments become filled with hydration products, mainly dense CH crystals, which bind filaments together (Reference 41).

These changes in the interfacial microstructure are associated with the special structure of the reinforcing unit in GFRC, which is a strand composed of about 200 filaments grouped together, and not single filaments surrounded by cement matrix. In the production of GFRC, glass roving is chopped and sprayed over a mold, simultaneously with spraying of a cement mortar mix. In the spray process, the roving is dispersed into the strands which compose it, but the filaments in each strand are kept together and the whole strand unit is surrounded by the cementitious matrix. The spaces between the filaments are smaller than about 3 μm , and therefore cement grains cannot penetrate between them. The formation of hydration products in these zones is apparently slow, and is associated probably with deposition from the pore solution, which penetrates into these spaces. The process involved is a nucleation and growth one, with the glass surfaces serving as nucleation sites. Usually there is preferential growth

of CH on such surfaces and therefore, in many instances, the hydration products formed between the filaments are rich in CH (Reference 41).

It has been suggested that the densification of the matrix microstructure at the glass interface can lead to embrittlement. This can be explained either by the effective increase in the fiber-matrix bond or by the generation of local flexural stresses (Reference 41).

2.7.6 Accelerated Aging Test:

According to Litherland, et. al. (1981), Reference 44, the prediction of long-term strength of GFRC can be made by the use of accelerated aging tests. Changes in strength of strands of AF-glass fiber in Portland Cement were accelerated by aging in hot water at several temperatures. Similar accelerated aging tests were carried out with GFRC composites and the results were compared with strength changes in materials exposed to natural weathering in a variety of climates. Then predictions could be given for expected strength of GFRC composites over a period of one hundred years.

The long-term strength predictions are based on the availability of three main bodies of experimental data:

- (i) Knowledge of the direct tensile strength of strands of AR-glass fiber reinforced in cement environments, after exposure to hot, wet conditions;

- (ii) Knowledge of the strengths of GFRC composites after accelerated aging in similar aggressive conditions; and
- (iii) Knowledge of the strengths of GFRC composites after weathering for some years in a variety of real climates (as a basis for comparison).

2.7.6.1 Direct Tensile Strength of Glass Fiber Strands:

In the case of glass fiber reinforced cements and mortars the strength behavior of the cement or mortar matrix was reasonably well understood and was predictable over a period of several years. The strength of fiber/matrix bonds was less well known, but it was the strength behavior of the AR-glass fiber itself which was least understood (it was assumed that the strength of the composite is not directly controlled by the strength of the fibers). It is now important to be able to directly measure the tensile strength of glass fiber strands in a hardened and cured cement environment which represents the conditions in the composite as closely as possible (Reference 44).

For this purpose, the strand-in-cement test (SIC test) was devised. In this test a small block of cement paste or mortar is cast around part of a typical multifilament strand. The strand outside the cement is strengthened and protected by impregnation with resin, and this is continued for a short distance into the cement to prevent damage and flexing at the edge of the block. Adhesion between resin and cement is prevented by small plasticine grommets and a

final protection is given to the strand outside the cement by a coat of wax. Typical dimensions and construction of an SIC specimen are shown in Figure 2.7.11 (Reference 44).

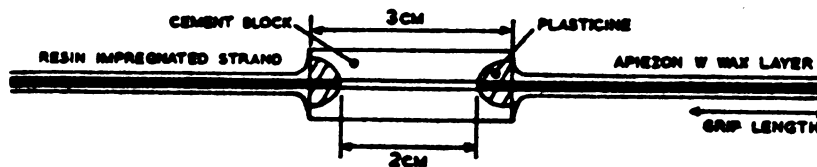


Figure 2.7.11 Strand-In-Cement (SIC) Specimen (Reference 41).

After casting the cement is allowed to set and "cure" for 24 hours at 100% RH at room temperature. Specimens are then transferred to a suitable storage environment for the required period, removed and tested in direct tension, with the strand ends being gripped in pneumatically operated grips. The tensile strength of the strand is then calculated from the breaking load, measured strand tex, and fiber density (Reference 44).

For studies of fiber strength loss under accelerated aging conditions reported by Litherland, et. al. (1981), Reference 41, several groups of specimens were immersed in water at various temperatures. A group of ten specimens was

removed at intervals and the mean strength of these ten specimens taken as a measure of the glass fiber strength. The results of many such accelerated aging tests with AR-glass fiber in rapid hardening Portland cement mortar blocks are shown in Figure 2.7.12, where each test point is the average strength of a group of ten individual SIC specimens (Reference 44).

If the rate of loss of strength of the glass fiber is directly related to the rate of some chemical reaction (e.g. at the cement/fiber interface), and further if the time taken for the SIC strength to fall to any given value (σ_{SIC}) be regarded as an inverse measure of the rate of strength loss, then an Arrhenius type relationship may be expected between the time taken for the SIC strength to fall to a given value in a particular accelerated test, and the temperature of that test (Reference 44);

$$\text{i.e., } \log_{10}(\text{time to reach } \sigma_{SIC}) \propto 1/T$$

Where; T is the absolute temperature of the accelerated test.

A family of such plots is shown in Figure 2.7.13 covering the time taken to reach strengths ranging from 1000 MN/m² to 300 MN/m² in experiments conducted at temperatures between 4°C and 80°C. The individual points were read off the best fit curves shown in Figure 2.7.12 and were restricted to the regions of Figure 2.7.12 for which actual strength measurements has been taken. This means that no extrapolation has been done at this stage; the points on the

350 MN/m² line in Figure 2.7.13 are restricted to temperatures above 39°C because strength had not yet fallen to that value in the lower temperature experiments and the one 4°C result only occurs on the 1000 MN/m² line (Reference 44).

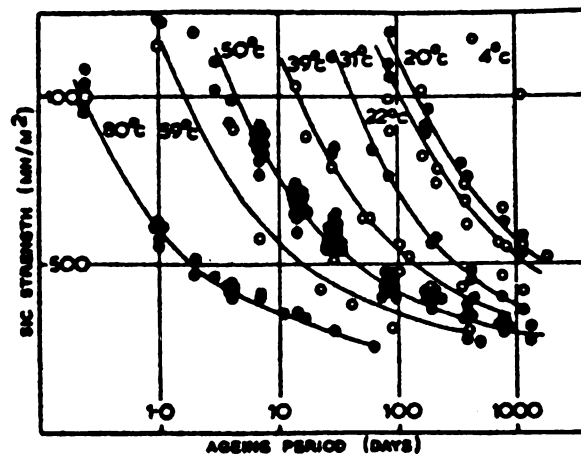


Figure 2.7.12 SIC Strength Retention in Water at Various Temperatures (Reference 44).

In Figure 2.7.13 the data points at all strength loss levels are well fitted by a family of parallel straight lines, showing good agreement with the assumed Arrhenius type relationship and also indicating a similar temperature dependence over the whole range of strength covered by the curves in Figure 2.7.12. It can be concluded from this that

the form of the SIC curves in Figure 2.7.12 is the same at all temperatures and that knowledge of the complete strength loss curves obtained at high temperatures may be used to predict the values of strengths expected at very long times and lower temperatures. Interpolation on, and extrapolation of, the straight lines in Figure 2.7.13 thus provides the means of constructing SIC strength-time curves at any chosen temperature in the range 0-100°C and of extending the existing low temperature curves in Figure 2.7.12 to very long time (Reference 44).

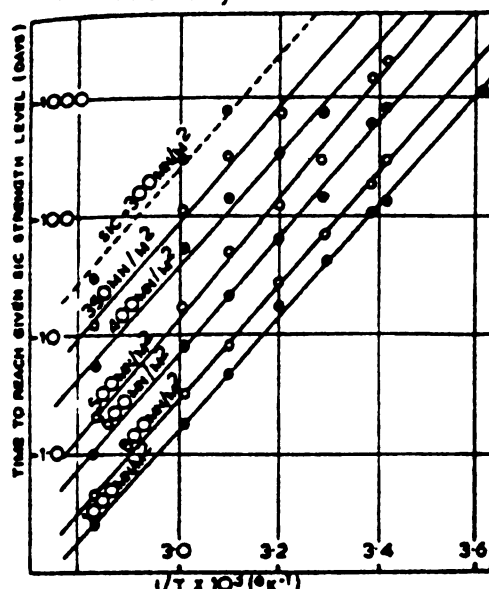


Figure 2.7.13 "Arrhenius" Plots (Reference 44).

50°C has been the most widely used acceleration temperature because it gives results within a reasonable experimental time scale without excessive danger of altering the nature of the chemical reactions between glass and cement. Because the $\log(\text{time})$ vs. $1/T$ lines in Figure

2.7.13 are all parallel to each other, it is possible to "normalize" them into one single line by plotting the log of the time at some temperature T relative to the time at some standard temperature-against $1/T$. This effectively combines and averages all the data for different strength levels given in Figure 2.7.13, into one overall picture of the relative acceleration of strength loss at different temperatures. It is also a convenient way of correlating strength changes expected over very long periods of time at much lower temperatures (Reference 44).

This normalization has been carried out to produce Figure 2.7.14, taking the widely used 50°C condition as the standard for comparison. The logarithm of the ratio of the time taken for the SIC strength to fall to a given value at $t^{\circ}\text{C}$ relative to the time to fall to that value at 50°C was plotted against the inverse of the absolute temperature corresponding to $t^{\circ}\text{C}$ - the times being read off the fitted curves in Figure 2.7.12 (Reference 44).

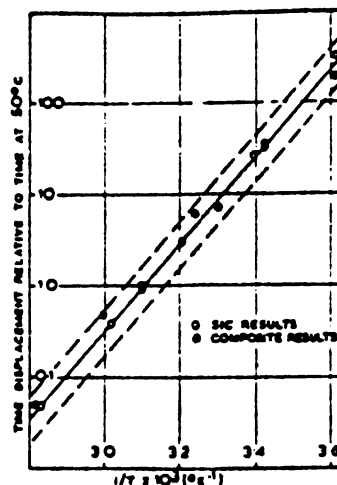


Figure 2.7.14 "Normalized Arrhenius" Plot (Reference 44).

The good linearity of the $\log(\text{time})$ vs. $1/T$ plot shown in Figure 2.7.13 and 2.7.14 indicates that essentially one chemical reaction or corrosion mechanism is controlling the strength changes over the whole experimental temperature range of 20°C to 80°C . This, taken with the good reproductivity of the results, gives confidence in the use of accelerated tests, completed in short and convenient experimental times, to predict strength behavior at low temperatures over longer times. Despite the earlier reservations regarding possible changes in the nature of the reactions involved, it now appears reasonable to use higher temperatures than 50°C (122°F) for these accelerated tests and thus obtain information even more quickly (Reference 44).

2.7.6.2 Accelerated Aging of GFR Composites:

Earlier experiments had shown that the strength-time curves of composites immersed in hot water show two distinct regions; a steadily falling initial portion followed by a constant or near constant strength region. Separate experiments had established that the rate of loss of strength in the falling of region is uninfluenced by cycling between hot and cold, wet and dry, or hot wet and freezing conditions but is essentially governed by the time spent at the wet, elevated temperature condition. The initial strength fall occurred more rapidly at higher temperatures but the very long-term strength appeared to be approximately independent of temperature at higher temperatures - although

possibly slightly temperature-dependent at lower temperatures ($<50^{\circ}\text{C}$) - Reference 44.

Figure 2.7.15 shows the results of several series of tests in which strips of composite 150 mm (5.91 in.) long x 50 mm (1.97 in.) wide x 6-8 mm (0.24 - 0.31 in.) thick were immersed in water at temperatures ranging from 4°C to 80°C . Groups of six samples were removed after various aging periods and their flexural strengths measured. The points in Figure 2.7.15 represent the overall average of results of several repetitions of these experiments using different composite boards manufactured and aged on separate occasions (Reference 44).

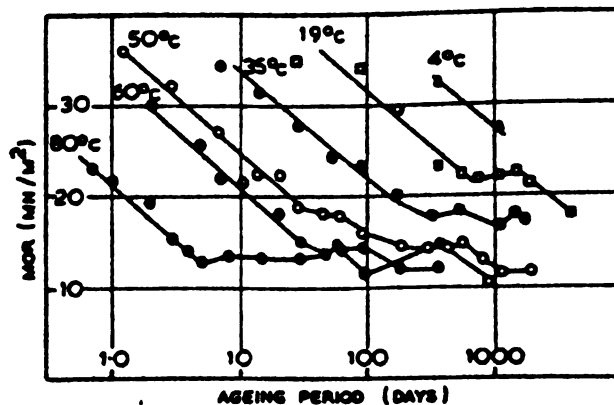


Figure 2.7.15 Strength Retention of GFRC Composites in Water at Various Temperatures (Reference 44).

From Figure 2.7.15 it can be seen that, at the higher accelerated aging temperatures of 60°C to 80°C, there is an initial fall in strength - and then a sharp transition to a constant strength region for the remainder of the aging period. Aging at the lower temperature of 50°C gives a similar fall in strength over the earlier portion of the curve; there is then a smoother, more gradual, transition to the same long-term strength at the end of the aging test. At even lower temperatures of 4°C, 19°C and 35°C, the initial falling portion of the curve is still parallel to the higher temperature results - but occurs much more slowly. Thus it seems reasonable to assume that, over a very long period, the strengths at these lower temperatures will ultimately reach the level indicated from the constant strength regions of the higher temperature curves (Reference 44).

It was concluded from these tests that:

- (a) Accelerated aging of composites over relatively short times in water at elevated temperatures could be used to produce materials in which the strength of the glass reinforcement had been reduced to a level corresponding of that attained over many years at lower temperatures; and
- (b) The temperature coefficient given in Figure 8.12 may be used to make quantitative estimates of particular time transpositions.

2.7.6.3 Weathering of GFRC Composites in Real Climate Conditions:

Figure 2.7.16 shows GFRC composite strengths after exposure to real weathering in comparison with strengths after the accelerated aging tests at 50°C, 60°C and 80°C described above. The weathering results extend up to 10 years in UK, five years in Toronto and two years in Bombay (Reference 44).

The form of the strength loss in real conditions is the same as that in the accelerated tests. As indicated by the early laboratory cycling tests, the changes in humidity and temperature which occur in real climate have not introduced sudden or unexpected changes in the pattern of strength behavior (Reference 44).

The fall in strength in real weathering occurs much more slowly than in the accelerated aging tests. However, there does appear to be a temperature-dependence as indicated by the relative positions of the curves for different climates with strength loss occurring most rapidly at Bombay and much more slowly at Toronto (Reference 44).

In fact the results show that temperature dependence in real weather is very similar to that in accelerated tests and that the mean annual temperature of a location or climate may be used to correlate the weathering strength losses with accelerated test results. This is shown in Figure 2.7.17 where the rate of strength changes at a number of sites around the world have been added to the Arrhenius

plot previously determined from accelerated strand and composite tests at different temperatures. Consider the very wide range of experiments and conditions, the agreement with the original straight line plot is very good. There is an indication that at Bombay the rate of strength loss is significantly less than predicted - perhaps due to the concentration of rainfall in a specific season followed by prolonged dry conditions in which glass/cement reactions are slowed down due to the reduced availability of water. There is a similar effect with preliminary results from a very dry site in Arizona. Generally, however, it appears possible to make a reasonable prediction of the strength loss behavior in a variety of climates from a knowledge of the mean annual temperature and accelerated composite aging test data (Reference 44).

It will be seen that strength is expected to fall slowly over some 30 to 40 years in cooler climate - but will fall more rapidly in hot climates. The very long-term strengths in both climates will be similar; the overall average value of the accelerated composite results for times equivalent to 40 to 600 years at 10°C being 13.6 MN/m² with a standard deviation of 1.6 MN/m² from tests at temperatures of 50°C, 60°C and 80°C (Reference 44).

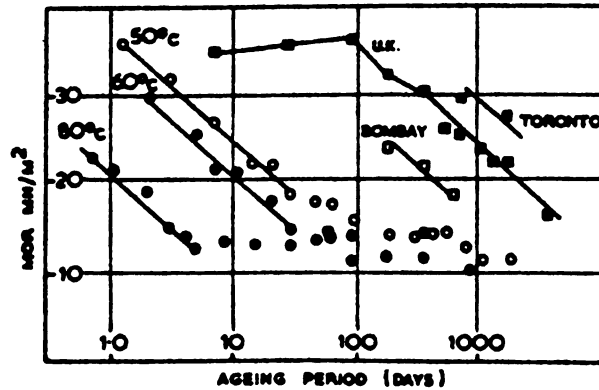


Figure 2.7.16 Strength Retention of GFR Composite in Water and Weathering (Reference 44).

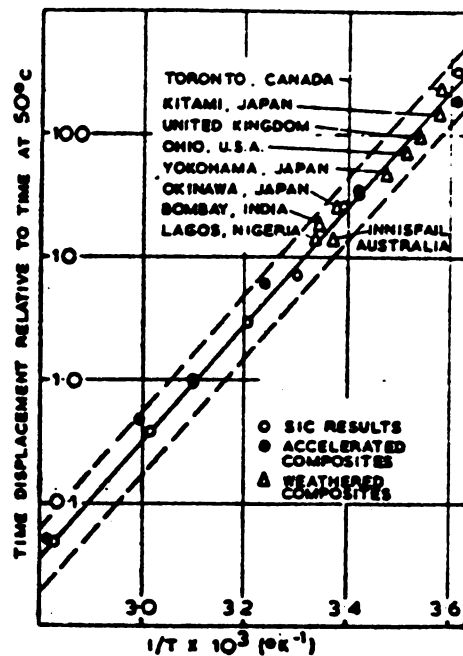


Figure 2.7.17 "Normalized Arrhenius" Plot Including Weathering Data (Reference 44).

2.7.7 Improvement of GFRC Durability:

The ways to improve durability of GFRC are summarized in Figure 2.7.18. The first way is to increase the durability of reinforcement in GFRC, that is, the glass fiber itself. This includes the improvement of glass composition by introducing oxides such as ZrO_2 , ThO_2 , SnO_2 , and improvement by the treatment of glass fiber surfaces. The second way is to improve GFRC durability by the modification of matrix. This could be accomplished by introducing pozzolan materials to reduce the $Ca(OH)_2$ formation; introducing polymer emulsions; using cements available other than Portland cement such as high alumina cement, slag cement, supersulphated cement; and using special cements developed for GFRC (Reference 7).

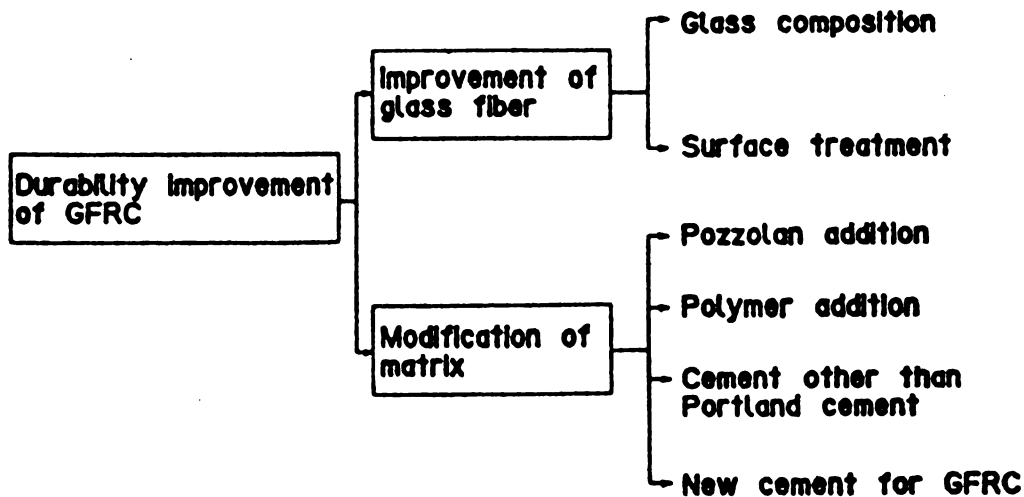


Figure 2.7.18 How to Improve Durability of GFRC (Reference 7).

2.7.7.1 Glass Composition Modification:

As mentioned in Section 2.1, high zirconia glass fibers, known as AR-glass fibers, are widely used for the purpose of increasing the alkali resistivity of glass fibers.

2.7.7.2 Surface Treatment:

According to Hayashi, et. al. (1985), Reference 7, alkali resistivity in cement environment of AR-glass fibers can be largely improved by applying alkali resistant organic materials on zirconia-containing glass fiber. Figure 2.7.19 illustrates the durability improvement of AR-glass fiber with various coatings such as Phenol, Furan, and polyvinyl alcohol (PVA) as evaluated by the strand in wet OPC paste test at 80°C (122°F). The AR-glass fibers coated with PVA (heat treated) and Furan displayed noticeable improvements in tensile strength retention over conventional AR-glass fiber. These improvements were brought about probably because the chemical reaction between glass fiber and calcium hydroxide was reduced by the Furan and PVA coatings on the glass fiber. Figure 2.7.20 shows the MOR of sprayed GFRC (5% GF) using PVA coated AR-glass fiber after accelerated aging in 80°C water. The mortar was prepared with a water-to-cement ratio of 0.36 and sand-to-cement ratio of 0.6 (Reference 7).

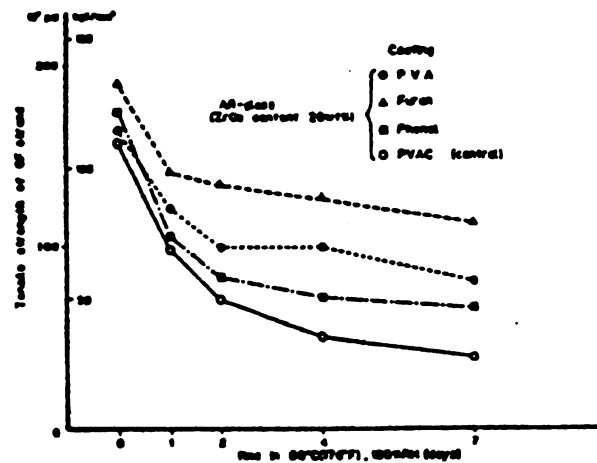


Figure 2.7.19 Strength of Glass Fiber Strand with Various Coatings in Wet OPC Paste at 80°C (176°F) - Reference 7.

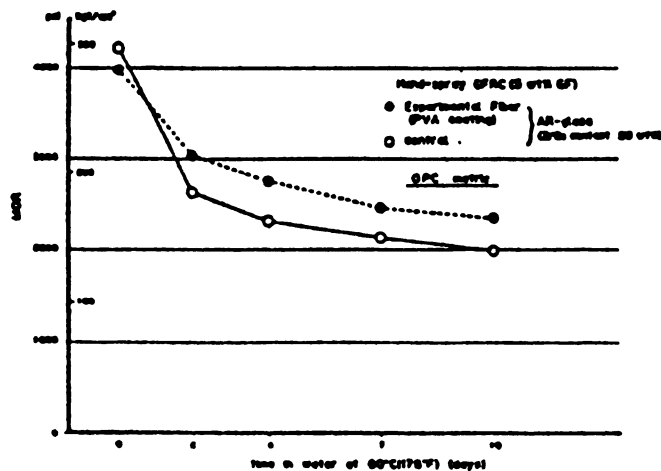


Figure 2.7.20 MOR of GFRC Using Specially Coated AR-Glass Fiber After Accelerated Aging in 80°C (176°F) Water (Reference 7).

2.7.7.3 Pozzolan Addition:

(a) Fly Ash:

Singh, et. al. (1984), Reference 18, suggested that the trends in the change of properties of fly ash containing GFRC with time are similar to those of composites made from neat OPC (Figure 2.7.21 to 2.7.23). In a relatively dry condition, there is very little change with time but in wet conditions and under natural weathering various strength properties show reductions from their peak values. Compared to their neat OPC counterpart, GFRC materials containing fly ash have lower initial strength and LOP values. The changes in these properties with time depend on the environment of storage. When kept continuously under water, in the 40% fly ash composite for instance, there is a substantial increase in the LOP value reflecting greater hydration of the cement but this is accompanied by a significant reduction in MOR from the peak value of 32 MPa (4.6 ksi) reached after one year. Under water the impact strength of the material is also reduced to a quarter of its initial value. In relatively dry air, there is virtually no change in properties from 28 days to 11 years. Natural weathering results show more or less the same trend as in water (Reference 18).

However, according to Leonard, et. al. (1984), Reference 4, fly ash improves the durability of GFRC when fly ash is used to prevent the growth of CH in between the filaments. Leonard used blended cements prepared with two

fly ashes as matrices in GFRc composites in an attempt to improve their durability. The hydrated matrices from the two blended cements investigated had similar strength and composition. Both fly ashes reduced the CH content to the same extent but in both cases the pH level was only slightly reduced compared to the Portland cement matrix. In spite of these similarities, the GFRc prepared with one fly ash showed considerable improvements in durability while the other one had only a small positive effect as shown in Figures 2.7.24 and 2.7.25. SEM observations indicated that the improved durability in one case was associated with modifications in the microstructure of hydration products deposited in between the glass filaments, resulting in a

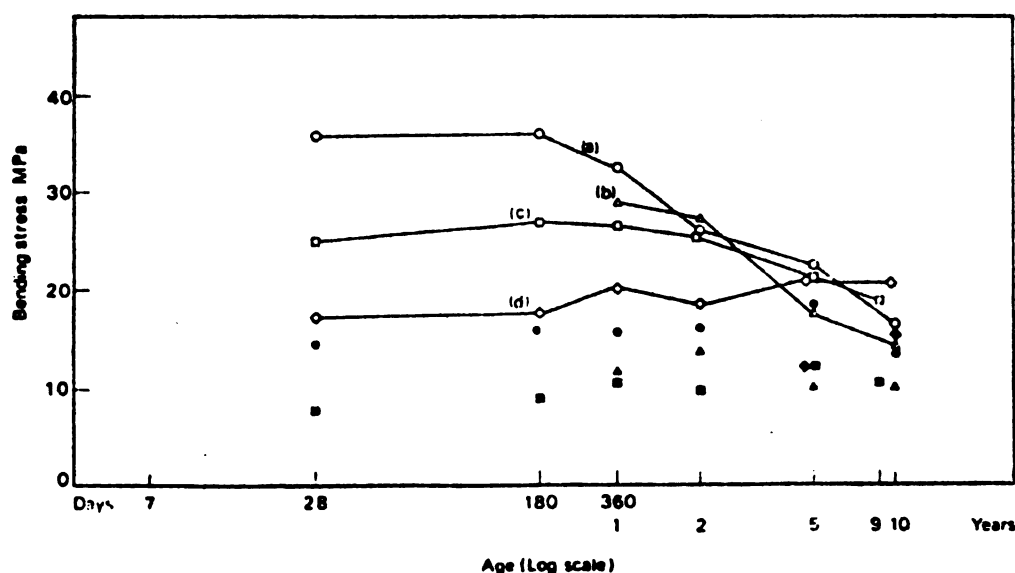


Figure 2.7.21 MOR (Open Symbols) and LOP (Solid Symbols) of GFRc Composites Containing (a) OPC, (b) 60% OPC, 40% Fly Ash, (c) Pozament, and (d) 60% OPC, 40% Fly Ash Modified by Styrene Butadiene, Stored in Natural Weather in UK (Reference 18).

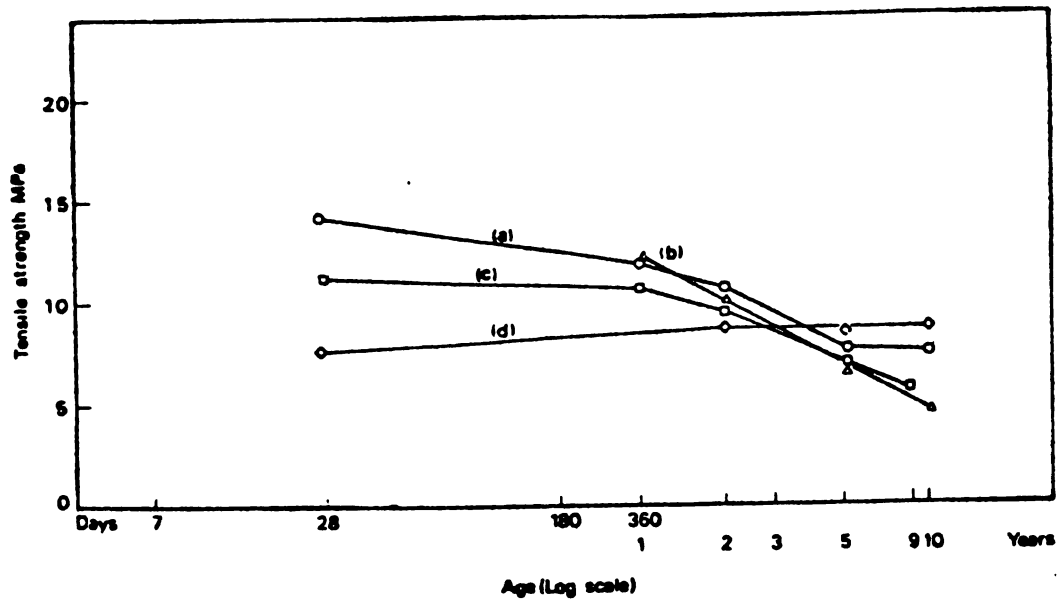


Figure 2.7.22 Ultimate Tensile Strength of GFRc Composites Containing (a) OPC, (b) 60% OPC, 40% Fly Ash, (c) Pozament, and (d) 60% OPC, 40% Fly Ash Modified by Styrene Butadiene, Stored in Natural Weather in UK (Reference 18).

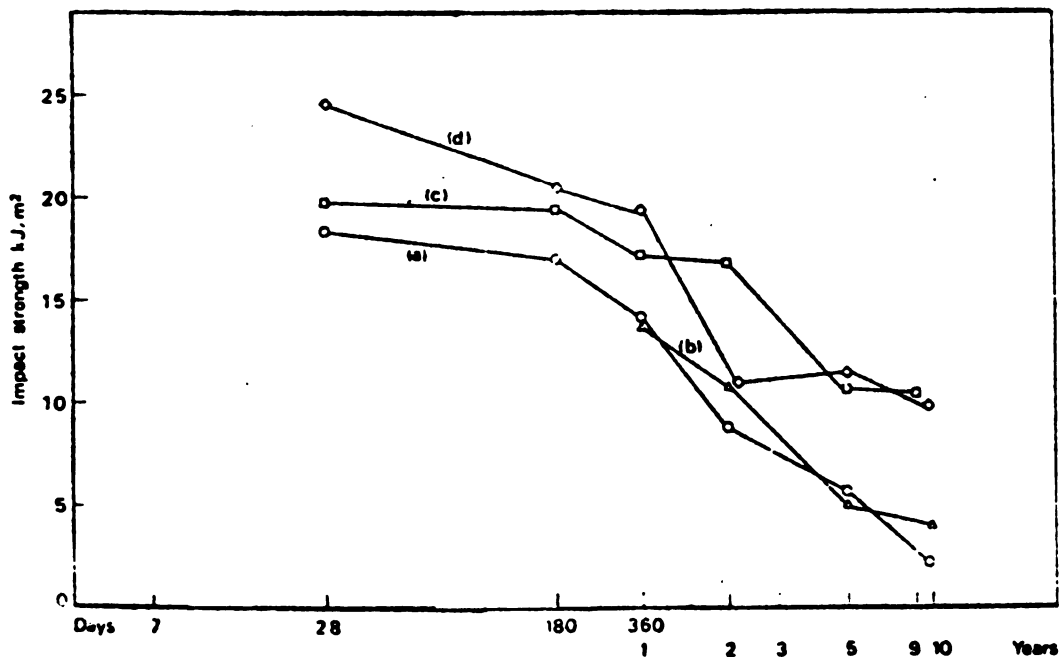


Figure 2.7.23 Impact Strength of GFRc Composite Containing (a) OPC, (b) 60% OPC, 40% Fly Ash, (c) Pozament, and (d) 60% OPC, 40% Fly Ash Modified by Styrene Butadiene, Stored in Natural Weather in UK (Reference 18).

much more open structure compared to that of Portland cement matrix or the other blended cement. It is therefore suggested that the potential of the blended cement matrix to improve the durability of GFRc is associated with its ability to modify the microstructure of the paste at the glass fiber interfaces (Reference 4).

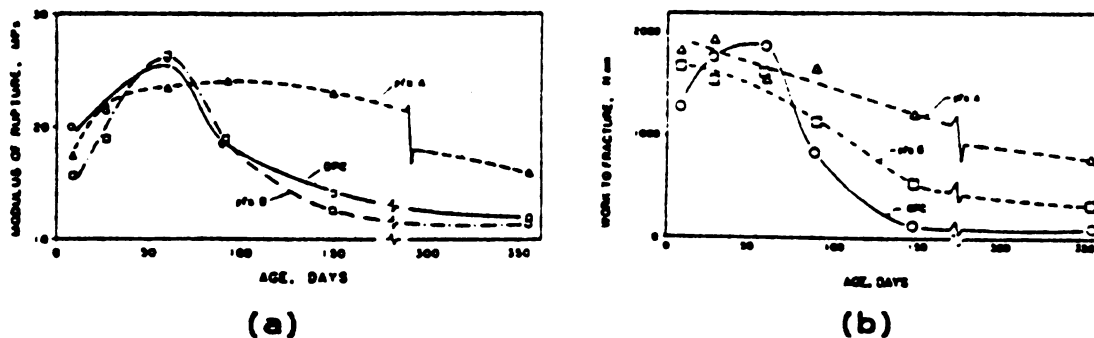


Figure 2.7.24 Effect of Aging in Water at 20°C on the (a) MOR, and (b) Toughness (W.F.) of GFRc Composites Prepared from Matrices of OPC and Blended Cements with 5% Fly Ash (Reference 4).

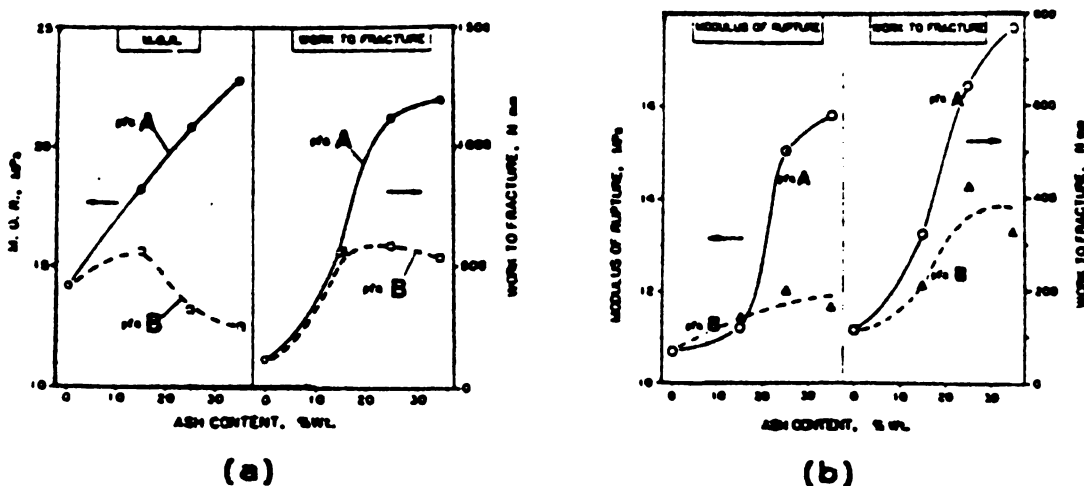


Figure 2.7.25 Effect of Fly Ash Content on the MOR and Toughness (W.F.) Values of GFRc Composites Aged in Water at 20°C for (a) 150 Days, (b) 1 Year (Reference 4).

(b) Silica Fume:

According to Bentur (1987), Reference 45, direct incorporation of silica fume in the glass fiber strand prior to the incorporation of strands in cement-based materials was found to be an effective means for obtaining a composite of improved durability. Two treatments were studied by Bentur: fiber treatment obtained by immersion of the reinforcing strand in the slurry, prior to their incorporation in the composite, and modification of the matrix by replacing 10% of cement with silica fume. The fiber treatment was achieved by immersing the glass fiber roving in silica fume slurry for 10 minutes, followed by air drying for 15 minutes. Figure 2.7.26 illustrates the effect of accelerated aging on the MOR and toughness (WOR) of the composites (References 19, 45). GFRc composites in which the fibers were not treated with silica fume eventually became brittle during the accelerated aging treatment, and they lost more than 85% of their initial toughness. The use of silica fume for fiber treatment resulted in a marked improvement, and prevented the embrittlement of composites which retained more than 50% of their original toughness after 5 months of accelerated aging. The combination of fiber treatment and matrix modification (by replacing 10% of cement with silica fume) gave some added benefits over the fiber treatment when judged on the basis of WOF retention. However, treatment of the matrix only did not result in any significant improvement in durability (Reference 19).

Evaluation of the aging trends based on the MOR values leads to similar conclusions regarding the effect of silica fume treatment. The MOR dropped to about 50% of its initial value when no fiber treatment was provided. This value is not much higher than the matrix cracking stress. The treatment of fibers resulted in the elimination of much of this drop in MOR, and supplementary treatment, to replace 10% of the Portland cement matrix with silica fume, did not result in improved durability performance in MOR over that already gained by fiber treatment. However, matrix treatment, not accompanied by fiber treatment, did not lead to any significant change in the durability performance evaluated on the basis of the MOR curves (References 19, 45).

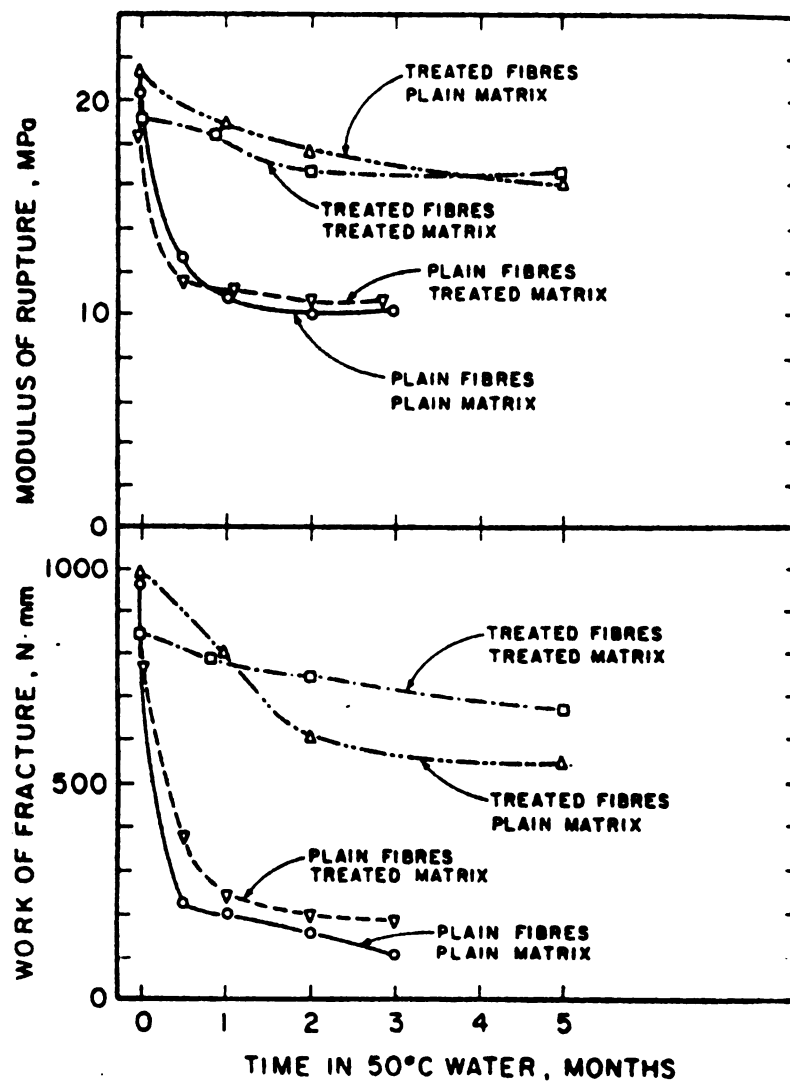


Figure 2.7.26 Effect of Accelerated Aging in 50°C Water on MOR and Toughness (WOR) of composites with AR-Glass Fibers with Various Treatments of Silica Fume (Reference 19).

2.7.7.4 Polymer Addition:

Bijen (1983), Reference 21, showed some improvements in the durability of GFRC composite by adding polymer into the matrix. The polymer-modified glass fiber reinforced cement (Forton P-GFRC) composite contained E-glass fibers instead of AR-glass fibers and a thermoplastic polymer in the form of water-dispersed particles (latex). This polymer emulsion is mixed with cement and sand to form a mortar. It is claimed that when the fiber bundles are mixed with this mortar, the glass fiber filaments are surrounded by the polymer particles and thus are screened off and protected against the migration of cement hydration products, as well as possible chemical attack.

Figure 2.7.27 shows typical stress-strain curves for GFRC with AR-glass fibers and Forton P-GFRC after 28 days (a) and after further aging of ten weeks at 50°C (122°F) (b). Figure 2.7.28 and 2.7.29 give comparative values for tensile and bending strength of composites aged submerged at 20°C (68°F) water temperature and at 20°C (68°F) and 65% RH. Figure 2.7.30 shows the results concerning impact strength. Results of the accelerated tests where the specimens had been submerged in 50°C (122°F) water are shown in Figure 2.7.31 through 2.7.36 (References 21, 46).

The AR-GFRC and Forton P-GFRC tested have almost the same tensile strength after curing for 28 days (Figure 2.7.28). When aged under conditions of 20°C (68°F), the Forton P-GFRC shows a slight increase in tensile strength,

while under accelerated aging conditions, a slight decrease is observed. The tensile strength of the AR-GFRC decreases with time. Under conditions of accelerated aging, this decline is found to proceed much faster than for Forton P-GFRC (Figure 2.7.31). A remarkable difference observed under accelerated aging conditions is that Forton P-GFRC does not show a significant change in properties after one week, while most properties in the AR-GFRCs do not obtained a constant level even after 26 weeks of accelerated aging (References 21, 46).

At 28 days, the deformation capacity (Figure 2.7.32) of the AR-GFRC is about twice as high as that of Forton P-GFRC. However, under conditions of accelerated aging, the deformation capacity of the AR-GFRC declines faster than that of Forton P-GFRC. The ultimate level of the Forton P-GFRC is higher (References 21, 46).

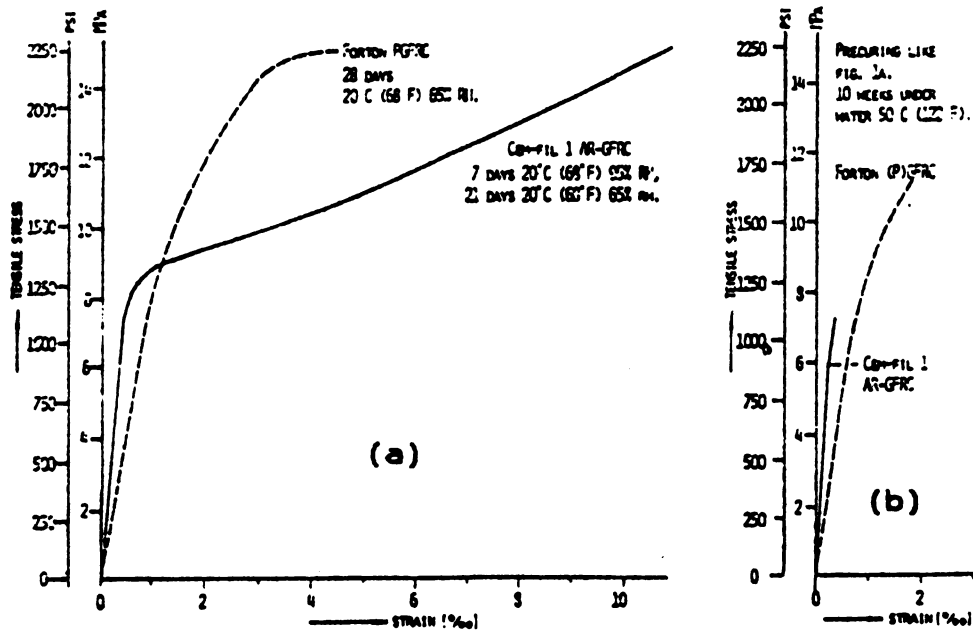


Figure 2.7.27 Typical Tensile Stress-Strain Curve for AR-GFRC and Forton P-GFRC after (a) 28 Days Curing at 20°C (68°F) and (b) the Next 26 Weeks Under Water at 50°C (122°F) - Reference 21.

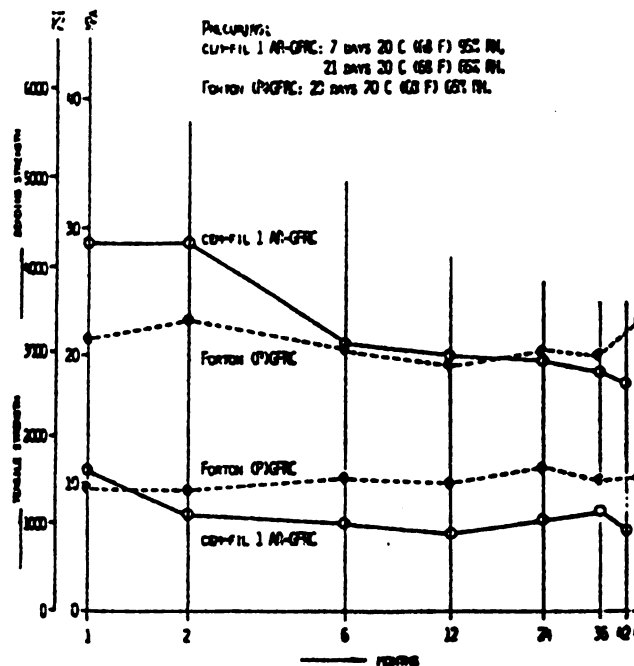


Figure 2.7.28 Bending and Tensile Strength Development as a Function of Time, Curing Under Water at 20°C (68°F) - Reference 21.

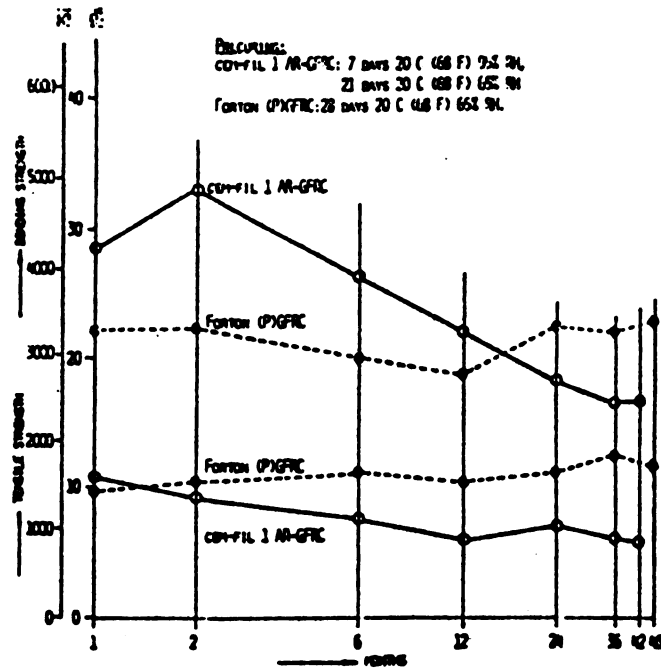


Figure 2.7.29 Bending and Tensile Strength Development, Curing at 20°C (68°F) and 65% RH (Reference 21).

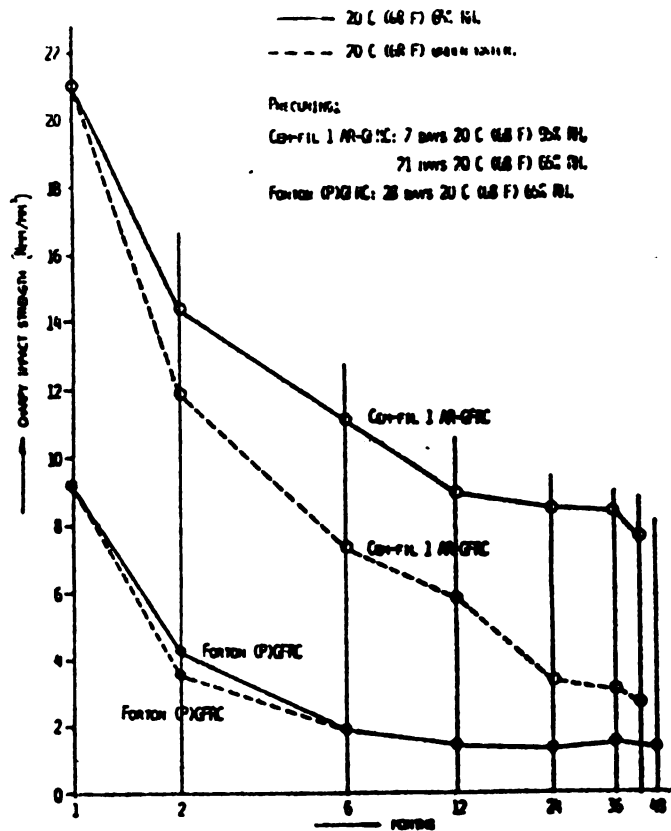


Figure 2.7.30 Impact Strength Development (Reference 21).

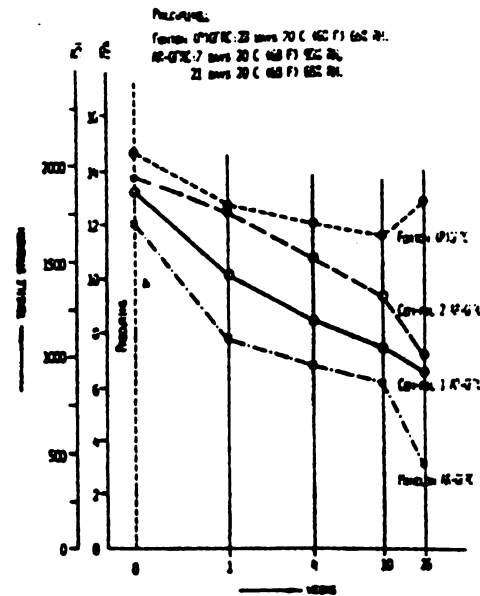


Figure 2.7.31 Tensile Strength Development Under Accelerated Aging at 50°C (122°F) Under Water (Reference 21).

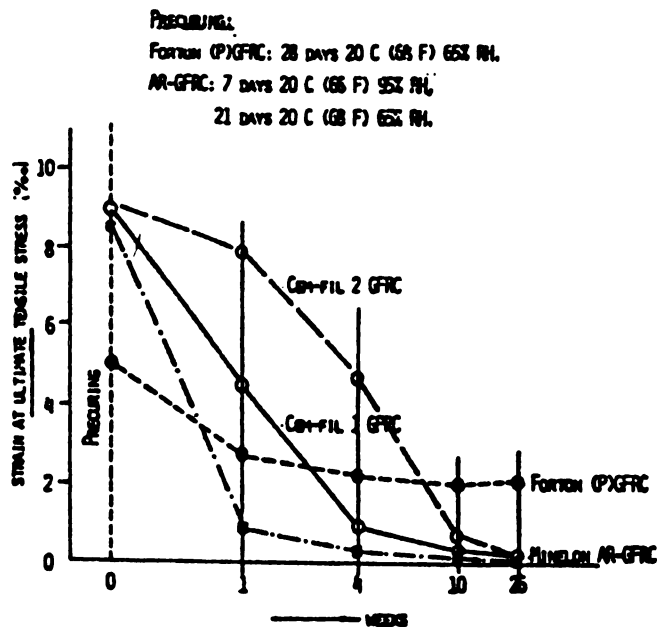


Figure 2.7.32 Development Strain at Ultimate Tensile Stress Under Accelerated Aging at 50°C (122°F) Under Water (Reference 21).

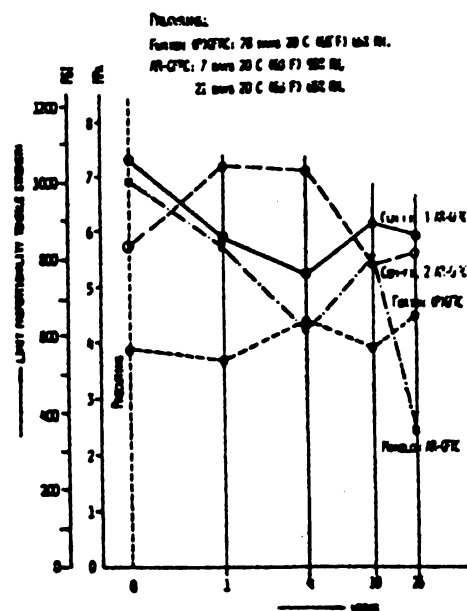


Figure 2.7.33 Development of Limit Proportionality in Tension Under Accelerated Aging at 50°C (122°F) Under Water (Reference 21).

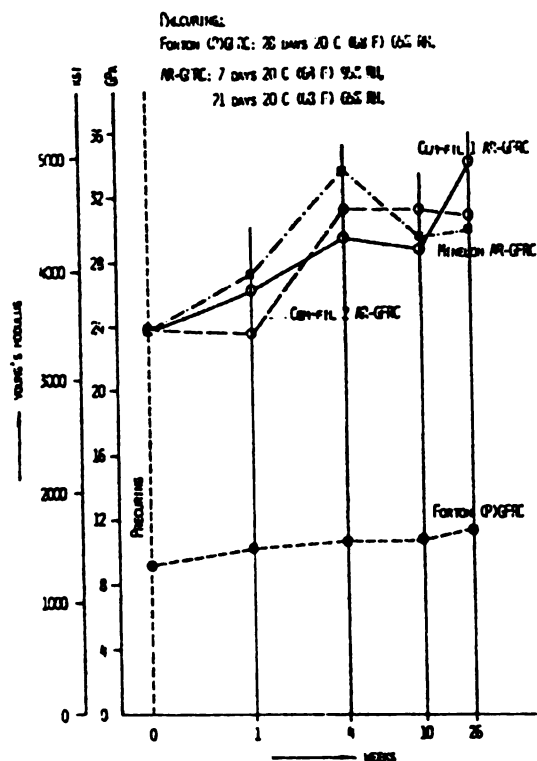


Figure 2.7.34 Tensile Young's Modulus Development Under Accelerated Aging at 50°C (122°F) Under Water (Reference 21).

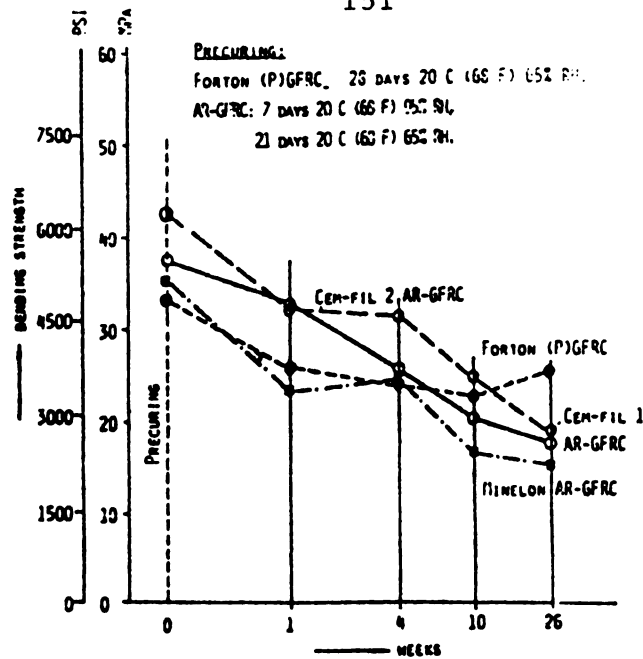


Figure 2.7.35 Bending Strength Development Under Accelerated Aging at 50°C (122°F) Under Water (Reference 21).

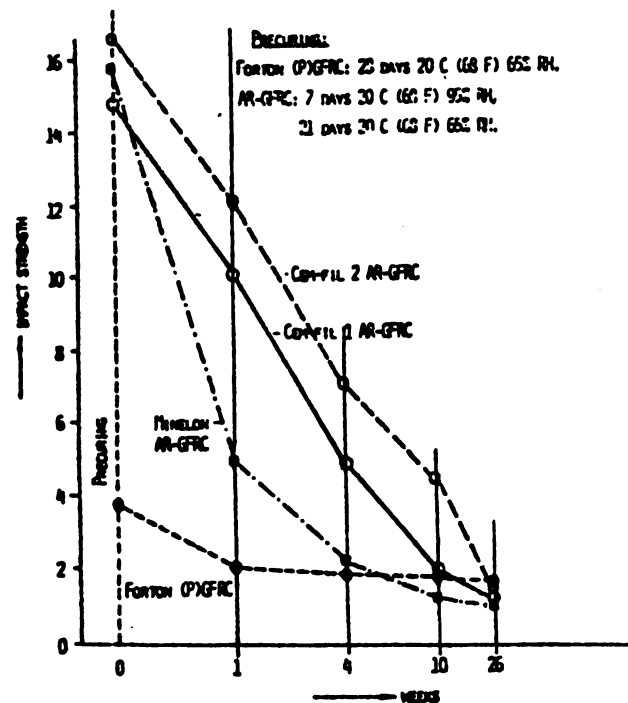


Figure 2.7.36 Impact Strength Development Under Accelerated Aging at 50°C (122°F) Under Water (Reference 21).

The limit of proportionality (Figure 2.7.33) does not show any coherent behavior for the AR-GFRCs nor for the Forton P-GFRC. Young's modulus (Figure 2.7.34) also increases over time for all GFRCs but only to a limited extent for P-GFRC. The increase in the Young's modulus will be due to both an increase of modulus of the matrix as well as an improvement in the fiber-matrix bond. The modulus of the AR-GFRC is higher than that of the Forton P-GFRC; polymer in the matrix of the latter reduces the modulus, as is expected with polymer-modified mortars (Reference 21).

Initially, the AR-GFRCs have a higher bending strength than the P-GFRC; this is due to their greater strain capacity. Over time, the bending strength of AR-GFRC declines more than that of P-GFRC. In the end, the bending strength of the AR-GFRC is lower than that of the Forton P-GFRC (Reference 21).

The impact resistance development (Figures 2.7.30 and 2.7.36) is similar to the development of the deformation capacity or, even more, to that of the energy of failure, although the latter shows a smaller decrease (Reference 21).

2.7.7.5 Cements Other Than Portland Cement for GFRC:

(a) High-Alumina Cement (HAC):

HAC is well-known for its rapid hardening and less alkalinity when compared with Portland cement. Majumdar (1981), Reference 6, has produced ten-year durability results for HAC composites reinforced with AR-glass fibers

and E-glass fibers kept in various environments (Figure 2.7.37 through 2.7.41).

In wet conditions a reduction in strength is observed to take place. In natural weather in UK the 10-year modulus of rupture and impact strength values are 22.8 MN/m^2 and 6.7 KJ/m^2 , respectively, corresponding to the 28-day values of 41.2 MN/m^2 and 22.8 KJ/m^2 . These values are better than the corresponding results obtained with Portland cement composites made from AR-glass fibers (Reference 6).

The results presented in Figure 2.7.35, 2.7.39 and 2.7.40 show quite clearly that in HAC composites stored under water, the AR-glass fiber provides a more durable reinforcement than E-glass (Reference 6, 47).

Under wet conditions the failure strains are significantly reduced with time. In the case of HAC composites made from E-glass the failure strain was only 200 micro-strains after 51 months whereas for the AR-glass fiber reinforced material the corresponding value was about 3000 micro-strains (Reference 6, 47).

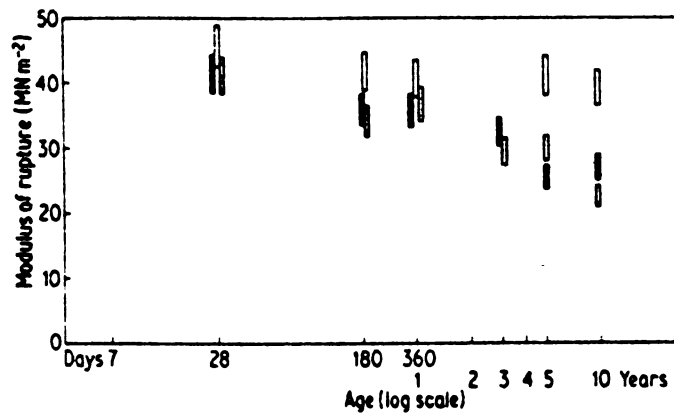


Figure 2.7.37 MOR of GFRC Made from HAC and AR-Glass Fibers. In Air at 20°C, 40% RH. □ , in Water at 20°C ■ , and Under Natural Weathering ◐ , (Reference 6).

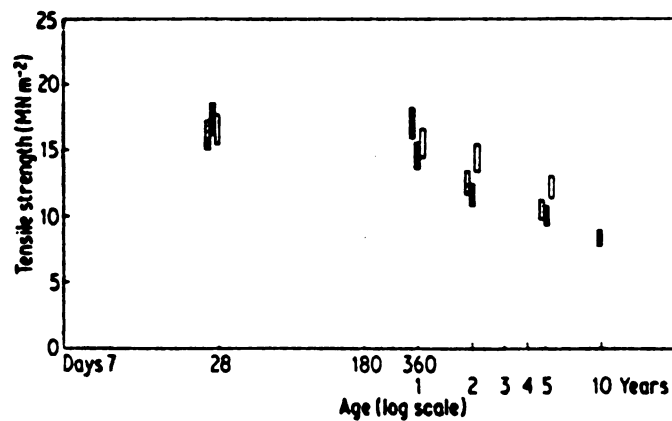


Figure 2.7.38 UTS of GFRC Made from HAC and AR-Glass Fibers Stored in Air 40% RH □ , Water at 20°C ■ , and Under Natural Weathering ◐ , (Reference 6).

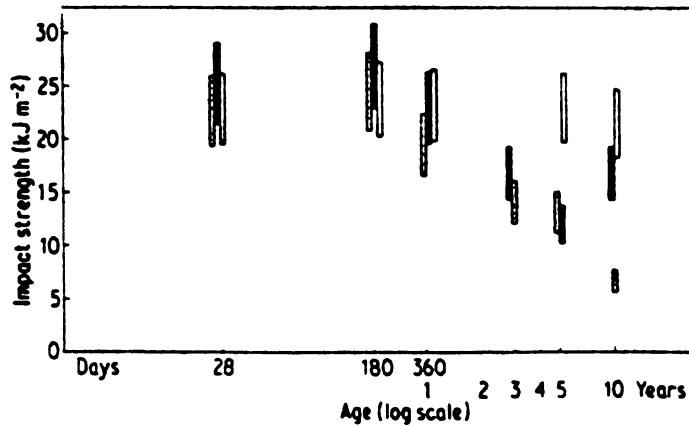


Figure 2.7.39 Impact Strength of AR-GFRC with HAC Stored in Air 40% RH \square , Water at 20°C \blacksquare , and Under Natural Weathering \hatched , (Reference 6).

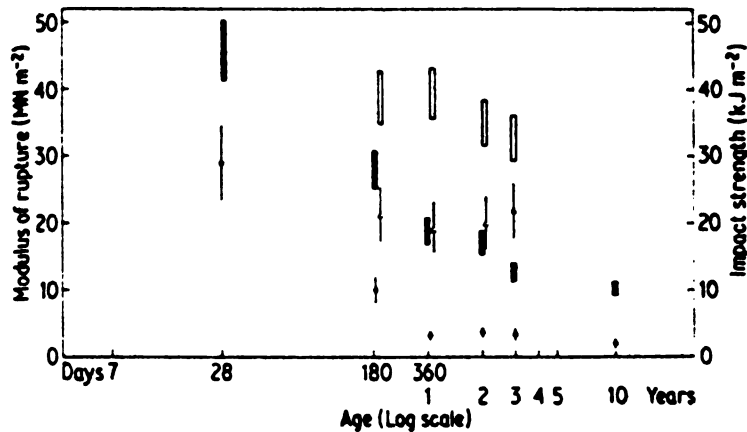


Figure 2.7.40 MOR and Impact Strength of GFRC with E-Glass. MOR Air Stored \square , MOR Water Stored \blacksquare , Impact Strength Air Stored \uparrow , and Impact Strength Water Stored \downarrow , (Reference 6).

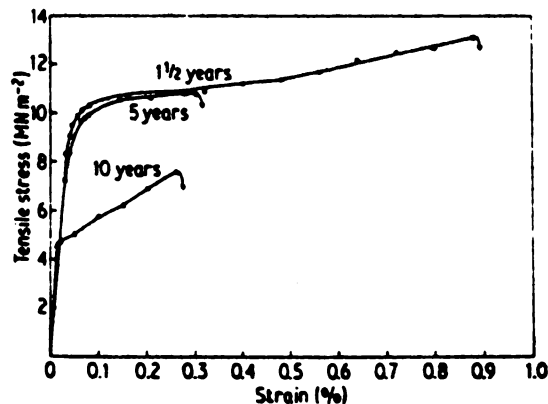


Figure 2.7.41 Stress-Strain Diagram of AR-GFRC/HAC, Water Stored, (Reference 6).

(b) Supersulphated Cement (SSC):

Supersulphated cement made by mixing granulated blast-furnace slag, calcium sulphate and a small quantity of an activator has been used in Europe for many years. This cement has proven particularly useful in applications where resistance to seawater, sulphates, weak acids and other aggressive agents is of prime importance. This increased resistance compared to that of OPC is generally ascribed to the lesser amount of free calcium hydroxide present in set SSC. Furthermore, the solution phase present in SSC is likely to be far less alkaline than its counterpart in OPC. The alkalinity of the cement matrix is the major factor in the reduction of the strength properties of glass-reinforced cement with aging in a wet environment (Reference 5).

The strength properties of alkali-resistant glass fiber-reinforced supersulphated cement have been studied by Majumdar, et. al. (1981), Reference 5, for periods of up to five years in comparison with similar materials made from OPC, and have given very encouraging results. The MOR and Izod impact strength (IS) values obtained with GFRC composites made from Frodingham SSC and the experimental quick-setting variety and kept under water at 20°C up to 5 years are shown in Figures 2.7.43 and 2.7.43. For comparison, results obtained with OPC composites are also given. The tensile stress strain curves obtained with AR-GFRC made from Frodingham SSC and kept under three different environments for 5 years are shown in Figure 2.7.44. The

changes in the ultimate failure strain that occurred in these samples with age are plotted in Figure 2.7.45 (Reference 5).

From Figures 2.7.42 and 2.7.43 it is clear that in wet conditions the bending and impact strengths of GFRC made from SSC are reduced to a lesser extent with time relative to the OPC composite, and the LOP in bending show a small increase in both cases. Of the two varieties of SSC, composites made from Frodingham cement appear to have retained larger proportions of their initial strength over the five year period of durability tests. From the results shown in Figure 2.7.44 it may be noted that even under the continuous immersion condition the failure strain of the SSC composites has remained fairly high after five years and this largely explains the superior impact strength of SSC/GFRC in wet environments to their OPC counterparts (Figure 2.7.43). Figure 2.7.45 shows that the quick setting SSC/GFRC is inferior to the Frodingham cement/GFRC in this respect. After 5 years natural weathering, composites made from both types of SSC have good impact resistance, but the tensile and the flexural strength of composites made from the quick setting varieties are lower than expected (Reference 5).

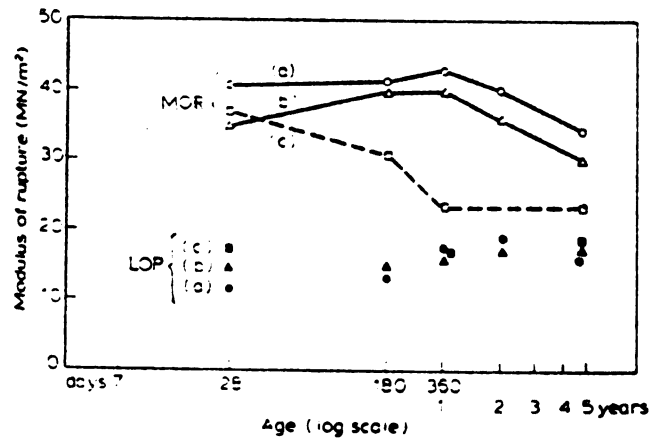


Figure 2.7.42 MOR and LOP in Bending for GFRC Made with: (a) Frodingham Supersulphated Cement, (b) Quick-Setting Supersulphated Cement, and (c) OPC; Stored Under Water at 20°C (Reference 5).

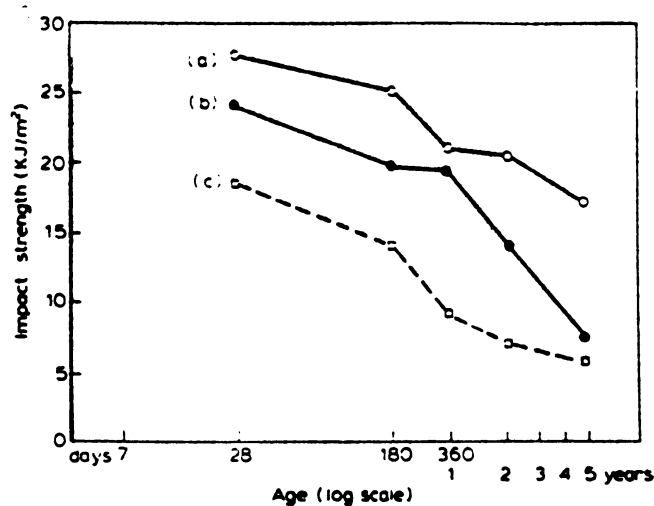


Figure 2.7.43 Impact Strength for GFRC Made with: (a) Frodingham Supersulphated Cement, (b) Quick-Setting Supersulphated Cement and (c) OPC; Stored Under Water at 20°C (Reference 5).

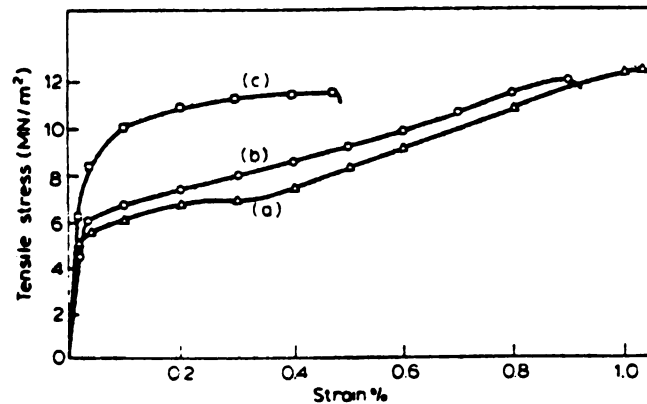


Figure 2.7.44 Tensile Stress-Strain Curves for GFRC Made With Frodingham Supersulphated Cement Stored: (a) in Air at 65% RH; (b) on Natural Weathering Site at UK; and (c) Under Water at 20°C for 5 Years (Reference 5).

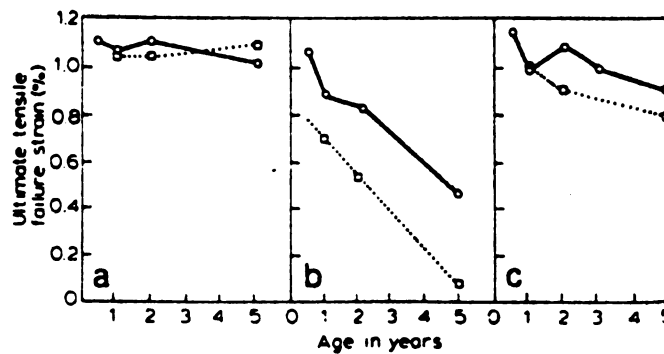


Figure 2.7.45 Ultimate Failure Strain in Tension of GFRC Made With Frodingham (o) and Quick-Setting (□) Supersulphated Cement Stored in (a) Air at 65% RH, (b) Water at 20°C and (c) Natural Weathering (Reference 5).

(c) Calciunsilicate- $C_4A_3\bar{S}$ - $C\bar{S}$ -Slag Type Low Alkaline Cement (CGC):

A special cement for use in GFRC was developed in Japan. Calciunsilicate- $C_4A_3\bar{S}$ - $C\bar{S}$ -Slag is a Low Alkaline Cement consists of mainly calcium silicates (C_3S and C_2S), calcium aluminate sulfate ($C_4A_3\bar{S}$), calcium sulfate ($C\bar{S}$) and water quenched blast furnace slag. The hydration products of this cement are mainly calcium silicate hydrate (C-S-H) and ettringite ($C_3A \cdot 3C\bar{S} \cdot H_52$), but is so designed that $Ca(OH)_2$ not be produced (Reference 7, 58).

According to Tanaka, et. al. (1985), Reference 58, the durability of GFRC improves significantly when this type of cement is used as the matrix for GFRC composite. The long-term change in strength was studied by accelerated aging tests. The results are illustrated in Figure 2.7.46. With GFRC using CGC that was immersed in water at $70^\circ C$, strength hardly declined and MOR of about 30 N/mm^2 and Izod impact strength of about 10 N/mm^2 were maintained, even after immersion for 91 days. With GFRC using OPC, both the MOR and Izod impact strength declined sharply and became constant after immersion for 14 days (Reference 7, 58).

In Figure 2.7.47, changes in strength under natural exposure are presented. GFRC was cured in a $20^\circ C$ thermostatic chamber for 28 days after molding and then was allowed to stand outdoors for exposure to the climatic effects such as rain and sunlight. With GFRC using OPC, after 24 months of natural exposure both the MOR and Izod

impact strength declined markedly. For the GFRC with CGC, on the other hand, the strength decline was not significant (Reference 58).

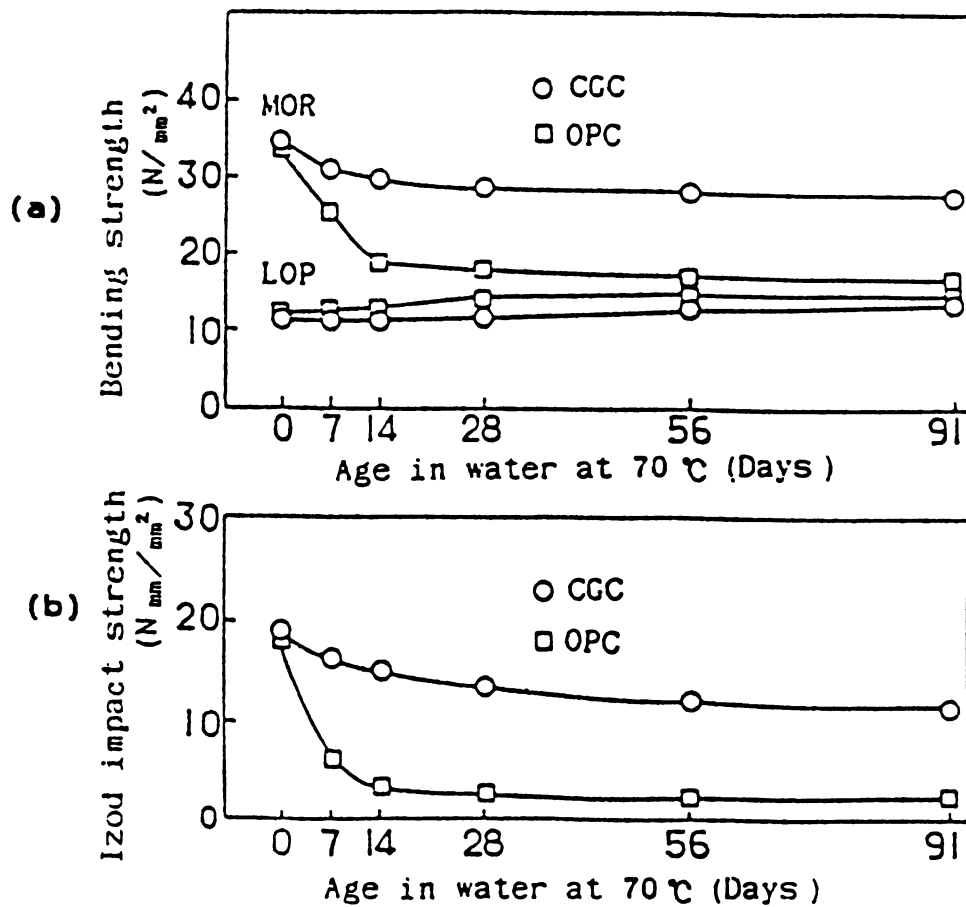


Figure 2.7.46 Changes in (a) The Bending, and (b) Impact Strength of GFRC by the Accelerative Test (Reference 58).

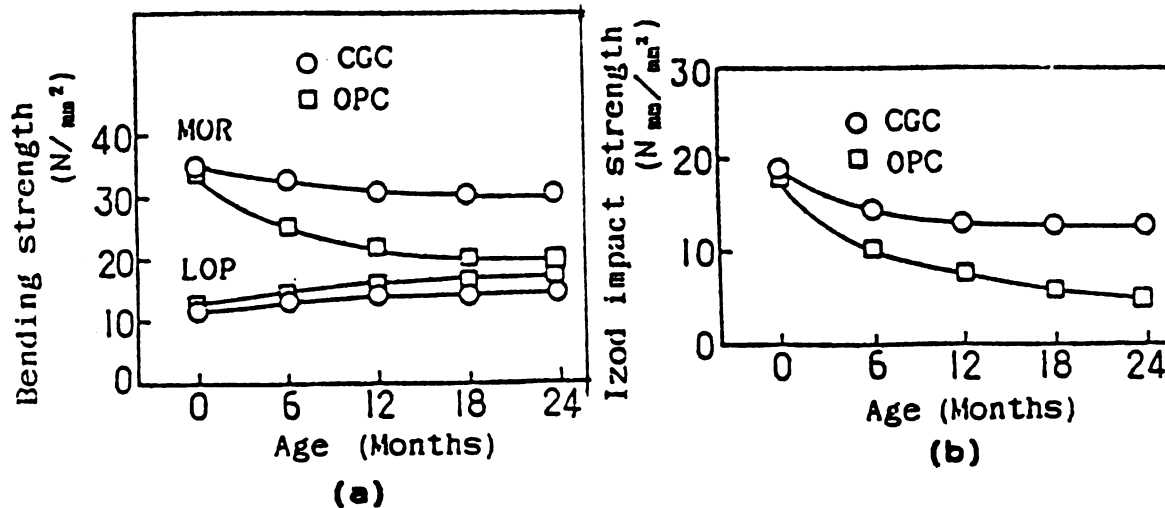


Figure 2.7.47 Changes in (a) The Bending and (b) Impact Strength of GFRP Under Natural Exposure (Reference 58).

2.8 BOND AND INTERFACE ZONE

2.8.1 Bond Characteristics of Glass Fiber:

Okada, et. al. (1982), Reference 49, investigated bond characteristics of glass fibers using pull-out tests of fibers from cement mortar. Figure 2.8.1 shows the schematic view of specimens. An artificial slit is provided to simulate a crack of matrix in the narrowest part of the specimen, and a fiber chopped in fixed length is anchored through the artificial slit. All of specimens have kept inside the molds for 24 hours and then in the moist room for more than 6 days at relative humidity of more than 90% and temperature of 20°C until the tests began.

Prior to the pull-out tests, the tensile strength of glass fiber was measured by the direct tensile test, and the average tensile strength was about 23.5 N per strand. Maximum tensile load of glass fiber in the matrix is increased to the anchor length as shown in Figure 2.8.2. These results are quite reasonable because the relationships between the pull-out force and the bond stress of fiber is theoretically given as follows (Reference 49);

$$P_t = \tau \cdot d_f \cdot l_a \quad \text{where } \tau: \text{bond stress between fiber and mortar}$$

d_f : perimeter of fiber

l_a : anchor length of fiber

Two types of failure, pull-out and break of fiber are observed when anchor length is 15 mm (0.59 in.). Fibers more than 15 mm of anchor length are damaged only in break. Thus, anchor length of 15 mm (0.59 in.) is considered to be the critical anchor length which is most effective for reinforcement. The maximum tensile load is almost constant when fiber is broken, and is corresponds to the direct tensile strength of glass fiber in the previous test (Reference 49).

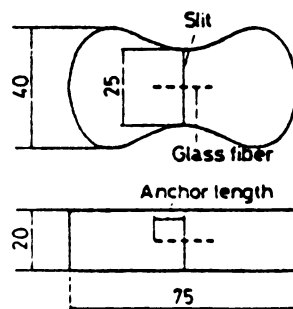


Figure 2.8.1 Schematic View of Specimen (Reference 49).

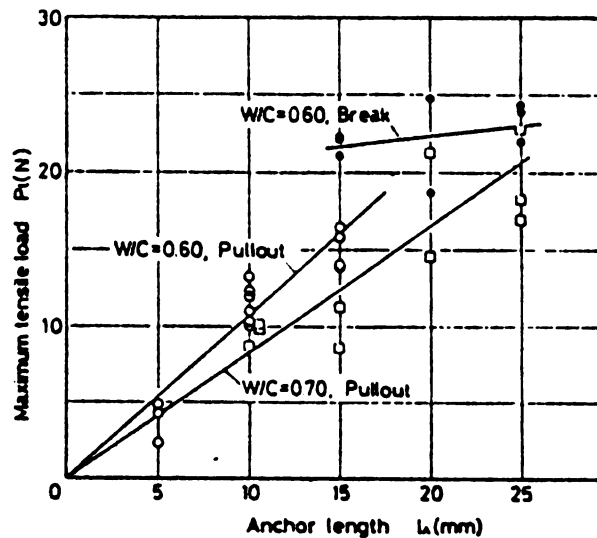


Figure 2.8.2 Relationship Between Tensile Load and Anchor Length (Reference 49).

The ratio of increase of maximum tensile load in accordance with the increase of anchor length is reduced when the water/cement ratio of matrix increases, but the maximum pull-out load increases as the water/cement ratio increases. This means that the critical fiber length or the critical anchor length is influenced by the properties of matrix mortar (Reference 49).

In Figure 2.8.3 the results of various angle of anchor are shown. The maximum tensile load is reduced to a half at angle 45° and to one third at angle 60° (Reference 49).

The specimen having anchor length of 20 mm (0.79 in.) and anchor angles of 30° and 45° show the maximum tensile

load nearly the same as that of specimens of anchor length of 10 mm (0.59 in.) and anchor angles of 30° and 45° , respectively. Reinforcing fibers with anchor lengths of 10 mm (0.59 in.) and 20 mm (0.79 in.) are broken or chopped at the location of artificial slit except in the case with anchor angle of 0 (Reference 49).

The maximum strength of specimen seems scarcely related to the anchor length or fiber length but related to anchor angle, when any magnitude of angle between fiber and applying load exists.

The strength of concrete generally decreases with increase of water/cement ratio. The effect of water/cement ratio on the fiber pull-out resistance are shown in Figure 2.8.4. The transitions of failure type from pull-out to break occur at water/cement ratio 0.65 for anchor length of 20 mm (0.79 in.) as shown in Figure 2.8.4 and water/cement ratio of 0.60 for anchor length of 15 mm (0.59 in.) as shown in Figure 9.5. In above cases, the transition from pull-out to break is discontinuous in the critical condition (Reference 49).

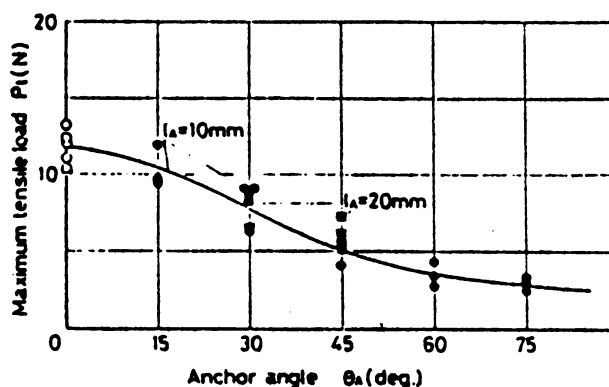


Figure 2.8.3 Relationship Between Tensile Load and Anchor Angle (Reference 49).

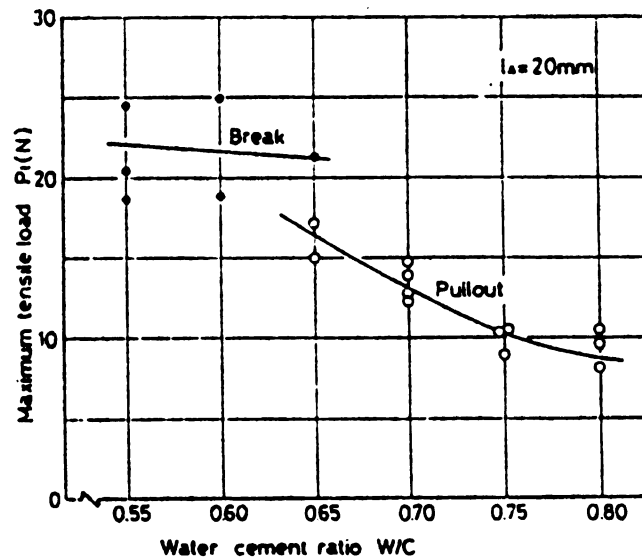


Figure 2.8.4 Relationship Between Tensile Load and W/C (Reference 49).

2.8.2 Aging Effect on Fiber Pull-Out Behavior:

Although the ultimate causes of the wet aging response are still debated, the process involves filling up of spaces between individual glass fibers. This cements glass fiber filaments together into fully bonded strands, and prevents individual fiber pullout before fracture. Both filling up process and the loss of individual fiber pullout capacity can be checked readily by scanning electron microscopy (SEM) - Reference 8.

A glass fiber strand is comprised of approximately 204 filaments. A sizing (or coating) keeps the 204 filaments intact throughout chopping and the GFRG spray-up fabrication process. The diameter of the glass filaments is

approximately 10 microns (0.0004 in.). The average space between individual filaments is approximately 2 to 3 microns (0.00008 to 0.00012 in.) and the average size of a cement particle is approximately 30 microns (0.0019 in.).

Therefore, cement particles cannot penetrate the fiber bundles and early bonding of cement paste is restricted to the outside filaments in a bundle (Reference 43).

For a young (non-embrittled) GFRc specimen loaded to failure in either tension or flexure, the failure mode is characterized by extensive pull-out or slippage of glass filaments located in the interior of the fiber bundle. Resistance to the applied load is developed through sliding friction as filaments pull out (Reference 43).

If the GFRc is allowed to age in a moist environment, the cement hydration progresses and spaces between individual glass filaments become packed with hydration products (specifically calcium hydroxides) and the glass fiber composite becomes embrittled. The embrittlement process is time related in that cement hydration is time related. In dry environments where cement hydration ceases, the embrittlement process also ceases and early composite strengths are maintained (Reference 43).

Mills (1981), Reference 48, in studies on precipitation of Calcium Hydroxide on AR-glass fiber, pointed out that CH has a remarkable affinity for AR-glass fiber, pointed out that CH has a remarkable affinity for AR-glass whatever counter-attractions are offered. The Portland cement binder

is apparently able to release sufficient CH to create an extremely dense layer of crystals on the glass, and these crystals appear to have a strong axis normal to the longitudinal axis of the glass. The structural fabric of crystals and fibers between cement grains was seen to be engulfed by precipitated CH in a manner consistent with the structure revealed by ion etching in a reverse process.

The glass can only act effectively if it can transmit force across a crack. If slippage in the glass is prevented, the opening of such a crack would lead to high localized strain in the glass, inevitably leading to its failure. The morphology of CH deposited on glass suggested that any tendency of the fiber to move relative to the matrix would result in principal compressive stress perpendicular to the fiber axis. This would reduce the longitudinal strength. Embrittlement of GFRC with age may be attributed to the affinity of CH with AR-glass fiber and the morphology of CH precipitate (Reference 48).

2.9 FAILURE MECHANISM AND THEORETICAL STUDIES

2.9.1 Tensile Stress-Strain Behavior of GFRC Composites:

When GFRC specimens are subjected to uniaxial tension, the response is linearly elastic until the initial matrix cracking. In the inelastic range (between the first cracking and the peak) progressive debonding and frictional slip at the fiber matrix interfaces occur. The relative stress-strain curves in tension for a strong fiber (steel,

glass, asbestos, polypropylene, sisal, kevler, etc.) and a brittle matrix (Portland cement, gypsum, etc.) are shown in Figure 2.9.1 (Reference 50). The strain at fracture for the brittle matrix is considerably smaller (less than 1/50) than that for the fiber. As a result, when a fiber reinforced brittle matrix composite is loaded, the matrix will crack long before the fiber can be fractured. Once the matrix is cracked, one of the following types of failure of the composite occurs (Reference 50):

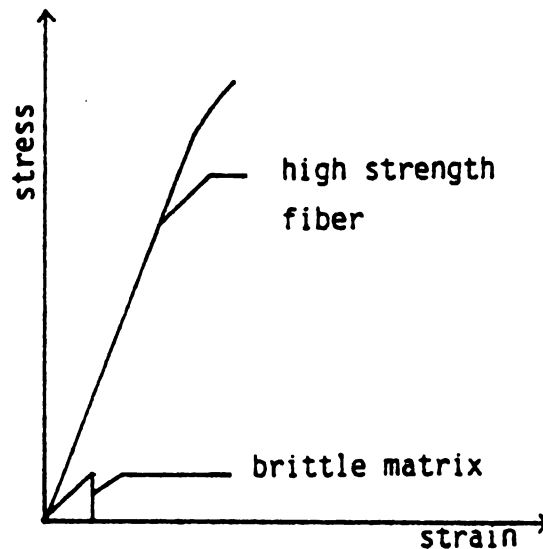


Figure 2.9.1 Stress Strain Curves of Strong Fibers and Brittle Matrices (Reference 50).

- (a) The composite fractures immediately after the matrix cracking. This type of behavior is shown in Figure 2.9.2 a.

- (b) Although the maximum load on the composite is essentially the same as that of the matrix alone, the composite continues to carry decreasing load after the peak, as shown in Figure 2.9.2 b. The post-cracking resistance is primarily provided by the pulling out of fibers from the cracked surfaces. Although no significant increase in the tensile strength of the composite is observed, a considerable increase in the toughness of the composite can be obtained.

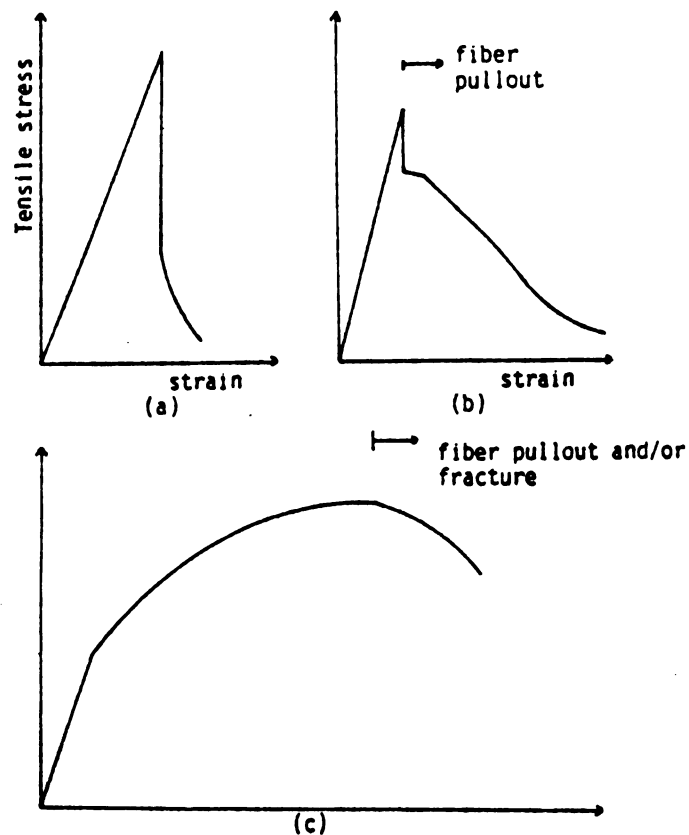


Figure 2.9.2 Ranges of Composite Stress-Strain Curves Made With Brittle Matrices and Strong Fibers (Reference 50).

- (c) Even after the cracking of the matrix, the composite continues to carry increasing tensile stresses; the peak stress and the strain at peak stress of the composite are greater than those of the matrix alone (Figure 2.9.2 c).

2.9.2 Constitutive Modeling of the Tensile Behavior of GFRc:

Figure 2.9.3 shows stress-strain curves in a three-part form discussed in this section. Initially, fibers and the matrix are strained equally and stress rises linearly until the matrix cracks; there is then a horizontal region of considerable strain in which parallel cracking develops in the matrix, and all the load is transferred to the fibers at the crack positions. Finally the stress rises again, being carried by the fibers, and composite stiffness and strength in this region are governed entirely by fiber content, modulus and strength (References 51, 52).

Aveston, et. al. (1971), Reference 51, derived quantitative expressions for many aspects of the stress-strain curve, including the strain at the end of the multiple cracking region (ϵ_{mc}) and the final failure strain of the composite (ϵ_{cu}) in terms of fiber and matrix properties.

Practical machine-sprayed or hand-sprayed GFRc composites differ from this ideal material in that fibers are normally incorporated as chopped strands, i.e. they are in the form of bundles containing about 200 glass filaments

and of length 30 to 40 mm (1.18 in. to 1.57 in.). The bundles themselves are approximately randomly oriented in the plane of the GFR sheet. It is easy to show that the strain, $\epsilon_f(\theta)$, in a fiber lying at an angle θ to the composite strain direction is less than that in an aligned fibers, given by:

$$\epsilon_f(\theta) = \epsilon_c \cos^2 \theta \quad (1)$$

where ϵ_c is the strain in the composite. Thus orientation of fibers at an angle to the applied load reduces their effectiveness as reinforcement, and numerical estimates of around 1/3 for the value of an orientation factor K_o which is used as multiplier of the fiber content when estimating the strength or stiffness of planar random fiber composites. Other similar "efficiency factors" are often used in composites calculations to take account of effects, such as poor bonding or the use of fibers in bundles, which may also lead to a degree of ineffectiveness in the utilization of fiber properties (References 51, 52).

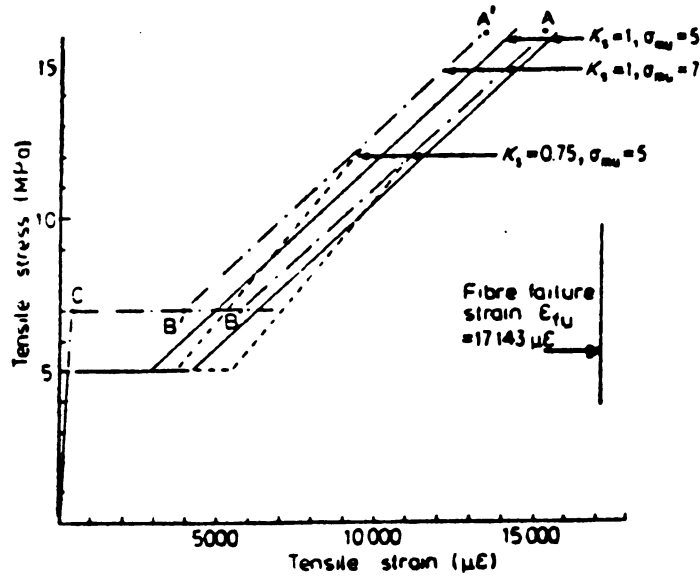


Figure 2.9.3 Typical Stress-Strain Curves for GFRc Materials Calculated from Equations 4, 6, 7 and 8 (Reference 52).

Aveston, et. al. (1971), Reference 51, pointed out that when the matrix cracks an additional load, equivalent to that being borne by the matrix, is placed on the bridging fibers. If fibers and matrix volume fractions are respectively V_f , V_m , fiber and stiffness E_f , E_m and matrix cracking strain ϵ_{mu} , this leads to an additional strain $\Delta\epsilon_f$ in the fibers at the crack position given by

$$\Delta\epsilon_f = \alpha \epsilon_{mu} \quad (2)$$

where $\alpha = E_m V_m / E_f V_f$. As one moves away from the crack position and the additional fiber stress is transferred back into the matrix and the additional fiber strain reduces to a value between zero and $\Delta\epsilon_f / 2$. Thus the total composite strain at the end of multiple cracking (ϵ_{mc}) lies between

and $\epsilon_{mc} = \epsilon_{mu} (1 + \alpha/2)$

$$= \epsilon_{mu} (1 + 3\alpha/4) \quad (3)$$

for crack spacings of $2x$ or x , respectively, where x is the minimum possible crack spacing (Reference 51).

For the case of a random fiber mat of chopped strands with an efficiency factor for orientation of K_o , and for strand effects (such as poor bonding to some fibers and lengths effects) of K_s , the effective stiffness of the fiber mat is reduced and additional strain is increased to

$$\Delta \epsilon_f (\text{mat}) = \alpha \epsilon_{mu} / K_o K_s$$

The expressions for strain at the end of multiple cracking then become

to $\epsilon_{mc} (\text{mat}) = \epsilon_{mu} \left(1 + \frac{\alpha}{2 K_o K_s} \right)$

$$= \epsilon_{mu} \left(1 + \frac{3\alpha}{4 K_o K_s} \right) \quad (4)$$

for crack spacings $2x$ to x , respectively (Reference 51).

At end of multiple cracking the composite strain (as given by Equations 3 or 4) is also equal to the strain in the fibers at the crack position less the amount of the matrix restraint (since load is transferred back from fiber to matrix between cracks). The amount of matrix restraint can therefore be obtained from the difference between fiber strain at the matrix cracking stress level and that given by Equations 3 and 4. As the stress on the composite is further increased, failure will finally occur when fiber strain reaches its failure value at the crack position. The

composite strain will then be equal to the fiber failure strain less the previously defined matrix restraint.

Expressions for the range of aligned composite failure strain

$$\epsilon_{cu} = (\epsilon_{fu} - \alpha \epsilon_{mu}/2)$$

to

$$= (\epsilon_{fu} - \alpha \epsilon_{mu}/4) \quad (5)$$

for crack spacings of $2x$ and x , respectively, where ϵ_{fu} = fiber failure strain (Reference 51).

For random chopped-strand composites the second terms are modified by $K_o K_s$ efficiency factors as before, since they have been derived from the matrix-restraint and load-transfer expressions used to obtain Equation 4. From Equation 1, fibers lying at an angle to the load are strained less than those aligned with the load. The latter will be the first to fail. Their failure will throw additional load on the remaining fibers and rapidly initiate failure of the whole mat. The term therefore does not need to be modified by a K_o factor. If, however, fiber strength is used ineffectively due to poor bonding or length effects then K_s may still apply; this is now most appropriately derived empirically from ultimate strength test data rather than post-cracking stiffness data (Reference 51).

The modified expressions for composite failure strain thus become:

$$\epsilon_{cu} = \left(K_s \epsilon_{fu} - \frac{\alpha \epsilon_{mu}}{2 K_o K_s} \right)$$

to

$$= \left(K_s \epsilon_{fu} - \frac{\alpha \epsilon_{mu}}{4 K_o K_s} \right) \quad (6)$$

for crack spacing of $2x$ to x , respectively (Reference 51).

Consider a GFRC composite containing 4% by volume (V_f) of glass-fiber strands whose strength (σ_{fu}) is 1200 MPa and Young's modulus (E_f) is 70 GPa. Assume that these strands are randomly oriented in the plane of the GFRC sheet so that $K_o=1/3$, and further assume initially that there is no inefficiency due to their use in chopped-strand form, i.e. $K_s=1$. Let the fibers be incorporated in a cement or mortar matrix with a cracking stress (σ_{cw} , commonly called the BOP, of 5MPa and Young's modulus 20 GPa). If the composite fails by breaking of the fibers bridging one of the matrix cracks when the aligned fibers reach their failure strain, then the composite strength σ_{cu} is given by

$$\sigma_{cu} = K_o K_s \sigma_{fu} V_f \quad (7)$$

The range of stress-strain behavior for such a composite, computed from the above data and from Equations 4, 6 and 7, is shown by the continuous lines in Figure 2.9.3 for the possible range of crack spacings $2x$ to x (Reference 51).

If the fibers in the strand are used less effectively, e.g. $K_s=0.75$, then the composite strength and strain to failure are significantly reduced whilst the strain to the end of multiple cracking is increased, as shown by the region of calculated properties defined by the dashed lines in Figure 2.9.3.

Two main changes are to be expected on prolonged wet aging of the composite: the strength of the matrix will increase and the strength of the fiber reduced. Consider these in two stages for the case when $K_s=1$ (Reference 51).

(a) Assuming that the BOP increases on aging from 5 to 7 MPa, this leads to a small increase in the strain at the end of multiple cracking (ϵ_{mc}) and a small decrease in the strain to failure, as shown by the chain-dotted lines in Figure 2.9.3.

(b) Loss of fiber strength on aging directly controls the term in Equations 6 and 7. The composite failure point will move lines AB or A'B' until Point B or B' is reached. The fibers are then no longer strong enough to bear the load when the matrix cracks, i.e. their strength has fallen below a critical value of given by

$$K_o K_s \sigma_f V_f < \sigma_{mu} \quad (8)$$

and the composite failure strain drops suddenly to Point C. The effect of the increase of BOP on aging is to increase the stress and strain levels at which this sudden drops occurs. Although not illustrated in Figure 2.9.3 it is important to note that an increase in fiber content will reduce the value of σ_{crit} calculated from Equation 8 and hence delay the onset of sudden embrittlement by the BC or B'C transition on aging (Reference 51).

The failure strain calculated here does not include, and is not dependent on, any gross fiber pull-out which may or may not occur at final failure. Fiber pull-out may help

to give a controlled crack growth once final failure has started, but it does not necessarily give rise to a strain deformation distributed along the gauge length of the specimen prior to final failure (Reference 51).

It can also be seen that composite failure strain is directly related to fiber failure strain and the efficiency of using fiber strain (or strength) through the first term in Equation 6, which predominates for "unaged" composites containing strong fibers. Fiber content and orientation affect the second term in Equation 6 and these factors become more significant in influencing fiber failure strain as fiber strength and strain are reduced by aging and the second term in Equation 6 becomes comparable with the term, when increasing fiber content leads to increased strain to failure. Other factors, such as matrix strength and stiffness, or the detailed crack spacing have relatively little influence on final failure - again except in the case of an aged composite, where fiber strength is reduced to near Point B or B' and an increase in matrix strength and/or lower fiber content may cause the critical fiber stress to be exceeded and result in a sudden reduction in failure strain from Point B or B' to C (Reference 51).

2.9.3 Failure Mechanism of GFRP:

According to Stucke and Majumdar (1976), Reference 53, the experimental evidence suggests that GFRP failures occur when the bending stresses in the fibers at the surface of a

transverse crack exceed a certain stress value. This stress, σ_f , will be given by the Griffith relation,

$$\sigma_f = \left(\frac{2\pi E}{\pi C} \right)^{1/2} \quad (1)$$

where π is the surface energy of fracture of the glass fiber, E is its Young's modulus and C is the length of a surface flaw. In unaged glass fibers ($\sigma_f = 1.8 \text{ GNm}^{-2}$, $\pi = 5 \text{ Jm}^{-2}$ and $E = 20 \text{ GNm}^{-2}$) giving a value of the flaw size of 0.06 micron (Reference 53).

The micrographs of the surfaces of aged fibers show that the flaw size is considerably larger than this (about 0.15 micron). The weakening of the fibers will not, however, drastically alter the toughness of the composite but will result in a reduction of the ultimate strength (Reference 53).

Figure 2.9.4 shows schematically how a fiber, oriented at an angle θ with respect to the applied tensile stress, is bent when a transverse crack is opened by a displacement ϵ_c . A considerable bending strain will be experienced by the fiber where it emerges from the crack face at X and X' . Accordingly, stresses will also be produced in the matrix. The stress at the surface of the fiber will depend on the radius of curvature, R , at these points. Using simple bending theory and assuming the uniaxial tensile stress on the fibers is small compared to

the bending stresses, the stress in the fiber on its outer surface σ_b is,

$$\sigma_b = \frac{Er}{(R+r)} \quad (2)$$

where r is the radius of the fiber cross-section. Assuming that $\sin \theta/2 \approx \frac{1}{2}R$, where l is the length of the bent region of fiber, then,

$$\sigma_b \approx \frac{2Er \sin \theta/2}{l + 2r \sin \theta/2} \quad (3)$$

Substituting appropriate value of $\sigma_b \approx \sigma_f = 1.8 \text{ GNm}^{-2}$, for unaged fibers and $r=5$ micron; then for bending to occur without failure $l > 200$ micron for all values of θ from 0 to 90 deg. Thus we can see that for all fibers to remain unbroken during fracture, and assuming they are undamaged by corrosion, the value of l or the radius of curvature of the bent fiber is large. It is, therefore, possible to relate most fiber failures in GFRP to certain microstructural features which will limit to less than 200 microns (Reference 53).

Generally, l is observed to be greater than 200 microns in the 90 day old materials due to three possible microstructural features: (1) the presence of wide cracks around the fiber bundles resulting from the delamination of the composite, (ii) the crumbling of the matrix around the bundles, probably due to the stresses imposed on the matrix by the bent fibers, and (iii) the absence of hydration products between the fibers within the strands. On the

other hand, the absence of these features in the older water stored and naturally-weathered GFRG typically limits l to a few microns (Reference 53).

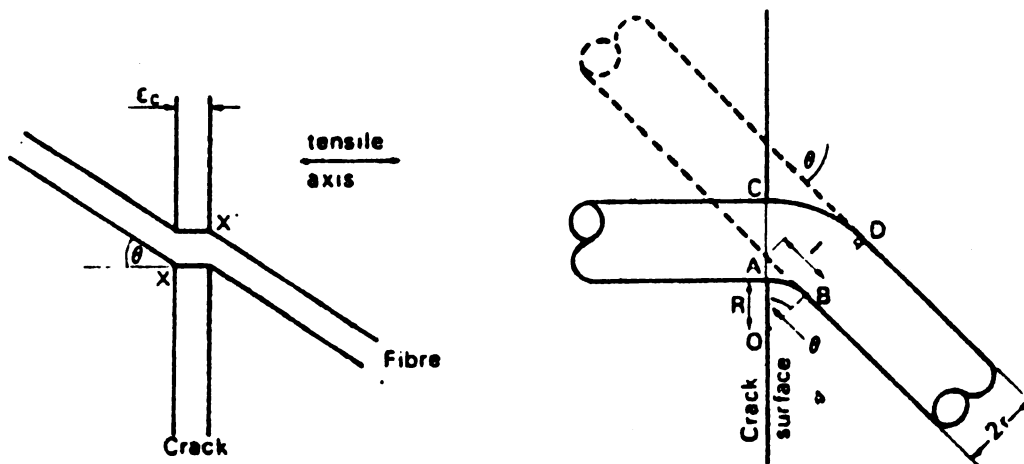


Figure 2.9.4 Schematic Representation of the Bending of Fibers Bridging a Transverse Crack During Fracture (Reference 53).

The fiber-matrix interface in any composite material is important since it can affect the transfer of stress from the matrix to the fibers and the propagation of cracks in the matrix in the vicinity of the fibers. The interface in the dry air stored materials will be inherently weak due to the small contact area between the matrix and the fibers. However, they will be very compliant due to the numerous separate bonds between the fibers and the whisker-like

crystals and the high porosity. The failure of such an interface will tend to be gradual with progressive failure of the individual bonded crystals and, therefore, should contribute significantly to the toughness of the composite as a whole (Reference 53).

Furthermore, this type of porous interface could provide an effective barrier to the propagation of cracks. The stress concentration at the tip of a crack approaching the fibers will be relaxed at the interface since the porous and compliant interface region will be able to accommodate much of the strain at the crack tip. This will then slow down the moving of crack around the fiber strand, and if the strands are close enough together the entire length of the crack front may be halted, at least temporarily. This will necessitate the propagation of subsidiary cracks in the matrix to accommodate further applied strain. The formation of the subsidiary crack structure in dry stored GFRG, resulting in a large fracture surface area, gives rise to the high energy failures associated with the observed values of toughness, "ductility" and impact strength (Reference 53).

The dense type of interface present in water-stored GFRG will be much less compliant than the porous types, although the shear strength will be higher due to the increased frictional components. These interfaces will be less able to relax the stress concentrations at the crack tip and thus the primary crack will be able to propagate

relatively freely around the fiber bundles until, ultimately, complete failure of the matrix occurs. The stress on the composite will then be supported by the fibers alone. Thus the failure surface area will be small, approximately equal to the cross-sectional area of the test specimen, and accordingly the toughness will be relatively low (Reference 53).

2.10 DESIGN

2.10.1 Design Considerations:

The approach to design with GFRC is no different from that for any other material. There are three basic steps to be taken.

- (i) A study of the material - its constituents, behavior and properties;
- (ii) A study of how it is made and used in practice and the effect this has on the material and its properties; and
- (iii) Finally, having gained an understanding of the material and how it is made and having identified its essential properties and limitations, design methods may be developed which properly take these into account.

Thus design can be seen to lie between research and manufacture and the designer must translate theories into practical design methods (Reference 54).

From studying the materials, their constituents and properties, methods of manufacture and the influence these have on material properties, and having considered how the material is used in practice, a basis for design can be established. Although GFRG is not a single material and covers a range of materials with properties dependent on the particular formulation used, most information is available on certain standard mixes which form the basis of those currently used. However, long-term data are only available on materials with a neat cement matrix made by the machine spray and dewatering process. The main properties and factors which need to be considered are:

1. Strength properties of GFRG
2. Shrinkage, moisture and thermal movements
3. Manufacturer's limitations
4. Material properties and control tests
5. Behavior of full size components
6. Associated materials

The design method has to incorporate these factors into a logical framework and should also be such that, as more knowledge and confidence are gained about the materials, refinements and adjustments can be made (Reference 55).

2.10.1.1 Strength Properties:

For most applications the designer is particularly concerned with flexural behavior, as tensile stresses under

flexure will generally be the critical stress. The limit of proportionality in bending (LOP) is adopted as the basic for design, rather than the modulus of rupture (MOR), for the following reasons:

- * There is insufficient knowledge of the stress-strain behavior of GFRC up to failure, and MOR is therefore not meaningful as a measure of the actual stress in the material at failure.
- * Below the LOP, simple bending theory is applicable.
- * The designer is mostly concerned with the avoidance of cracking in the matrix.
- * The LOP is less variable and its behavior in different environments is more predictable than the MOR. It should be noted, however, that there is a variation between the LOP results as measured by different operators and instruments, but this is a function of the test method rather than the material behavior.
- * At stress levels below the LOP, fatigue and stress rupture will not be critical.

Although design is based on the LOP, the pseudo-ductile behavior of GFRC above LOP up to the MOR provides the ultimate factor of safety against failure. The loss of this pseudo-ductility and the fall in the MOR in wet or natural weathering conditions thus reduce the ultimate factor of safety from its initial value (Reference 55).

2.10.1.2 Shrinkage, Moisture and Thermal Movements:

When movements are restrained, tensile stresses will be induced in GFRC. Their magnitude depends on the degree of restraint and the stress-strain characteristics of the material at the particular age under consideration. When the ultimate drying shrinkage of a standard GFRC mix, typically about 0.15%, is compared with the tensile cracking strain under of about 0.05% it is clearly very important to consider the factory which would restrain the shrinkage movements (Reference 55).

The restraint may be external or internal, caused by factors such as variations within the material, variations in drying rates, and incorporation of other materials. The effects of restraint have to be considered together with the value of Young's modulus for the material at a particular age and relaxations which will occur through creep in tension. It is apparent from studies of neat cement mortars and concretes that the restraint stresses are not secondary, and they may be of a similar magnitude as those resulting from applied loads and could lead to cracking in the matrix (Reference 52).

2.10.1.3 Manufacturer's Limitations:

The design method has to recognize the difference between materials produced by the manufacturer and those produced in the laboratory. It has been observed that where the manufacturer's control is good the material produced compares well with the laboratory material, but poor control

leads to lower and more variable results. In addition, there may also be differences between materials in the actual product and the test board used for quality recording. These differences may arise from the spraying process or from the curing method. The differences may therefore be put into two categories:

- * Normal variations which arise in any manufacturing process; and
- * Other variations which are particular to GFRC and are mainly due to fiber Orientation and the dispersion and curing effects.

Account must also be taken of possible variations in skin thickness which may be undetected in the product. With thin sheet materials, small variations can cause significant stress increases, and it has been observed that large variations are possible (Reference 55).

2.10.1.4 Material Properties and Control Tests:

The combination of fiber content, LOP and MOR testing is required for proper control of GFRC production to give a check on the adequacy and strength of the material being produced. Normal statistical methods may then be used to establish characteristic values to be employed in design and to check compliance during manufacture (Reference 55).

2.10.1.5 Behavior of Full Size Components:

Account must be taken of the differences in the behavior of full-size components with the standard test coupon in bending. This is essentially a question of

assessing strain gradients across the section under consideration and taking account of size and shape effects (Reference 55).

2.10.1.6 Associated Materials:

These may include infills, surface coatings, fixings and jointing materials. The interaction of GFRC with infills is of particular importance. Naturally, where they are used as a structural element in design, the interfacial bond with the GFRC and the stress-strain characteristics of the infill must be known (Reference 55).

2.10.2 Design Loads:

GFRC is designed for stripping, handling and installation loads. Service loads are set by the governing building code and are multiplied by the appropriate load factors from "Building Code Requirements for Reinforced Concrete (ACI 318-83)," Section 9.2, to determine design loads (Reference 56).

2.10.2.1 Service Loads:

GFRC design must consider both dead and live loads including wind, earthquake (if applicable), and temperature and moisture effects. Service loads set by the governing building code should be considered only as minimum requirements. There may be situations where additional considerations with respect to service loads should be considered, such as:

Gravity Load Effects: Gravity loads associated with the weight of GFRC often do not result in pure compressive stresses. GFRC skin bending stresses associated with gravity loads should be considered in design.

Wind Load Effects: Variation in wind loads due to surrounding structures or to the geometry of the structure should be considered in design.

Earthquake Load Effects: Internal forces developed in GFRC during seismic events must be capable of being transferred to anchors without causing excessive stresses. Special consideration should be given to three-dimensional GFRCs where inertial forces can potentially result in skin bending stresses (Reference 56).

2.10.2.2 Load Factors and Load Combinations:

Minimum design loads stated in the governing building code, along with the additional service loads should be considered when assessing various load combinations, as typically presented below:

$0.75[1.4D + 1.7(\text{greater of } L, W \text{ or } 1.1E) + 1.6(\text{greater of } M \text{ or } T)]$

where:

D=dead load

E=earthquake load

L=live load

M=self-straining forces and effects arising from
contraction or expansion due to moisture changes

T=self-straining forces and effects arising from
contraction or expansion due to temperature changes

W=wind load

The factor for moisture and temperature change may be considered greater than that shown in ACI 318 due to the uncertainties in values and calculation procedures, and also due to the greater potential effect if underestimated (Reference 56).

2.10.3 Mechanical Design:

The design of any product has to satisfy many requirements. Adequate strength against specified loads is an obvious requirement, and therefore mechanical design will commonly be performed to ensure satisfactory performance. The loads to which a product may be subjected during demoulding and handling should not be ignored (Reference 57).

2.10.3.1 The Approach to Mechanical Design in GFRC:

As with other materials in the allowable stress method of design, it is normal practice to design at stresses below

the elastic limit. The elastic limits of GFRP in compression, bending (LOP), tension (BOP) and shear do not change significantly in most environments; the initial property values can thus be used as a reference.

Design stresses are also selected with respect to long-term strength values. In conditions where there is a reduction of ultimate strength, accelerated aging tests (Figure 2.10.1) indicate that the strength stabilizes. Design stresses should be based on this stable value, allowing a suitable factor of safety (Reference 57).

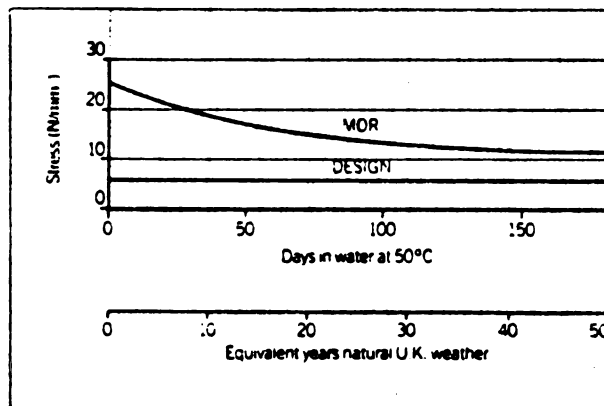


Figure 2.10.1 Reduction of MOR (Reference 57).

In terms of the bending strength of a good quality hand sprayed GFRP, a typical design stress is 6 N/mm^2 , which covers both of these requirements (Figure 2.10.2). The high initial ultimate properties of the material are a bonus in

the early life of the product, allowing the use of higher design stresses for structures such as formwork, which may require high strength only in the early life of the product (Reference 57).

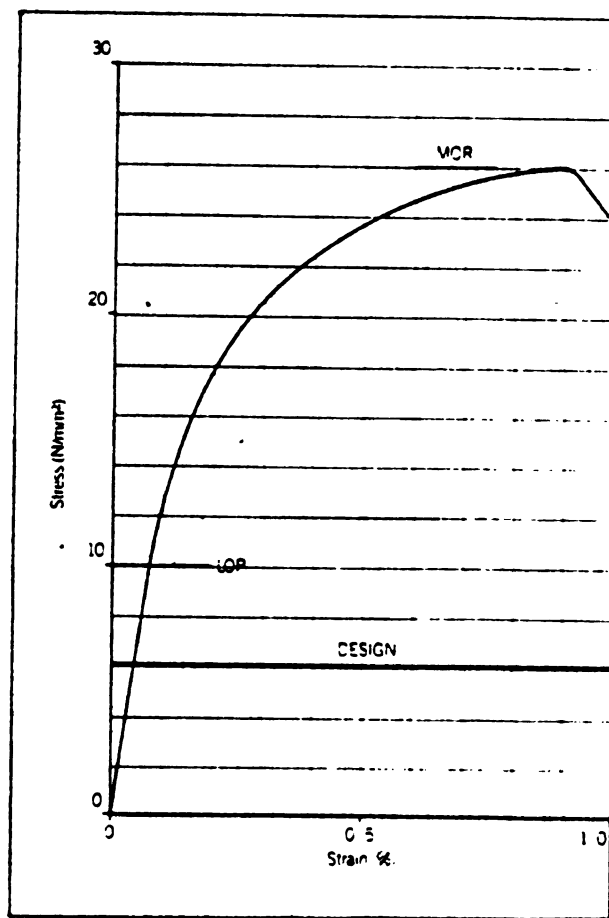


Figure 2.10.2 Bending Behavior of GFRC (Reference 57).

2.10.3.2 Design Stresses:

The normal test data available from a GFRC manufacturer relates to bending tests on small coupons of GFRC. The

results can be statistically analyzed to give values of the initial LOP and MOR. Other mechanical properties of GFRC can be divided into those which are; (1) strongly dependent upon the matrix (compressive strength and inter-laminar shear strength); (2) related to the LOP; strongly dependent upon the glass fiber content (UTS and in-plane shear); and (4) related to the MOR.

For instance:

Compressive strength	6-10xLOP
Inter-laminar shear strength	0.4-0.5xLOP
UTS	0.4xMOR
In-plane shear strength	0.4xMOR

Hence an estimate can be made of the characteristic values of these properties if the LOP and MOR are known (Reference 57).

Table 2.10.1 gives typical design stresses for GFRC, which are obtained by applying a factor of approximately 1.8 to the long term cracking strength (e.g. LOP, BOP) of GFRC.

GFRC is often used in constructions where the stress is neither pure bending nor pure tension. Bending of box-sections (often used to strengthen GFRC products) is an example. In this case the design stress will be between the values for bending and tension (Reference 57).

The values of design stress may be increased where loads are of limited duration and occur early in the life of the material (e.g. permanent formwork), and reduced values (e.g. one third of the normal values) may be desirable when

considering the stresses imposed by demoulding a product at an early stage in the curing cycle when the LOP of the material may be low. Consideration may be given to reducing the design stresses if a permanent load is to be applied to the GFRC in order to take account of the effects of creep (Reference 57).

Table 2.10.1 Typical Design Stresses for GFRC (Reference 57).

Stress Type	Loading Example	Design Stresses N/mm ²	
		5% spray GRC	3½% premix GRC
Compressive	Compressive	12	12
Bending	Bending solid beams or plates	6	4
Tensile	Cylindrical hoop stress	3	2
Tensile	Bending sandwich panels	3	2
Web Shear	In-plane shear of webs in box sections	2	1
Bearing Shear	Shear loading at bearing positions	1	1

2.10.3.3 Analysis:

GFRC products can usually be subdivided into interacting parts, each of which can be tested individually as a beam or plate element and analyzed according to using formulae available in standard texts (Reference 57).

The stresses and deflections for beams can be calculated using the following formulae.

$$\text{Stress } f = \frac{WL}{k_1 Z}$$

$$\text{Deflection } y = \frac{WL^3}{k_2 EI}$$

where W is the total load on the beam (N).

L is the length of the beam (mm).


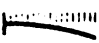
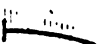



E is the modulus of the material (N/mm²).

k_1 and k_2 depend on the beam support and the load type.

Z (mm³) and I (mm⁴) depend on the shape of the beam.

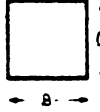

For some of the more common cases of loading types and support conditions, Table 2.10.2 gives values for K_1 and K_2 (Reference 57).

Table 2.10.2 Values for K_1 and K_2 (Reference 57).

Load Type	Support Condition	Diagram	k_1	k_2
Point load	Cantilever		1	3
Uniform	Cantilever		2	8
Hydrostatic	Cantilever		3	15
Point load	End supports		4	48
Uniform	End supports		8	77
Hydrostatic	End supports		7.8	77

For two of the more common shapes of beams found in GFRC construction the values of Z and I presented in Table 2.10.3 can be calculated. Section properties of other shapes can be calculated by normal procedures (Reference 57).

Table 2.10.3 Values for Z and I (Reference 57).

Beam Shape	Section Modulus Z	Second Moment of Area I
Solid 	$\frac{BD^2}{6}$	$\frac{BD^3}{12}$
Box Section 	$\frac{BD^3 - bd^3}{6D}$	$\frac{BD^3 - bd^3}{12}$

The formula for deflection gives an estimate of the short term deflections. For the sustained loads or dead weight, the creep of GFRP should be considered. A simple method is to multiply the immediate deflections under sustained loads by a factor of 3 to obtain the long term deflection (Reference 57).

2.10.4 Physical Design:

2.10.4.1 Thermal Movement:

Thermal dimension changes in GFRP can be calculated from the formula:

$$\Delta L = \alpha \Delta T L$$

where α is the coefficient of thermal expansion.

ΔT is the change in temperature.

L is the length over which the dimension change is measured.

and ΔL is the change in length.

Hence for a 2 m long GRC component undergoing a temperature rise of 30°C

$$\Delta L = 20 \times 10^{-6} \times 30 \times 2000 = 1.2 \text{ mm}$$

assuming a coefficient of thermal expansion of $20 \times 10^{-6}/^\circ\text{C}$.

Cladding panels on a building may experience surface temperatures varying from -10°C to 60°C (light colors) or 80°C (dark colors) over the period of the year in the U.K., so substantial expansion or contraction may take place, up to 1.8 mm (0.07 in.) per meter length (Reference 57).

2.10.4.2 Moisture Movement:

Moisture movements in GFRC comprise two components. These are irreversible shrinkage and reversible shrinkage. Both components are present at all times, but the relative amounts of each depend on the conditions. Irreversible shrinkage will occur under all conditions, but more slowly if the GFRC has a high moisture content. Reversible shrinkage depends only on fluctuations in moisture content (Reference 57).

Wet-cured GFRC with a sand:cement ratio of 0.5:1 will probably experience 0.05% dimensional change due to irreversible shrinkage and of up to 0.15% reversible moisture movement subsequently. Since shrinkage occurs at a greater rate immediately after cure it is sensible to allow GFRC product to dry or acclimatize away from exposure to sun or winds for a period immediately after cure. In this way a large portion of the irreversible shrinkage may take place prior to installation of a component. The amount of shrinkage or moisture movement which may realistically be seen in service is up to 0.15% or 1.5 mm/metric length. Such an amount of movement requires design consideration in many ways, e.g. allowance for movement at fixing positions and selection of joint widths (Reference 57).

2.10.4.3 Stresses and Deflections due to Moisture and Thermal Movement:

Moisture and temperature gradients within GFRC products will induce stresses and/or deflections in the product. Since GFRC is normally made in relatively thin sections the possibility of significant differences in temperature through the thickness of the material is small, but moisture differentials can occur and the product will tend to bow out of its plane. For instance, if a damp flat GFRC sheet is placed upon a flat surface, the upper surface of the GFRC will start to dry by evaporation while the lower surface will not. The resulting bow is usually a temporary state since the effect is normally reversible. If different areas

of a product are subject to different conditions of temperature and moisture the product will tend to change shape to accommodate the induced movement, but under certain circumstances the product may be restrained, e.g. by its own shape, resisting the change of shape. When restraint occurs stresses are induced and these stresses can exceed the failure stress of the GFRC, resulting in what are termed "shrinkage" cracks (Reference 57).

The calculation of such stresses and deflections is complex in most cases and also inaccurate, since the conditions of moisture and temperature can only be estimated. However, if all movement of the GFRC is totally restricted then the stress which would be developed may be unacceptably high. For example, restraint of 0.15% shrinkage, assuming a modulus of 20,000 N/mm² could induce a stress

$$f = .0015 \times 20,000 = 30 \text{ N/mm}^2$$

This is substantially higher than the tensile strength of most GFRC formulations (Reference 57).

Good design of GFRC products would include a minimal number of fixings, making sure that these allow movement in the plane of the GFRC, and would also restrict the number of changes of section, ensuring smoothness of those which are necessary.

2.11 APPLICATIONS

With a fuller understanding of the particular benefits offered by GFRC, applications are becoming more varied and more widespread. GFRC products may be based upon thin and moulded plates; combination of these in sandwich panels; and in the form of the heavier-section, lower performance, premixed composite (References 59, 60).

2.11.1 Cladding Panels:

GFRC cladding is particularly noted for its relative lightness and 'freedom of design shape' in comparison with conventional concrete cladding. Additional stiffness, load carrying capacity and substantial improvements in insulation can be achieved by sandwich panel systems which combine GFRC surface skins of 6-10 mm (0.25-0.4 in.) thickness with a structural foam core that bonds the GFRC skins and provides a sandwich system with distinct and viable properties. Figures 2.11.1 and 2.11.2 show GFRC cladding panels used as replacement for heavy concrete sections (Reference 60).

Non-burning and incombustible characteristics of GFRC claddings can also be used in the replacement of certain timber forms and FRP panels. The replacement of timber forms is shown in Figures 2.11.3 and 2.11.4, and Figure 2.11.5 shows FRP panel replacement application (References 59, 60).

2.11.2 Formwork Applications:

Due to the inherent properties of GFRC it has considerable potential as a permanent rather than re-usable formwork material. In particular advantages offered are:

1. Pre-inspection and approval of the units can be made before casting-in.
2. Production of a uniform finished face.
3. The possibility of using expensive finishes in the ideal conditions of a precast works (Reference 59).

Bridge decking formwork (Figure 2.11.6) has proved to be a success story in its own right. From the early applications of high alumina cement and E-glass fiber using single skin profiles sheets, to the sandwich panel systems in use today, the product has evolved to fulfill the needs of the bridge designer in a number of ways (Reference 59).

The water industry adopted GFRC formwork to reinstate many miles of sewer systems in UK due to poor structural conditions that have developed. GFRC offers a cost-effective method of relining. Figure 2.11.7 show sewer linings whose GFRC units were manufactured in two pieces with overlap joints that run horizontally (References 59, 60).

Figure 2.11.8 shows a GFRC coffered ceiling that was formed from units of approximately 1.2 m cube (4 ft. cube). The principle of a coffered ceiling is well understood, but conventional methods employ FRP shutters that have to be struck and subsequent defects made good. The units also

come only in standard sizes offering little aesthetic scope for interior design considerations (Reference 59).

2.11.3 General Applications:

Figures 2.11.9 (a) and 2.11.9 (b) show GFRC roof tiles which used to be made by asbestos cement. GFRC properties of prime interest for the replacement of asbestos cement are (1) no health hazard with glass fiber as the reinforcement, (2) no brittle fracture mechanism under impact load, and (3) greater flexibility in matching composite formation to performance requirements for particular applications (Reference 60).

Figures 2.11.10 through 2.11.13 show general applications of GFRC products for several industrial market areas. Obviously there are many other GFRC product systems for particular industrial areas, for example, fire protective ducting and fire doors for the fire protection industry, noise barrier systems for urban motorways, and field drainage elements and railing fencing for agricultural industry (Reference 56).

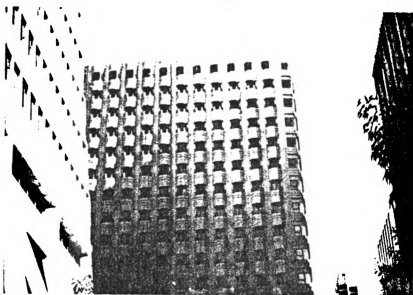


Figure 2.11.1 GFRC Cladding Panels (Reference 60).

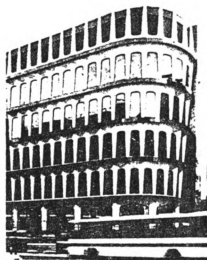


Figure 2.11.2 Replacement of Conventional Cladding Panels (Reference 60).

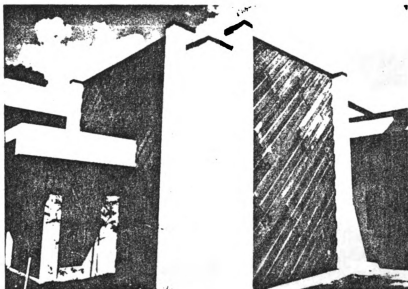


Figure 2.11.3 Timber Replacement (Reference 60).

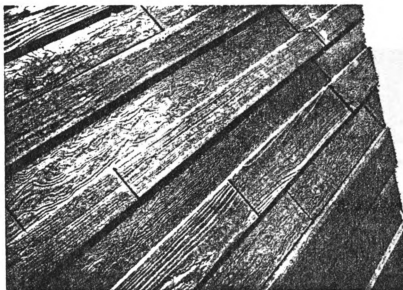


Figure 2.11.4 GFRP 'Timber' Cladding Detail (Reference 60).

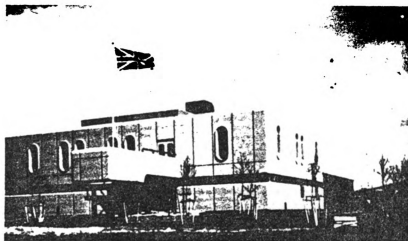


Figure 2.11.5 FRP Panel Replacement Application (Reference 59).

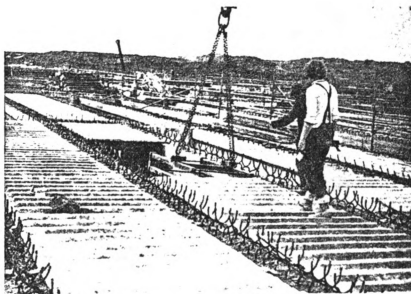


Figure 2.11.6 Permanent Formwork (Reference 60).

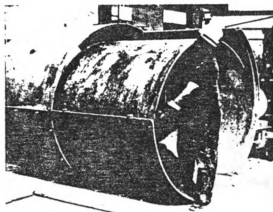


Figure 2.11.7 Sewer Linings (Reference 59).

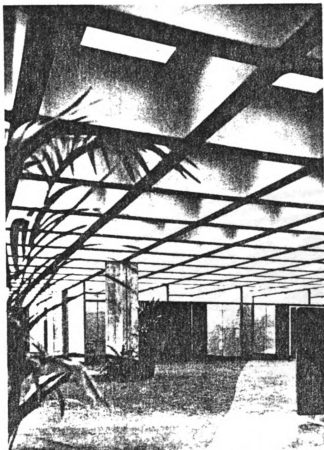
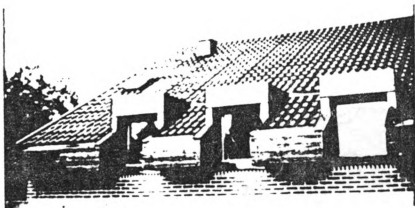
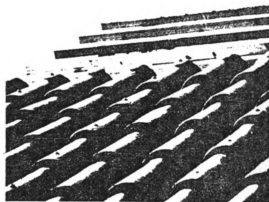


Figure 2.11.8 GFR Permanent Coffier Units (Reference 59).



(a) Roof Tiles



(b) Roof Tiles Detail

Figure 2.11.9 Asbestos Cement Replacement (Reference 60).

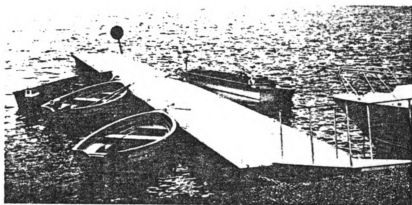


Figure 2.11.10 The Marine Industry. Floating Pontoons (Reference 60).

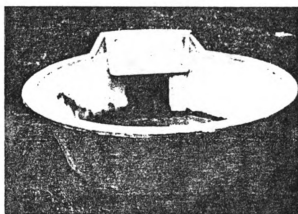


Figure 2.11.11 The Agricultural Industry. Field Drinking Trough (Reference 60).

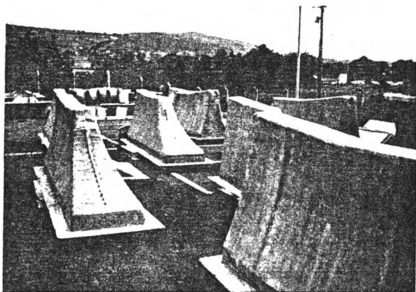


Figure 2.11.12 The Agricultural Industry. Sheep Dip Troughs (Reference 60).



Figure 2.11.13 The Leisure Industry. Kiosk (Reference 60).

CHAPTER 3

EXPERIMENTAL PROGRAM

3.1 OBJECTIVE

An experimental study was conducted in order to reach the following objectives:

1. Establish the durability characteristics of polymer modified GFRC with different polymer additions; assess the effects of polymer modification.
2. Identify the failure and aging mechanisms of conventional and polymer-modified GFRC.

3.2 EXPERIMENTAL DESIGN

3.2.1 Variables:

The key variables of the experimental study were: (1) polymer content at four levels; (2) aging environments (two conditions); and (3) aging duration after precuring (nine levels).

The "levels" of these variables considered in this experimental study are introduced below:

Polymer contents (polymer/cement wt%): 0%(control), 5%,
10% and 15%,

Aging environments (curing condition after 28 days of precuring):

dry air (20°C, 68°F, 40% RH)

hot water (50°C, 122°F)

Aging durations (after 28 days of precuring):

0 (28th day after casting), 12 hours,

1, 5, 10, 15, 20, 30, 50 days

The polymer contents selected for use in this investigation represent typical values used in practice. The maximum aging duration was selected as 50 days because, as reported in Reference 61, most of the strength and toughness losses caused by immersion in 50°C water take place within the first 30 days immersion.

3.2.2 Testing:

Durability characteristics were assessed through flexural tests in accordance with ASTM C 947-81 (Standard Test Method for Flexural Properties of Thin-Section Glass-Fiber-Reinforced Concrete Using Simple Beam With Third-Point Loading). Scanning electron microscope (SEM) observations were used to identify the mechanisms of failure and aging in GFRC.

In the flexural test, LOP (limit of proportionality), MOR (modulus of rupture), and flexural toughness were measured. More than eight specimens were tested at ages of 0 and 50 days; four specimens were tested at other ages for each mix proportion and aging condition.

3.3 MATERIALS, MIX PROPORTIONS & CONSTRUCTION

3.3.1 Materials:

The materials used in this investigation were:

- (a) AR-glass fiber; Nippon Electric Glass AR-2500H-103 (see Table 3.1).
- (b) Cement; Davenport Type I Portland cement.
- (c) Silica sand; Unimin Granusil 40 (see Table 3.2 for gradation).
- (d) Polymer; acrylic emulsion M2250 supplied at 47% solids content by weight of the polymer latex compound.
- (e) Superplasticizer; W.R. Grace WRDA 19.

3.3.2 Mix Proportions:

The GFRC panels tested in this investigation were made using mix proportions presented below.

- (a) Glass fiber content; 6 wt% of GFRC chopped to 2 in. length.
- (b) Water content; water/cement ratio of 0.3.
- (c) Sand content; sand/cement ratio of 0.5.
- (d) Superplasticizer; 6 to 20 oz. addition for 100 lb. of cement (no adjustment for water content).
- (e) Polymer content (variable); 0, 5, 10, 15 wt% of cement (solid/cement ratio), and water content was adjusted for the water from polymer latex compound.

Table 3.1 Properties of AR-Glass Fiber (Reference 62).

Item		Unit	Properties
Density		pcf	170
Fiber Diameter		inch	0.00053
Tensile Strength		psi	more than 1.85×10^6
Young's Modulus		psi	1.1×10^7
Strain		%	more than 1.5
Alkali-resis-tivity	Weight ¹⁾ Loss	ARG Fiber	% 0.85
		E-type glass fiber	% 10.5
	Tensile ²⁾ Strength Retention	ARG Fiber	% 75
		E-type glass fiber	% 14

1) Weight loss rate (%) of strand, held at 176°F for 200 hours in saturated cement solution

2) Tensile strength retention rate (%) of cement paste applied strand, held at 122°F for 300 hours in 100%RH.

Table 3.2 Silica Sand Sieve Analysis.

ASTM E-11 Sieve No.	Mean % Retained on Individual Sieves
20	Trace
30	6.9
40	43.5
50	44.7
pan	4.9

3.3.3 Construction:

Seven GFRP panels with dimension of 15 x 30 x 1/2 in. (38 x 76 x 1.3 cm) were manufactured for each polymer content (total of 28 panels). The direct spraying method with single head gun (as discussed in Chapter 2) was used for the construction of panels. Char mixer was used to

achieve uniform and pumpable GFRC mortar mixtures. The output rate of mortar pump was 20 lb. of mortar per minute and that of chopper gun was 1.3 lb. of glass fiber per minute.

After spraying, the panels were covered with plastic sheets and stored at 20°C (68°F), and demolded after overnight curing. At this point, the polymer-modified GFRC panels (polymer contents of 5, 10, 15%) were simply cured in dry air (20°C, 68°F, 40% RH) for additional 27 days of precuring; while non-polymer-modified GFRC panels (polymer content of 0%) were continuously covered with plastic sheets for the remaining 27 days of precuring in order to maintain moisture at 80-90% RH. Note that in case of polymer-modified GFRC a continuous polymer tends to be formed in air, and thus optimum properties can be achieved by dry air curing although this does not allow full strength of the paste to be developed (Reference 20).

3.4 TEST PROCEDURES

Test procedures were as follows:

1. After the 28-day precuring period all panels were saw-cut into 2 x 15 x 0.5 in. (5 x 38 x 1.3 cm) specimens. Figure 3.1 shows a polymer-modified GFRC panel and two specimens cut from another panel.
2. Half of the specimens from panels manufactured with each mix proportion (45 specimens for each polymer content) were selected randomly and immersed in 50°C

(122°F) water for accelerated aging; the remaining specimens were either tested (age 0) or placed in dry air curing (20°C, 68°F, 40% RH). Random selection of specimens for different aging condition and periods helped eliminate potential errors caused by panel-to-panel and section-to-section (within a panel) variations. Figure 3.2 shows the water bath used for accelerated aging.

3. At each predetermined age, both the dry air and hot water cured specimens with different polymer contents were subjected to third-point flexural loading on a span of 12 in. (30.5 cm). The crosshead speed was kept below 0.1 in./min. (2.5 mm/min.). A load cell and two displacement transducers were used to measure load and deflection at mid-span of the beam (Figure 3.3). A computer-based data acquisition system (Figure 3.4) was used to record load-deflection curves, Flexural strengths and flexural toughness.
4. After flexural testing specimens aged in air and hot water were thoroughly saw cut into smaller specimens for SEM observation of their fractured surfaces. The SEM used in this investigation was JEOL T-330 (Figure 3.5).



Figure 3.1 GFRP Panel and Specimens.



Figure 3.2 Water Bath for Accelerated Aging.

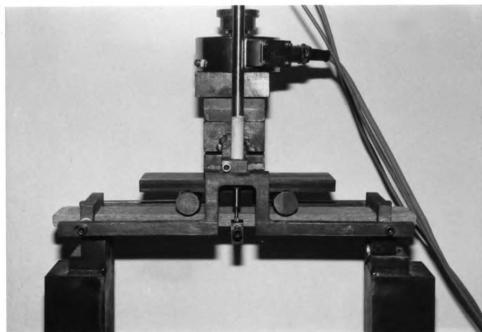


Figure 3.3 Third-Point Loading with a Load Cell and Two Transducers.

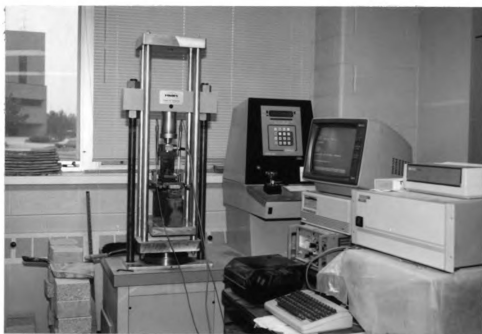


Figure 3.4 Computer-Based Data Acquisition System.



Figure 3.5 JEOL T-330 SEM.

CHAPTER 4

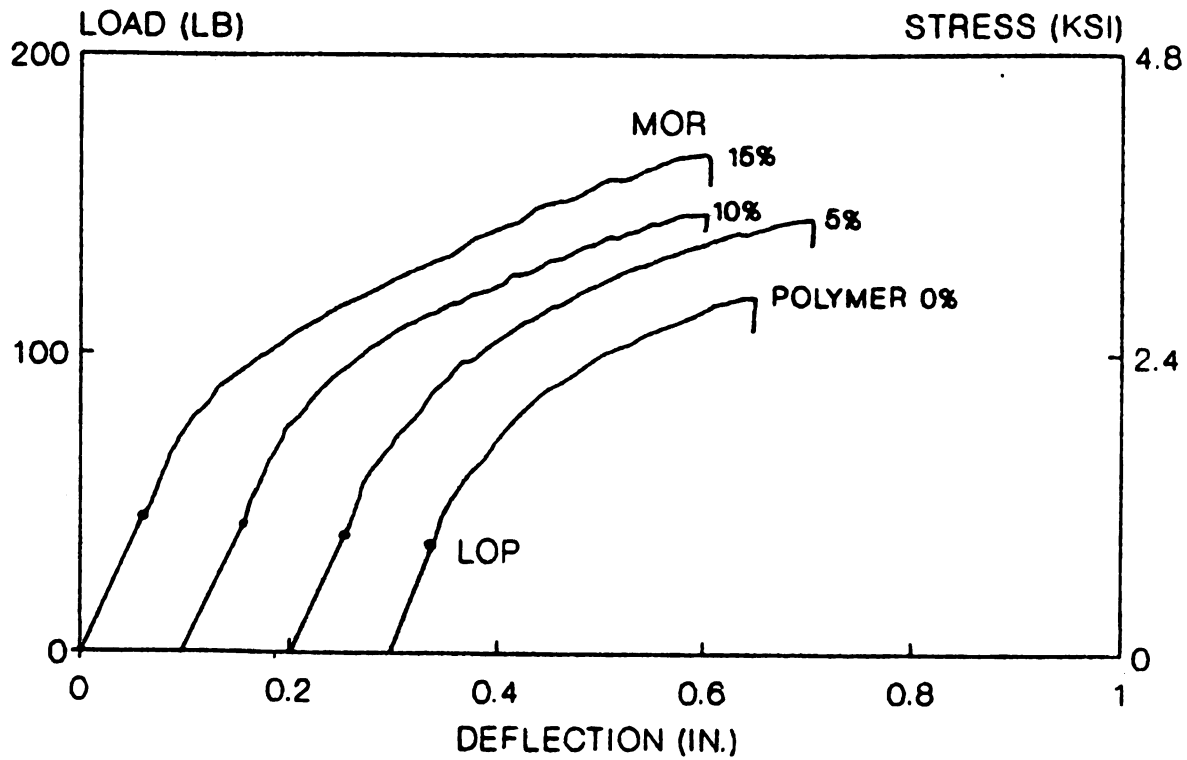
EXPERIMENTAL RESULTS & DISCUSSION

The test data generated in this investigation together with the conclusions derived based on statistical analyses of results are presented in this chapter.

4.1 FLEXURAL LOAD-DEFLECTION BEHAVIOR

Figure 4.1 shows typical flexural load-deflection curves for unaged GFRC with different polymer contents. For unaged GFRC, polymer addition leads to improvements in both strength (LOP and MOR) and toughness characteristics. An enlargement of the multiple crack region (between LOP and MOR in load-deflection curves) is caused by polymer modification. At 15% polymer addition, the amount of hair crack visible under loading at the tension side of specimens was about twice as many as that for specimens with no polymer addition (see Figure 4.2).

Figure 4.3 presents typical flexural load-deflection curves for aged GFRC specimens after 50-days of immersion in hot water at 50°C (122°F). The multiple cracking region was reduced significantly after aging in hot water and brittle mode of fracture with no visible hair cracks prior to peak load was common in aged specimens. Although the MOR (Modulus of Rapture) and toughness of polymer modified GFRCs were somehow higher than unmodified mixture after aging for 50 days in hot water, severe deteriorations were still observed at all polymer addition levels.



2X15X0.5 IN. SPECIMEN (SPAN=12')

Figure 4.1 Typical Load-Deflection Curves-Unaged GFRC.

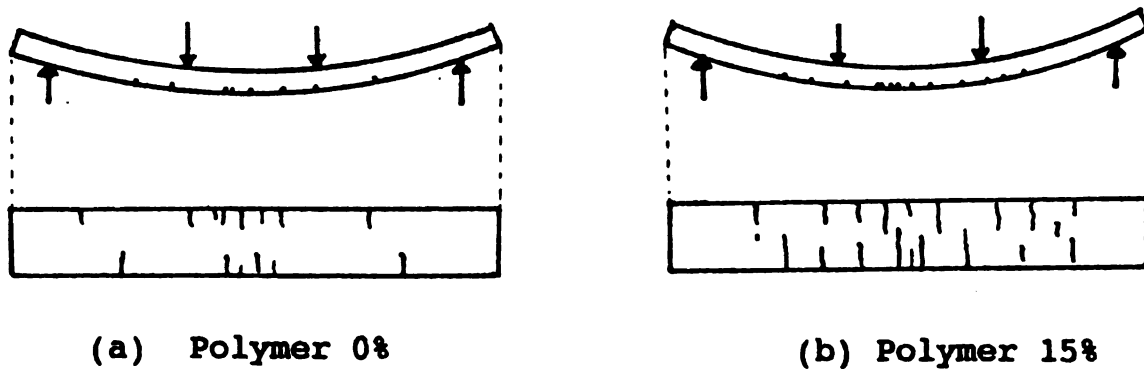
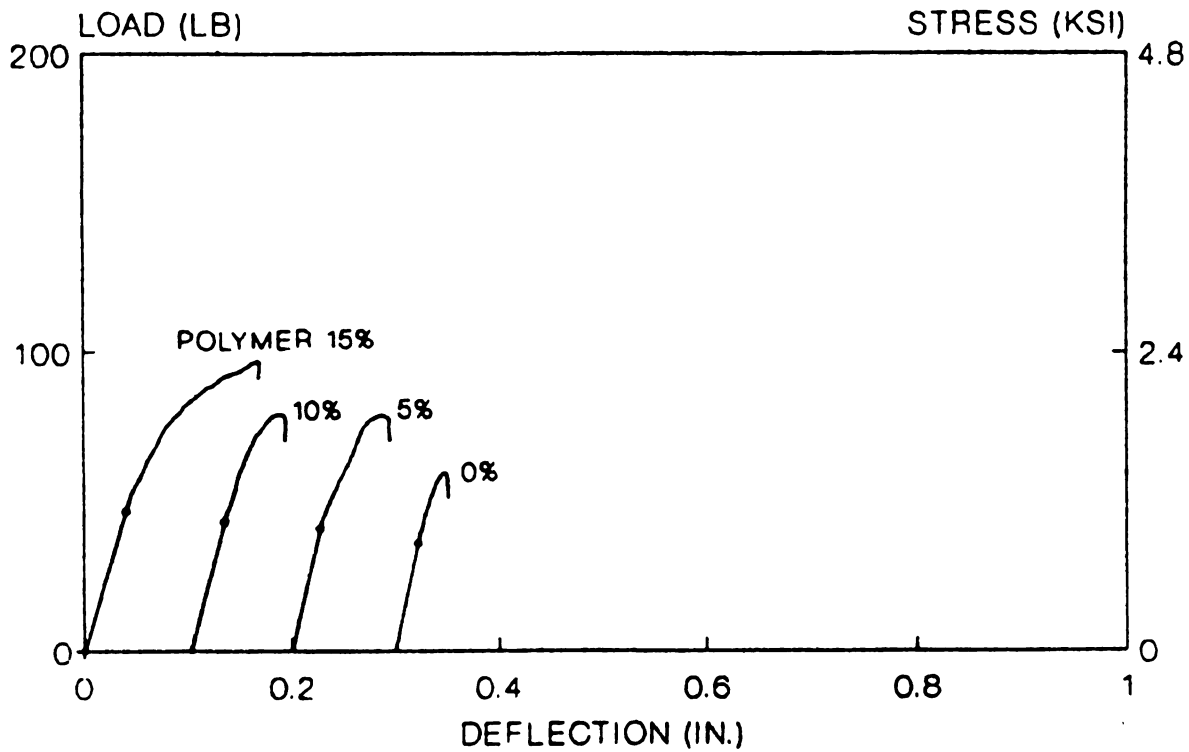


Figure 4.2 Multiple Cracking.



2X.15X0.5 IN SPECIMEN (SPAN=12")

Figure 4.3 Typical Load-Deflection Curves - Aged GFRC (50 Days in 50°C, 122°F Water).

4.2 FLEXURAL STRENGTH AND TOUGHNESS TEST RESULTS

Tables 4.1 through 4.9 present the average values of LOP, MOR and flexural toughness obtained in flexural tests performed at different aging periods. Flexural toughness was defined as the area under load-deflection curve up to MOR divided by the cross-sectional area of the beam (Reference 61).

The effects of aging on LOP and MOR values for all tested specimens are plotted in Figures 4.4 through 4.7, and on flexural toughness in Figures 4.8 through 4.11. These indicate that polymer addition improves flexural characteristics, and aging in hot water reduces LOP, MOR and

toughness while aging in air does not seem to have significant effects on the flexural performance of GFRC. There are, however, relatively large variations in the flexural test results (particularly for MOR and Flexural toughness), necessitating the use of statistical methods to analyze the test results.

Table 4.1 Flexural Test Results - Unaged GFRC.

AGE 0 (28TH DAY FROM CASTING)			
POLYMER P/C wt%	LOP psi	MOR psi	TOUGHNESS lb/in.
0%	824	2795	37.00
5%	957	3345	61.33
10%	976	3237	61.91
15%	1142	3923	89.20
AVERAGE OF 13-15 SPECIMENS			

AGE 12 HOURS						
POLYMER P/C wt%	LOP psi		MOR psi		TOUGHNESS lb/in.	
	AIR	WATER	AIR	WATER	AIR	WATER
0%	938	799	3017	2166	42.55	29.17
5%	910	835	3291	2631	63.44	37.28
10%	983	887	3318	2592	59.60	42.24
15%	1024	953	3802	3195	71.99	63.26

AIR-20C (68F), 40%RH. WATER-50C (122F)

AVERAGE OF FOUR SPECIMENS

Table 4.3 Flexural Test Results - 1 Day Aging.

AGE 1 DAY						
POLYMER P/C wt%	LOP psi		MOR psi		TOUGHNESS lb/in.	
	AIR	WATER	AIR	WATER	AIR	WATER
0%	861	669	2788	1873	37.06	20.51
5%	864	868	3244	2659	54.73	38.66
10%	890	798	3400	2392	66.53	40.74
15%	1230	920	3976	3445	83.05	68.86

AIR-20C (68F), 40%RH. WATER-50C (122F)

AVERAGE OF FOUR SPECIMENS

Table 4.4 Flexural Test Results - 5 Day Aging.

AGE 5 DAYS						
POLYMER P/C wt%	LOP psi		MOR psi		TOUGHNESS lb/in.	
	AIR	WATER	AIR	WATER	AIR	WATER
0%	945	824	3114	1856	46.11	14.07
5%	923	877	3481	2278	58.07	24.58
10%	990	734	2997	2092	63.80	22.72
15%	1164	1066	3668	3134	77.65	48.78

AIR-20C (68F), 40%RH. WATER-50C (122F)

AVERAGE OF FOUR SPECIMENS

Table 4.5 Flexural Test Results - 10 Day Aging.

AGE 10 DAYS						
POLYMER P/C wt%	LOP psi		MOR psi		TOUGHNESS lb/in.	
	AIR	WATER	AIR	WATER	AIR	WATER
0%	865	806	2855	2143	35.08	17.02
5%	917	859	3454	2122	58.93	16.93
10%	1060	832	3854	2111	75.79	14.88
15%	1076	966	4116	3008	87.95	36.06

AIR-20C (68F), 40%RH. WATER-50C (122F)

AVERAGE OF FOUR SPECIMENS

Table 4.6 Flexural Test Results - 15 Day Aging.

AGE 15 DAYS						
POLYMER P/C wt%	LOP psi		MOR psi		TOUGHNESS lb/in.	
	AIR	WATER	AIR	WATER	AIR	WATER
0%	923	823	2901	1710	35.75	10.43
5%	1038	888	3830	1923	66.38	13.53
10%	1243	857	3881	2166	70.71	11.79
15%	1121	947	4422	2555	99.60	26.41

AIR-20C (68F), 40%RH. WATER-50C (122F)

AVERAGE OF FOUR SPECIMENS

Table 4.7 Flexural Test Results - 20 Day Aging.

AGE 20 DAYS						
POLYMER P/C wt%	LOP psi		MOR psi		TOUGHNESS lb/in.	
	AIR	WATER	AIR	WATER	AIR	WATER
0%	960	867	2577	1821	34.57	11.00
5%	988	808	3901	2050	79.34	11.91
10%	1054	933	3511	1970	69.74	9.61
15%	1167	997	4466	2661	97.22	32.33

AIR-20C (68F), 40%RH. WATER-50C (122F)

AVERAGE OF FOUR SPECIMENS

AGE 30 DAYS						
POLYMER P/C wt%	LOP psi		MOR psi		TOUGHNESS lb/in.	
	AIR	WATER	AIR	WATER	AIR	WATER
0%	880	799	2655	1532	32.86	4.20
5%	944	948	3495	2070	59.65	11.06
10%	1032	955	3884	2267	75.65	6.83
15%	1101	965	4244	2572	94.50	18.37

AIR-20C (68F), 40%RH. WATER-50C (122F)

AVERAGE OF FOUR SPECIMENS

Table 4.9 Flexural Test Results - 50 Day Aging.

AGE 50 DAYS						
POLYMER P/C wt%	LOP psi		MOR psi		TOUGHNESS lb/in.	
	AIR	WATER	AIR	WATER	AIR	WATER
0%	900	833	2887	1455	37.36	2.60
5%	943	980	3439	1923	62.67	5.04
10%	1057	1028	3586	1876	65.11	4.09
15%	1094	1065	3877	2351	88.29	15.52

AIR-20C (68F) , 40%RH. WATER-50C (122F)

AVERAGE OF 8-11 SPECIMENS

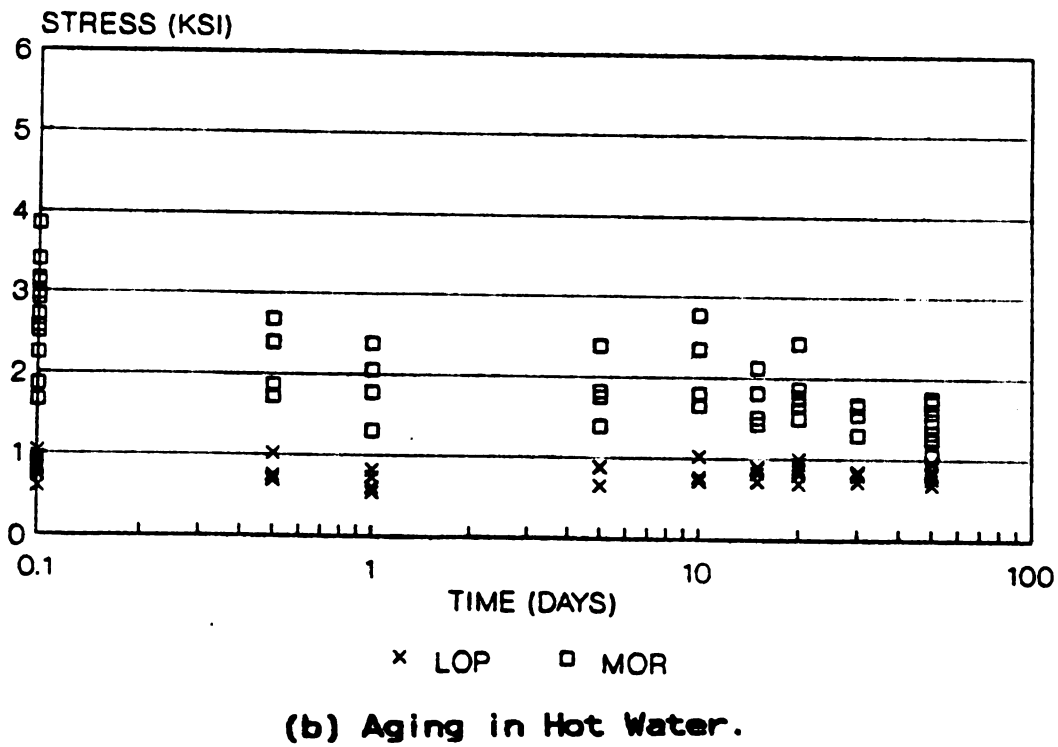
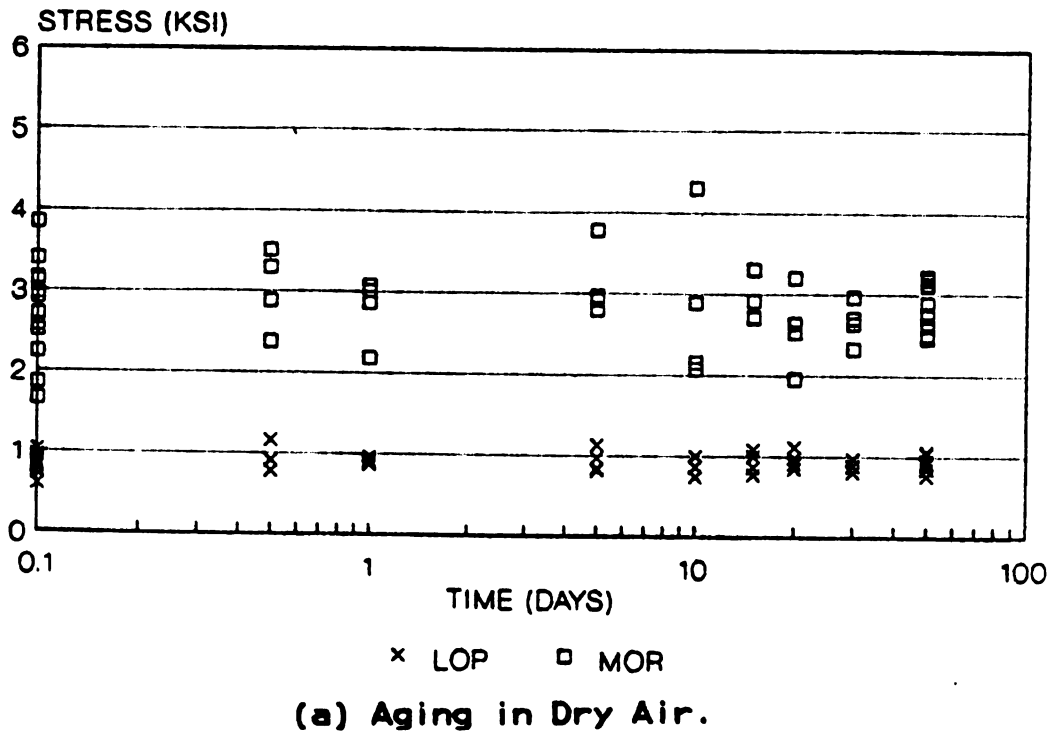


Figure 4.4 LOP, MOR vs. Time-Polymer 0%.

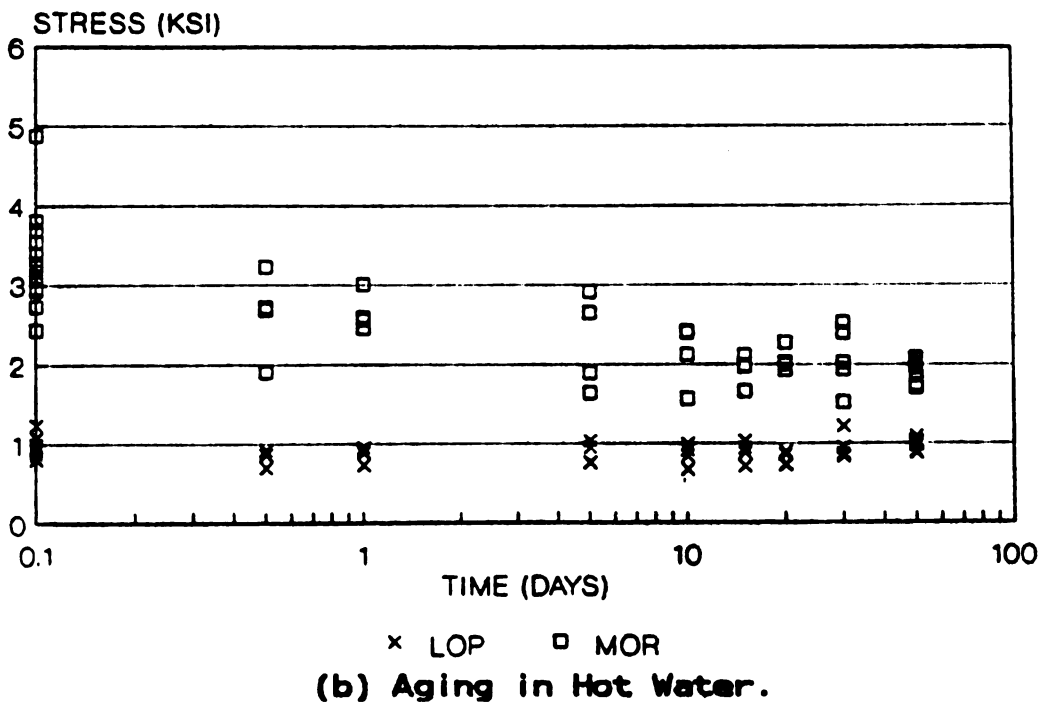
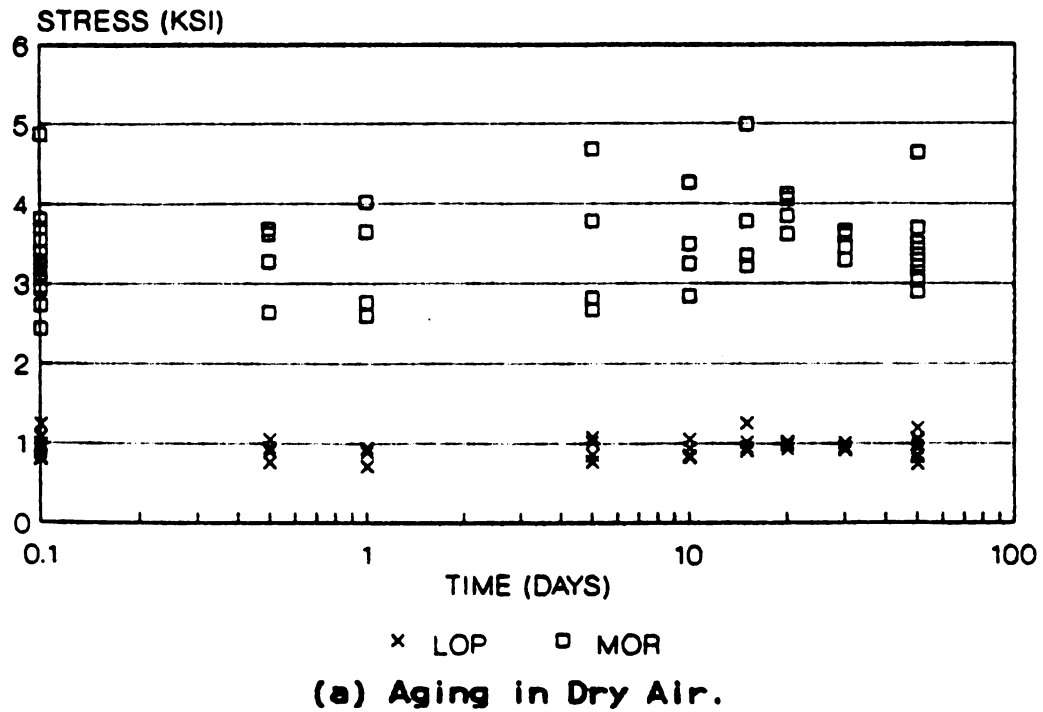
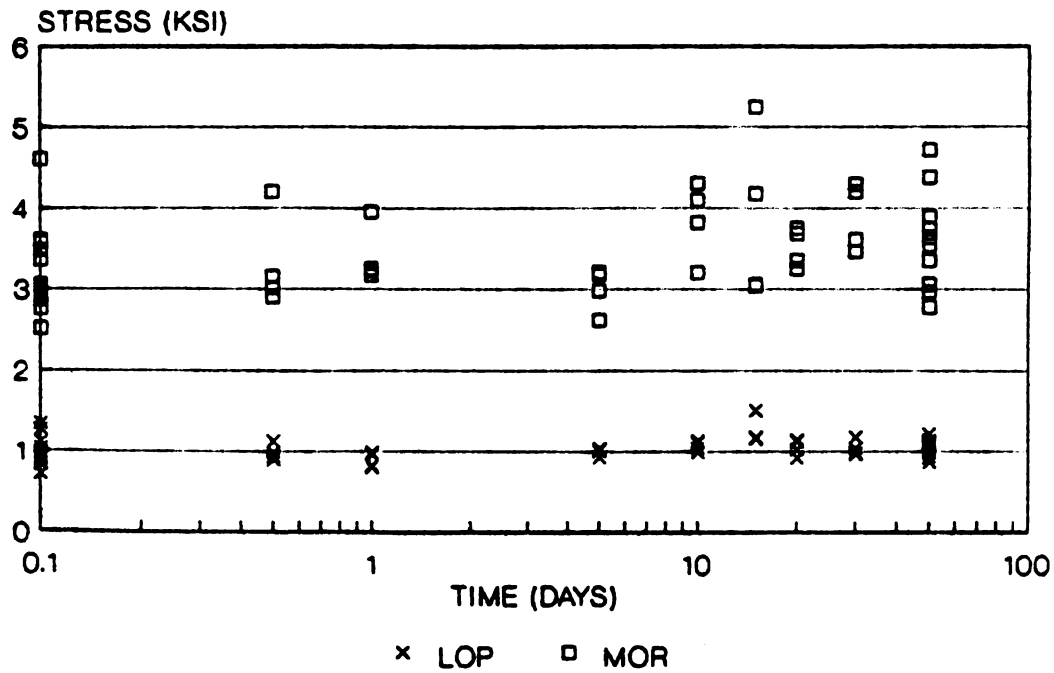
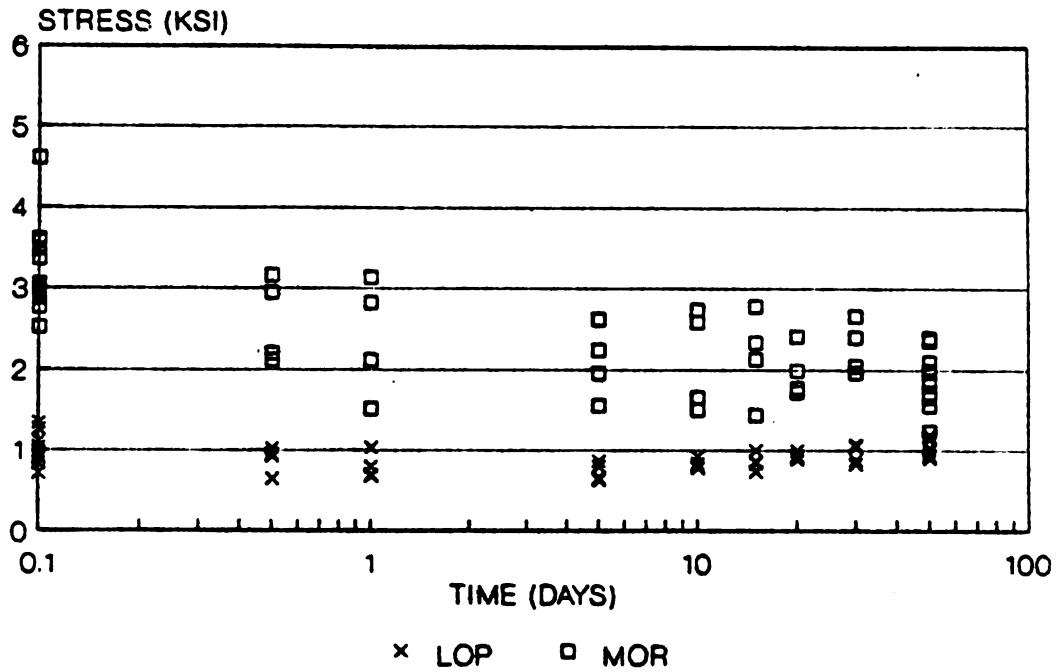


Figure 4.5 LOP, MOR vs. Time-Polymer 5%.

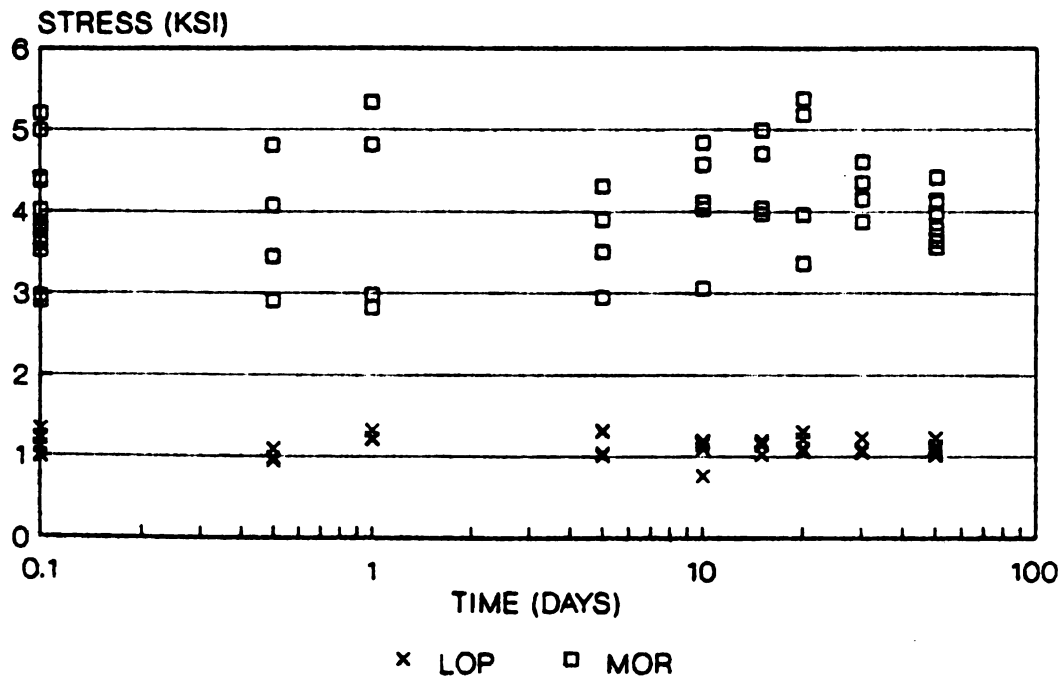


(a) Aging in Dry Air.

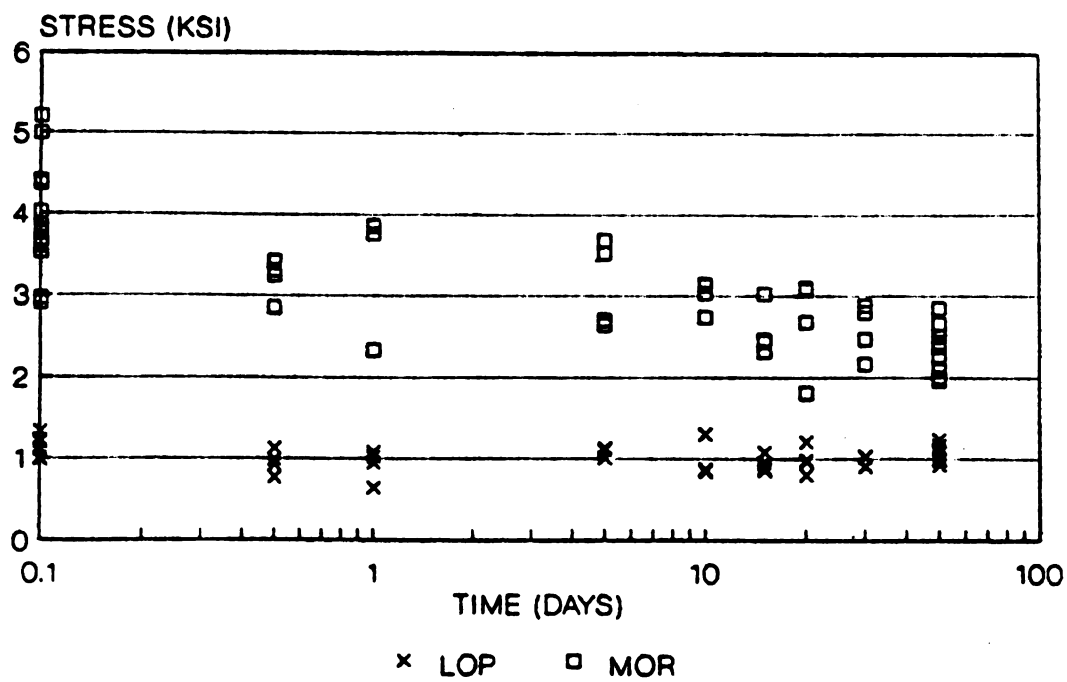


(b) Aging in Hot Water.

Figure 4.6 LOP, MOR vs. Time-Polymer 10%.

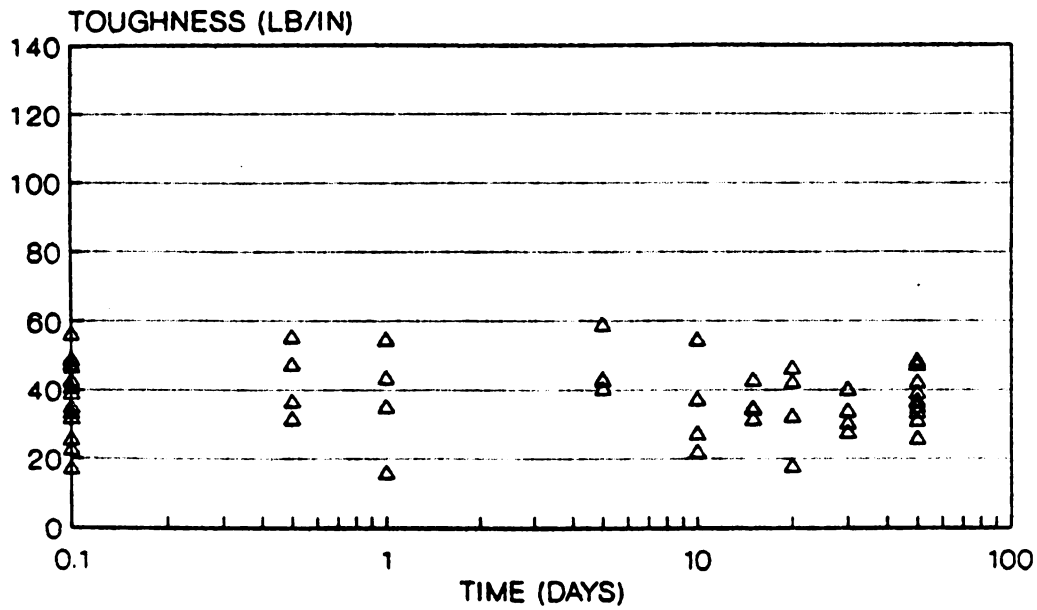


(a) Aging in Dry Air.

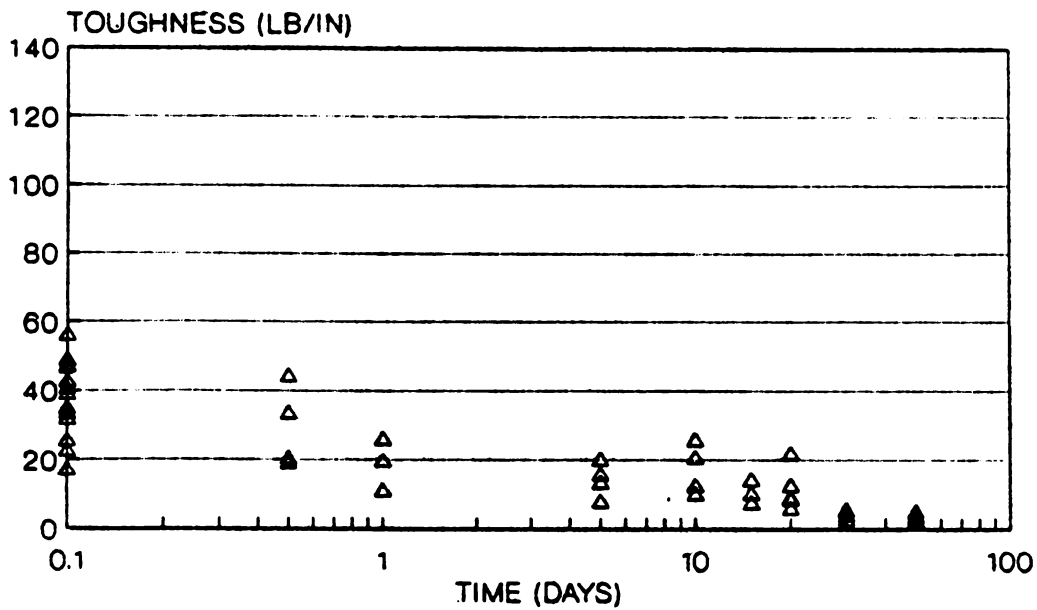


(b) Aging in Hot Water.

Figure 4.7 LOP, MOR vs. Time-Polymer 15%.

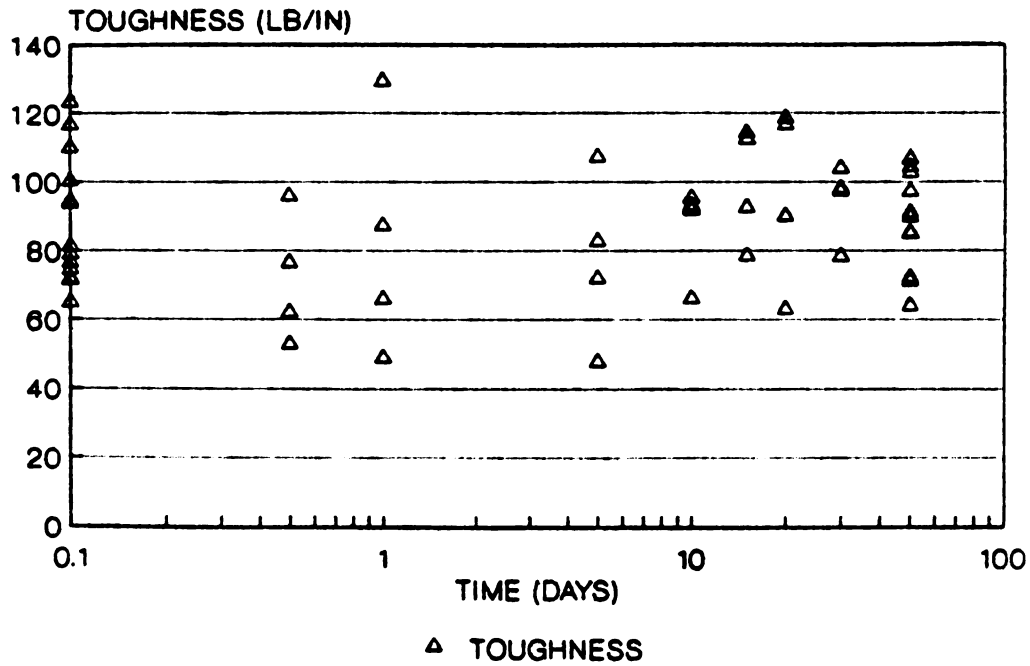


△ TOUGHNESS
(a) Aging in Dry Air.

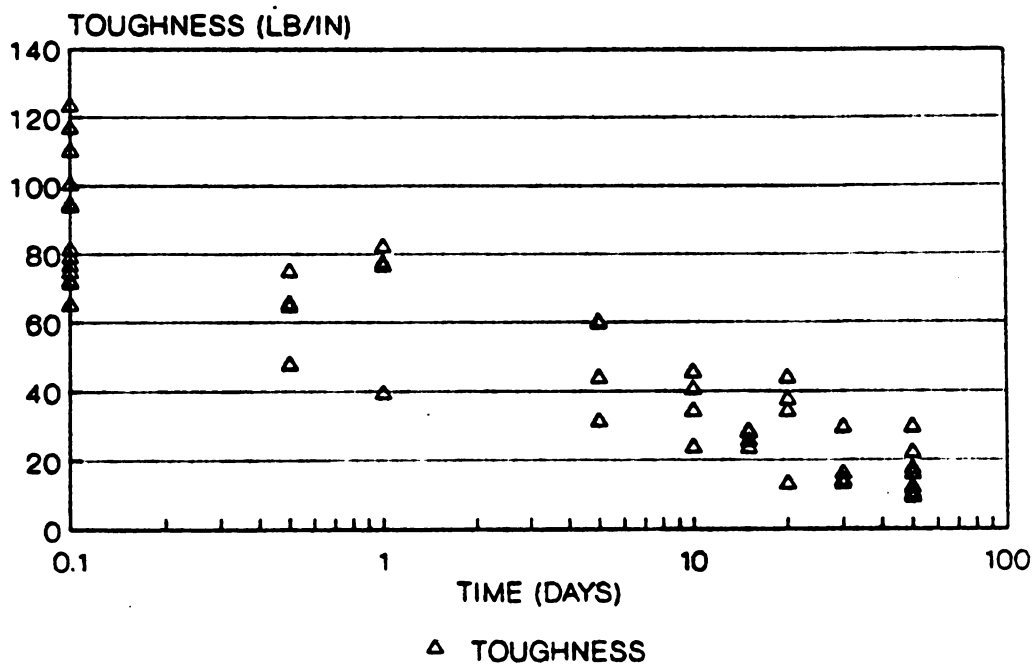


△ TOUGHNESS
(b) Aging in Hot Water.

Figure 4.8 Toughness vs. Time-Polymer 0%.

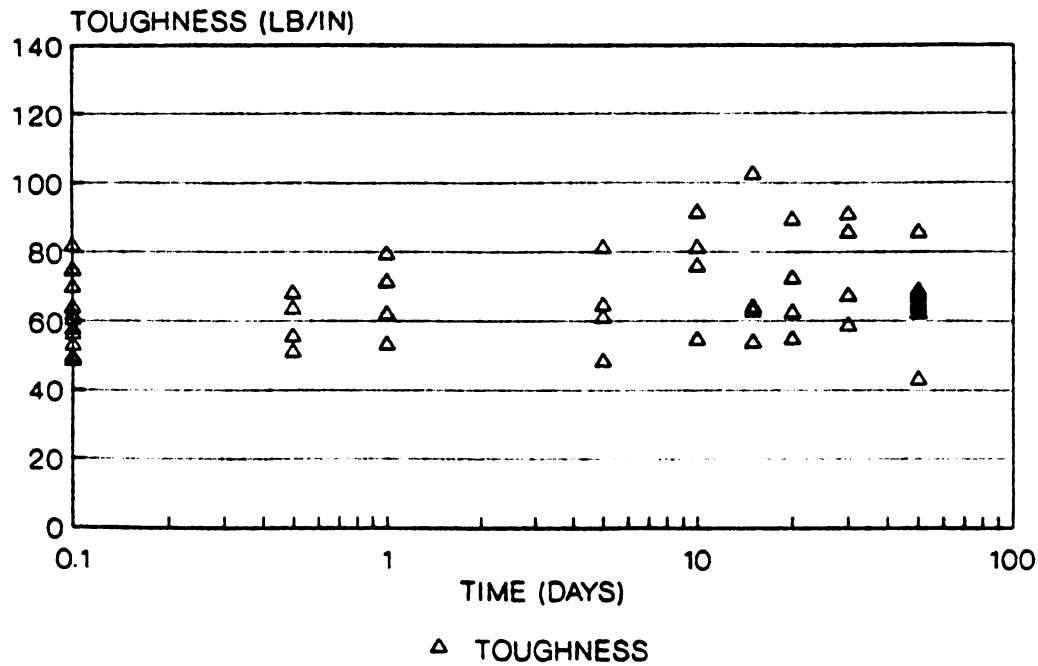


(a) Aging in Dry Air.

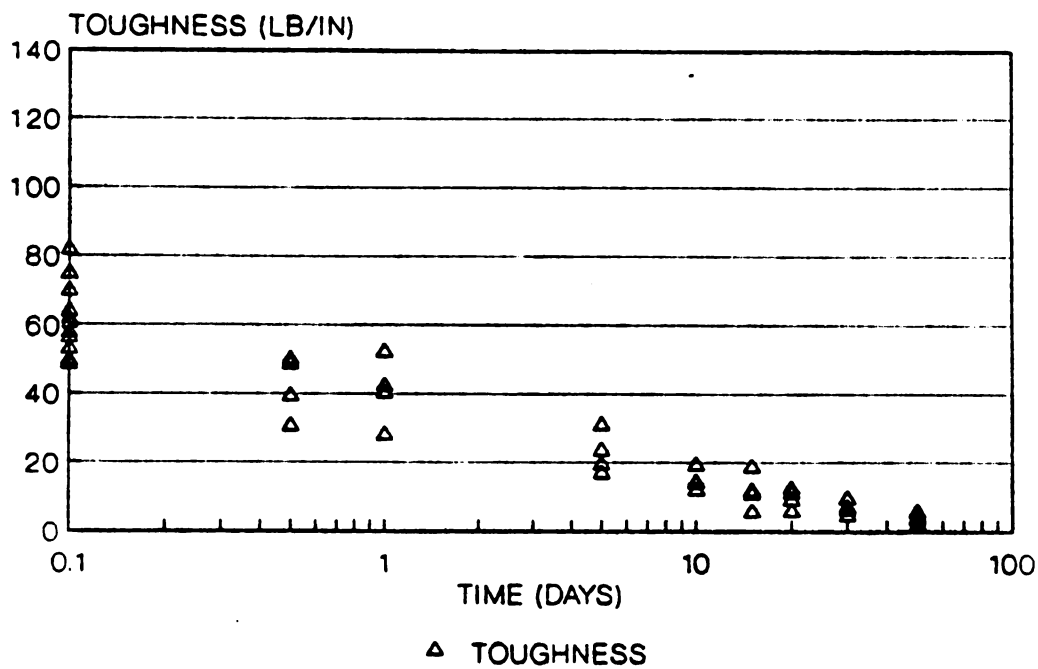


(b) Aging in Hot Water.

Figure 4.9 Toughness vs. Time-Polymer 5%.



(a) Aging in Dry Air.



(b) Aging in Hot Water.

Figure 4.10 Toughness vs. Time-Polymer 10%.

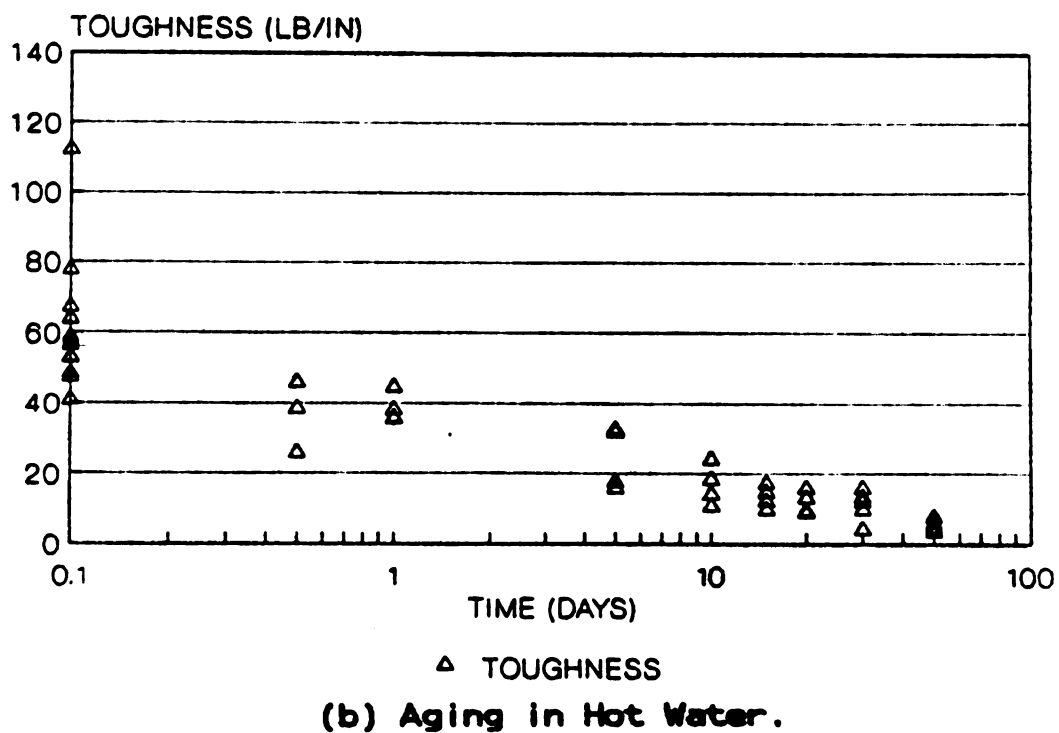
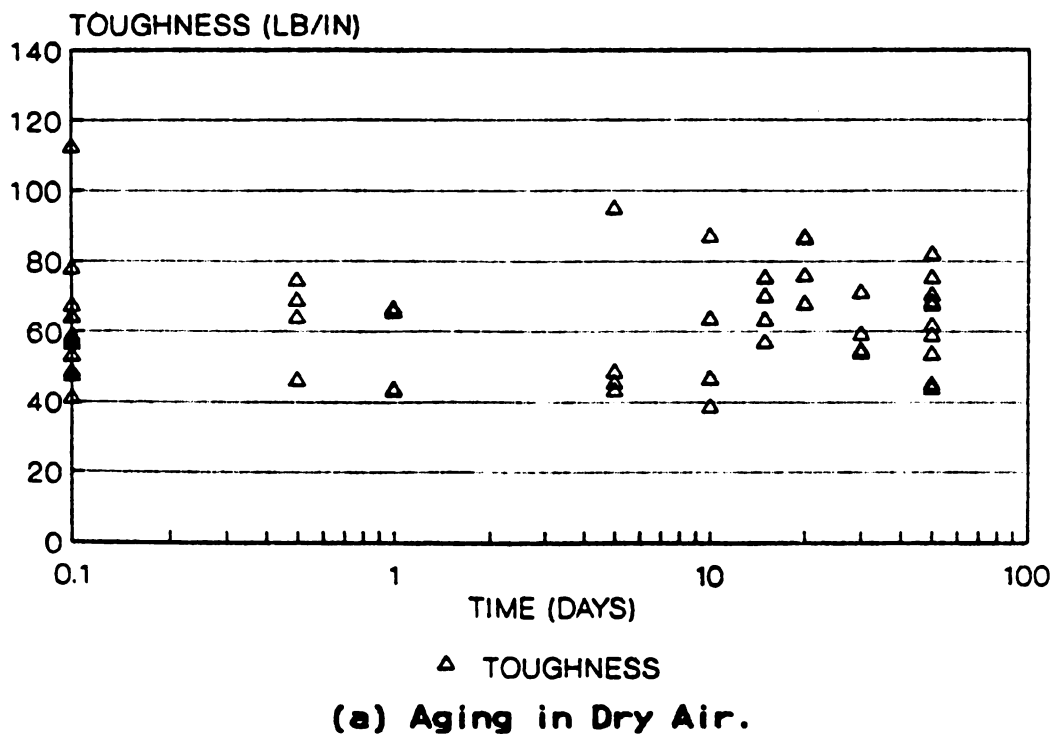


Figure 4.11 Toughness vs. Time-Polymer 15%.

4.3 POLYMER EFFECTS ON AGING IN AIR

Figures 4.12 and 4.13 show the average flexural strength and toughness of unaged GFRC (285h day after casting) and GFRC aged in air for 50 days (50 days after 28-day precuring), with different polymer addition. Figures 4.14 and 4.15 also present the change of LOP, MOR and flexural toughness with time for each polymer content. These flexural characteristics seem to improve with the increase of polymer addition, and polymer modified GFRCs show slight increase in MOR and toughness with time; however, because of relatively large variations in test results statistical analysis were conducted as described below, in order to confirm observations. It should be noted that about 10 replications were made for each mix conditions at ages 0 and 50 days, and 4 replications were made at other ages.

One-way analysis of variance with Scheffe's procedure was the statistical technique used in this phase of study. By using this technique, no differences in LOP, MOR and toughness with aging period could be detected any pair of ages and for any polymer content, at 5% level of significance. Hence aging in air after 28 days of precuring does not have any important effects, negative or positive, at 5% level of significance with LOP, MOR and flexural toughness of unmodified and polymer modified GFRC.

In order to analyze the polymer modification effects, considering the relatively small effects of aging in air,

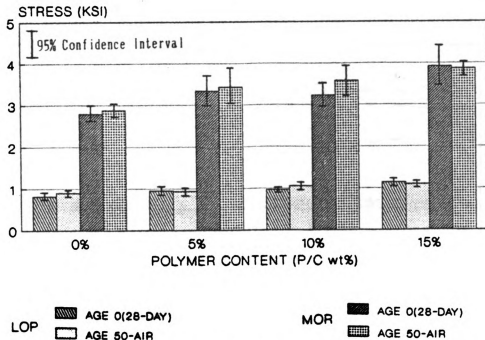


Figure 4.12 LOP and MOR of Unaged and Aged in Air.

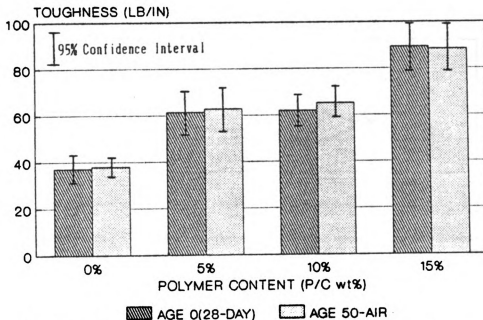


Figure 4.13 Toughness of Unaged and Aged in Air.

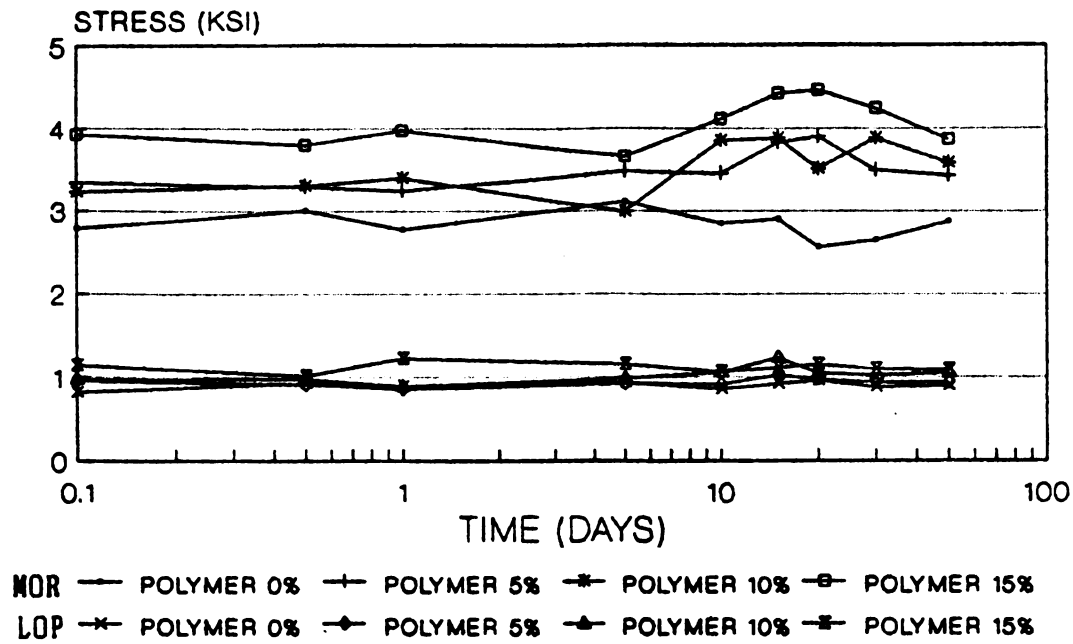


Figure 4.14 LOP and MOR with Time-GFRC Aged in Air.

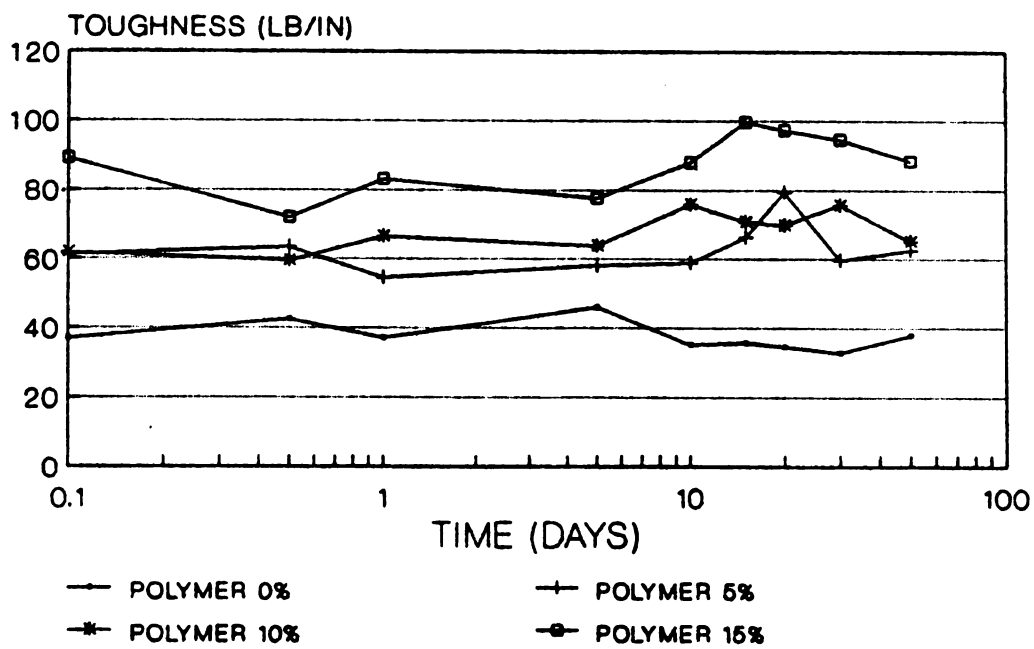


Figure 4.15 Toughness with Time-GFRC Aged in Air.

all the test data obtained after different periods of aging in air were grouped together; this gave more than 50 data points for each mix condition. Tables 4.10 to 4.12 show statistical characteristics for LOP, MOR and flexural toughness. Polymer modification, at 15% polymer-cement ratio, led to about 40% increase in MOR and about 100% in flexural toughness when compared with unmodified GFRc. The results of one-way analysis of variance are summarized in Tables 4.13 through 4.15. Asterisks (*) in these tables suggest significant differences detected at 5% level of significance between the pairs of polymer contents on the corresponding row and columns of the tables. Polymer addition at 5% has major effects on MOR and toughness, but not on LOP, at 5% level of significance. Polymer addition at 10% and 15% have major effects on MOR, toughness and also LOP, when compared with unmodified GFRc. Except for LOP, increasing from 5% to 10% polymer content does not have major effects on flexural performance. However, increasing the polymer content from 10% to 15% positively influenced all aspects of flexural behavior, at 5% level of significance.

All GFRc specimens, unaged or aged in air, showed a ductile mode of failure. Figure 4.16 shows the cracking pattern of these ductile GFRcs, which was always marked by an inclined crack. Figure 4.17 shows the fractured surface of unaged GFRc. SEM observation of fractured surfaces is shown in Figure 4.18 indicates that all fiber filaments have

Table 4.10 Statistical Characteristics for LOP-Aging in Air.

Polymer	Count	Mean (psi)	Standard Deviation	95% Conf. Int. for Mean			Min.	Max.
0%	55	883	109	853	to	912	589	1148
5%	52	941	117	908	to	973	703	1246
10%	53	1021	141	983	to	1060	704	1495
15%	53	1118	108	1089	to	1148	753	1320

Table 4.11 Statistical Characteristics for MOR-Aging in Air.

Polymer	Count	Mean (psi)	Standard Deviation	95% Conf. Int. for Mean			Min.	Max.
0%	55	2833	483	2703	to	2964	1653	4296
5%	52	3457	571	3298	to	3615	2430	4981
10%	53	3469	575	3310	to	3627	2511	5238
15%	53	4005	662	3823	to	4188	2813	5376

Table 4.12 Statistical Characteristics for Flexural Toughness-Aging in Air.

Polymer	Count	Mean lb/in.	Standard Deviation	95% Conf. Int. for Mean			Min.	Max.
0%	55	37.43	10.29	34.65	to	40.22	15.75	58.65
5%	52	62.45	15.15	58.23	to	66.67	38.63	112.15
10%	53	66.23	12.61	62.75	to	69.71	43.01	102.41
15%	53	88.05	19.26	82.74	to	93.86	47.92	129.48

Table 4.13 Polymer Effects in LOP-Aging in Air.

Mean (psi)	Polymer	0%	5%	10%	15%
883	0%				
941	5%				
1021	10%	*	*		
1118	15%	*	*	*	

(*) denotes significant differences at 5% level
of significance for the pairs of polymer content.

Table 4.14 Polymer Effects in MOR-Aging in Air.

Mean (psi)	Polymer	0%	5%	10%	15%
2833	0%				
3457	5%	*			
3469	10%	*			
4005	15%	*	*	*	

(*) denotes significant differences at 5% level
of significance for the pairs of polymer content.

Table 4.15 Polymer Effects in Flexural Toughness-Aging in Air.

Mean lb/in	Polymer	0%	5%	10%	15%
37.43	0%				
62.45	5%	*			
66.23	10%	*			
88.05	15%	*	*	*	

(*) denotes significant differences at 5% level
of significance for the pairs of polymer content.

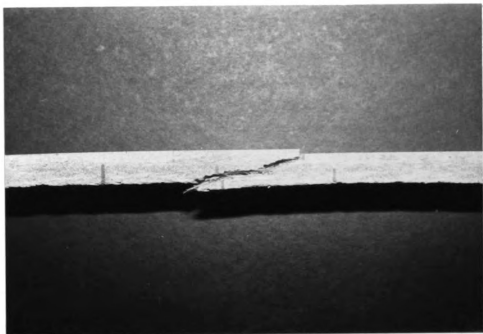


Figure 4.16 Inclined Crack-Unaged GFRC.



Figure 4.17 Fractured Surface-Unaged GFRC.

pulled out without any damage to the filaments. Figure 4.19 shows the smooth surface of a single filament with no chemical attack when aged in air. Figures 4.20 and 4.21 show the fiber-matrix interface zone of unaged GFRC after 0 and 50 days of aging in air, respectively. Both photographs suggest no cement hydration products deposited in between filaments.

Figure 4.22 shows a crack developed along glass fiber in unbrittle GFRC, and Figure 4.23 presents a view showing the debonding between fiber filaments and matrix. For the case of unaged GFRC and GFRC aged in air, the interface zones are the weakest points in the composite, and the crack directions are governed by the orientation of glass fibers.

At 15% polymer content, some fiber filaments and showed quite different appearance from those from non-polymer-modified GFRC (compare Figure 4.24 and Figure 4.25) indicating the possible accumulation of polymer particles near the surface of filaments. Figure 4.26 also shows the polymer particles attached to a fiber filament. This appearance of polymer particles on filament surfaces was, however, seen only at 15% polymer addition.

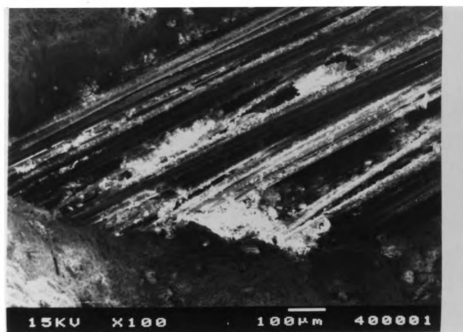


Figure 4.18 Fiber Pull-Out With No Fracture of Filaments.

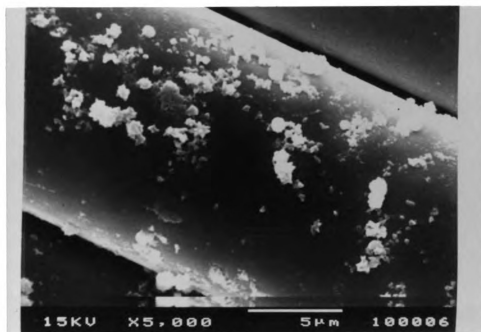


Figure 4.19 Smooth Surface of Filament-Aging in Air.

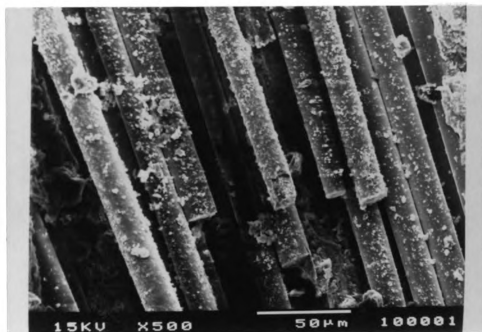


Figure 4.20 Free Space In-Between Filaments-Unaged GFRP.

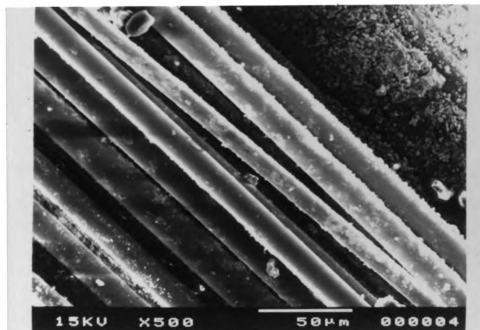


Figure 4.21 Free Space In-Between Filaments-Aging in Air.

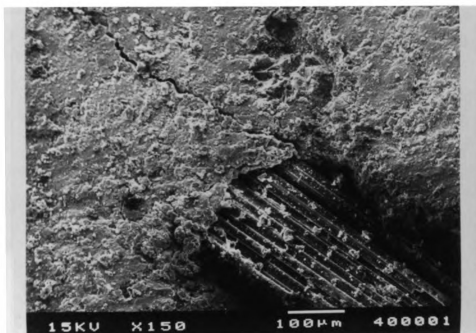


Figure 4.22 Crack Developed Along Fiber-Aging in Air.

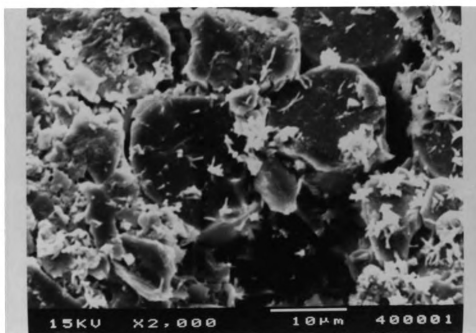
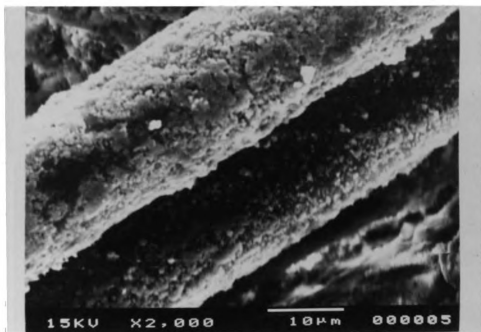
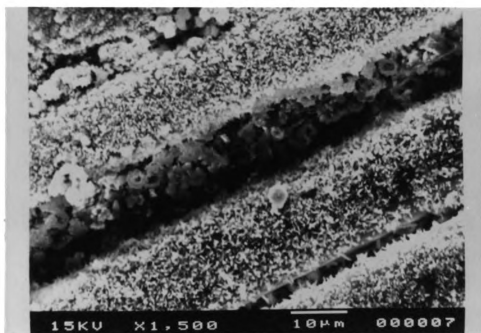


Figure 4.23 Debonding Between Matrix and Filaments.



**Figure 4.24 Hydration Products Attracted to Filaments-
Polymer 0%.**



**Figure 4.25 Polymer Particles Attracted to Filaments-
Polymer 15%.**

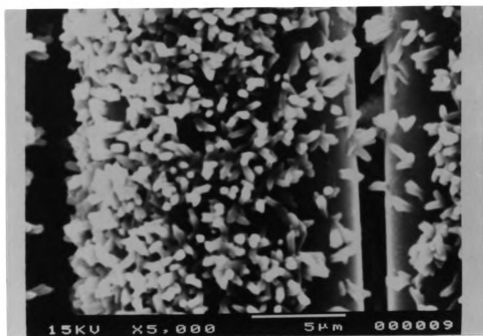


Figure 4.26 Polymer Particles - Polymer 15%.

4.4 POLYMER EFFECTS ON AGING IN HOT WATER

Figures 4.27 and 4.28 show the comparison of flexural characteristics between unaged GFRC and aged in hot water for 50 days (50 days immersion in 50°C, 122°F water) with different polymer additions. No change in LOP with time could be detected at the significance level of 5%.

However, MOR and flexural toughness were reduced significantly as result of aging in hot water (MOR and flexural toughness of GFRC aged in hot water for 50 days are significantly different from those of unaged GFRC at 5% level of significance).

In order to compare aging behavior for different polymer addition, regression analysis was performed for all the data points shown in Figures 4.3 through 4.10. A linear model in logarithmic scale was adopted in the regression analysis. Figures 4.29 and 4.30 show these linear regression curves for MOR and flexural toughness with mean values at each age (note that all the test data, not means at different ages, were used for regression analysis).

Although polymer-modified GFRCs show better performance in MOR and flexural toughness at all ages, losses in these characteristics with aging in hot water seem to have occurred faster than in unmodified GFRC especially for flexural toughness as indicated by the steeper regression lines in the case of polymer modified GFRC specimens in Figures 4.29 and 4.30.

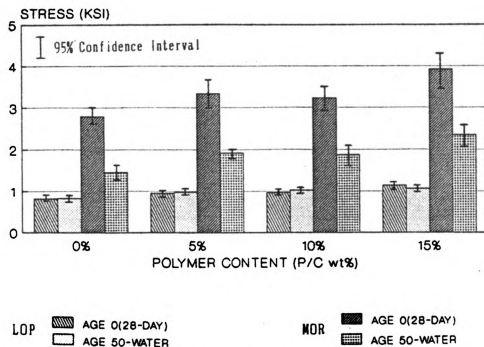


Figure 4.27 LOP and MOR of Unaged and Aged in Hot Water.

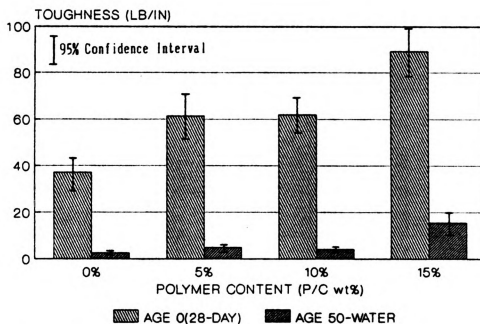


Figure 4.28 Toughness of Unaged and Aged in Hot Water.

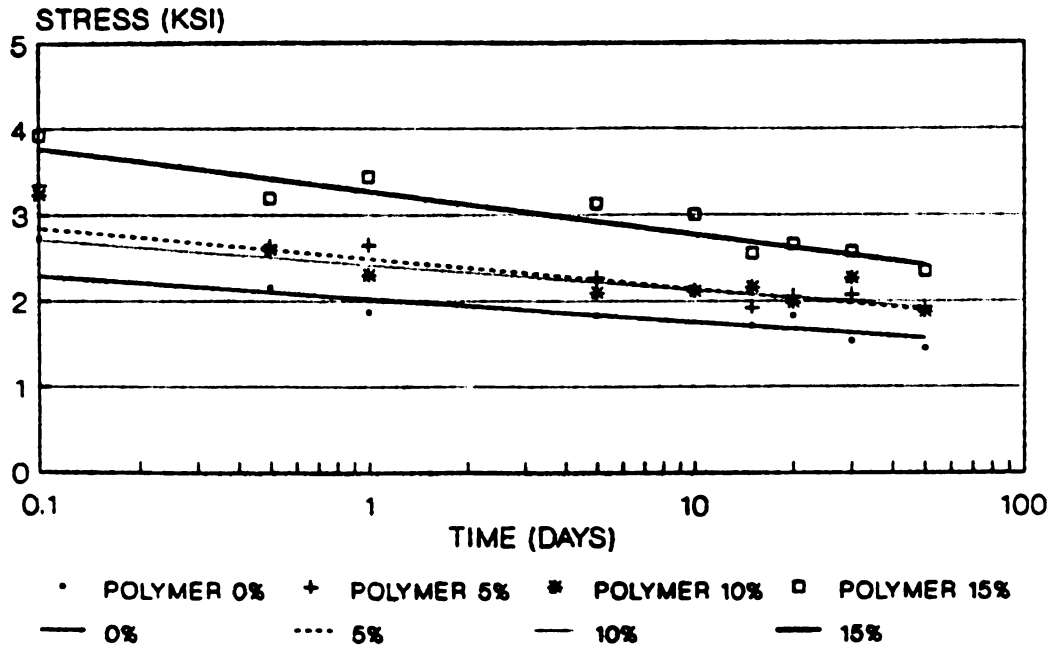


Figure 4.29 Linear Regression Curves of MOR with Time-Aging in Hot Water.

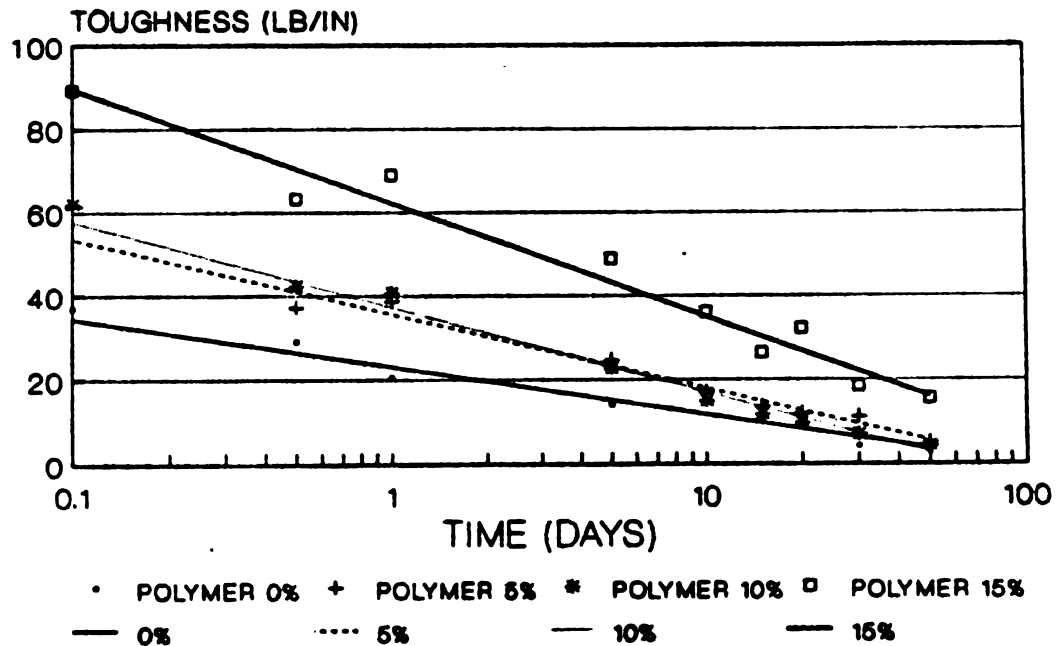


Figure 4.30 Linear Regression Curves of Toughness with Time-Aging in Hot Water.

Tables 4.16 through 4.18 present statistical characteristics, and Tables 4.29 through 4.21 show polymer effects detected at 5% level of significance for specimens aged in hot water for 50 days. Polymer additions at 5% and 10% show major effects on MOR, but not on toughness, compared with unmodified GFRC at 5% level of significance. 15% polymer content still have major effects on both MOR and Flexural toughness even after aging in hot water for 50 days, when compared with the other polymer contents.

Brittle mode of failure was obvious even for 15% polymer addition, after 50 days of aging in hot water. Figures 4.31 and 4.32 show the cracking pattern and fractured surface of these brittle specimens. GFRC after aging in hot water failed in flexure by the appearance of a perpendicular crack with the smallest fractured surface possible, and all fibers on the fractured surface were broken, showing almost no pull-out behavior.

SEM observations of fractured surfaces of the brittle specimens are shown in Figures 4.33 and 4.34. These figures clearly indicate the penetration of cement hydration products in-between fiber filaments; even 15% polymer addition could not prevent the filling-up process.

No fiber degradation caused by alkali attack could be seen on single filament. In fact, even for fully aged specimens (50 days in 50°C, 122°F water), the surface of glass filaments remained as smooth as before aging (Figure 4.35).

Table 4.16 Statistical Characteristics for LOP-50 Days in Hot Water.

Polymer	Count	Mean (psi)	Standard Deviation	95% Conf. Int. for Mean		Min.	Max.
0%	9	829	87	762	to 896	675	956
5%	8	978	73	917	to 1039	862	1087
10%	11	1024	110	952	to 1099	888	1188
15%	10	1060	101	988	to 1132	919	1230

Table 4.17 Statistical Characteristics for MOR-50 Days in Hot Water.

Polymer	Count	Mean (psi)	Standard Deviation	95% Conf. Int. for Mean		Min.	Max.
0%	9	1453	252	1259	to 1648	1044	1753
5%	8	1919	139	1803	to 2034	1694	2074
10%	11	1875	340	1647	to 2103	1230	2387
15%	10	2345	284	2142	to 2548	1952	2840

Table 4.18 Statistical Characteristics for Flexural Toughness - 50 Days in Hot Water.

Polymer	Count	Mean lb/in.	Standard Deviation	95% Conf. Int. for Mean		Min.	Max.
0%	9	2.56	1.18	1.70	to 3.50	1.26	4.92
5%	8	5.04	1.33	3.92	to 6.16	3.44	7.71
10%	11	4.09	1.28	3.22	to 4.95	1.93	5.82
15%	10	15.51	6.42	10.93	to 20.11	9.09	29.66

Table 4.19 Polymer Effects in LOP-50 Days in Hot Water.

Mean (psi)	Polymer	0%	5%	10%	15%
829	0%				
978	5%	*			
1024	10%	*			
1060	15%	*			

(*) denotes significant differences at 5% level of significance for the pairs of polymer content.

Table 4.20 Polymer Effects in MOR-50 Days in Hot Water.

Mean (psi)	Polymer	0%	5%	10%	15%
1453	0%				
1918	5%	*			
1875	10%	*			
2345	15%	*	*	*	

(*) denotes significant differences at 5% level of significance for the pairs of polymer content.

Table 4.21 Polymer Effects in Flexural Toughness-50 Days in Hot Water.

Mean lb/in	Polymer	0%	5%	10%	15%
2.60	0%				
5.04	5%				
4.09	10%				
15.52	15%	*	*	*	

(*) denotes significant differences at 5% level of significance for the pairs of polymer content.

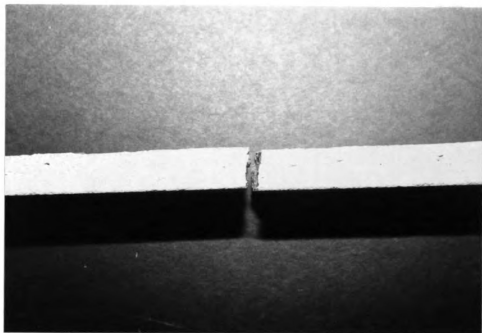


Figure 4.31 Perpendicular Crack-Aging in Hot Water.



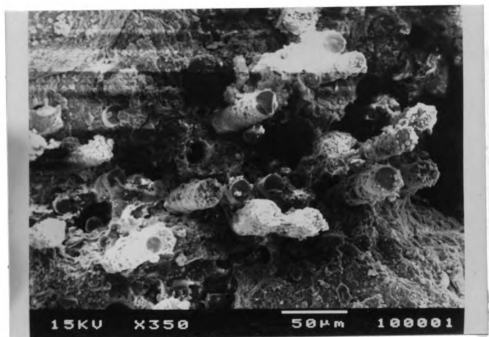
Figure 4.32 Fractured Surface-Aging in Hot Water.

Further indications of the tendency towards fiber rupture, instead of pull-out, in GFRc specimens aged in hot water are presented in Figures 4.36 and 4.37. The growth of hydration products within the glass fiber filaments seem to provide excessive bonding between fibers and the matrix which eliminates fiber pull-out prior to rupture. The fact that relatively large amount of frictional energy are dissipated during fiber pull-out illustrates why the loss of pull-out in hot water aged GFRc specimens leads to loss of ductility. Polymer modification had no significant effects in the process of aging in GFRc.

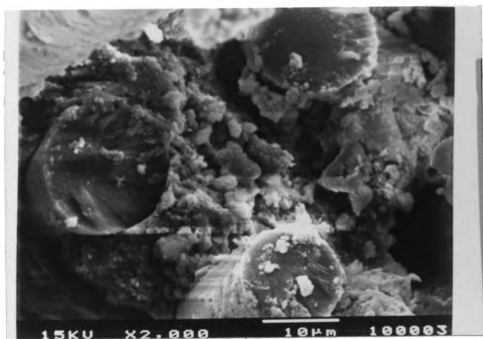
It is important to note that aging in hot water was used as an accelerating aging process which simulate a natural weathering. According to Litherland, et. al. (1981), Reference 44, flexural characteristics of GFRc aged for 1 day in 50°C (122°F) water represents those of GFRc 101 days of natural weathering exposure in the United Kingdom. The use of accelerated aging in hot water may cause complexions due to the differences between hydration products in hot water and in ambient conditions (Reference 61), and also due to the potentially adverse effects of hot water on the polymer phase in polymer-modified GFRc.

In order to find the actual durability characteristics of polymer-modified GFRc, GFRc panels are now subjected to natural weathering at a site on Michigan State University campus (Figure 3.38); the results of natural weathering tests, and correlations between natural weathering and hot

water aging will not be analyzed later (this work was outside the scope of the research reported herein).

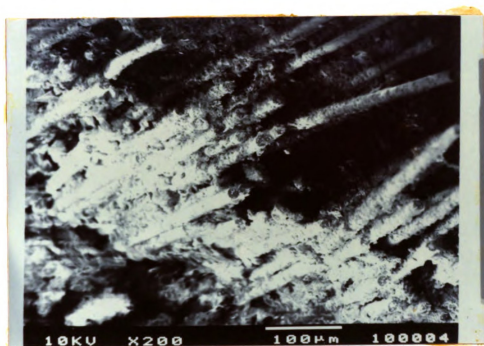


(a) Magnification 350

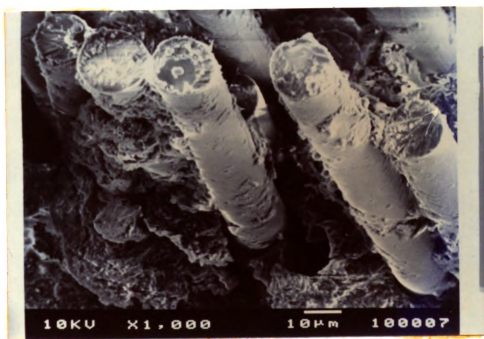


(b) Magnification 2000

Figure 4.33 Penetration of Hydration Products-Polymer 0%.

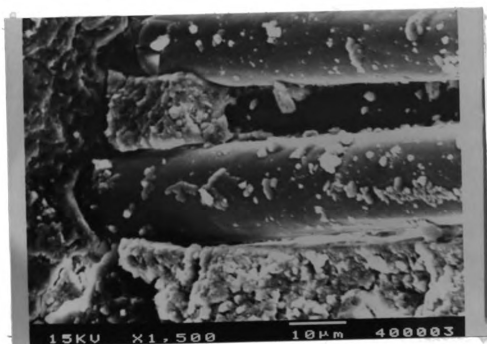


(a) Magnification 200

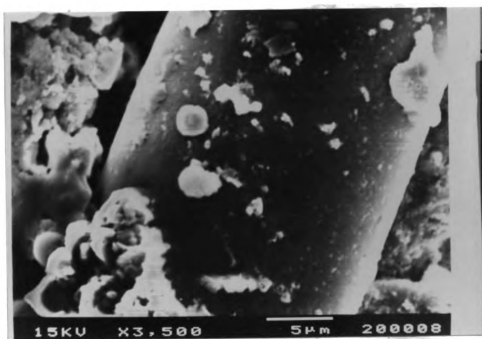


(b) Magnification 1000

Figure 4.34 Penetration of Hydration Products-Polymer 15%.



(a) Polymer 0% (50 Days in Hot Water)



(b) Polymer 15% (50 Days in Hot Water)

Figure 4.35 Smooth Surface of Filaments.

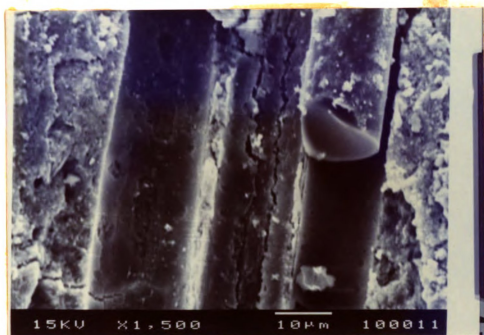


Figure 4.36 Fractured Filament and Grooves Caused by Pull-Out.

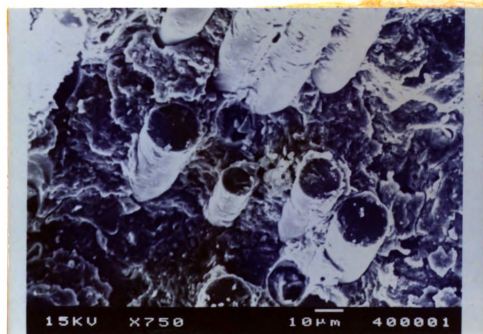


Figure 4.37 Fractured Filaments with Little Pull-Out.



Figure 4.38 Natural Weathering Exposure at Michigan State University.



CHAPTER 5

SUMMARY & CONCLUSION

The effects of aging in air and in hot water on the flexural performance of GFRC specimens with different polymer contents were investigated experimentally. The direct spraying technique was used to prepare 15 x 30 x 0.5 in. (38 x 76 x 1.3 cm) panels, from which the 2 x 15 x 0.5 in. (5 x 38 x 1.3 cm) flexural specimens were cut. The polymer content selected in this investigation represents typical values used in practice (0%, 5%, 10%, and 15% polymer/cement ratio by weight). Third-point loading flexure tests with a span length of 12 in. were performed at predetermined aging periods (0, 12 hours, 1, 5, 10, 15, 20, 30, 50 days) for GFRC specimens aged in air (20°C, 68°F, 40% RH) and in hot water (50°C, 122°F, water immersion). SEM observations were also performed to identify failure and deterioration mechanisms in GFRC. The polymer used in this investigation was acrylic emulsion, and the glass fiber was AR-glass fiber. The findings from this investigation are summarized below.

1. 15% polymer addition (polymer/cement wt%) led to 25% increase in LOP, 40% increase in MOR and more than 100% in toughness of unaged non-polymer-modified GFRC.
2. 5% and 10% polymer additions also improved MOR of unaged non-polymer-modified GFRC by 25% and its flexural toughness by 70%, however, increase in polymer

content from 5% to 10% did not cause any significant improvements in flexural behavior.

3. Polymer modifications led to significant increase in the multiple cracking region of the flexural load-deflection curve (between LOP and MOR) of unaged GFRC.
4. At 15% polymer addition, SEM observations showed an accumulation of polymer particles on glass fiber filaments.
5. Aging in air (50 days in 20°C, 68°F, 40% RH) did not affect the above flexural performance characteristics of unmodified and polymer-modified GFRC.
6. Aging in hot water (immersion in 50°C, 122°F water) led to rapid loss of strength (MOR) and flexural toughness for all polymer contents.
7. MOR values of GFRC aged in hot water for 50 days were about one-half those of unaged GFRC, and most of toughness was diminished during the 50 days of hot water aging period; polymer modification could not prevent those losses.
8. LOP values did not show significant drops even after 50 days of aging in hot water.
9. Although polymer modified GFRC showed flexural characteristics better than those of non-modified GFRC during the hot water aging period, polymer-modified GFRC lost their strength and particularly toughness in a faster rate than non-polymer-modified GFRC.

10. SEM observations suggested that the losses in flexural toughness and strength with aging in hot water were caused by the penetration of cement hydration products in between glass filaments. This densification led to stress concentrations and excessive bonding between fiber filaments and matrix, which caused the lack of pull-out behavior.
11. Ductile GFRC specimens failed in flexure with an inclined crack having large fracture surfaces, while the brittle GFRC specimens (after aging in hot water) failed with a crack perpendicular to the beam axis having relatively small fracture surfaces.

LIST OF REFERENCES

LIST OF REFERENCES

1. Biryukovich, K.L., Biryukovich, Yu.L. "Glass Fibre Reinforced Cement," Budivel'nik, CERA Translation No. 12 1964.
2. Majumdar, A.J., and Nurse, R.W., "Glass Fibre Reinforced Cement," Materials Science and Engineering 15, 1974, pp. 107-127.
3. Pilkinton Reinforcements, "Cem-Fil GRC Technical Data," Published by Pilkinton Brothers Ltd., 1984.
4. Leonard, S., and Bentur, A., "Improvement of the Durability of Glass Fiber Reinforced Cement Using Blended Cement Matrix," Cement and Concrete Research, Vol. 14, 1984, pp. 717-728.
5. Majumdar, A.J., and Singh, B., "Glass Fiber Reinforced Sulfate Cement," Composites, July 1981, pp. 177-183.
6. Majumdar, A.J., Singh, B., and Ali, M.A., "Properties of High-Alumina Cement Reinforced with AR Glass Fibers," Journal of Materials Science 16, 1981, pp. 2597-2607.
7. Hayashi, M., Sato, S., and Fujii, H., "Some Ways to Improve Durability of GFRC," Proceedings-Durability of Glass Fiber Reinforced Concrete Symposium, Prestressed Concrete Institute, Chicago, Illinois, November 1985, pp. 270-284.
8. Diamond, S., "The GFRC Durability Problem: Nature, Characteristics and Test Methods," Proceedings-Durability of Glass Fiber Reinforced Concrete Symposium, Prestressed Concrete Institute, Chicago, Illinois, November 1985, pp. 199-209.
9. Mashima, M., "Glass Fiber Reinforced Concrete," Fiber Reinforced Cement Concrete Composite Material, Japan Concrete Institute, October 1986, pp. 12-24.
10. True, G., "Constituent Materials," GRC-Production and Uses, published by A Viewpoint Publication, 1986, pp. 33-34.
11. Lee, J.A., "GRC-The Material," GRC and Buildings, Chapter 2, published by Butterworths Ltd., 1983, pp. 6-27.

12. Fordyce, M.W., and Wodehouse, R.G., "Manufacturing Method," GRC and Buildings, published by Butterworths Ltd., 1983, pp. 74-87.
13. True, G., "Production Equipment," GRC-Production and Uses, published by A Viewpoint Publication, 1986, pp. 5-23.
14. True, G., "Moulds and Moulding Techniques," GRC-Production and Uses, published by A Viewpoint Publication, 1986, pp. 24-32.
15. PCI Committee, "Recommended Practice for Glass Fiber Reinforced Concrete Panels," published by Prestressed Concrete Institute, 1987, pp. 8-10.
16. Bayasi, Z., and Soroushian, P., "Optimum Use of Pozzolan Materials in Steel Fiber Reinforced Concrete," Seminar Proceedings in Fiber Reinforced Concrete: Design and Applications, East Lansing, Michigan, February 1987, pp. 80-110.
17. Mindess, S., and Young, J., "Admixtures for Concrete," Concrete, Published by Prentice-Hall Inc., 1981, pp. 166-200.
18. Sign, B., Majumdar, A.J., and Ali, M.A., "Properties of GRC Containing pfa," The International Journal of Cement Composites and Lightweight Concrete, Vol. 6, Number 2, May 1984, pp. 67-74.
19. Benture, A., "Silica Fume Treatments as Means for Improving Durability of Glass Fiber Reinforced Cements," Journal of Materials in Civil Engineering, Vol. 1, No. 3, August 1989, pp. 167-183.
20. Mindess, S., and Young, J., "Modern Developments," Concrete, published by Prentice-Hall Inc., 1981, pp. 615-645.
21. Bijen, J., "Durability of Some Glass Fiber Reinforced Cement Composites," ACI Journal, July-August 1983, pp. 305-311.
22. PCI Committee, "Manufacturing," Recommended Practice for GRC Panels, published by Prestressed Concrete Institute, 1987, pp. 35-42.
23. True, G., "Mixers, Mix Designs and Mixing Procedures," GRC-Production and Uses, published by A Viewpoint Publication, 1986, pp. 40-43.
24. True, G., "Curing," GRC-Production and Uses, published by A Viewpoint Publication, 1986, pp. 51-53.

25. True, G., "Finishes," GRC-Production and Uses, published by A Viewpoint Publication, 1986, pp. 54-56.
26. Fordyce, M.W., and Wodehouse, R.G., "Construction Details," GRC and Buildings, published by Butterworths Ltd., 1983, pp. 153-173.
27. PCI Committee, "Quality Control," Recommended Practice for GRC Panels, published by Prestressed Concrete Institute, 1987, pp. 43-46.
28. True, G., "Quality Control, Testing Methods and Statistical Evaluation of Results," GRC-Production and Uses, published by A Viewpoint Publication, 1986, pp. 63-80.
29. Chiyoda Technical and Industrial Co., Ltd., "Experimental Research for GRC Premix-Using an Omni-Mixer," Technical Report No. 10-2, May 1979.
30. Pilkinton Reinforcements, "Principles of Glass Fiber Reinforcement," Cem-Fil GRC-Technical Data, Chapter 4, published by Pilkinton Brothers Ltd., 1984.
31. PCI Committee, "Physical Properties," Recommended Practice for Glass Fiber Reinforced Concrete Panels, published by Prestressed Concrete Institute, 1987, pp. 10-17.
32. Fordyce, M.W., and Wodehouse, R.G., "Material Properties," GRC and Buildings, published by Butterworths Ltd., 1983, pp. 28-55.
33. Sign, B., Walton, P.L., and Stucke, M.S., "Test Methods Used to Measure the Mechanical Properties of Fiber Cement Composite at the Building Research Establishment," Proceedings-RILEM Symposium on Testing and Test Method of Fiber Cement Composite, Sheffield, 1978, pp. 377-387.
34. Procter, B.A., "Properties and Performance of GRC," Proceedings-Symposium on Fibrous Concrete, London, 1980, pp. 69-89.
35. Majumdar, A.J., Sign, B., Langley, A.A., and Ali, M.A., "The Durability of Glass Fiber Cement-The Effect of Fiber Length and Content," Journal of Materials Science 15, 1980, pp. 1085-1096.
36. Pilkinton Reinforcements, "Mechanical Properties of GRC," Cem-Fil GRC Technical Data, Chapter 5, published by Pilkinton Brothers Ltd., 1984.

37. Pilkinton Reinforcements, "Physical and Mechanical Properties of GRC," Cem-Fil GRC Technical Data, Chapter 6, published by Pilkinton Brothers Ltd., 1984.
38. Fordyce, M.W., and Wodehouse, R.G., "Mechanical Properties," GRC and Buildings, published by Butterworths Ltd., 1983, pp. 74-87.
39. True, G., "Typical Properties," GRC-Production and Uses, published by A Viewpoint Publication, 1986, pp. 98-104.
40. Shah, S.P., Ludirdja, D., Daniel, J.I., and Mobasher, B., "Toughness-Durability of Glass Fiber Reinforced Concrete System," ACI Materials Journal, September-October 1988, pp. 352-360.
41. Bentur, A., "Mechanism of Potential Embrittlement and Strength Loss of Glass Fiber Reinforced Cement Composites," Proceedings-Durability of Glass Fiber Reinforced Concrete Symposium, Prestressed Concrete Institute, Chicago, Illinois, November 1985, pp. 109-123.
42. Singh, B., and Majumdar, A.J., "The Effect of Fiber Length and Content on the Durability of Glass Reinforced Cement - Ten-Year Results," Journal of Materials Science Letters 4, 1985, pp. 967-971.
43. Daniel, J.I., "Durability of Glass Fiber Reinforced Concrete Systems," Proceedings-Durability of Glass Fiber Reinforced Concrete Symposium, Prestressed Concrete Institute, Chicago, Illinois, November 1985, pp. 174-198.
44. Litherland, K.L., Oakley, D.R., and Proctor, B.A., "The Use of Accelerated Ageing Procedures to Predict the Long Term Strength of GRC Composites," Cement and Concrete Research, Vol. 11, 1981, pp. 455-466.
45. Bentur, A., and Diamond, S., "Direct Incorporation of Silica Fume into Glass Fiber Strands as a Means for Developing GFR Composites of Improved Durability," The International Journal of Cement Composites and Lightweight Concrete, Vol. 9, No. 3, August 1987, pp. 127-135.
46. Bijen, J., and Jacobs, M., "Properties of Glass Fiber-Reinforced Polymer-Modified Cement," Materiaux et Constructions, Vol. 15, No. 89, 1982.

47. Chan, H.C., and Patterson, W.A., "Effects of Ageing and Weathering on the Tensile Strength of Glass Fiber Reinforced High-Alumina Cement," *Journal of Materials Science* 6, 1971, pp. 342-346.
48. Mills, R.H., "Preferential Precipitation of Calcium Hydroxide on Alkali-Resistant Glass Fibers," *Cement and Concrete Research*, Vol. 11, 1981, pp. 689-697.
49. Okada, K., Mise, T., and Mashima, M., "Bond Characteristics of Glass Fiber with Cement Mortar," *Proceedings-The 25th Japan Congress on Materials Research*, 1983, pp. 191-194.
50. Shah, S.P., "Reinforced Mechanism in GFRG Composites," *Proceedings-Durability of Glass Fiber Reinforced Concrete Symposium*, Prestressed Concrete Institute, Chicago, Illinois, November 1985, pp. 90-108.
51. Aveston, J., Cooper, G.A., and Kelly, A., "Single and Multiple Fracture," *Proceedings-NPL Conference on the Properties of Fibrous Composites*, IPC Science and Technology Press, Guildford, UK, 1971, pp. 15-35.
52. Proctor, B.A., "The Stress-Strain Behaviour of Glass-Fiber Reinforced Cement Composites," *Journal of Materials Science* 21, 1986, pp. 2441-2448.
53. Stucke, M.S., and Majumdar, A.J., "Microstructure of Glass Fiber-Reinforced Cement Composites," *Journal of Materials Science* 11, 1976, pp. 1019-1030.
54. Fordyce, M.W., and Wodehouse, R.G., "Design," *GRC and Buildings*, published by Butterworths Ltd., 1983, pp. 88-89.
55. True, G., "Design," *GRC-Production and Uses*, published by A Viewpoint Publication, 1986, pp. 57-62.
56. PCI Committee, "Design," *Recommended Practice for Glass Fiber Reinforced Concrete Panels*, published by Prestressed Concrete Institute, 1987, pp. 18-33.
57. Pilkinton Reinforcements, "Design Principles," *Cem-Fil GRC Technical Data*, Chapter 7, published by Pilkinton Brothers Ltd., 1984.
58. Tanaka, M., and Uchida, I., "Durability of GFRG with Calciumsilicate-Slag Type Low Alkaline Cement," *Proceedings-Durability of Glass Fiber Reinforced Concrete Symposium*, Prestressed Concrete Institute, Chicago, Illinois, November 1985, pp. 305-314.

59. True, G., "Product Range," GRC-Production and Uses, published by A Viewpoint Publication, 1986, pp. 83-95.
60. Tallentire, A.G., "Application & Uses," GRC and Buildings, published by Butterworths Ltd., 1983, pp. 56-73.
61. Shah, S.P., Daniel, J.I., Ludirdja, D., "Toughness of Glass Fiber Reinforced Concrete Panels Subjected to Accelerated Aging," PCI Journal, September-October 1987, pp. 82-99.
62. Nippon Electric Glass Co., Ltd., "High Zirconia Alkali-Resistant Glass Fiber: ARG," published by Nippon Electric Glass Co., Ltd., April 1986, pp. 4-11.